



ČESKÁ
KARDIOLOGICKÁ
SPOLEČNOST

XXIX.

VÝROČNÍ SJEZD
ČESKÉ KARDIOLOGICKÉ
SPOLEČNOSTI

TO NEJLEPŠÍ Z **ČESKÉ KARDIOLOGIE**
ZA ROK

2020

Nejlepší původní české práce publikované v roce 2020

Tato sekce prezentuje každoročně na výročním sjezdu ČKS **nejlepší původní vědecké práce členů ČKS**, vzniklé na pracovištích v ČR a publikované v předchozím kalendářním roce v mezinárodních časopisech s impakt faktorem $>2,0$. Tři nejlepší jsou rovněž **oceněny výběrem ČKS**. Práce jsou řazeny dle IF.

Podmínky:

- Práce musí být publikována v časopise s impakt faktorem $> 2,0$ v průběhu posledního kalendářního roku před sjezdem ČKS, na který je přihlášena
- Práce musí vzniknout na pracovišti v České republice
- Prvním autorem musí být člen ČKS
- Musí jít o původní práci, prezentující vlastní výzkumné výsledky (nemůže se jednat o přehledný článek, editorial, abstrakt ani o kasuistiku)
- Nemůže se jednat ani o práci vzniklou v zahraničí (např. při studijním pobytu českého lékaře)
- Současně s přihlášením práce je autor povinen zaslat do sekretariátu ČKS e–mailem PDF verzi originálního článku s přihlášenou prací. Bez tohoto textu „in extenso“ nemůže být práce přijata.

Patent Foramen Ovale Closure Is Effective in Divers: Long-Term Results From the DIVE-PFO Registry

J. Honěk a kol.

Left Atrial Appendage Closure versus Non-Vitamin K Anticoagulants in High Risk Patients with Atrial Fibrillation: The PRAGUE-17 Trial

P. Osmančík a kol.

Dysregulation of epicardial adipose tissue in cachexia due to heart failure: the role of natriuretic peptides and cardiolipin

V. Melenovský a kol.

Impact of access route to the left ventricle on asymptomatic periprocedural brain injury: the results of a randomized trial in patients undergoing catheter ablation of ventricular tachycardia

E. Borišincová a kol.

Deleterious Effects of Hyperactivity of the Renin-Angiotensin System and Hypertension on the Course of Chemotherapy-Induced Heart Failure after Doxorubicin Administration: A Study in Ren-2 Transgenic Rat

P. Kala a kol.

MicroRNA-331 and microRNA-151-3p as biomarkers in patients with ST-segment elevation myocardial infarction

M. Horváth a kol.

Exercise dynamics of cardiac biomarkers and hemoconcentration in patients with chronic systolic heart failure

J. Beneš a kol.

Complete recovery of fulminant cytotoxic CD8 T-cell-mediated myocarditis after ECMELLA unloading and immunosuppression

I. Jurčová a kol.

Desminopathy: Novel Desmin Variants, a New Cardiac Phenotype, and Further Evidence for Secondary Mitochondrial Dysfunction

M. Kubánek a kol.

Modified Strategies for Invasive Management of Acute Coronary Syndrome during the COVID-19 Pandemic

P. Toušek a kol.

Effectiveness of alcohol septal ablation for hypertrophic obstructive cardiomyopathy in patients with late gadolinium enhancement on cardiac magnetic resonance

E. Polaková a kol.

Long-term outcome of repeated septal reduction therapy after alcohol septal ablation for HOCM

J. Veselka a kol.

Patients with hypertrophic obstructive cardiomyopathy after alcohol septal ablation have favorable long-term outcome irrespective of their genetic background

J. Bonaventura a kol.

J. Honěk a kol.

Patent Foramen Ovale Closure Is Effective in Divers: Long-Term Results From the DIVE-PFO Registry

Journal of The American College of Cardiology
Impact Factor: 20,589

See discussions, stats, and author profiles for this publication at: <https://www.researchgate.net/publication/343848212>

Patent Foramen Ovale Closure Is Effective in Divers

Article in *Journal of the American College of Cardiology* · September 2020

DOI: 10.1016/j.jacc.2020.06.072

CITATIONS

0

READS

7

10 authors, including:



Jakub Honěk

University Hospital Motol

28 PUBLICATIONS 119 CITATIONS

SEE PROFILE



Martin Srámek

Charles University in Prague

33 PUBLICATIONS 78 CITATIONS

SEE PROFILE



Tomáš Honek

Charles University in Prague

24 PUBLICATIONS 239 CITATIONS

SEE PROFILE



Ales Tomek

Charles University in Prague

109 PUBLICATIONS 358 CITATIONS

SEE PROFILE

Some of the authors of this publication are also working on these related projects:



Statins prior to PCI [View project](#)



Post-cardiac arrest care [View project](#)

Letters

Patent Foramen Ovale Closure Is Effective in Divers



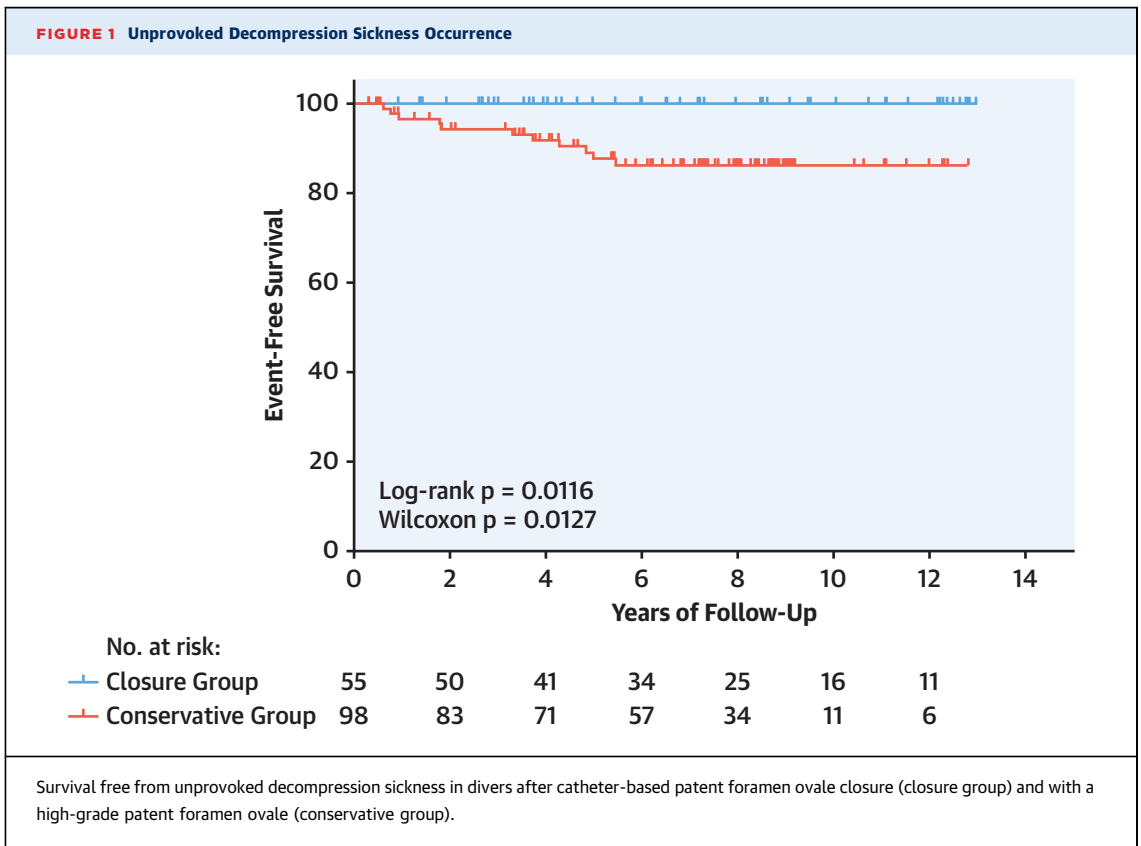
Long-Term Results From the DIVE-PFO Registry

Patent foramen ovale (PFO) is associated with increased risk of decompression sickness (DCS) in divers because of paradoxical embolization of nitrogen bubbles (1). These events can be unpredictable in divers with a PFO (2). Catheter-based PFO closure led to the elimination of arterial emboli after simulated dives (3). However, the evidence of its clinical effectiveness is sparse (4). This study aimed to evaluate the long-term clinical effectiveness of catheter-based PFO closure in the prevention of unprovoked DCS.

A total of 829 consecutive divers were prospectively included in the DIVE-PFO (Decompression

Illness Prevention in Divers with a Patent Foramen Ovale) registry between January 2006 and December 2018. The study was approved by the Ethics Committee of University Hospital Motol. Transcranial color-coded sonography (TCCS) was used for the detection and grading of a right-to-left shunt, as previously described (2). Demographic data, diving experience, and details of any DCS were collected by means of questionnaires at enrollment and on a telephone follow-up visit. For divers for whom follow-up was not available, survival was checked in the National Database of Deaths. Transesophageal echocardiography was offered to divers with: 1) DCS history; 2) high-grade shunt on TCCS; or 3) unsuccessful TCCS examination (insufficient bone window). If the result of transesophageal echocardiography was available, the higher grade of the 2 examinations was counted.

The PFO closure procedures were performed in 5 centers. The Amplatzer Septal Occluder (AGA Medical



Corporation, Golden Valley, Minnesota) was used in 10 (18%) divers, and the Occlutech Figulla PFO Occluder N (Occlutech GmbH, Jena, Germany) was used in 46 (82%). The indication for the procedure was the presence of a grade 3 PFO and either: 1) a history of unprovoked DCS; or 2) diver's preference (not able to adapt to conservative diving recommendations, i.e., professionals). Minor bleeding occurred in 2 divers (3.6%); no other procedure-related complications occurred.

The endpoint of the study was unprovoked DCS (2). Estimates for long-term event-free survival were made by the Kaplan-Meier method, and differences were assessed by the log-rank test and the Gehan-Breslow-Wilcoxon method.

The follow-up was available for 748 (90%) divers, of whom 702 continued diving. Of these, a high-grade PFO was diagnosed in 153 (22%) divers: 55 underwent a catheter-based PFO closure (closure group), and 98 were advised to dive within the limits of recreational diving (conservative group). The mean follow-up time was 7.1 ± 3.8 years and 6.5 ± 3.2 years ($p = 0.339$), numbers of new dives were 30,684 and 25,328 ($p < 0.001$), mean ages were 40.0 ± 7.9 and 37.3 ± 9.8 years ($p = 0.079$), and 78.2% and 79.6% ($p = 0.893$) of divers were male for the closure group and conservative group, respectively. An unprovoked DCS occurred in 11 (11%) divers in the conservative group versus 0 in the closure group ($p = 0.012$) (Figure 1).

There is still a large knowledge gap regarding the optimal risk stratification and management strategy in divers with PFO. To date, there are no prospective studies to assess the clinical benefit of PFO closure in divers. The present study is unique in its uniform screening method and prospective participant inclusion. The results are consistent with previous findings that: 1) PFO closure eliminates arterial gas emboli; and 2) PFO is a major risk factor for unprovoked DCS (2,3). PFO closure is a safe procedure with a very low complication rate (5). According to our data, PFO closure is recommended in divers with a high-grade PFO, with a history of unprovoked DCS, or at the diver's preference. Besides protection from DCS, PFO closure also offers the diver lifelong protection from PFO-associated stroke.

This study is subject to inherent limitations, including selection bias. Although this study is, to our knowledge, the largest available, the number of endpoints is still low. The self-reporting of endpoints is another limitation; the majority of cases were not examined by a specialist at the time of the DCS event.

The results of the DIVE-PFO registry demonstrated that catheter-based PFO closure was more effective in

DCS prevention than the conservative approach in divers with a high-grade PFO.

*Jakub Honěk, MD, PhD
Martin Šrámek, MD
Tomáš Honěk, MD, PhD
Aleš Tomek, MD, PhD
Luděk Šefc, PhD
Jaroslav Januška, MD, PhD
Jiří Fiedler, MD
Martin Horváth, MD
Štěpán Novotný, MD
Josef Veselka, MD, PhD

*Department of Cardiology
Motol University Hospital
V Úvalu 84, 150 06, Praha 5
Czech Republic

E-mail: jakub.honek@gmail.com

<https://doi.org/10.1016/j.jacc.2020.06.072>

© 2020 by the American College of Cardiology Foundation. Published by Elsevier.

Please note: This study was supported by project 00064203, for conceptual development of a research organization, from the Ministry of Health, Czech Republic. The authors have reported that they have no relationships relevant to the contents of this paper to disclose.

The authors attest they are in compliance with human studies committees and animal welfare regulations of the authors' institutions and Food and Drug Administration guidelines, including patient consent where appropriate. For more information, visit the [JACC author instructions page](#).

REFERENCES

1. Bove AA. Diving medicine. *Am J Respir Crit Care Med* 2014;189:1479-86.
2. Honěk J, Šrámek M, Šefc L, et al. High-grade patent foramen ovale is a risk factor for unprovoked decompression sickness in recreational divers. *J Cardiol* 2019;74:519-23.
3. Honěk J, Šrámek M, Šefc L, et al. Effect of catheter-based patent foramen ovale closure on the occurrence of arterial bubbles in scuba divers. *J Am Coll Cardiol Intv* 2014;7:403-8.
4. Anderson G, Ebersole D, Covington D, Denoble PJ. The effectiveness of risk mitigation interventions in divers with persistent (patent) foramen ovale. *Diving Hyperb Med* 2019;49:80-7.
5. Wintzer-Wehekind J, Alperi A, Houde C, et al. Long-term follow-up after closure of patent foramen ovale in patients with cryptogenic embolism. *J Am Coll Cardiol* 2019;73:278-87.

The Need for and Benefits of an International Database for Cardiac Tumors



The report by Sultan et al. (1) is an excellent review that confirms both the rarity and poor long-term prognosis of cardiac tumors. It represents the largest collection of these tumors published to date.

Finally, we have a reasonably large group of patients with the diagnosis of primary cardiac

P. Osmančík a kol.

*Left Atrial Appendage Closure versus Non-Vitamin K
Anticoagulants in High Risk Patients with Atrial Fibrillation:
The PRAGUE-17 Trial*

Journal of The American College of Cardiology
Impact Factor: 20,56

Left Atrial Appendage Closure Versus Direct Oral Anticoagulants in High-Risk Patients With Atrial Fibrillation



Pavel Osmancik, MD, PhD,^a Dalibor Herman, MD, PhD,^a Petr Neuzil, MD, CSc,^b Pavel Hala, MD,^b Milos Taborsky, MD, CSc,^c Petr Kala, MD, PhD,^d Martin Poloczek, MD,^d Josef Stasek, MD, PhD,^e Ludek Haman, MD, PhD,^e Marian Branny, MD, PhD,^f Jan Chovancik, MD,^f Pavel Cervinka, MD, PhD,^g Jiri Holy, MD,^g Tomas Kovarnik, MD, PhD,^h David Zemanek, MD, PhD,^h Stepan Havranek, MD, PhD,^h Vlastimil Vancura, MD, PhD,ⁱ Jan Opatrny, MD,ⁱ Petr Peichl, MD, PhD,^j Petr Tousek, MD, PhD,^a Veronika Lekesova, MD,^b Jiri Jarkovsky, RNDr, PhD,^k Martina Novackova, MGR,^k Klara Benesova, MGR,^k Petr Widimsky, MD, DrSc,^{a,*} Vivek Y. Reddy, MD,^{b,l,*} on behalf of the PRAGUE-17 Trial Investigators

ABSTRACT

BACKGROUND Percutaneous left atrial appendage closure (LAAC) is noninferior to vitamin K antagonists (VKAs) for preventing atrial fibrillation (AF)-related stroke. However, direct oral anticoagulants (DOACs) have an improved safety profile over VKAs, and their effect on cardiovascular and neurological outcomes relative to LAAC is unknown.

OBJECTIVES This study sought to compare DOACs with LAAC in high-risk patients with AF.

METHODS Left Atrial Appendage Closure vs. Novel Anticoagulation Agents in Atrial Fibrillation (PRAGUE-17) was a multicenter, randomized, noninferiority trial comparing LAAC with DOACs. Patients were eligible to be enrolled if they had nonvalvular AF; were indicated for oral anticoagulation (OAC); and had a history of bleeding requiring intervention or hospitalization, a history of a cardioembolic event while taking an OAC, and/or a CHA₂DS₂-VASc of ≥ 3 and HAS-BLED of > 2 . Patients were randomized to receive LAAC or DOAC. The primary composite outcome was stroke, transient ischemic attack, systemic embolism, cardiovascular death, major or nonmajor clinically relevant bleeding, or procedure-/device-related complications. The primary analysis was by modified intention to treat.

RESULTS A high-risk patient cohort (CHA₂DS₂-VASc: 4.7 ± 1.5) was randomized to receive LAAC (n = 201) or DOAC (n = 201). LAAC was successful in 181 of 201 (90.0%) patients. In the DOAC group, apixaban was most frequently used (192 of 201; 95.5%). At a median 19.9 months of follow-up, the annual rates of the primary outcome were 10.99% with LAAC and 13.42% with DOAC (subdistribution hazard ratio [sHR]: 0.84; 95% confidence interval [CI]: 0.53 to 1.31; p = 0.44; p = 0.004 for noninferiority). There were no differences between groups for the components of the composite endpoint: all-stroke/TIA (sHR: 1.00; 95% CI: 0.40 to 2.51), clinically significant bleeding (sHR: 0.81; 95% CI: 0.44 to 1.52), and cardiovascular death (sHR: 0.75; 95% CI: 0.34 to 1.62). Major LAAC-related complications occurred in 9 (4.5%) patients.

CONCLUSIONS Among patients at high risk for stroke and increased risk of bleeding, LAAC was noninferior to DOAC in preventing major AF-related cardiovascular, neurological, and bleeding events. (Left Atrial Appendage Closure vs. Novel Anticoagulation Agents in Atrial Fibrillation [PRAGUE-17]; [NCT02426944](https://doi.org/10.1016/j.jacc.2020.04.067)) (J Am Coll Cardiol 2020;75:3122-35)
© 2020 by the American College of Cardiology Foundation.



Listen to this manuscript's audio summary by Editor-in-Chief Dr. Valentin Fuster on JACC.org.

From the ^aCardiocenter, Third Faculty of Medicine, Charles University Prague and University Hospital Kralovske Vinohrady, Prague, Czech Republic; ^bCardiocenter, Department of Cardiology, Na Homolce Hospital, Prague, Czech Republic; ^cCardiocenter, Department of Cardiology, University Hospital Olomouc, Olomouc, Czech Republic; ^dClinic of Cardiology, Masaryk University and University Hospital Brno, Brno, Czech Republic; ^eFirst Department of Internal Medicine, Faculty of Medicine, University Hospital Hradec Kralove, Charles University Prague, Prague, Czech Republic; ^fDepartment of Cardiology, Cardiocenter, Hospital Podlesí a.s., Trinec, Czech Republic; ^gDepartment of Cardiology, Krajská zdravotní a.s., Masaryk Hospital and J.E.Purkyne University, Usti nad Labem, Czech Republic; ^hCardiocenter, Second Internal Clinic—Cardiology and Angiology, Charles University, General Faculty Hospital, Prague, Czech Republic; ⁱDepartment of Cardiology, University Hospital and Faculty of Medicine Pilsen, Pilsen, Czech Republic; ^jCardiocenter, Institute of Clinical and Experimental Medicine, Prague, Czech Republic; ^kMasaryk University, Institute of Biostatistics and Analyses, Brno, Czech Republic; and the ^lHelmsley Electrophysiology Center, Icahn School of Medicine at Mount Sinai, New York, New York. *Drs. Widimsky and Reddy are co-senior authors. This work was supported by a research grant from

Vitamin K antagonists (VKAs) such as warfarin had long served as the therapeutic mainstay for preventing stroke in atrial fibrillation (AF). However, VKAs are limited by a narrow therapeutic profile, numerous diet-drug interactions, and requisite blood level monitoring. Accordingly, a novel site-specific therapeutic alternative, mechanical left atrial appendage closure (LAAC), entered clinical practice (1). In 2 randomized trials, LAAC was noninferior to VKAs for all stroke or systemic embolism and was associated with 78% and 52% reductions in hemorrhagic stroke and cardiovascular mortality, respectively (2).

SEE PAGE 3136

Coincident with these LAAC trials, the pharmacological options for stroke prevention expanded significantly with the advent of 4 direct oral anticoagulants (DOACs) that inhibit either factor IIa (dabigatran) or factor Xa (rivaroxaban, apixaban, and edoxaban) (3-6). In total, DOACs were associated with 19%, 51%, and 10% reductions in stroke or systemic embolism, hemorrhagic stroke, and mortality, respectively (7). Similar to the benefit of LAAC over VKAs, the benefit of DOACs over VKAs was related to a decrease in intracranial hemorrhage. Not surprisingly, DOACs have largely replaced VKAs as first-line therapy for AF stroke prevention.

The efficacy and safety of LAAC compared to oral anticoagulation in this era of more effective and safer anticoagulants is unknown, because, to our knowledge, there has never been a direct comparison of LAAC with DOACs. Accordingly, in patients with nonvalvular AF, we compared DOACs with LAAC using commercially available closure devices for the prevention of stroke, transient ischemic attack (TIA), systemic embolism, cardiovascular death, clinically significant bleeding, or procedure-/device-related complications.

METHODS

TRIAL DESIGN. The PRAGUE-17 (Left Atrial Appendage Closure vs. Novel Anticoagulation Agents

in Atrial Fibrillation; NCT02426944) trial was an investigator-initiated, multicenter, prospective, open-label, randomized, non-inferiority trial conducted at 10 cardiac centers in the Czech Republic (8). The trial was coordinated at Charles University and University Hospital Kralovske Vinohrady, Prague. Database management and primary analyses were performed at the Institute for Biostatistics and Analyses, Masaryk University, Brno. The multicenter ethics committee at University Hospital Kralovske Vinohrady and the ethics committees at participating centers approved the protocol. All patients provided written informed consent. Patient enrollment began in October 2015 and concluded in January 2019, with follow-up of the last enrolled patient occurring at least 6 months post-randomization.

PARTICIPANTS. Moderate- or high-risk patients with nonvalvular AF were eligible if indicated for anticoagulation and had: 1) history of bleeding requiring intervention or hospitalization; 2) history of a cardioembolic event while taking anticoagulation agents; or 3) a moderate to high risk profile, defined as CHA₂DS₂-VASc (congestive heart failure, hypertension, age ≥ 75 years, diabetes mellitus, prior stroke, transient ischemic attack, or thromboembolism, vascular disease, age 65-74 years, sex category [female]) of ≥ 3 plus HAS-BLED (uncontrolled hypertension, abnormal renal or liver function, stroke, bleeding, labile international normalized ratio, elderly, drugs or alcohol) of ≥ 2 . These CHA₂DS₂-VASc and HAS-BLED scores have been previously defined (9). Key exclusion criteria include mechanical valve prosthesis, mitral stenosis, comorbidities other than AF mandating anticoagulation, patent foramen ovale with large atrial septal aneurysm, mobile aortic plaque, symptomatic carotid arterial atherosclerosis, clinically significant bleeding within 30 days,

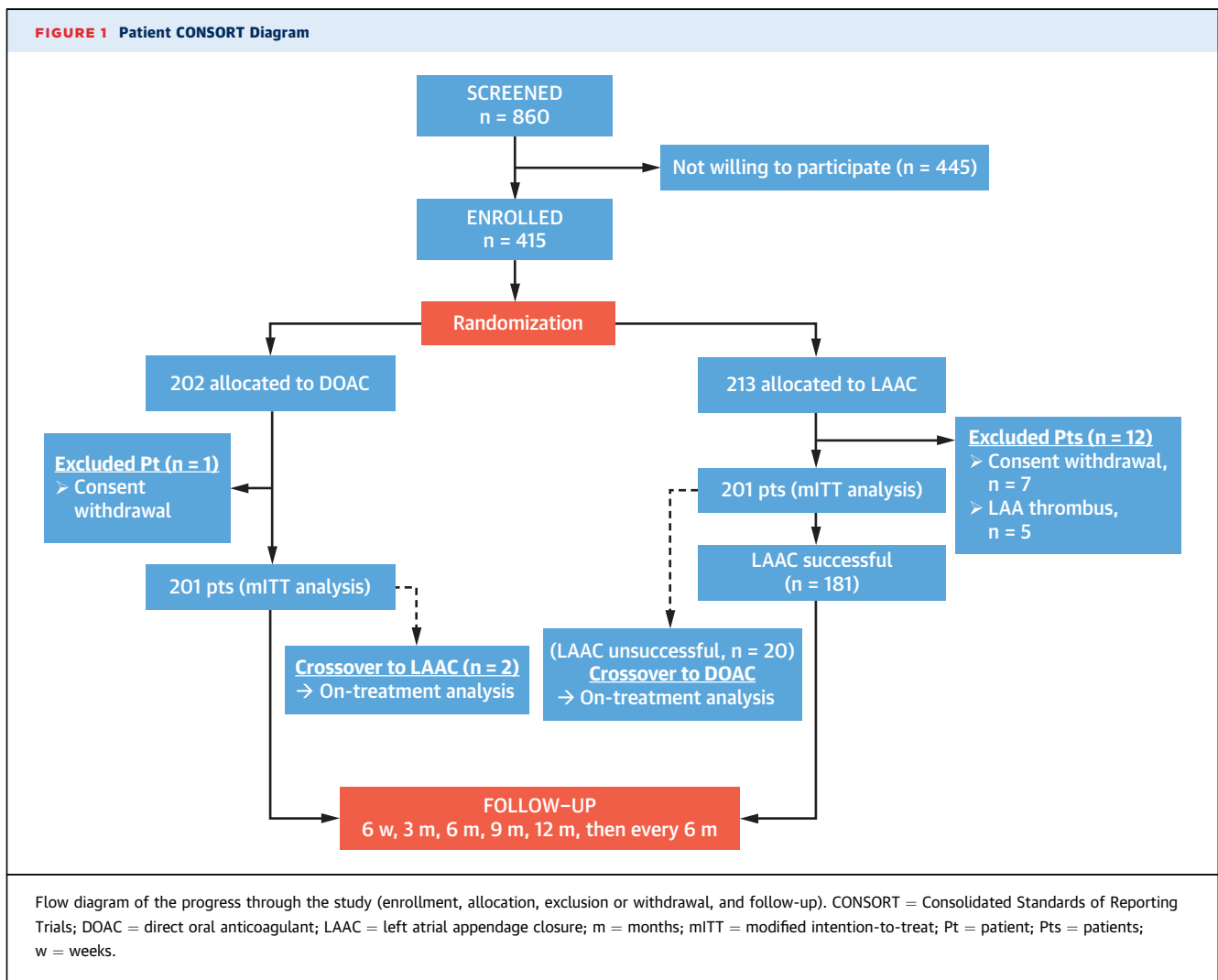
ABBREVIATIONS AND ACRONYMS

AF	= atrial fibrillation
CEC	= clinical endpoint committee
CI	= confidence interval
DAPT	= dual antiplatelet treatment
DOAC	= direct oral anticoagulant
DSMB	= Data Safety and Monitoring Board
HR	= hazard ratio
IQR	= interquartile range
LAA	= left atrial appendage
LAAC	= left atrial appendage closure
mITT	= modified intention-to-treat
NMCRB	= nonmajor clinically relevant bleeding
OAC	= oral anticoagulant
sHR	= subdistribution hazard ratio
TEE	= transesophageal echocardiography
TIA	= transient ischemic attack
VKA	= vitamin K antagonists

the Ministry of Health, Czech Republic (AZV 15-29565A). Dr. Osmancik has received occasional speaking honoraria from Bayer and Abbott. Dr. Taborsky has served on the Advisory Boards for Bayer and Pfizer. Dr. Kala has served on the Speakers Bureau and Advisory Board for Bayer; and has served on the Advisory Board and as a consultant for Boston Scientific. Dr. Poloczek has received speaking honoraria from Abbott. Dr. Haman has received speaking honoraria from Pfizer. Dr. Zemanek has received speaking honoraria from Abbott and Bayer. Dr. Widimsky has received honoraria from Bayer, Pfizer, and Boehringer Ingelheim. Dr. Reddy has received consulting income and grant support from Abbott Inc. and Boston Scientific Inc. All other authors have reported that they have no relationships relevant to the contents of this paper to disclose. Jacqueline Saw, MD, served as Guest Associate Editor for this paper. Deepak L. Bhatt, MD, MPH, served as Guest Editor-in-Chief for this paper.

The authors attest they are in compliance with human studies committees and animal welfare regulations of the authors' institutions and Food and Drug Administration guidelines, including patient consent where appropriate. For more information, visit the [JACC author instructions page](#).

Manuscript received January 30, 2020; revised manuscript received April 20, 2020, accepted April 20, 2020.



cardioembolic event within 30 days, and creatinine clearance of <30 ml/min. If randomized to LAAC, transesophageal echocardiography (TEE) was performed to exclude left atrial thrombi. Consistent with clinical necessity, the protocol mandated only TEE in the LAAC group, and not before DOAC initiation. The presence of a thrombus in the left atrial appendage (LAA) or left atrium was a pre-specified additional exclusion criterion (8).

RANDOMIZATION AND MASKING. With a centralized computer system, patients were randomly assigned to LAAC or DOAC in a 1:1 ratio, with block sizes of 18 to 22 patients (this variance prevented sites from deducing treatment assignment near the end of a block) and stratified by center to ensure comparable CHA₂DS₂-VASc scores between groups. Patient data were uploaded into a database by using a secure web interface. Treatment allocation was not blinded to

participants and local investigators; however, as best as possible, members of the clinical endpoint committee were blinded to patient allocation.

STUDY TREATMENT AND PROCEDURES. Patients randomized to the DOAC group could receive either rivaroxaban, apixaban, or dabigatran at the manufacturer-recommended dose. Investigators were instructed to reserve crossover from DOAC to LAAC for patients with bleeding while taking the prescribed DOAC and not simply based on patient preference. Medication compliance was monitored by querying patients about regular medication use during each visit.

Patients randomized to LAAC underwent implantation with a commercially available Amulet (Abbott Inc., St. Paul, Minnesota) or Watchman/Watchman-FLX (Boston Scientific Inc., St. Paul, Minnesota) device. Device selection was at the discretion of

the implanting center. Centers without previous LAAC experience were mandated to perform procedures before study initiation and to perform the first 5 study procedures with active proctoring by an experienced operator (10). Under conscious sedation or general anesthesia, after femoral venous access and transseptal puncture, the LAAC device was placed at the appendage ostium by using a combination of fluoroscopy and either TEE or intracardiac echocardiography at centers experienced with this technology.

After LAAC, the recommended antithrombotic regimen was aspirin 100 mg/day plus clopidogrel 75 mg/day for 3 months. If a TEE then showed no device-related thrombus or leak of ≥ 5 mm, clopidogrel was withdrawn; aspirin was continued indefinitely. Based on patient characteristics and device type, this post-implant antithrombotic regimen could be individualized and was ultimately left to physician discretion. In patients at high risk for bleeding, dual antiplatelet treatment (DAPT) could be shortened to 6 weeks. Conversely, in patients with a very high thrombotic risk, alternative regimens included DOAC substitution for DAPT for up to 3 months or DOACs for 6 weeks followed by DAPT for 6 weeks (10).

For both groups, outpatient follow-up occurred at 6 weeks and 3, 6, 9, and 12 months and every 6 months thereafter. The minimum follow-up for the last enrolled patient was the 6-month visit. During each visit, patients were asked about the endpoint occurrence, all other changes in clinical status, hospitalization or other health care utilization, and medication changes.

STUDY OUTCOMES. Because the risks associated with each treatment strategy are significantly different, the primary endpoint was a composite of safety and efficacy characteristics of both strategies: 1) stroke (ischemic or hemorrhagic) or TIA; 2) systemic embolism; 3) clinically significant bleeding; 4) cardiovascular death; or 5) a significant peri-procedural or device-related complications. Clinically significant bleeding was a composite of major and nonmajor clinically relevant bleeding (NMCRB), according to the International Society on Thrombosis and Hemostasis (ISTH) criteria. Major bleeding includes either a decrease in hemoglobin of ≥ 2.0 g/dl during a 24-h period, transfusion of ≥ 2 units of packed red cells, bleeding at a critical site (intracranial, intraspinal, intraocular, pericardial, intramuscular with compartment syndrome, or retroperitoneal), or fatal bleeding. NMCRB is defined as bleeding requiring hospitalization or an invasive procedure but not meeting ISTH major criteria (11). Complications included pericardial effusion requiring drainage/pericardiocentesis or

TABLE 1 Baseline Characteristics and Risk Factors of Participants

	DOAC (n = 201)	LAAC (n = 201)	Missing Values
Demographics			
Age, yrs	73.2 \pm 7.2	73.4 \pm 6.7	—
<75	122 (60.7)	116 (57.7)	—
>75	79 (39.3)	85 (42.3)	—
Male	130 (64.7)	134 (66.7)	—
Weight, kg	88.1 \pm 16.2	86.9 \pm 17.6	—
Clinical history			
AF type			
Paroxysmal	67 (33.3)	53 (26.4)	—
Persistent	46 (22.9)	47 (23.4)	—
Long-standing persistent	16 (8.0)	18 (9.0)	—
Permanent	72 (35.8)	83 (41.3)	—
CHA ₂ DS ₂ -VASc	4.7 \pm 1.5	4.7 \pm 1.5	—
CHA ₂ DS ₂ -VASc ≤ 3	50 (24.9)	48 (23.9)	—
CHA ₂ DS ₂ -VASc = 4	40 (19.9)	47 (23.4)	—
CHA ₂ DS ₂ -VASc = 5	57 (28.4)	50 (24.9)	—
CHA ₂ DS ₂ -VASc ≥ 6	54 (26.9)	56 (27.9)	—
HAS-BLED	3.0 \pm 0.9	3.1 \pm 0.9	—
Heart failure	90 (44.8)	88 (43.8)	—
Hypertension	186 (92.5)	186 (92.5)	—
Diabetes mellitus	90 (44.8)	73 (36.3)	—
History of cardioembolic event	69 (34.3)	73 (36.3)	—
Of which stroke	63 (91.3)	66 (90.4)	—
History of MI	39 (19.4)	30 (14.9)	—
Randomized at experienced centers	140 (69.7)	141 (70.1)	—
Prior antithrombotic treatment			
Warfarin	104 (51.7)	85 (42.3)	—
DOACs	55 (27.4)	66 (32.8)	—
If no OAC, new AF appearance	30 (71.4)	38 (76)	—
Aspirin	32 (15.9)	39 (19.4)	—
Clopidogrel	11 (5.5)	17 (8.5)	—
Dual antiplatelet treatment	6 (3.0)	7 (3.5)	—
Other (low-dose LMWH, none)	19 (9.5)	24 (11.9)	—
Values are mean \pm SD or n (%).			
AF = atrial fibrillation; CHA ₂ DS ₂ -VASc = congestive heart failure, hypertension, age ≥ 75 years, diabetes mellitus, prior stroke, transient ischemic attack, or thromboembolism, vascular disease, age 65-74 years, sex category (female); HAS-BLED = uncontrolled hypertension, abnormal renal or liver function, stroke, bleeding, labile international normalized ratio, elderly, drugs or alcohol; LAAC = left atrial appendage closure; LMWH = low-molecular-weight heparin; MI = myocardial infarction; DOAC = direct oral anticoagulant; OAC = oral anticoagulant.			

surgery, cardioembolism, peri-procedural bleeding requiring surgical revision or transfusion, device embolization, device-related thrombus with cardioembolism, or others as assessed by the operator and clinical endpoint committee (CEC). Secondary endpoints included the individual components of the primary endpoint. Detailed endpoint definitions are provided in the [Supplemental Appendix](#).

An independent CEC adjudicated events, and an independent data safety and monitoring board (DSMB) monitored adverse events associated with the LAAC procedure. The DSMB was immediately informed of any procedural adverse events. In addition to the sum of adverse events, the DSMB also

TABLE 2 Procedural Characteristics of the LAAC Group (N = 181)

Procedure duration, min	60 (45-85)
Fluoroscopy, min	11 (6-16)
Device type	
Amulet	111 (61.3)
Watchman	65 (35.9)
Watchman-FLX	5 (2.8)
Procedures requiring >1 device	17 (9.4)
Size of the final device	
Amulet	25.5 ± 4.1
Watchman	27.3 ± 3.8
Watchman-FLX	26.4 ± 1.3
Leak on the device by TEE or ICE imaging	7 (3.9)
Qualitative assessment of device position*	
Optimal	172 (95.0)
Suboptimal	7 (3.9)
Poor	2 (1.1)
Temporary thrombus during procedure†	2 (1.1)
Ultrasound navigation	
TEE	92 (50.8)
ICE	74 (40.9)
TEE + ICE	15 (8.3)
Sedation	
General anesthesia	55 (30.4)
Deep analgesedation	28 (15.5)
Mild analgesedation	98 (54.1)
Mild pericardial effusion (post-procedural)‡	4 (2.2)
Antithrombotic treatment at discharge	
Aspirin	149 (82.3)
Clopidogrel	149 (82.3)
DOAC	20 (11.1)
Warfarin	9 (5.0)
LMWH	9 (5.0)

Values are median (interquartile range), n (%), or mean ± SD. *Procedures continued and were successfully performed without complications. †These effusions did not require intervention. ‡This was a qualitative assessment by the operator.
ICE = intracardiac echocardiography; TEE = transesophageal echocardiography; other abbreviations as in [Table 1](#).

received aggregated outcome data from all study participants (patient recruitment, baseline characteristics, and aggregate rate of endpoints) on an annual basis and was responsible for comparing the actual to expected event rates. This was necessary to potentially stop the study if the recruitment was insufficient or if the endpoints occurred with significantly less frequency than expected. No between-group statistical comparisons were planned or performed during these interim DSMB analyses.

STATISTICAL ANALYSIS. The primary hypothesis was that LAAC would be noninferior to DOACs for the primary endpoint. The primary analysis was pre-specified to be performed on a modified intention-to-treat (mITT) basis, including all randomized patients without an LAA thrombus by TEE. Based on previous

randomized DOAC trials and randomized and observational LAAC trials, we estimated that 13% and 10% of the DOAC and LAAC cohorts, respectively, would experience the primary endpoint annually (1,3-6,12-16). We determined that a minimum of 396 study participants would provide 80% power at a 2-sided alpha level of 0.05 for a noninferiority margin of 5% (or 1.469, expressed as a hazard ratio [HR]). Estimating the noninferiority margin is complicated by the absence of any trial comparing DOACs with placebo; therefore, one must estimate the minimum treatment effect of DOACs over placebo in high-risk patients with AF. Importantly, this margin is concordant with (and, indeed, somewhat stricter than) the U.S. Food and Drug Administration guidance: for active control event rates below 20%, a 1.67 margin for the odds ratio should be used. Also, the 1.469 margin is similar to that used in the prior DOAC trials (3-5).

Because ITT outcomes can potentially bias non-inferiority trials toward the null hypothesis, post hoc secondary on-treatment and per protocol analyses were performed. The [Supplemental Appendix](#) contains details regarding patients censored in these secondary analyses.

The primary endpoint power analysis was computed for the differences in proportions of the 1-year endpoint occurrence; the Barnard-Rohmel-Kieser test was used for testing the noninferiority hypothesis. The power analysis was computed with PASS 13 software (NCSS, LLC, Kaysville, Utah). Cumulative incidence functions and Fine-Gray competing risk regression models were adopted for data visualization and description. The trial statistical plan included Kaplan-Meier curves and Cox proportional hazard models for data description (see [Supplemental Appendix](#)) and did not pre-specify any adjustment for the competing risk of mortality. However, at trial conclusion, consistent with the prevailing change in convention of statistical methodology, all primary analyses were conducted after adjusting for the competing risk for mortality. Accordingly, for the primary composite and cardiovascular mortality endpoints, calculations adjusted for noncardiovascular mortality. Similarly, other (nonmortality) endpoints were adjusted for all-cause mortality.

For other data, standard descriptive statistical methods were used: absolute and relative frequencies for categorical data and the median (interquartile range [IQR]) or mean ± standard deviation for continuous data. The influence of patient characteristics on the occurrence of endpoints was calculated using the Fine-Gray regression models with the study

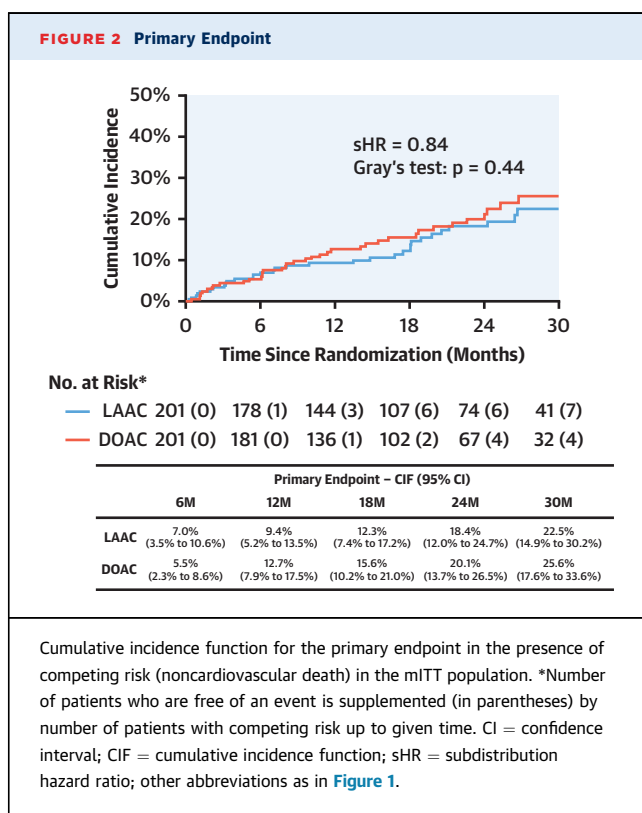
group as a covariate and is reported as sub-distribution hazard ratios (sHRs). Statistical analyses were done using SPSS, version 25.0, software (IBM Corporation, Armonk, New York).

RESULTS

PATIENTS AND FOLLOW-UP. Between October 2015 and January 2019, of 860 patients screened at 10 centers, 415 patients were enrolled in the study. Thirteen patients were excluded, 8 for informed consent withdrawal and 5 for the presence of LAA thrombus on TEE before the procedure (Figure 1). The baseline characteristics of these 13 excluded patients were not different from those of the remaining LAAC cohort (Supplemental Table 1). Regarding the 5 patients excluded for LAA thrombus, there were no strokes during follow-up; rather, there were 2 late ISTH major bleeds in patients taking VKAs (at 498 and 1,159 days post-randomization) and 1 non-cardiovascular death. Patients withdrawing informed consent refused study follow-up; ultimately, 402 patients were randomized (201 to each group). History of bleeding was present in 192 patients and history of a cardioembolic event in 142 patients; 112 patients were entered only on the basis of the CHA₂DS₂-VASc and HAS-BLED scores. The median follow-up was 21.1 months (IQR: 11.8 to 28.9 months) in the DOAC group and 19.3 months (IQR: 12.4 to 28.3 months) in the LAAC group, for an aggregate of 695.9 patient-years. One patient in the LAAC group was lost to follow-up after the 6-month visit because of migration.

The groups were well-balanced for clinical characteristics (Table 1 and Supplemental Table 2). The mean age was 73.3 years, and 34.3% were women. The cohort was high risk, with a mean CHA₂DS₂-VASc of 4.7 ± 1.5 and >25% with a CHA₂DS₂-VASc of >6, prior cardioembolism in 35.3%, and prior bleeding in 47.8%. Most patients had previously received anticoagulants, either VKAs (47.0%) or DOACs (30.1%). In most of the remaining patients (74%), AF was recently diagnosed.

TREATMENT CHARACTERISTICS. Of patients randomized to LAAC, 7.0% (14 of 201) did not undergo the procedure because of either patient refusal (n = 9) or anatomic considerations: overly large LAA in 3 patients, pre-existing pericardial effusion in 1 patient, and suspicion for infective endocarditis on TEE in 1 patient. All 14 patients agreed to continued follow-up, and 12 crossed over to the DOAC group (Figure 1). Ultimately, 187 patients underwent LAAC, and the LAA was successfully occluded in 96.8% (181 of 187) of procedure attempts, or in 90% (181 of 201) of patients assigned to LAAC. The implanted devices



were either Amulet, Watchman, or Watchman-FLX in 61.3%, 35.9%, or 2.8%, respectively. Four of the 10 enrolling centers were de novo centers (Supplemental Table 3). Most patients (148; 81.8%) received DAPT upon discharge (8 for 6 weeks only), 25 (13.8%) patients received apixaban for 3 months followed by aspirin, and 8 (4.4%) patients received apixaban for 6 weeks followed by DAPT for 6 weeks. Procedure details are shown in Table 2.

TEE imaging was performed at 3 months in 178 LAAC patients. Device-related thrombi were observed in 6 (3.4%) patients, 5 of which resolved with 4 weeks of low-molecular-weight heparin treatment, whereas the last patient underwent surgical extraction. Regarding peri-device leak into the LAA past the device, a >5-mm leak was seen in 4 (2.2%) patients, 1- to 5-mm leaks in 20 (11.2%), and no leak in 154 (86.5%).

In the DOAC group, the most frequently used anticoagulant was apixaban, in 192 patients (95.5%): 5 mg and 2.5 mg twice daily in 159 (79.1%) and 33 (16.4%) patients, respectively. Among patients with reduced dose, the criteria for dose reduction recommended by the manufacturer were not met in 16 (48.5%) of them. These patients had similar CHA₂DS₂-VASc scores as the remaining patients (4.68 ± 1.19 vs. 4.70 ± 1.5) but had higher HAS-BLED scores (3.4 ± 0.8

TABLE 3 Incidence of Composite Primary Endpoint and its Components in the Presence of Competing Risk (Noncardiovascular Death for Primary Endpoint and Cardiovascular Death, All-Cause Death for Other Endpoints) in the Intention-to-Treat Populations

	DOAC (n = 201)			LAAC (n = 201)			Subdistribution Hazard Ratio (95% CI)	p Value	p Value for Noninferiority
	No. of Patients With Event	No. Events	Event Rate/Yr	No. of Patients With Event	No. Events	Event Rate/Yr			
Primary endpoint	41	47	13.42	35	38	10.99	0.84 (0.53-1.31)	0.44	0.004
Cardiovascular death	15	15	4.28	11	11	3.18	0.75 (0.34-1.62)		
All stroke/TIA	9	9	2.57	9	9	2.60	1.00 (0.40-2.51)		
Ischemic stroke/TIA	8	8	2.28	9	9	2.60	1.13 (0.44-2.93)		
Systemic embolism	1	1	0.29	0	0	0.00	—		
Procedure/device related complications	—	—	—	9	9	2.60	—		
ISTH major/nonmajor bleeding	22	26	7.42	18	19	5.50	0.81 (0.44-1.52)		
ISTH major/nonmajor bleeding not related to device	22	26	7.42	12	13	3.76	0.53 (0.26-1.06)		

CI = confidence interval; ISTH = International Society on Thrombosis and Hemostasis; TIA = transient ischemic attack; other abbreviations as in Table 1.

vs. 2.95 ± 0.89). No cardioembolic events and 1 major bleeding event occurred during follow-up in these patients. Dabigatran was used in 8 patients: 150 mg and 110 mg twice daily in 7 (3.5%) and 1 (0.5%) patients, respectively. Rivaroxaban 20 mg daily was used in 1 (0.5%) patient.

PRIMARY ENDPOINT. By mITT, the primary outcome occurred in 35 patients with LAAC (10.99% per 100 patient-years) compared to 41 patients with DOACs (13.42% per 100 patient-years; sHR: 0.84; 95% confidence interval [CI]: 0.53 to 1.31; $p = 0.44$) (Figure 2, Table 3). The upper bound of the 95% CI in the LAAC group was 16.1%, which was substantially less than the event rate in the DOAC group plus noninferiority margin (18.42%); therefore, the study met the criteria for noninferiority of LAAC relative to DOACs ($p = 0.004$ for noninferiority) (Central Illustration). The Kaplan-Meier estimate yielded similar outcomes (Supplemental Figure 1). This result was consistent across all subgroups with no statistically significant interactions (Figure 3). Similarly, no significant between-center differences were found: the overall sHR for all centers was within the CI of the individual sHRs (Supplemental Figure 2).

SECONDARY ENDPOINTS IN THE INTENTION-TO-TREAT ANALYSIS. The annual rate of all stroke/TIA was 2.60% with LAAC compared to 2.57% with DOACs (sHR: 1.00; 95% CI: 0.40 to 2.51) (Figure 4A, Table 3). There were 8 and 7 strokes and 1 and 2 TIAs in the LAAC and DOAC groups, respectively. Mean stroke severity as assessed by modified Rankin score at discharge was 2.38 ± 1.5 in the LAAC group and 2.29 ± 0.76 in the DOAC group. There was 1 intracranial hemorrhage with DOACs and none with LAAC; all other strokes were ischemic in origin, as confirmed by computed tomography. No intraprocedural stroke or TIA occurred during LAAC.

The annual rate of cardiovascular mortality was 3.18% with LAAC compared to 4.28% with DOACs (sHR: 0.75; 95% CI: 0.34 to 1.62) (Figure 4B, Table 3). Two deaths in the LAAC group were classified as being procedure or device related. The rates of noncardiovascular and all-cause mortality were also similar between groups (sHR: 1.16; 95% CI: 0.42 to 3.18; and HR: 0.88; 95% CI: 0.48 to 1.63, respectively) (Supplemental Figures 3 and 4).

The bleeding rate was similar between the LAAC and DOAC groups (Figure 4C, Table 3). The annual rate of ISTH major/NMCRB was 5.50% with LAAC compared with 7.42% with DOAC (sHR: 0.81; 95% CI: 0.44 to 1.52). The distribution between ISTH major and NMCRB was 13 and 6 with LAAC and 14 and 12 with DOACs, respectively. Six (31.6%) of the LAAC bleeding events were procedure/device related. After excluding these procedural/device bleeding events, the annual rate of ISTH major/NMCRB was 3.76% with LAAC (sHR: 0.53; 95% CI: 0.26 to 1.06) (Figure 4D, Table 3).

PER PROTOCOL ANALYSIS. In the post hoc per protocol analysis, 181 and 199 patients were included in the LAAC and DOAC groups, respectively. (Details of patient assignment and censoring are noted in the Supplemental Appendix.) LAAC was noninferior to DOAC for the primary endpoint outcome (sHR: 0.82; 95% CI: 0.52 to 1.30; $p = 0.40$; $p = 0.003$ for noninferiority) (Figure 5A). There were also no significant differences between groups for the embolic events: all stroke/TIA (2.20% with LAAC vs. 2.68% with DOACs; sHR: 0.81; 95% CI: 0.30 to 2.15) and ischemic stroke/TIA (2.20% with LAAC vs. 2.38% with DOACs; sHR: 0.91; 95% CI: 0.33 to 2.48). Similar rates were also seen for ISTH major/NMCRB (sHR: 0.89; 95% CI: 0.48 to 1.65) and cardiovascular death (sHR: 0.74; 95% CI: 0.33 to 1.67) (Supplemental Figure 5).

ON-TREATMENT ANALYSIS. The post hoc on-treatment analysis ultimately included 184 and 216 patients in the LAAC and DOAC groups, respectively. (Details of patient assignment and censoring are noted in the [Supplemental Appendix](#).) LAAC was again noninferior to DOAC for the primary endpoint outcome ($p = 0.013$), and again, there were no significant differences between groups for either the primary endpoint (sHR: 0.79; 95% CI: 0.49 to 1.25; $p = 0.31$) ([Figure 5B](#)) or its individual components: all stroke/TIA (sHR: 0.70; 95% CI: 0.28 to 1.78), ISTH major/NMCRB (sHR: 0.91; 95% CI: 0.48 to 1.72), and cardiovascular death (sHR: 0.68; 95% CI: 0.30 to 1.54) ([Supplemental Figure 6](#)).

LAAC DEVICE OR PROCEDURE-RELATED COMPLICATIONS. As shown in [Table 4](#) and [Supplemental Table 4](#), significant complications occurred in 9 patients (4.5%, or 4.8% of procedural attempts), including 4 (2.1%) within 7 days of the procedure and 5 (2.7%) occurring 104 ± 57 days post-procedure. (Characteristics of patients with complications are shown in [Supplemental Table 4](#).) Among these was a procedure-related death in a patient with a groin bleed requiring vascular surgery complicated by a large myocardial infarction that culminated in death; an autopsy revealed previously unrecognized severe 3-vessel coronary artery disease. Also, a device-related death occurred approximately 6 weeks post-procedures as a result of a late pericardial tamponade (details in the [Supplemental Appendix](#)).

DISCUSSION

To our knowledge, among patients with nonvalvular AF at high risk for stroke, PRAGUE-17 is the first randomized trial comparing percutaneous LAAC with DOACs, primarily apixaban, for the prevention of all-cause stroke, systemic embolism, cardiovascular death, clinically significant bleeding, or procedure-/device-related complications. LAAC was noninferior to DOACs for this composite endpoint, in both the pre-specified mITT primary analysis and the post hoc on-treatment and per protocol analyses ([Central Illustration](#)). Furthermore, there were no significant differences in any particular component of the primary endpoint.

Evidence for LAAC first came from 2 trials, PROTECT-AF (Watchman Left Atrial Appendage System for Embolic Protection in Patients With Atrial Fibrillation) and PREVAIL (Prospective Randomized Evaluation of the Watchman Left Atrial Appendage Closure Device in Patients With Atrial Fibrillation Versus Long-Term Warfarin Therapy), in which VKA-eligible patients were randomized to either the

TABLE 4 LAAC Device- or Procedure-Related Complications

	Early (≤7 Days) Occurrence	Late (>7 Days) Occurrence	Total
Pericardial effusion	0	2*	2
Device embolization	1†	0	1
Device-related death	0	1‡	1
Procedure-related death	1‡	0	1
Vascular complications	2§	0	2
Other complications	0	2	2
Total	4	5	9

*Late pericardial effusions occurred at 89 and 194 days after implantation with the Amulet device. One was treated with pericardiocentesis and the other conservatively; both patients had good outcomes. †Acute device embolization during the procedure, requiring surgical removal. ‡See details in the [Supplemental Appendix](#). §Includes 1 femoral pseudoaneurysm and 1 large groin hematoma, both treated with vascular surgery. ||One device malposition at the left inferior pulmonary vein, with successful removal and reimplantation. One large device-related thrombus was diagnosed by TEE imaging 113 days after implantation. The thrombus was considered potentially malignant (although no embolic event had occurred), so surgical removal was successfully performed.

LAAC = left atrial appendage closure.

Watchman device or VKAs (1,13). LAAC proved noninferior to VKAs for the composite primary endpoint of all-cause stroke, systemic embolism, or cardiovascular death. An approximately 80% reduction in intracranial hemorrhage significantly contributed to the positive effect of LAAC, including an approximately 50% cardiovascular mortality benefit. However, as with all procedures, LAAC is susceptible to complications. Furthermore, there was a contemporaneous introduction into clinical practice of new non-VKA anticoagulants with more favorable risk-benefit profiles. DOACs also resulted in an approximately 50% reduction in hemorrhagic stroke and an approximately 10% mortality benefit (7). Because decreased intracranial hemorrhage with LAAC contributed significantly to the positive outcomes in PROTECT-AF and PREVAIL, and because DOACs are also associated with a reduced rate of intracranial hemorrhage, a randomized study comparing these 2 treatment options was warranted.

In contrast to OAC-versus-OAC comparisons, the risks and benefits of the treatment strategies in PRAGUE-17 differ significantly. Long-term OAC use increases hemorrhagic risk, whereas LAAC is associated with procedural complications. Therefore, a composite clinical endpoint was selected to encapsulate both efficacy, such as stroke and critical outcomes like mortality, and the completely disparate risks plausibly associated with each treatment modality.

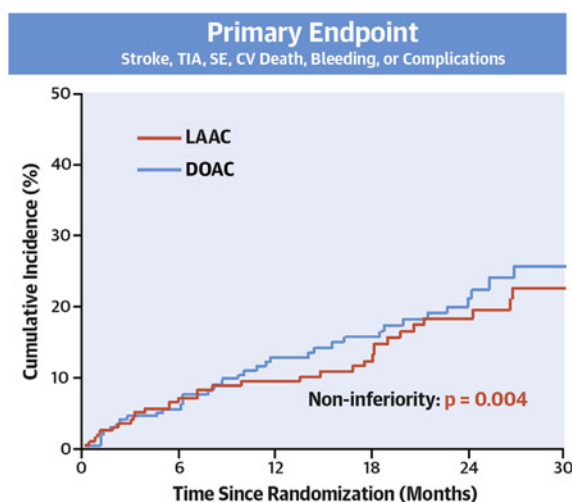
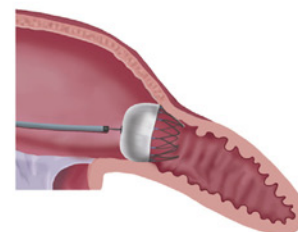
STROKE AND TIA. In our high-risk cohort, the annual incidence of both all-stroke/TIA and ischemic stroke/TIA was similar between groups whether analyzed by mITT (sHRs: 1.00 and 1.13, respectively), per protocol

CENTRAL ILLUSTRATION The PRAGUE-17 Trial

PRAGUE-17 Randomized Clinical Trial



- 402 High-Risk AF Pts → Randomized
CHA₂DS₂-VASc = 4.7 ± 1.5
HAS-BLED = 3.1 ± 0.9
- Follow-up: 20.8 ± 10.8 mo (695 pt-year)



	sHR (95% CI)	p value
Primary Endpoint		
mITT	0.84 (0.53-1.31)	0.44
Per Protocol	0.82 (0.52-1.30)	0.40
On-Treatment	0.79 (0.49-1.25)	0.31
All-Stroke/TIA	1.00 (0.40-2.51)	0.99
CV Death	0.75 (0.34-1.62)	0.46
Major + NMCR Bleeding		
All	0.81 (0.44-1.52)	0.51
Nonprocedural	0.53 (0.26-1.06)	0.07

Osmancik, P. et al. J Am Coll Cardiol. 2020;75(25):3122-35.

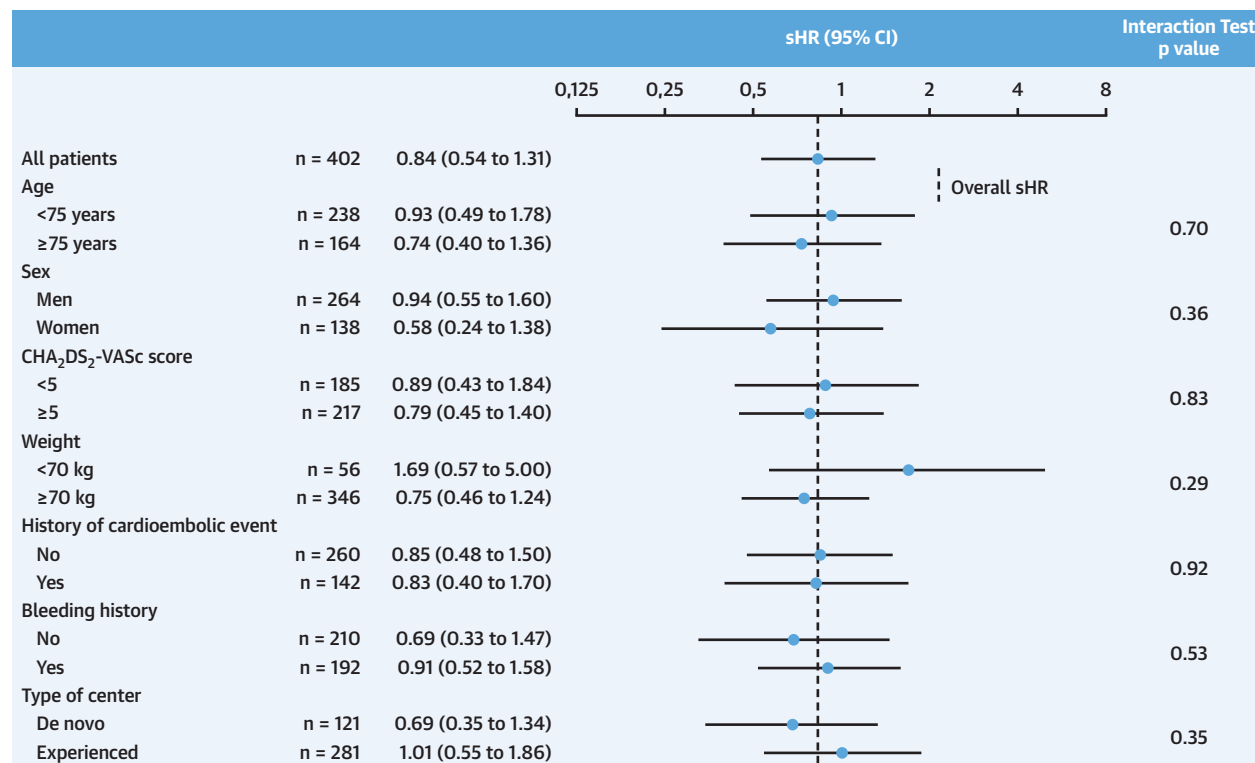
Shown are the patient characteristics, cumulative incidence function for the primary endpoint in the modified intention-to-treat population, and the subdistribution hazard ratios of the various secondary endpoints. AF = atrial fibrillation; CHA₂DS₂-VASc = congestive heart failure, hypertension, age ≥75 years, diabetes mellitus, prior stroke, transient ischemic attack, or thromboembolism, vascular disease, age 65-74 years, sex category (female); CI = confidence interval; CV = cardiovascular; DOAC = direct oral anticoagulant; HAS-BLED = hypertension, abnormal renal or liver function, stroke, bleeding, labile international normalized ratio, elderly, drugs or alcohol; LAAC = left atrial appendage closure; mITT = modified intention-to-treat; NMCR = nonmajor and major clinically relevant; PRAGUE-17 = Left Atrial Appendage Closure vs. Novel Anticoagulation Agents in Atrial Fibrillation; Pt = patient; SE = systemic embolism; sHR = subdistribution hazard ratio; TIA = transient ischemic attack.

(sHRs: 0.81 and 0.91, respectively), or on treatment (sHRs: 0.70 and 0.77, respectively) and was substantially lower if compared to the expected rate of ischemic stroke according to the CHA₂DS₂-VASc score (7.57% per year). The corresponding annualized ischemic stroke/TIA/systemic embolism rates were recently reported from 2 large observational LAAC registries with similarly high-risk AF cohorts: 2.3% in the Amplatzer Cardiac Plug registry of 1,047 patients (CHA₂DS₂-VASc: 4.5 ± 1.6; stroke/TIA history in 39%) and 2.0% in the Watchman EWOLUTION (Evaluate Real-World Clinical Outcomes in Patients With AF and High Stroke Risk-Treated With the WATCHMAN

Left Atrial Appendage Closure Technology) registry of 1,020 patients (CHA₂DS₂-VASc: 4.5 ± 1.6; stroke/TIA history in 30.5%) (14,15). Although our study was not powered to compare the rates of cardioembolic events alone, together, all these data bolster support for the role of the LAA in stroke pathogenesis and reinforce the hypothesis that site-specific therapy with LAAC can serve as an OAC alternative.

Aspirin, the background long-term antithrombotic therapy after LAAC, reduces the risk of stroke by about a fifth compared with placebo. In an analysis of the secondary prevention patients of the AVERROES (Apixaban in Patients With Atrial Fibrillation) trial

FIGURE 3 Subgroup Analysis

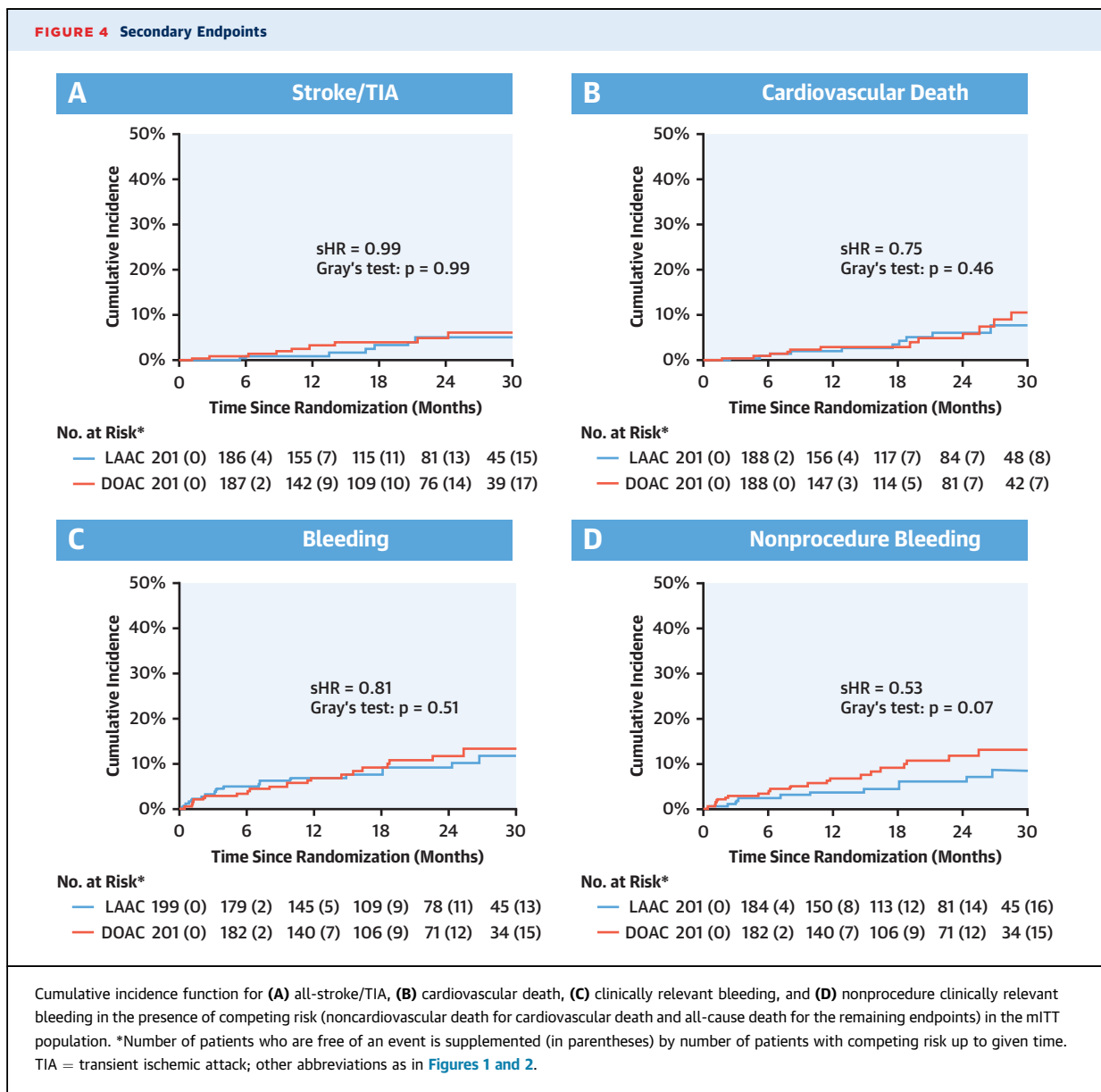


Incidence of the primary endpoint in the MITT population by subgroups in the presence of competing risk (noncardiovascular death). CHA₂DS₂-VASc = congestive heart failure, hypertension, age ≥75 years, diabetes mellitus, prior stroke, transient ischemic attack, or thromboembolism, vascular disease, age 65-74 years, sex category (female); other abbreviations as in [Figures 1 and 2](#).

(i.e., patients with a history of stroke/TIA), the annualized incidence of stroke or systemic embolism was 9.16% with aspirin versus 2.39% with apixaban (17). Furthermore, the annualized ischemic stroke rates in the aspirin arm of AVERROES were 3.49% and 8.75% in the CHA₂DS₂-VASc 3 to 5 and 6 to 8 cohorts, respectively; the corresponding apixaban rates were 1.29% and 4.19% (HRs: 0.37 and 0.47) (18). Thus, the similar incidence of stroke in the 2 arms of PRAGUE-17 cannot be explained by any beneficial effect of aspirin in the LAAC group. Again, however, as highlighted by the wide 95% confidence bounds of the sHR point estimate (95% CI: 0.40 to 2.51), the limited number of patients in PRAGUE-17 precludes definitive conclusions about this endpoint. However, approximately 7,000 patients would be required for a noninferiority study of LAAC versus DOAC with a composite primary endpoint including only all stroke, TIA, or systemic embolism (details in the [Supplemental Appendix](#)).

BLEEDING. Despite their significant reduction in hemorrhagic stroke, DOACs are associated with an

increase of other bleeding, such as gastrointestinal bleeding (7). In our trial, ISTH major/NMCRB occurred in 7.42% of patients annually in the DOAC arm. In ROCKET-AF (Rivaroxaban Once Daily Oral Direct Factor Xa Inhibition Compared with Vitamin K Antagonism for Prevention of Stroke and Embolism Trial in Atrial Fibrillation), ISTH major/NMCRB with rivaroxaban was 14.9% annually (3). However, the most commonly used DOAC in our study was apixaban, which in ARISTOTLE (Apixaban for Reduction in Stroke and Other Thromboembolic Events in Atrial Fibrillation) and AVERROES exhibited ISTH major/NMCRB rates of 4.07% and 4.5%, respectively (5,12). The ARISTOTLE and AVERROES populations were at lower risk (CHADS₂ [congestive heart failure, hypertension, age ≥75 years, diabetes mellitus, prior stroke or transient ischemic attack]: 2.1 and 2.0, respectively), however, and had an infrequent bleeding history (16.7% and 3%, respectively). In comparison, the PRAGUE-17 DOAC patients were higher risk (CHA₂DS₂-VASc: 4.7 ± 1.5; 47.3% bleeding history)—likely the explanation for the disparate bleeding rates.

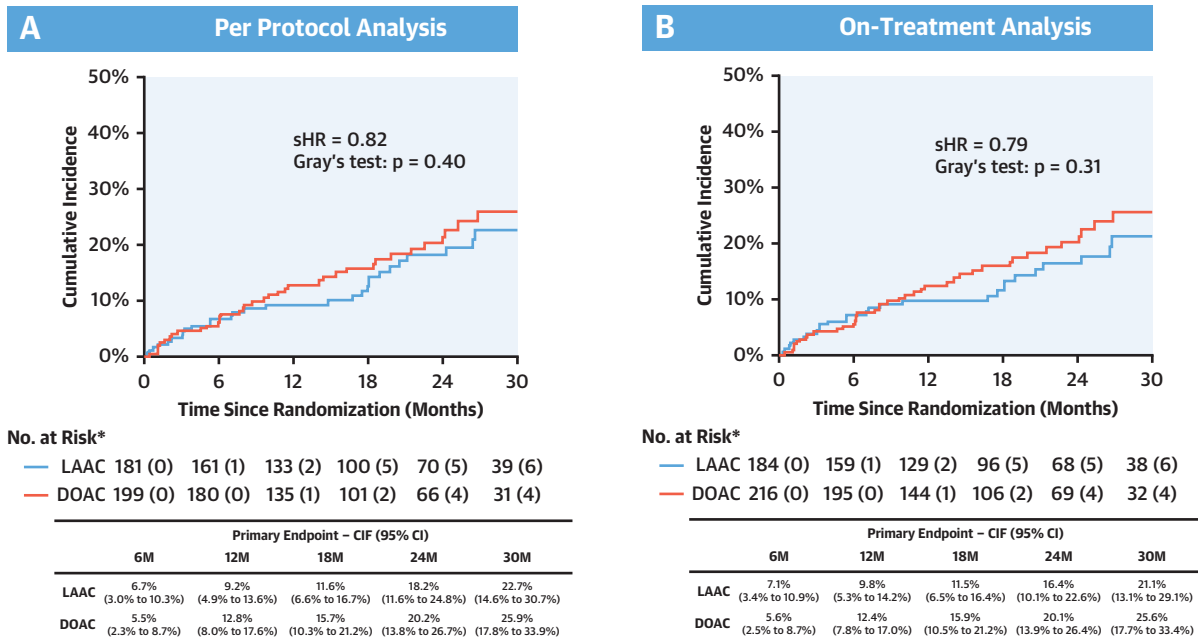
FIGURE 4 Secondary Endpoints

Similarly, in the LAAC arm of our study, ISTH major/NMCRB occurred in 5.50% annually, which was higher than observed with aspirin in AVERROES (3.9%). In the analysis of AVERROES by CHA₂DS₂-VASc, major bleeding occurred in 1.34% of patients per year in the CHA₂DS₂-VASc 3 to 5 population taking aspirin but in only 0.53% patients per year with a CHA₂DS₂-VASc of 2 in the aspirin arm (18). These data further support the explanation of higher bleeding rates in our study compared to AVERROES being due to the higher risk profile of our cohort.

There were similar rates of ISTH major/NMCRB between groups (SHR: 0.81). This ostensibly unexpected outcome is explained, first, by the fact that 6

of 9 complications were bleeds. Indeed, if one excludes these device/procedure bleeding events, thereby comparing spontaneous ISTH major/NMCRB events between aspirin (the background antithrombotic after LAAC) with DOACs (mainly apixaban), LAAC had numerically fewer bleeds (SHR: 0.53; p = 0.07). This is consistent with the on-treatment analysis of AVERROES: major bleeding was more frequent with apixaban than aspirin (HR: 1.54; 95% CI: 0.96 to 2.45; p = 0.07) (12). Statistical significance was not reached because of insufficient statistical power for this particular endpoint in both studies. Indeed, longer follow-up may demonstrate differences of bleeding. Moreover, use of a truncated

FIGURE 5 Secondary Analyses



Cumulative incidence functions for the primary endpoint in the presence of competing risk (noncardiovascular death) in the (A) per protocol and (B) on-treatment populations. *Number of patients who are free of an event is supplemented (in parentheses) by number of patients with competing risk up to given time. Abbreviations as in Figures 1 and 2.

post-LAAC antithrombotic regimen that minimizes bleeding while still preventing device-related thrombosis may further enhance LAAC outcomes.

These data also highlight the relatively low rate of bleeding with apixaban, with the absolute reduction relative to VKAs being in the highest-risk cohorts. In ARISTOTLE, annualized major bleeding was reduced from 3.55% to 2.60% in patients with CHA₂DS₂-VASc of ≥3 and from 4.7% to 3.46% in patients with HAS-BLED ≥3 (19). Thirty-three (16.4%) DOAC patients received low-dose apixaban, appropriately in 16 (48.5%). Dose reduction is relatively common in clinical practice, especially with apixaban (20). In a population-based study of >10,000 patients with AF, 21.6% received inappropriate apixaban underdosing. Compared to appropriately dosed patients, underdosed patients had higher HAS-BLED scores (2.0 vs. 1.6), suggesting that underdosing may be related to the clinical fear of bleeding.

COMPLICATIONS. Various randomized and observational LAAC studies have documented a steady decline in complication rates. Complications occurred in 8.7% in PROTECT-AF, including a 4.3% rate of pericardial tamponade, but then decreased in the

Amplatzer Cardiac Plug and EWOLUTION registries to overall complication and tamponade rates of 4.97% and 2.7%, and 1.2% and 0.3%, respectively (1,14,15,21). In PRAGUE-17, the short-term (up to 7 days or discharge) complication rate was 2.1%, consistent with this improving trend. However, the 2.7% late complication rate, including 3 late pericardial effusions, with 1 resulting in death, is suboptimal. Given the overall similar rate of primary events in the arms of the study, the safety of the LAAC is paramount and requires further improvement.

On the other hand, a strength of PRAGUE-17 was its real-world implications: 4 of the 10 implanting centers were truly de novo, initiating their LAAC experience in this trial itself. For the remaining 6 centers, in the year preceding trial commencement, only 18.7 ± 11.8 LAAC procedures had been performed per center (range 8 to 40) (Supplemental Table 3).

STUDY LIMITATIONS. PRAGUE-17 is underpowered to evaluate the relative differences in the individual components of the primary endpoint. Regarding the primary endpoint, stroke reduction may be more important than bleeding reduction. The composite endpoint was chosen to cover the risks and benefits of

2 very different treatment modalities. On the other hand, this trial enrolled one of the highest-risk AF populations ever studied in an AF stroke prevention trial. The consequent high event rate allowed sufficient power to assess the primary endpoint. Although the mean follow-up is substantial (20.8 ± 10.8 months), additional follow-up is needed to determine the relative long-term differences between groups. In the DOAC group, no medication logs were kept; however, the observed ischemic stroke rate suggests reasonable DOAC compliance.

The results may not apply to all with AF who are indicated for a DOAC (e.g., those at low bleeding risk). Five LAAC patients with LAA thrombi on pre-procedural TEE were excluded. However, a post hoc pure intention-to-treat analysis including these patients yielded similar results (sHR: 0.85; 95% CI: 0.55 to 1.32; $p = 0.48$; $p = 0.003$ for noninferiority) (Supplemental Figure 7). Furthermore, imputation of these 5 patients has minimal effect on the per protocol and on-treatment analyses, because these patients received VKA. The crossover of 14 LAAC patients to DOACs would bias toward the null hypothesis; however, the per-protocol and on-treatment analyses yielded similar results.

CONCLUSIONS

Among patients with nonvalvular AF at high risk for stroke and increased risk of bleeding, mechanical LAAC was noninferior to DOACs for the composite of cardioembolic events, cardiovascular death, clinically significant bleeding, or procedure-/device-related complications. However, safety issues remain with LAAC, warranting further refinements in both operator technique and device technology.

ACKNOWLEDGMENTS The authors are grateful to the members of the DSMB and CEC, as well as the whole team of information technology specialists and statisticians responsible for the development of the randomization software and e-database and all statistical analyses.

ADDRESS FOR CORRESPONDENCE: Dr. Pavel Osmancik, Cardiocenter, Charles University Prague, Third Internal-Cardiology Clinic, Srobarova 50, 10034 Prague, Czech Republic. E-mail: pavel.osmancik@gmail.com. Twitter: @POsmancik. OR Dr. Vivek Y. Reddy, Helmsley Electrophysiology Center, Icahn School of Medicine at Mount Sinai, One Gustave L. Levy Place, Box 1030, New York, New York 10029. E-mail: vivek.reddy@mountsinai.org.

PERSPECTIVES

COMPETENCY IN PATIENT CARE AND

PROCEDURAL SKILLS: Among selected patients with AF at risk for stroke and bleeding, LAAC provides protection against stroke, systemic embolism, and bleeding comparable to DOACs.

TRANSLATIONAL OUTLOOK: Although enhancements in LAAC technology improve the safety of the device-based strategy, longer-term follow-up of larger numbers of patients will be needed to establish relative risks and benefits and inform selection of these alternative treatments.

REFERENCES

- Holmes DR, Reddy VY, Turi ZG, et al. Percutaneous closure of the left atrial appendage versus warfarin therapy for prevention of stroke in patients with atrial fibrillation: a randomised non-inferiority trial. *Lancet* 2009;374:534-42.
- Holmes DR Jr., Doshi SK, Kar S, et al. Left atrial appendage closure as an alternative to warfarin for stroke prevention in atrial fibrillation: a patient-level meta-analysis. *J Am Coll Cardiol* 2015;65:2614-23.
- Patel MR, Mahaffey KW, Garg J, et al. Rivaroxaban versus warfarin in nonvalvular atrial fibrillation. *N Engl J Med* 2011;365:883-91.
- Connolly SJ, Ezekowitz MD, Yusuf S, et al. Dabigatran versus warfarin in patients with atrial fibrillation. *N Engl J Med* 2009;361:1139-51.
- Granger CB, Alexander JH, McMurray JJ, et al. Apixaban versus warfarin in patients with atrial fibrillation. *N Engl J Med* 2011;365:981-92.
- Giugliano RP, Ruff CT, Braunwald E, et al. Edoxaban versus warfarin in patients with atrial fibrillation. *N Engl J Med* 2013;369:2093-104.
- Ruff CT, Giugliano RP, Braunwald E, et al. Comparison of the efficacy and safety of new oral anticoagulants with warfarin in patients with atrial fibrillation: a meta-analysis of randomised trials. *Lancet* 2014;383:955-62.
- Osmancik P, Tousek P, Herman D, et al. Interventional left atrial appendage closure vs novel anticoagulation agents in patients with atrial fibrillation indicated for long-term anticoagulation (PRAGUE-17 study). *Am Heart J* 2017;183:108-14.
- Pisters R, Lane DA, Nieuwlaat R, et al. A novel user-friendly score (HAS-BLED) to assess 1-year risk of major bleeding in patients with atrial fibrillation: the Euro Heart Survey. *Chest* 2010;138:1093-100.
- Enomoto Y, Gadiyaram VK, Gianni C, et al. Use of non-warfarin oral anticoagulants instead of warfarin during left atrial appendage closure with the Watchman device. *Heart Rhythm* 2017;14:19-24.
- Schulman S, Kearon C. Subcommittee on Control of Anticoagulation of the Scientific and Standardization Committee of the International Society on Thrombosis and Haemostasis. Definition of major bleeding in clinical investigations of anti-hemostatic medicinal products in non-surgical patients. *J Thromb Haemost* 2005;3:692-4.

- 12.** Connolly SJ, Eikelboom J, Joyner C, *et al.* Apixaban in patients with atrial fibrillation. *N Engl J Med* 2011;364:806-17.
- 13.** Holmes DR Jr., Kar S, Price MJ, *et al.* Prospective randomized evaluation of the Watchman Left Atrial Appendage Closure device in patients with atrial fibrillation versus long-term warfarin therapy: the PREVAIL trial. *J Am Coll Cardiol* 2014;64:1-12.
- 14.** Boersma LV, Ince H, Kische S, *et al.* Evaluating real-world clinical outcomes in atrial fibrillation patients receiving the WATCHMAN left atrial appendage closure technology. *Circ Arrhythm Electrophysiol* 2019;12:e006841.
- 15.** Tzikas A, Shakir S, Gafoor S, *et al.* Left atrial appendage occlusion for stroke prevention in atrial fibrillation: multicentre experience with the AMPLATZER cardiac plug. *EuroIntervention* 2016;11:1170-9.
- 16.** Reddy VY, Mobius-Winkler S, Miller MA, *et al.* Left atrial appendage closure with the Watchman device in patients with a contraindication for oral

- anticoagulation: the ASAP study (ASA Plavix Feasibility Study With Watchman Left Atrial Appendage Closure Technology). *J Am Coll Cardiol* 2013;61:2551-6.
- 17.** Diener HC, Eikelboom J, Connolly SJ, *et al.* Apixaban versus aspirin in patients with atrial fibrillation and previous stroke or transient ischaemic attack: a predefined subgroup analysis from AVERROES, a randomised trial. *Lancet Neurol* 2012;11:225-31.
- 18.** Lip GY, Connolly S, Yusuf S, *et al.* Modification of outcomes with aspirin or apixaban in relation to CHADS(2) and CHA(2)DS(2)-VASc scores in patients with atrial fibrillation: a secondary analysis of the AVERROES study. *Circ Arrhythm Electrophysiol* 2013;6:31-8.
- 19.** Lopes RD, Al-Khatib SM, Wallentin L, *et al.* Efficacy and safety of apixaban compared with warfarin according to patient risk of stroke and of bleeding in atrial fibrillation: a secondary analysis of a randomised controlled trial. *Lancet* 2012;380:1749-58.

- 20.** Rodríguez LAG, Martín-Pérez M, Vora P, *et al.* Appropriateness of initial dose of non-vitamin K antagonist oral anticoagulants in patients with non-valvular atrial fibrillation in the UK. *BMJ Open* 2019;9:e031341.

- 21.** Boersma LV, Schmidt B, Betts TR, *et al.* Implant success and safety of left atrial appendage closure with the WATCHMAN device: peri-procedural outcomes from the EWOLUTION registry. *Eur Heart J* 2016;37:2465-74.

KEY WORDS atrial fibrillation, cardioembolic event, direct oral anticoagulant, left atrial appendage, stroke

APPENDIX For a list of investigators, expanded Methods and Results sections as well as supplemental tables and figures, please see the online version of this paper.

V. Melenovský a kol.

Dysregulation of epicardial adipose tissue in cachexia due to heart failure: the role of natriuretic peptides and cardiolipin

Journal of Cachexia, Sarcopenia and Muscle
Impact Factor: 9,802

Dysregulation of epicardial adipose tissue in cachexia due to heart failure: the role of natriuretic peptides and cardiolipin

Petra Janovska² , Vojtech Melenovsky^{1*} , Michaela Svobodova², Tereza Havlenova¹ , Helena Kratochvilova¹ , Martin Haluzik¹ , Eva Hoskova¹ , Terezie Pelikanova¹ , Josef Kautzner¹ , Luca Monzo¹ , Ivana Jurcova¹ , Katerina Adamcova² , Lucie Lenkova², Jana Buresova² , Martin Rossmeisl² , Ondrej Kuda² , Tomas Cajka²  & Jan Kopecky^{2*} 

¹Department of Cardiology, Institute for Clinical and Experimental Medicine - IKEM, Prague, Czech Republic, ²Institute of Physiology of the Czech Academy of Sciences Prague 4, Czech Republic

Abstract

Background Cachexia worsens long-term prognosis of patients with heart failure (HF). Effective treatment of cachexia is missing. We seek to characterize mechanisms of cachexia in adipose tissue, which could serve as novel targets for the treatment.

Methods The study was conducted in advanced HF patients ($n = 52$; 83% male patients) undergoing heart transplantation. Patients with $\geq 7.5\%$ non-intentional body weight (BW) loss during the last 6 months were rated cachectic. Clinical characteristics and circulating markers were compared between cachectic ($n = 17$) and the remaining, BW-stable patients. In epicardial adipose tissue (EAT), expression of selected genes was evaluated, and a combined metabolomic/lipidomic analysis was performed to assess (i) the role of adipose tissue metabolism in the development of cachexia and (ii) potential impact of cachexia-associated changes on EAT-myocardium environment.

Results Cachectic vs. BW-stable patients had higher plasma levels of natriuretic peptide B (BNP; 2007 ± 1229 vs. 1411 ± 1272 pg/mL; $P = 0.010$) and lower EAT thickness (2.1 ± 0.8 vs. 2.9 ± 1.4 mm; $P = 0.010$), and they were treated with ~ 2.5 -fold lower dose of both β -blockers and angiotensin-converting enzyme inhibitors or angiotensin receptor blockers (ACE/ARB-inhibitors). The overall pattern of EAT gene expression suggested simultaneous activation of lipolysis and lipogenesis in cachexia. Lower ratio between expression levels of natriuretic peptide receptors C and A was observed in cachectic vs. BW-stable patients (0.47 vs. 1.30), supporting activation of EAT lipolysis by natriuretic peptides. Fundamental differences in metabolome/lipidome between BW-stable and cachectic patients were found. Mitochondrial phospholipid cardiolipin (CL), specifically the least abundant CL 70:6 species (containing C16:1, C18:1, and C18:2 acyls), was the most discriminating analyte (partial least squares discriminant analysis; variable importance in projection score = 4). Its EAT levels were higher in cachectic as compared with BW-stable patients and correlated with the degree of BW loss during the last 6 months ($r = -0.94$; $P = 0.036$).

Conclusions Our results suggest that (i) BNP signalling contributes to changes in EAT metabolism in cardiac cachexia and (ii) maintenance of stable BW and 'healthy' EAT-myocardium microenvironment depends on the ability to tolerate higher doses of both ACE/ARB inhibitors and β -adrenergic blockers. In line with preclinical studies, we show for the first time in humans the association of cachexia with increased adipose tissue levels of CL. Specifically, CL 70:6 could precipitate wasting of adipose tissue, and thus, it could represent a therapeutic target to ameliorate cachexia.

Keywords Heart failure; Lipolysis; Natriuretic peptides; Adipose tissue; Cardioliipin; Cardiac cachexia

Received: 1 April 2020; Revised: 3 September 2020; Accepted: 4 September 2020

*Correspondence to: Vojtech Melenovsky, Department of Cardiology, Institute for Clinical and Experimental Medicine - IKEM, Videňská 1958/9, Prague 140 28, Czech Republic. Phone: 420-732-816-242, Fax: 420-261-362-486, Email: vojtech.melenovsky@ikem.cz

Jan Kopecký, Laboratory of Adipose Tissue Biology, Institute of Physiology of the Czech Acad Sciences, Videnska 1083, Prague 14020, Czech Republic. Phone: 420-720-555-501, Email:jan.kopecky@fgu.cas.cz
Petra Janovska and Vojtech Melenovsky contributed equally to this study.

Introduction

Despite the fact that obesity is a strong risk factor for heart failure (HF) in the general population, obese patients with already established HF have better long-term prognosis than their non-obese counterparts, a situation sometimes referred to as ‘an obesity paradox’.^{1–3} In patients with advanced HF, fat mass seems to be associated with better survival^{2,4} while non-intentional weight loss, the defining feature of cardiac cachexia,^{3,5–7} is a strong independent risk factor for mortality from HF.^{1,3} Other chronic conditions such as cancer or chronic obstructive pulmonary disease often also lead to cachexia, which compromises treatment options and survival.⁸ Thus, distinct diseases may trigger a final common mechanism that leads to chronic body wasting and promotes other organ dysfunctions. Importantly, cachexia could not be reversed using conventional nutritional support, and effective mechanism-based treatment of cachexia needs to be developed.⁸

Disturbed energy handling in adipose tissue represents an early event in the development of cancer cachexia,^{8–10} but the role of metabolic, immune, and secretory alterations of adipose tissue in the development and/or progression of cardiovascular diseases (including HF) is poorly understood.^{11–13} In particular, epicardial adipose tissue (EAT) was in the focus of very few studies.^{12–14} Due to its close proximity and shared microvascular network, the EAT-myocardium microenvironment can be a place of intensive exchange of paracrine regulators or metabolic substrates, and it may serve as a transducer of systemic metabolic state, inflammation, or neurohumoral activation on the cardiac muscle.^{15,16}

Fatty acids released from adipose tissue are crucial for cardiac function, because a majority of cardiac ATP comes from fatty acid β -oxidation and oxidative phosphorylation in mitochondria.¹⁷ Activation of fatty acid metabolism is common in advanced stages of HF, due to enhanced adipose tissue lipolysis.¹¹ Lipolysis is activated in HF due to activation of the sympathetic nervous system, renin-angiotensin-aldosterone system (RAAS)^{17–20} and elevated circulating levels of natriuretic peptides A and B (ANP and BNP)^{11,18} that are secreted directly by the heart.^{18,19,21} Adipose tissue inflammation and insulin resistance further contribute to altered adipose tissue metabolism in HF patients.^{8,17} In advanced HF, excessive fatty acid mobilization leads to a switch in substrate utilization by the myocardium, from β -oxidation to energetically less effective glycolysis,^{17,22} and eventually to oxidation of ketone bodies.²²

In order to identify potential therapeutic targets to reduce body wasting and improve HF outcomes, we conducted a

study that compared clinical characteristics, circulating markers, and notably, EAT gene expression and metabolome in advanced HF patients with or without cardiac cachexia.

Materials and methods

Study cohort

Study cohort ($n = 52$) consisted of consecutive patients with end-stage HF who underwent heart transplantation at the Institute for Clinical and Experimental Medicine (IKEM) in Prague, Czech Republic. Subjects with body weight (BW)-reducing therapy or endocrine disease were excluded. Samples of EAT from the HF patients were harvested from the anterior interventricular groove immediately after explantation of the heart and were placed into liquid nitrogen and stored at -80°C until analysis. BW-trajectories during the last 6 months before transplantation were obtained by direct questioning and from medical records. Cachexia was defined as non-intentional non-edematous BW loss of at least 7.5% during the previous 6 months, as compared with BW-stable patients.³ This relatively high cut-off (other studies^{3, 5–7}) was used in order to maximally unmask the impact of BW-wasting on various parameters analysed using a relatively small patient’s cohort (Discussion).

Medical records were queried to obtain clinical history, echocardiographic, and haemodynamic examinations obtained before heart transplantation. The daily dose of β -adrenergic blockers was converted to equivalents dose of metoprolol (mg/day) using ratios of guidelines-recommended target doses (Table 7.2 in Ponikowski *et al.*⁶). In similar way, daily dose of RAAS activity inhibitors, namely angiotensin-converting enzyme (ACE) inhibitors or angiotensin receptor blockers (ARB), was converted to equivalent dose of ramipril (mg/day). None of the patients was treated by sacubitril/valsartan. The protocol was approved by the Ethics Committee of IKEM. All the patients signed informed consent approving their enrolment in the study and research analysis of the EAT and blood samples.

Epicardial adipose tissue gene expression

Analysis was performed using total RNA isolated from the tissue and quantitative real-time PCR. Results were normalized to geometric mean of three housekeeping genes: GAPDH, HPRT, and PPIA. For gene names, PCR primers and other details, see Supporting Information, Table S1.

Blood tests

Serum and plasma samples were stored at -80°C . Routine biochemical parameters were evaluated using an automated Abbott Architect ci1600 analyser. BNP concentrations were measured using a microparticle immunoassay (Architect BNP; Abbott Laboratories). Insulin was measured using RIA (Beckman-Coulter).

Metabolomic and lipidomic analysis

A combined targeted and untargeted workflow for the metabolome, lipidome and exposome characterization was performed using EAT extracts (Supporting Information, Method S1).

Statistical analyses

The data are presented as means \pm standard error or means \pm standard deviation, as indicated. Comparisons were

analysed using Student's *t*-test, and considered significant when $P \leq 0.05$. Spearman's rank correlation coefficients and linear regression were used to evaluate correlations between various parameters. To find fundamental relations between data sets, partial least squares discriminant analysis was performed using MetaboAnalyst 4.0 web portal.²³

Results

Clinical characteristics

The baseline characteristics of the patients are summarized in Table 1. The cohort consisted of predominantly middle-aged males, with prevailing non-ischemic HF aetiology. Twelve patients (23%) were treated for type 2 diabetes, 22 (42%) were overweight, and 6 (12%) were obese [body mass index (BMI) $> 30 \text{ kg}\cdot\text{m}^{-2}$]. Seventeen patients (33%) reported significant ($\geq 7.5\%$) non-intentional BW loss during the last 6 months—the defining feature of cardiac cachexia,⁴ which

Table 1 Clinical variables and medication

Variable	All patients <i>n</i> = 52	BW-stable <i>n</i> = 35	Cachexia <i>n</i> = 17	<i>P</i> value
Age	54 \pm 11	55 \pm 10	52 \pm 14	0.725
Gender (M; %)	83	86	76	0.409
Body mass index (kg/m^2)	25 \pm 4	26 \pm 4	22 \pm 3	<0.001
Body weight (BW) change (%)	-4.8 \pm 6.1	-1.3 \pm 3.3	-11.9 \pm 4.1	<0.001
NYHA class (1–4)	3.4 \pm 0.5	3.3 \pm 0.5	3.6 \pm 0.5	0.031
Non-ischemic HF (%)	65	57	82	0.073
HF duration (years)	5.2 \pm 4.1	5.4 \pm 3.9	4.7 \pm 4.4	0.556
Inotrope therapy (prior Tx; %)	21	14	35	0.082
Atrial fibrillation on ECG (%)	30	28	32	0.499
Echocardiography				
LV ejection fraction (%)	21 \pm 6	21 \pm 7	19 \pm 5	0.302
LV end-diastolic diameter (mm)	74 \pm 10	72 \pm 9	73 \pm 12	0.794
Mitral regurgitation (0–4)	2.4 \pm 1.1	2.3 \pm 1.1	2.6 \pm 1.1	0.307
Left atrial volume index (mL/m^2)	74 \pm 30	69 \pm 29	79 \pm 32	0.220
Right atrial area (cm^2)	25 \pm 8	25 \pm 7	26 \pm 9	0.904
Tricuspid regurgitation (grade 0–4)	2.1 \pm 0.9	2.0 \pm 1.0	2.1 \pm 0.9	0.751
RV diastolic diameter (mm)	46 \pm 8	45 \pm 8	47 \pm 9	0.407
RV dysfunction grade (0–4)	1.6 \pm 1.0	1.7 \pm 1.0	1.4 \pm 0.9	0.403
TAPSE (mm)	14 \pm 5	14 \pm 5	14 \pm 4	0.736
Epicardial fat thickness (mm)	2.6 \pm 1.3	2.9 \pm 1.4	2.1 \pm 0.8	0.010
Haemodynamics				
Heart rate (bpm)	77 \pm 13	77 \pm 13	77 \pm 13	0.710
Mean blood pressure (mmHg)	85 \pm 10	88 \pm 10	79 \pm 7	0.130
Cardiac output (L/min)	3.5 \pm 0.8	3.7 \pm 0.7	3.2 \pm 1.0	0.131
Right atrial pressure (mmHg)	9.4 \pm 4.4	10.1 \pm 4.9	8.1 \pm 3.4	0.043
PA mean pressure (mmHg)	33 \pm 9	34 \pm 10	32 \pm 8	0.384
PA wedge pressure (mmHg)	24 \pm 8	24 \pm 8	23 \pm 7	0.563
Medication				
Furosemide (mg/day)	168 \pm 164	155 \pm 125	193 \pm 226	0.534
^a β -blockers (mg/day)	40 \pm 50	50 \pm 56	20 \pm 25	0.011
^a ACE/ARB-inhibitors (mg/day)	1.4 \pm 2.0	1.7 \pm 2.1	0.7 \pm 1.3	0.035

β -blockers, dose in metoprolol equivalents, ACE/ARB-inhibitors, dose of angiotensin-converting-enzyme inhibitors or angiotensin receptor blockers in ramipril equivalents (Materials and methods); LV, left ventricular, RV, right ventricle; NYHA, New York Heart Association functional class; TAPSE, tricuspid annular plane systolic excursion; Tx, transplantation; PA, pulmonary artery.

Data are shown for all the patients, or two subgroups of the patients split based on their BW trajectories during the previous 6 months (BW-stable vs. Cachexia). Data are means \pm SD. Bold, statistical significant difference.

^aEight out of 52 patients received neither β -blockers nor ACE/ARB-inhibitors, and 34 patients received a combination of the two.

[Correction added on 12 November 2020, after first online publication: Tables 1 and 2 were previously incorrect and have been replaced in this current version.]

discriminated them from BW-stable patients ($n = 35$; 67%). Cachectic patients were more symptomatic, had higher New York Heart Association class and ~ 1.4 -fold lower EAT thickness, and tended to have lower systemic blood pressure and cardiac output. Cachectic patients had more often non-ischemic HF aetiology and were treated with ~ 2.5 -fold lower dose of β -blockers and ~ 2.4 -fold lower dose of ACE/ARB-inhibitors as compared with BW-stable patients. Cachectic vs. BW-stable HF-patients displayed ~ 1.4 -fold higher BNP plasma levels reflecting the higher myocardial stress, despite there was no significant difference in cardiac structure by echocardiography. Levels of plasma glucose tended to be lower, and that of haemoglobin A1C were lower in the cachectic patients (Table 2).

The impact of cachexia on epicardial adipose tissue expression of lipid metabolism, adipokines, and inflammatory genes

To characterize the role of adipose tissue immunometabolism in cachexia development, expression of selected genes in EAT was evaluated and compared between BW-stable and cachectic patients (Figure 1A–D; for fold change of the mean values, Supporting Information, Table S2). Concerning lipolysis (Figure 1A), expression of lipolysis-promoting natriuretic peptide receptor A (NPRA) gene was similar in both groups (for gene names, see Table S1). Mean expression of natriuretic peptide receptor C (NPRC, also called clearance receptor) gene was ~ 2.4 -higher in BW-stable patients. Lower

NPRC/NPRA transcript level ratio in cachectic vs. BW-stable patients (0.47 vs. 1.30; Table S2) suggested lower clearance of natriuretic peptides resulting in stimulation of lipolysis.^{19,21} Accordingly, both NPRC expression and NPRC/NPRA transcript level ratio correlated negatively with systemic levels of BNP, positively with BMI and BW change, daily dose of both β -blockers and ACE/ARB-inhibitors, and mean blood pressure (Figure 2). Genes for both PTGDS and ADORA1 tended to be up-regulated in association with cachexia (Figure 1A), suggesting increased production of prostaglandin D2 that exerted antilipolytic effect,²⁴ in concert with ADORA1 stimulation.²⁵ In spite of the up-regulation of PTGDS and ADORA1, genes for (i) the key lipases ATGL and HSL,⁸ (ii) PLIN1, which is required for activation of lipolysis,¹³ (iii) cell death-inducing DNA fragmentation factor (CIDEA), which counteracts inhibition of lipolysis by AMP-activated protein kinase,⁹ and (iv) zinc- $\alpha 2$ -glycoprotein, the lipolytic factor known to be induced in cancer cachexia,²⁶ tended to be up-regulated in cachectic patients (Figure 1A). With respect to genes engaged in triacylglycerols formation (Figure 1B), we focused on (i) FAS, which is essential for *de novo* lipogenesis, (ii) PEPCK, required for glyceroneogenesis, (iii) DGAT1 and DGAT2, engaged in fatty acid re-esterification/triacylglycerol synthesis, and (iv) FABP1, fatty acid transporter. Mean expression of FAS, and DGAT1 was ~ 2.9 -fold and ~ 1.6 -fold higher in cachectic than BW-stable patients, respectively. Also, expression of PEPCK, DGAT2, and FABP1 tended to be up-regulated in cachexia. Next, we focused on expression of genes engaged in control of lipid catabolism and mitochondrial functions (Figure 1C). These genes

Table 2 Plasma parameters

Parameter	^b Control range	All patients	BW-stable	Cachexia	<i>P</i> value
		<i>n</i> = 52	<i>n</i> = 35	<i>n</i> = 17	
^a BNP (pg/mL)	10–80	1606 ± 1278	1411 ± 1272	2007 ± 1229	* 0.010
Creatinine (μmol/L)	64–104	109 ± 42	106 ± 31	114 ± 60	0.596
Total protein (g/L)	64–79	62 ± 6	63 ± 7	61 ± 4	0.798
C reactive protein (g/L)	< 5	9 ± 12	8 ± 9	11 ± 17	0.525
Haemoglobin (g/L)	135–175	126 ± 15	127 ± 15	124 ± 13	0.437
Total cholesterol (mmol/L)	2.9–5.1	3.7 ± 1.1	3.7 ± 1.1	3.8 ± 1.1	0.782
Triglycerides (mmol/L)	0.5–1.7	1.3 ± 0.7	1.3 ± 0.8	1.2 ± 0.5	0.415
TSH (mIU/L)	0.4–4.9	3.9 ± 3.4	3.8 ± 3.8	4.2 ± 2.5	0.803
ft3 (pmol/L)	2.9–4.9	3.4 ± 0.8	3.4 ± 0.8	3.3 ± 0.9	0.655
ft4 (pmol/L)	9–19	14 ± 4	14 ± 3	16 ± 5	0.223
Cortisol (nmol/L)	166–507	436 ± 241	451 ± 265	407 ± 187	0.493
Fasting plasma glucose (mmol/L)	3.6–5.6	5.8 ± 1.2	6 ± 1.3	5.4 ± 1.1	0.112
Fasting plasma insulin (μIU/mL)		4.1 ± 3.8	4.2 ± 4.1	3.9 ± 3.1	0.846
HOMA-IR		1.0 ± 1.0	1.1 ± 1.1	0.9 ± 0.7	0.492
Haemoglobin A1C (mmol/mol)	20–42	49 ± 10	50 ± 12	44 ± 6	0.017
Bilirubin (μmol/L)	3–20	21 ± 11	21 ± 12	23 ± 11	0.584
Sodium (mmol/L)	137–144	135 ± 4	136 ± 4	134 ± 5	0.321
Potassium (mmol/L)	3.5–5.1	4.1 ± 0.6	4.1 ± 0.7	4.2 ± 0.4	0.219

Data are shown for all the patients, or two subgroups of the patients split based on BW trajectories during the previous 6 months (BW-stable vs. Cachexia). Data are means ± SD. Bold, statistical significant difference.

^aMedian (Q1–Q3) for BNP: all patients, 1283 (599–2413); BW-stable, 707 (445–1815); Cachexia 1650 (902–2506).

^bControl (normal) range at the IKEM Central Laboratory; data are for both genders, only the BNP data are for man at 55–65 years of age, for women of this age: 10–155 pg BNP/ml plasma. HOMA, homeostasis model assessment;

^cFor log-transformed data.

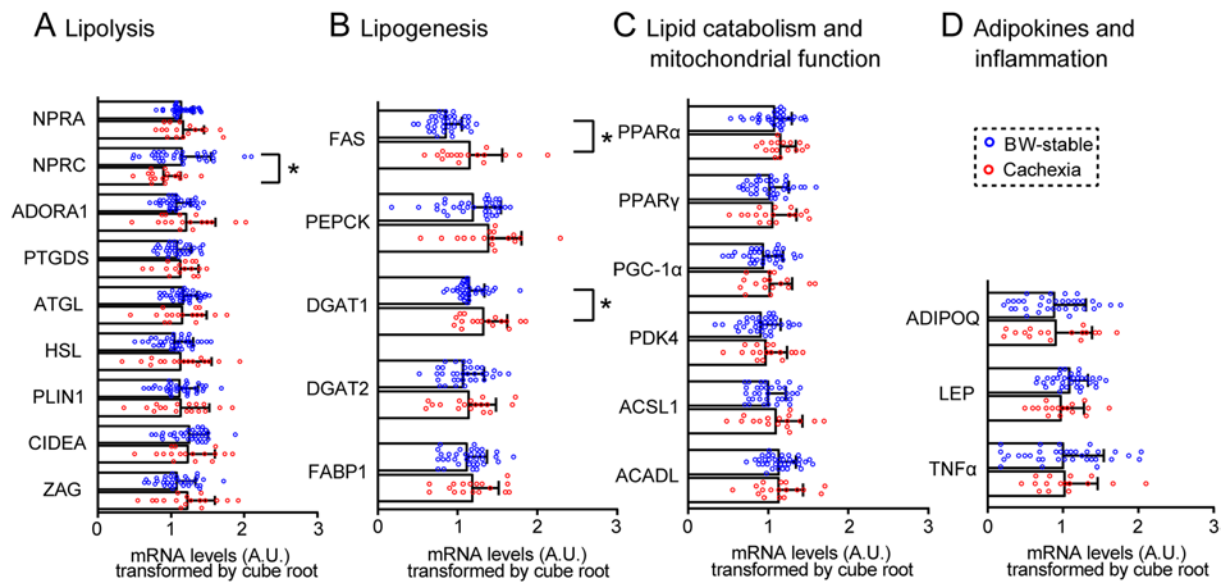


FIGURE 1 Expression of lipid metabolism, adipokines and inflammatory genes in epicardial adipose tissue. Comparison between body weight-stable ($n = 35$) and cachectic ($n = 17$) patients. (A–D) Transcripts grouped according to their functions. Transcript levels (A.U.) were normalized (i) to geometric mean of three housekeeping genes and (ii) by cube root transformation. Data are means \pm SE; Student's t -test. * Significant difference between the groups; for fold-change of the means, see Table S2. For gene names abbreviations, see the main text and Table S1.

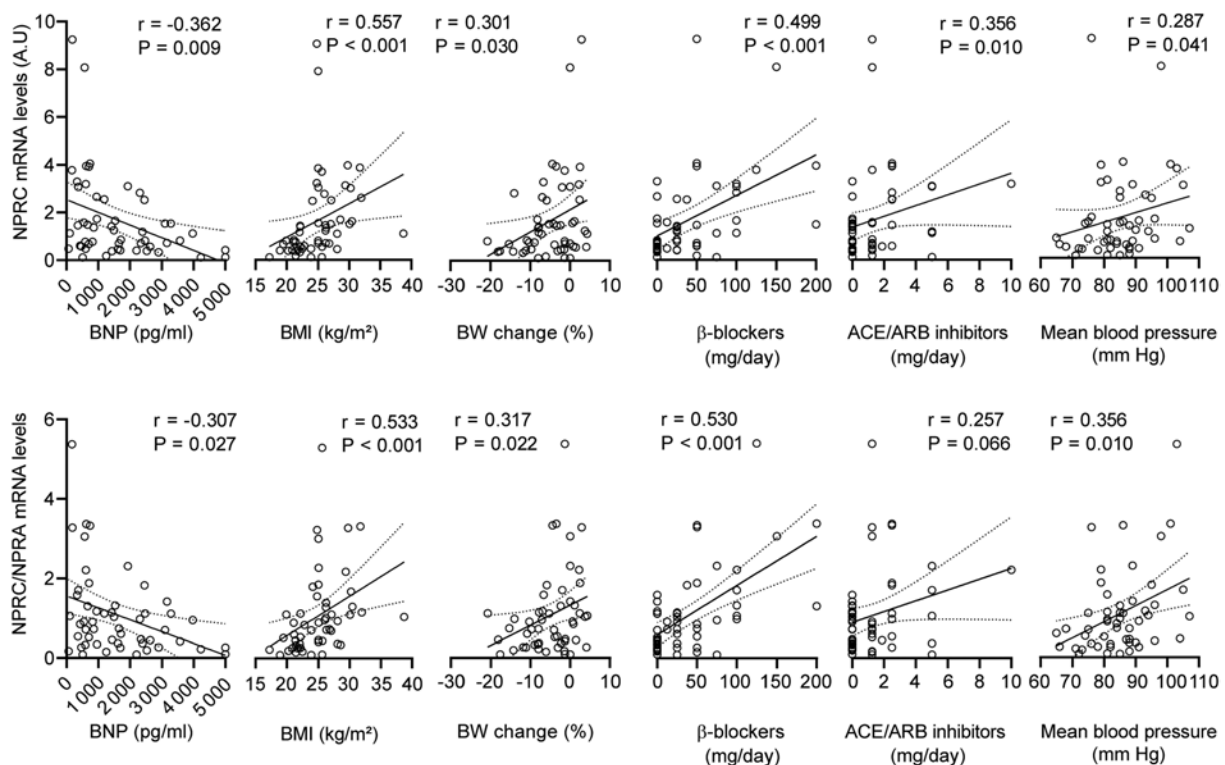


FIGURE 2 Correlation of gene expression markers of natriuretic peptide system activity with clinical parameters. Linear regression plot of the relationship between transcript levels of NPRC (upper panels), or the ratio between NPRC and NPRA transcript levels (NPRC/NPRA; lower panels), and the indicated parameters. Linear regression lines, including 95% confidence intervals, are shown. Spearman's rank correlation coefficients (r) and P value (indicated in the figures) were also calculated to assess the correlations between various parameters. For the source data, see Figure 1 and Tables S1, 1, and 2. ACE/ARB inhibitors, angiotensin-converting enzyme inhibitors/angiotensin receptor blockers; BNP, natriuretic peptides B; BMI, body mass index; BW, body weight; NPRC, natriuretic peptide receptor C

included (i) PPAR α , which acts both as a sensor for fatty acids and ligand-activated transcription factor enhancing lipid catabolism, (ii) PPAR γ , and its target PGC-1 α inducing mitochondrial biogenesis,²⁷ (iii) PDK4, which limits glucose oxidation by inhibiting pyruvate dehydrogenase and thus supports β -oxidation,²⁸ and (iv) ACSL1 and ACADL, which are engaged in mitochondrial β -oxidation of fatty acids. Expression of all these genes tended to be up-regulated in cachexia (Figure 1C). Regarding the secretory functions and immune status of EAT (Figure 1D), we focused on the expression of genes for adiponectin (ADIPOQ) and leptin (LEP), representing two major adipokines,²⁹ as well as pro-inflammatory TNF α gene. Expression of none of these genes was significantly affected by cachexia.

Although ionotropic support tended to be higher in cachectic patients prior the surgery (35% vs. 14%, Table 1), it had no impact on the expression of lipid metabolism, adipokines, and inflammatory genes in EAT (not shown).

Relatively small differences in the gene expression pattern between BW-stable and cachectic patients prompted us to explore the data by using a complex pathway analysis of EAT metabolism (Figure 3). All the differences in mean expression of the individual genes between BW-stable and cachectic patients were considered, irrespective of their statistical significance (Table S2). This approach revealed a broad induction of EAT lipid metabolism in cachexia. It can be assumed that adipose tissue wasting in cachexia is caused by a net loss of tissue triacylglycerols, which are stored in adipocytes. This implies higher stimulation of lipolytic and oxidative pathways activities, which lead to decrease in the intracellular triacylglycerol pool as compared with insufficient stimulation of glyceroneogenesis, *de novo* fatty acid synthesis and fatty acid re-esterification/triacylglycerol synthesis that are engaged in the replenishment of the pool.

Global impact of cachexia on epicardial adipose tissue metabolome

To get further insight into the mechanisms underlying the role of adipose tissue in the development of cardiac cachexia, we performed untargeted metabolomic and lipidomic analysis of EAT. Using six different gas chromatography–mass spectrometry platforms (Method S1), we annotated 750 compounds including polar metabolites, complex lipids, and various exposome compounds such as drugs (Supporting Information, Figure S1 and Dataset S1). All known from these analytes, except for drugs and other non-physiological analytes, that is the exposome compounds ($n = 47$; Supporting Information, Table S3), were used for further analysis.

Using partial least squares discriminant analysis, a supervised classification method, a separation between

BW-stable and cachectic patients, was observed indicating a fundamental difference between the two groups (Figure 4A). Variable importance in projection (VIP) identified the most discriminating analytes. Among the top 30 VIP analytes (Figure 4B), various (lyso)phospholipids represented a majority (60%), while triacylglycerols together with diacylglycerols were the second (13%) and ceramides the third (10%) most abundant classes among the discriminating analytes. However, cardiolipin (CL) 70:6 was clearly the single most important discriminating analyte. These results indicate that development of cachexia in HF-patients is linked with major changes in EAT metabolome and suggest an involvement of at least some of the VIP analytes in the mechanisms underlying pathological wasting of adipose tissue. Indeed, in preclinical studies, increase of CL levels in various tissues was causally linked to cancer cachexia.^{10,30–32} Therefore, CL in EAT of the HF-patients became the major focus of the next part of our study.

Involvement of epicardial adipose tissue cardiolipin in cachexia

Evaluation of the lipidomics data revealed presence of four different CLs in EAT, namely CL 70:6, CL 70:7, CL 72:7, and CL 72:8 (Figure 5A). Side chains of these CLs contained combinations of three different acyls, namely palmitoleic (C16:1), oleic (C18:1), and linoleic (C18:2) acid (Supporting Information, Table S4). Only CL 70:6 discriminated between BW-stable and cachectic patients, while it represented the least abundant CL species (Figure 5A). Its levels were ~1.5-fold higher in the cachectic patient's group (Table S4). EAT metabolome also contained several phosphatidylglycerol (PG) species, that is the building blocks in the synthesis of CL (Figure 5B). Levels of most of these PGs tended to be higher in cachectic as compared with BW-stable patients (Table S4).

Importantly, EAT levels of CL 70:6 significantly correlated with BW markers, that is negatively with both BMI and BW change. Similar trends were observed with CL 70:7. No correlation between the BW markers and the levels of either CL 72:7 or CL 72:8 was observed (Figure 5C). Thus, the strength of the association between various CLs and the degree of cachexia increased in the case of less abundant CL species (Figure 5A).

Hierarchical clustering of EAT analytes using only levels of the four CLs revealed two clusters of patients at the first level of hierarchy, Cluster A4 and Cluster B4, respectively (Figure 5D). Cluster A4 (13 cases) was composed exclusively of BW-stable patients. Cluster B4 (39 cases) represented a heterogeneous mixture of BW-stable (56%) and cachectic (44%) patients. EAT levels of most CLs and PGs were higher in Cluster B4-patients, with CL 70:6 showing the largest (~47-fold) difference (Table S4). In agreement with the comparison between BW-stable and cachectic patients (Tables 1

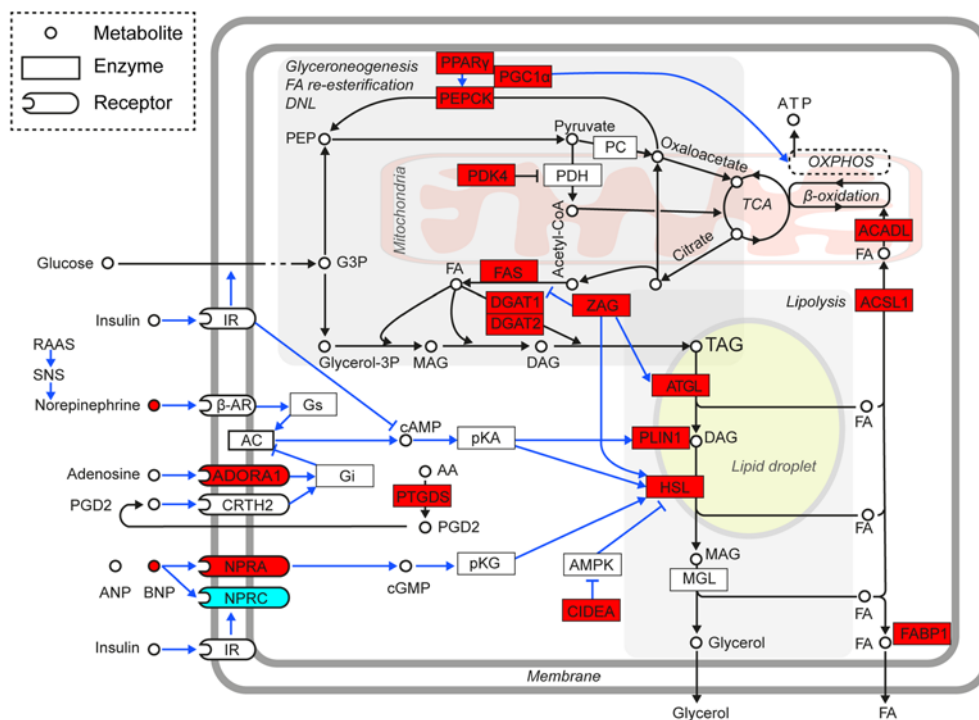


FIGURE 3 Induction of epicardial adipose tissue (EAT) lipid metabolism linked to cachexia. Gene expression data (Figure 1; and the FC values in Table S2) were collectively analysed to assess activity of the key regulatory and metabolic pathways in EAT adipocytes. Majority of the genes exerted higher mean expression levels (irrespective of the statistical significance of difference) in cachectic as compared with BW-stable patients; also plasma levels of BNP (Table 2) and adenosine EAT levels (Supporting Information, Dataset S2) were higher in cachectic patients (red colour). Only the NPRC expression in cachectic patients was relatively low (blue colour). Data suggest that stimulation of lipolysis in EAT of HF-patients by BNP (as well as sympathetic system and RAAS activity; Introduction; not measured here) is further augmented with adipose tissue wasting, in spite of the adaptive antilipolytic response at the PTGDS and ADORA1 gene expression level. Triacylglycerols (TAG) loss due to the increased lipolysis is not fully compensated by lipogenesis, which depends on glyceroneogenesis, *de novo* fatty acid synthesis (DNL) and fatty acid (FA) re-esterification. Energy requirements of these anabolic pathways are covered by increased ATP production in mitochondria that combust FA (Figure 7) and other energy fuels (Introduction). Metabolite fluxes and regulatory effects are indicated by black and blue lines, respectively. β -AR, β -adrenergic receptor; AA, arachidonic acid; AC, adenylate cyclase; ACADL, long-chain acyl-coenzyme A dehydrogenase, also called LCAD; ACSL1, acyl-CoA synthetase long chain family member 1; ADORA1, adenosine A1 receptor; AMPK, AMP-activated protein kinase; ANP, A-type natriuretic peptide; ATGL, adipose triglyceride lipase; BNP, B-type natriuretic peptide; cAMP, cyclic adenosine monophosphate; cGMP, cyclic guanosine monophosphate; CIDEA, cell death-inducing DNA fragmentation factor, alpha subunit-like effector A; CoA, coenzyme A; CRTH2, prostaglandin D2 receptor 2; DAG, diacylglycerol; DGAT1 and DGAT2, diacylglycerol O-acyltransferase 1 and 2, respectively; FABP1, fatty acid binding protein 1; FAS, FA synthase; G3P, glyceraldehyde 3-phosphate; Gi, G protein subunit alpha i1; Glycerol-3P, glycerol 3-phosphate; Gs, guanine nucleotide-binding protein G(s) subunit alpha; HSL, hormone-sensitive lipase; IR, insulin receptor; MAG, monoacylglycerol; MGL, monoacylglycerol lipase; NPR1, natriuretic peptide receptor 1; NPR3, natriuretic peptide receptor 3, also called clearance receptor; PC, pyruvate carboxylase; PDH, pyruvate dehydrogenase; PDK4, pyruvate dehydrogenase kinase 4; PEP, phosphoenolpyruvate; PEPCK, phosphoenolpyruvate carboxykinase; PGC-1 α , peroxisome proliferative-activated receptor γ coactivator 1 α ; PGD2, prostaglandin D2; PKA, protein kinase A; PKG, protein kinase G; PLIN1, perilipin 1; PPAR γ , peroxisome proliferator activated receptor γ ; PTGDS, prostaglandin D2 synthase; RAAS, renin-angiotensin-aldosterone system; SNS, sympathetic nervous system; TCA, tricarboxylic acid cycle; ZAG, zinc-binding alpha-2-glycoprotein 1.

and 2), the homogenous group of BW-stable patients in Cluster A4 exhibited lower plasma BNP levels and higher dose of both β -blockers and ACE/ARB-inhibitors as compared with Cluster B4-patients (Supporting Information, Table S5).

At the gene expression level, Cluster A4 patients showed relatively high NPRC and relatively low ADORA1 and FAS expression, consistent with the difference in gene expression pattern between BW-stable and cachectic patients (Table S2). Also minor differences in expression of the other genes between Cluster A4 and Cluster B4 patients were mostly in agreement with the corresponding differences between

BW-stable and cachectic patients; in addition, the Cluster A4 vs. Cluster B4 comparison unmasked higher expression of leptin gene in Cluster A4, that is in BW-stable patients (Table S2).

The above results documented the role of CL with a specific acyl side chains composition, namely the CL 70:6 containing C16:1, C18:1, and C18:2 acyls, in the development of cardiac cachexia. Therefore, we aimed to ascertain the mechanisms underlying the differential control of EAT levels of various CLs in cachexia. First, we focused on potential role of changes in EAT levels of PGs. Multiple significant positive

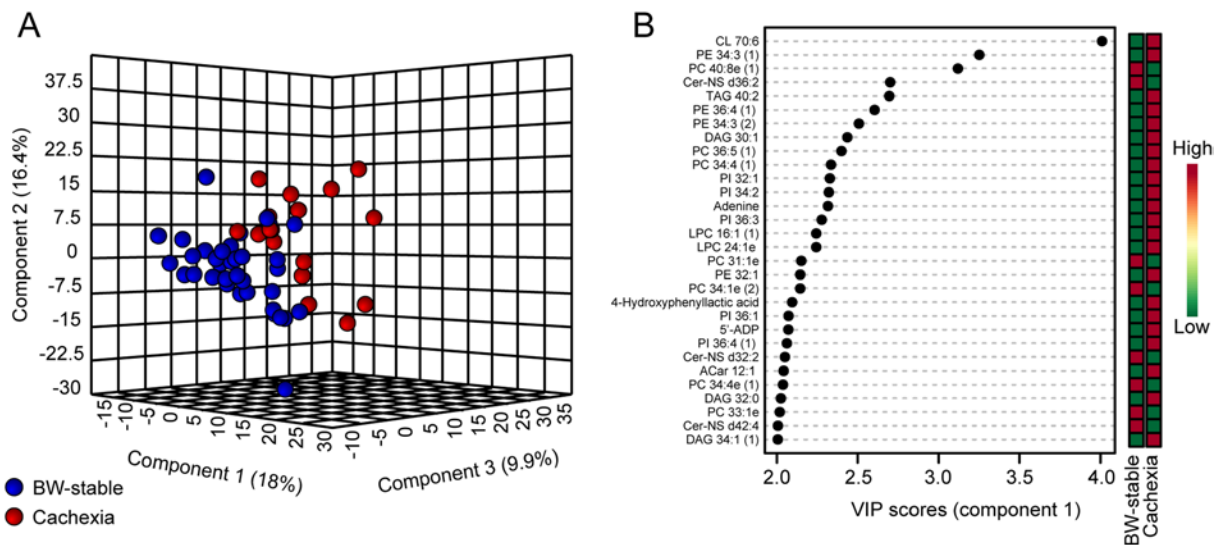


FIGURE 4 Multivariate analysis of epicardial adipose tissue (EAT) metabolome. Untargeted metabolomic and lipidomic analysis was performed using EAT extracts in all patients ($n = 52$) as described in *Method S1*. Dataset of all analytes with known structure detected in EAT (*Figure S1*), except for drugs and other non-physiological analytes (*Table S3*), was analysed using partial least squares discriminant analysis. (A) Score plot resulting from the analysis focused on the separation between the body weight (BW)-stable ($n = 35$) and cachectic ($n = 17$) patients (*Table 1*). (B) The corresponding variable importance in projection (VIP) plot with scores, to identify the top 30 most discriminating analytes. The coloured boxes indicate the relative concentrations of the corresponding analyte in each group; for fold-change, see *Dataset S2A*. 5'-ADP, adenosine-5'-diphosphate; Cer-NS, ceramide non-hydroxyfatty acid-sphingosine; CL, cardiolipin; DAG, diacylglycerol; LPC, lysophosphatidylcholine; LPE, lysophosphatidylethanolamine; PC, phosphatidylcholine; PE, phosphatidylethanolamine; PG, phosphatidylglycerol; PI, phosphatidylinositol; TAG, triacylglycerol. Lipid class $x : y$, acyl number of carbons : number of double bonds. Number in the brackets, isobar of the analyte.

correlations between the levels of either CL 70:6 or CL 70:7 and most PGs were found. For CL 72:7 or CL 72:8 species, the correlations were less frequent (*Figure S2*).

Secondly, we focused on the role of genes engaged in CL synthesis, PG synthase 1 (PGS1) and CL synthase 1 (CRLS1), and in remodelling of the acyl side chains of CL, acyl-CoA : lysocardiolipin acyltransferase 1 (LCLAT1). Expression of these genes was compared between BW-stable and cachectic patients, as well as between Cluster A4 and Cluster B4 patients (*Figure 6* and Supporting Information, *Table S6*). With PGS1 and LCLAT1, no significant differences between the groups were observed. However, CRLS1 expression was significantly higher (~1.7-fold) in Cluster B4 as compared with Cluster A4 patients, while expression of both PGS1 and LCLAT1 showed a similar trend.

These results suggested that differential increase in the EAT levels of various CLs in cachexia could reflect both (i) basal levels of PGs that are used for CL synthesis and (ii) activity of the genes engaged in CL synthesis and remodelling.

Discussion

To our knowledge, this is the first study focused on the role of EAT-myocardium microenvironment in the development of cardiac cachexia. A complex approach was used, which was

based on the characterization of both metabolome/lipidome and gene expression in EAT of the end-stage HF-patients with and without cardiac cachexia.

For the characterization of the impact of BW-wasting on various parameters in our study, the BW-stable and cachectic patients were discriminated using a non-edematous BW loss of at least 7.5% during the previous 6 months. This 7.5% cut-off, used also to define cardiac cachexia by Anker and colleagues in 1997,³ was higher as compared with that of 5% used in the 2008 cardiac cachexia definition⁵ or the 6% cut-off point in the ESC Guidelines from 2016⁶; Anker *et al.*⁷ When we have analysed the data at several cut-off points, equal to 5%, 6%, and 7.5% (not shown), we have found that the highest cut-off (7.5%) helped to uncover subtle links between the BW-loss and EAT gene expression (*Figure 1*), while the differences between BW-stable and cachectic patients (i) in the clinical variables and medication (*Table 1*) or plasma parameters (*Table 2*) and (ii) metabolome/lipidome (*Figures 4* and *5D*) were only marginally affected by various cut-off points. Thus, due to limited number of studied subjects, we choose the higher cut-off point of BW change to enhance the contrast between cachectic and BW-stable patients.

Our results demonstrate fundamental differences in metabolome/lipidome between BW-stable and cachectic patients. CL, a phospholipid of the inner mitochondrial membrane, specifically CL 70:6, was the most discriminating analyte. In preclinical models of cancer cachexia, intracellular

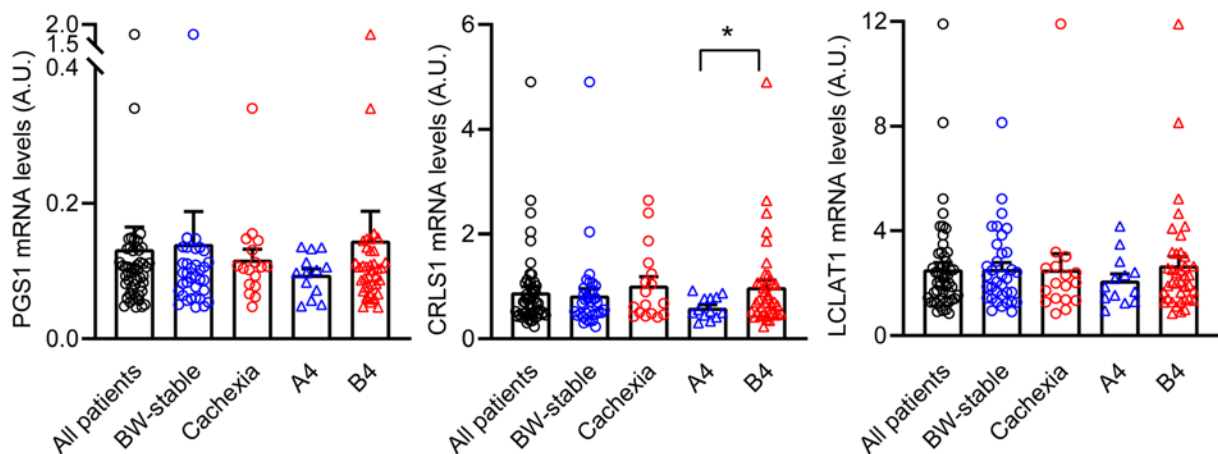


FIGURE 6 Expression of genes engaged in synthesis (PGS1 and CRLS1) and remodelling (LCLAT1) of cardioliipin across patient's subgroups. Transcript levels (A.U.) were normalized to geometric mean of three housekeeping genes. Data (Table S6) for all patients ($n = 52$), or the following subgroups: (i) BW-stable ($n = 35$) and cachectic ($n = 17$) patients; and (ii) Clusters A4 and B4 patients ($n = 13$ and $n = 39$, respectively), are shown. Data are means \pm SE; Student's *t*-test. *Significant difference between the groups. For gene names abbreviations, see the main text and Table S1.

importance for heart function due to the mutual interactions within the EAT-myocardium environment (Introduction).

Our results suggest that CL of a specific acyl profile could be causally involved in cachexia. Side chains of the four CLs contained in EAT represented combinations of only three different acyls, namely C16:1, C18:1, and C18:2, with the CL species abundance increasing with larger molecular mass and a higher degree of unsaturation and length of the acyl side chains (Table S4). It was not the major CL species, that is CL 72:8 (tetralinoleoyl-CL), which is normally present in insulin-sensitive tissues,³³ but the least abundant CL 70:6, which discriminated between BW-stable and cachectic patients. As suggested by the results of the animal study,³² CL70:6 could induce the uncoupling of oxidative phosphorylation in EAT mitochondria of cachectic patients. Its specific molecular acyl composition could underlie this effect.

Indeed, the changes in the tissue content of specific CL species and or changes in the acyl profile of CL could be the cause of specific pathologies: (i) Barth syndrome, a multisystem disorder characterized by cardiomyopathy, is associated with reduced levels of CL 72:8 (tetralinoleoyl-CL) in mitochondria, due to the defect of CL transacylase tafazzin, (ii) decrease of CL 72:8 preceded the development of HF in spontaneously hypertensive rats and correlated with a loss of mitochondrial cytochrome oxidase activity (reviewed in Saini-Chohan *et al.*³⁴), and (iii) replacement of C18:2 by docosahexaenoic acid (C22:6) in the CL side chains leads to mitochondrial dysfunction in diabetes and other metabolic diseases.³⁵ The mechanism of induction of CLs tissue levels in cachexia has yet to be characterized in detail. Our results in EAT of HF-patients show a link to increased tissue levels of PGs, the building blocks in the synthesis of CLs, suggesting an involvement of the enzymes engaged in CL synthesis and remodelling, especially the CL synthase CRLS1.

Previous studies focused on EAT gene expression either in patients with milder or no HF and compared subjects according to degree of left ventricular dysfunction¹² or according to the presence of coronary artery disease.¹³ Expression of the genes characterized here remained either unaffected (LEP, TNF α ; Fosshaug *et al.*¹²; and PLIN1, HSL, ATGL, ADIPOQ, LEP, IL6; Jaffer *et al.*¹³) or only marginally changed (PPAR α , IL6; Fosshaug *et al.*¹²). In this study, the overall pattern of EAT gene expression suggested simultaneous activation of lipolysis and lipogenesis in cachectic as compared with BW-stable HF-patients. Lipolysis was probably activated by the concert action of RAAS and sympathetic nervous systems^{17–20} and by natriuretic peptides.^{11,18} The prolipolytic factors contributing to cancer-related cachexia, CIDEA⁹ and zinc- α 2-glycoprotein,^{26,36} were probably also involved. Activation of both lipolysis and energy dissipating fatty acid/triacylglycerol futile cycling in EAT is consistent with the high catabolic activity of adipose tissue¹¹ and the overall catabolic dominance in HF-patients¹⁷ that was augmented further in association with adipose tissue wasting. Similar changes in adipose tissue metabolism were found in cancer cachexia.^{8,9} Presumably, the decrease in tissue triacylglycerol content due to increased lipolysis could not be compensated in full by activation of lipogenesis in EAT of cachectic patients. This is consistent with the effect of CL-induced uncoupling of oxidative phosphorylation in adipocytes^{37,38} when insufficient ATP production would limit several key biochemical activities engaged in triacylglycerols replenishment, such as glyceroneogenesis, *de novo* synthesis of fatty acids and their re-esterification (Figure 7 and Supporting Information, Figure S3). Relatively high ADORA1 expression found in BW-stable patients grouped in Cluster A4 is typical of EAT,²⁵ and ADORA1 up-regulation could contribute to the cardioprotection due to vasodilatation of coronary vessels²⁵

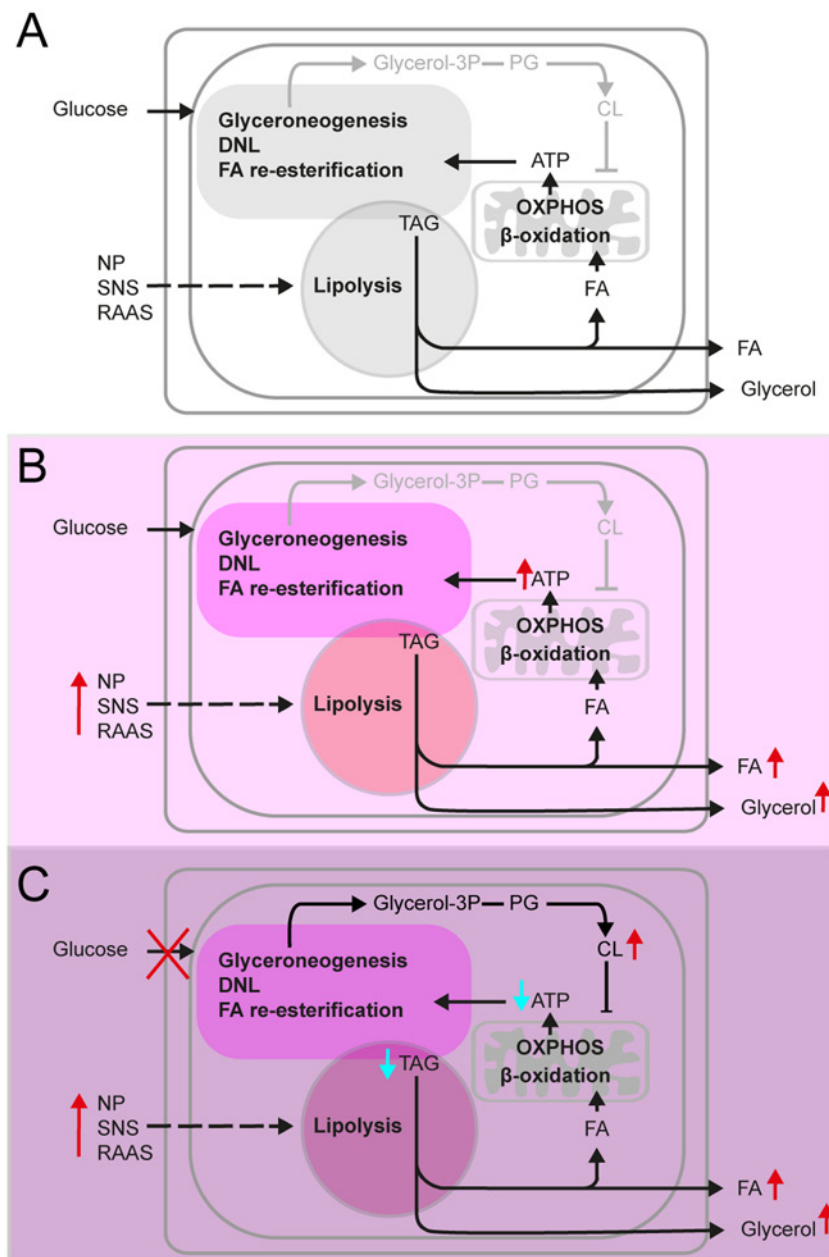


FIGURE 7 Changes in metabolism of EAT adipocytes during development of HF and cachexia. As compared with healthy subjects (A), in HF-patients (B and C), lipid metabolism in EAT adipocytes is activated in response to elevated plasma natriuretic peptides (NP) levels and increased activity of sympathetic nervous system (SNS) and RAAS. Activation of lipolysis results in increased efflux of fatty acids (FA) and glycerol from EAT. While FA could serve as energy fuels for myocardium, glycerol is used for hepatic glyceroneogenesis. In BW-stable HF-patients (B), breakdown of intracellular triacylglycerols (TAG) is balanced by TAG synthesis, which depends on glyceroneogenesis, *de novo* synthesis of FA (DNL), and FA re-esterification. These energy consuming reactions are driven by ATP, which is mostly synthesized by oxidative phosphorylation (OXPHOS) linked to β -oxidation of FA in mitochondria. In cachectic HF-patients (C), lipolysis is stimulated even more than in the BW-stable patients, in association with elevation of intracellular CL levels. This probably results from both, increased formation of phosphatidyl glycerols and dysregulation of enzymes engaged in CL synthesis and remodelling in cachexia. Aberrantly high levels of CL, namely the CL 70:6 species, induce uncoupling of OXPHOS. Low rate of ATP synthesis limits activity of the pathways contributing to TAG synthesis, resulting in insufficient replenishment of the TAG pool in fat cells and wasting of adipose tissue. For more details, see *Figure S3*.

and attenuation of β -adrenergic stimulation of lipolysis.²⁴ However, in general, the changes in EAT gene expression in cachexia were only mild. It should be learned if they take place also in other fat depots, which differ in their metabolic

features from EAT,^{12,13,25} and what is the contribution of the changes in adipose tissue metabolism to cardiac cachexia. For sure, due to its small mass, EAT plays an insignificant role in total energy balance.

Our study highlights the importance of the enhanced release of natriuretic peptides from the failing heart for the changes in EAT metabolism and development of cachexia,^{18,19,21} as suggested by the higher levels of BNP in cachectic patients. Adipose tissue sensitivity to natriuretic peptides is regulated by NPRC and NPRC/NPRA ratio.^{19,21} Hence, the relatively low NPRC/NPRA ratio in the cachectic patients, resulting in enhanced bioavailability of natriuretic peptides in the EAT-myocardium microenvironment, could be important. In addition, a negative correlation was found between the expression of NPRC and levels of CL 70:6 in EAT (Spearman's rank correlation coefficient = -0.561), supporting the role of NPRC in CL-induced changes of EAT metabolism in cachexia.

Comparisons between the subgroups of HF patients (i.e. BW-stable vs. cachectic, and Cluster A4 vs. Cluster B4 patients) revealed lower plasma BNP levels and higher daily doses of both β -blockers and ACE/ARB-inhibitors in the patients who were resistant to cachexia. These drugs prevent adverse neurohumoral activation that accompanies HF and, thus, represent the cornerstone of effective HF therapy, with their doses usually titrated to the maximally tolerated level. Therefore, HF patients who tolerated higher doses of these drugs were better protected against the development of cardiac cachexia. Indeed, β -adrenergic blockers and angiotensin II receptor antagonists have protective effects against fat loss due to cardiac cachexia (reviewed in Cabassi *et al.*²⁰). Anticachectic, adipose tissue-sparing effects of neurohumoral antagonist might therefore contribute to the favourable impact of these drugs on survival.

Our results support the idea that novel treatment strategies for HF-patients may be designed to target EAT metabolism and its secretory features, while changing EAT-myocardium microenvironment¹⁵ and, therefore, improving heart function. This could include neutralization of CIDEA activity to counteract excessive lipolysis in EAT, similarly as suggested for the treatment of cancer cachexia^{8,9} or inhibition of ATGL activity.¹⁴ Our findings here open a new possibility to treat cachexia by modulating CL biosynthesis and/or CL function. To this end, the use of cell-penetrating aromatic-cationic tetrapeptides that selectively target CL³⁹ should be explored.

In conclusion, we observed here in patients with advanced HF that BNP signalling probably contributed to changes in EAT metabolome/lipidome and gene expression, reflecting dysregulated induction of EAT lipid metabolism in cardiac cachexia. Concomitant modulation of EAT-myocardium microenvironment may be involved in the deterioration of heart function in the cachectic patients. Our results suggest that the maintenance of stable BW and 'healthy' EAT-myocardium microenvironment of the HF-patients is associated with their ability to tolerate higher therapeutic doses of conventional therapeutics, namely neurohumoral inhibitors (ACE/ARB inhibitors and β -adrenergic blockers). We showed that induction of

EAT levels of CL 70:6 could precipitate the wasting of adipose tissue. It is likely that an induction of minor CL species underlies energy dissipation in various tissues and represents one of the key events resulting in cachexia. Our results suggest that mitochondrial CL in EAT, as well as immunometabolic and secretory features of this tissue, could serve as a target for causal treatment of cardiac cachexia.

Acknowledgements

We would like to thank, Denisa Toulova, Petr Stavek, Regina Stupalova, and Nora Stankova for excellent technical assistance with this study. The authors certify that they comply with the ethical guidelines for publishing in the *Journal of Cachexia, Sarcopenia and Muscle*: update 2017.⁴⁰

Conflict of interest

None declared.

Funding

Ministry of Health (AZV ČR 17-28784A, AZV16-27496A and NV19-02-00118) and the project for the development of research organization 00023001 IKEM—institutional support.

Online supplementary material

Additional supporting information may be found online in the Supporting Information section at the end of the article.

Data S1. Method S1 Untargeted metabolomic and lipidomic analysis of EAT

Table S1. PCR primers

Table S2. Expression of selected genes in EAT

Table S3. Drugs and other non-physiological analytes in EAT extracts

Table S4. Cardiolipin and phosphatidylglycerol species levels in EAT

Table S5. Clinical variables, medication and plasma parameters in Cluster A4- and Cluster B4-patients

Table S6. Expression of selected genes involved in cardiolipin synthesis in EAT

Figure S1. Chemical classes of all the analytes with known structure detected in EAT.

Figure S2. Correlations between levels of CLs and PGs in EAT.

Figure S3. Induction of EAT lipid metabolism linked to cachexia – formation and role of CL.

Dataset S1. All 750 analytes with known structure detected in EAT extracts from HF-patients, including isobars.

Dataset S2. Analytes in EAT extracts with known structures and significantly different mean levels in (A) BW-stable and cachectic, and (B) Cluster A4- and Cluster B4-patients, respectively.

References

1. Kenchaiah S, Pocock SJ, Wang D, Finn PV, Zornoff LA, Skali H, et al. Body mass index and prognosis in patients with chronic heart failure: insights from the Candesartan in heart failure: assessment of reduction in mortality and morbidity (CHARM) program. *Circulation* 2007;**116**: 627–636.
2. Horwich TB, Fonarow GC, Clark AL. Obesity and the obesity paradox in heart failure. *Prog Cardiovasc Dis* 2018;**61**:151–156.
3. Anker SD, Ponikowski P, Varney S, Chua TP, Clark AL, Webb-Peploe KM, et al. Wasting as independent risk factor for mortality in chronic heart failure. *Lancet* 1997;**349**: 1050–1053.
4. Melenovsky V, Kotrc M, Borlaug BA, Marek T, Kovar J, Malek I, et al. Relationships between right ventricular function, body composition, and prognosis in advanced heart failure. *J Am Coll Cardiol* 2013; **62**:1660–1670.
5. Evans WJ, Morley JE, Argilés J, Bales C, Baracos V, Guttridge D, et al. Cachexia: a new definition. *Clin Nutr* 2008;**27**:793–799.
6. Ponikowski P, Voors AA, Anker SD, Bueno H, Cleland JG, Coats AJ, et al. 2016 ESC Guidelines for the diagnosis and treatment of acute and chronic heart failure: The task force for the diagnosis and treatment of acute and chronic heart failure of the European Society of Cardiology (ESC). Developed with the special contribution of the Heart Failure Association (HFA) of the ESC. *Eur J Heart Fail* 2016;**18**:891–975.
7. Anker SD, Negassa A, Coats AJ, Afzal R, Poole-Wilson PA, Cohn JN, et al. Prognostic importance of weight loss in chronic heart failure and the effect of treatment with angiotensin-converting-enzyme inhibitors: an observational study. *Lancet* 2003;**361**:1077–1083.
8. Rohm M, Zeigerer A, Machado J, Herzig S. Energy metabolism in cachexia. *EMBO Rep* 2019;**20**:e47258.
9. Rohm M, Schafer M, Laurent V, Ustunel BE, Niopek K, Algire C, et al. An AMP-activated protein kinase-stabilizing peptide ameliorates adipose tissue wasting in cancer cachexia in mice. *Nat Med* 2016;**22**: 1120–1130.
10. Halle JL, Pena GS, Paez HG, Castro AJ, Rossiter HB, Visavadiya NP, et al. Tissue-specific dysregulation of mitochondrial respiratory capacity and coupling control in colon-26 tumor-induced cachexia. *Am J Physiol Regul Integr Comp Physiol* 2019; **317**:R68–R82.
11. Szabo T, Postrach E, Mahler A, Kung T, Turhan G, von Haehling S, et al. Increased catabolic activity in adipose tissue of patients with chronic heart failure. *Eur J Heart Fail* 2013;**15**:1131–1137.
12. Fosshaug LE, Dahl CP, Risnes I, Bohov P, Berge RK, Nymo S, et al. Altered levels of fatty acids and inflammatory and metabolic mediators in epicardial adipose tissue in patients with systolic heart failure. *J Card Fail* 2015;**21**:916–923.
13. Jaffer I, Riederer M, Shah P, Peters P, Quehenberger F, Wood A, et al. Expression of fat mobilizing genes in human epicardial adipose tissue. *Atherosclerosis* 2012;**220**: 122–127.
14. Kintscher U, Foryst-Ludwig A, Haemmerle G, Zechner R. The role of adipose triglyceride lipase and cytosolic lipolysis in cardiac function and heart failure. *Cell Rep Med* 2020;**1**:1–21.
15. Packer M. Epicardial adipose tissue may mediate deleterious effects of obesity and inflammation on the myocardium. *J Am Coll Cardiol* 2018;**71**:2360–2372.
16. Salatzki J, Foryst-Ludwig A, Bentele K, Blumrich A, Smeir E, Ban Z, et al. Adipose tissue ATGL modifies the cardiac lipidome in pressure-overload-induced left ventricular failure. *PLoS Genet* 2018;**14**: e1007171.
17. Doehner W, Frenneaux M, Anker SD. Metabolic impairment in heart failure: the myocardial and systemic perspective. *J Am Coll Cardiol* 2014;**64**:1388–1400.
18. Polak J, Kotrc M, Wedellova Z, Jabor A, Malek I, Kautzner J, et al. Lipolytic effects of B-type natriuretic peptide 1-32 in adipose tissue of heart failure patients compared with healthy controls. *J Am Coll Cardiol* 2011;**58**:1119–1125.
19. Moro C, Lafontan M. Natriuretic peptides and cGMP signaling control of energy homeostasis. *Am J Physiol Heart Circ Physiol* 2013;**304**:H358–H368.
20. Cabassi A, Coghi P, Govoni P, Barouhiel E, Speroni E, Cavazzini S, et al. Sympathetic modulation by carvedilol and losartan reduces angiotensin II-mediated lipolysis in subcutaneous and visceral fat. *J Clin Endocrinol Metab* 2005;**90**:2888–2897.
21. Kovacova Z, Tharp WG, Liu D, Wei W, Xie H, Collins S, et al. Adipose tissue natriuretic peptide receptor expression is related to insulin sensitivity in obesity and diabetes. *Obesity (Silver Spring)* 2016;**24**:820–828.
22. Voros G, Ector J, Garweg C, Droogne W, Van Cleemput J, Peersman N, et al. Increased cardiac uptake of ketone bodies and free fatty acids in human heart failure and hypertrophic left ventricular remodeling. *Circ Heart Fail* 2018;**11**:e004953.
23. Chong J, Soufan O, Li C, Caraus I, Li S, Bourque G, et al. MetaboAnalyst 4.0: towards more transparent and integrative metabolomics analysis. *Nucleic Acids Res* 2018;**46**:W486–W494.
24. Wakai E, Aritake K, Urade Y, Fujimori K. Prostaglandin D2 enhances lipid accumulation through suppression of lipolysis via DP2 (CRTH2) receptors in adipocytes. *Biochem Biophys Res Commun* 2017; **490**:393–399.
25. Guauque-Olarte S, Gaudreault N, Piche ME, Fournier D, Mauriege P, Mathieu P, et al. The transcriptome of human epicardial, mediastinal and subcutaneous adipose tissues in men with coronary artery disease. *PLoS One* 2011;**6**:e19908.
26. Mracek T, Stephens NA, Gao D, Bao Y, Ross JA, Ryden M, et al. Enhanced ZAG production by subcutaneous adipose tissue is linked to weight loss in gastrointestinal cancer patients. *Br J Cancer* 2011;**104**: 441–447.
27. Masoodi M, Kuda O, Rossmeisl M, Flachs P, Kopecky J. Lipid signaling in adipose tissue: connecting inflammation & metabolism. *Biochim Biophys Acta* 1851;**2015**: 503–518.
28. Buresova J, Janovska P, Kuda O, Krizova J, der Stelt IR, Keijer J, et al. Postnatal induction of muscle fatty acid oxidation in mice differing in propensity to obesity: a role of pyruvate dehydrogenase. *Int J Obes (Lond)* 2018;**44**:235–244.
29. Funcke JB, Scherer PE. Beyond adiponectin and leptin: adipose tissue-derived mediators of inter-organ communication. *J Lipid Res* 2019;**60**:1648–1684.
30. Dumas JF, Peyta L, Couet C, Servais S. Implication of liver cardiolipins in mitochondrial energy metabolism disorder in cancer cachexia. *Biochimie* 2013;**95**:27–32.
31. Peyta L, Jarnouen K, Pinault M, Coulouarn C, Guimaraes C, Goupille C, et al. Regulation of hepatic cardiolipin metabolism by TNFalpha: implication in cancer cachexia. *Biochim Biophys Acta* 2015;**1851**: 1490–1500.
32. Julienne CM, Tardieu M, Chevalier S, Pinault M, Bougnoux P, Labarthe F, et al. Cardiolipin content is involved in liver mitochondrial energy wasting associated with cancer-induced cachexia without the involvement of adenine nucleotide translocase. *Biochim Biophys Acta* 2014; **1842**:726–733.
33. Schlame M, Rua D, Greenberg ML. The biosynthesis and functional role of cardiolipin. *Prog Lipid Res* 2000;**39**:257–288.
34. Saini-Chohan HK, Mitchell RW, Vaz FM, Zelinski T, Hatch GM. Delineating the role

- of alterations in lipid metabolism to the pathogenesis of inherited skeletal and cardiac muscle disorders: thematic review series: genetics of human lipid diseases. *J Lipid Res* 2012;**53**:4–27.
35. Li J, Romestaing C, Han X, Li Y, Hao X, Wu Y, et al. Cardiolipin remodeling by ALCAT1 links oxidative stress and mitochondrial dysfunction to obesity. *Cell Metab* 2010;**12**:154–165.
36. Zhu HJ, Ding HH, Deng JY, Pan H, Wang LJ, Li NS, et al. Inhibition of preadipocyte differentiation and adipogenesis by zinc-alpha2-glycoprotein treatment in 3T3-L1 cells. *J Diabetes Investig* 2013;**4**:252–260.
37. Rognstad R, Katz J. The effect of 2,4-dinitrophenol on adipose-tissue metabolism. *Biochem J* 1969;**111**:431–444.
38. Rossmeisl M, Syrový I, Baumruk F, Flachs P, Janovska P, Kopecký J. Decreased fatty acid synthesis due to mitochondrial uncoupling in adipose tissue. *FASEB J* 2000;**14**:1793–1800.
39. Szeto HH, Liu S. Cardiolipin-targeted peptides rejuvenate mitochondrial function, remodel mitochondria, and promote tissue regeneration during aging. *Arch Biochem Biophys* 2018;**660**:137–148.
40. von Haehling S, Morley JE, Coats AJS, Anker SD. Ethical guidelines for publishing in the Journal of Cachexia, Sarcopenia and Muscle: update 2019. *J Cachexia Sarcopenia Muscle* 2019;**10**:1143–1145.

E. Borišincová a kol.

Impact of access route to the left ventricle on asymptomatic periprocedural brain injury: the results of a randomized trial in patients undergoing catheter ablation of ventricular tachycardia

Europace
Impact Factor: 4,620

Impact of access route to the left ventricle on asymptomatic periprocedural brain injury: the results of a randomized trial in patients undergoing catheter ablation of ventricular tachycardia

Eva Boršincová *, Petr Peichl, Dan Wichterle, Marek Šramko, Bashar Aldhoon, Janka Franeková, Robert Čihák, and Josef Kautzner

Department of Cardiology, Institute for Clinical and Experimental Medicine, Vídeňská 1958/9, 140 21 Prague, Czech Republic

Received 10 May 2020; editorial decision 20 September 2020; accepted after revision 24 September 2020

Aims

Catheter ablation of ventricular tachycardia (VT) is an effective treatment in patients with structural heart disease (SHD) and recurrent arrhythmias. However, the procedure is associated with the risk of complications, including both manifest and asymptomatic cerebral thromboembolic events. We hypothesized that periprocedural asymptomatic brain injury (ABI) can be reduced by using transseptal instead of the retrograde access route to the left ventricle (LV).

Methods and results

Consecutive patients undergoing VT ablation for SHD were randomized 1:1 to either retrograde or transseptal LV access. All patients underwent radiofrequency ablation in conscious sedation with the use of an irrigated tip catheter. The degree of brain damage was evaluated by serum level of biomarker S100B. Significant ABI was defined as a post-ablation relative increase of S100B level >30%. A total of 144 patients (66 ± 9 years; 14 females; 90% coronary artery disease; LV ejection fraction: 30 ± 8%) were enrolled and 72 were allocated to each study groups. Symptomatic neurological complication of the procedure was not observed in any subject. A significant ABI was detected in 19.4% of patients. It was more commonly observed in subjects randomized to retrograde vs. transseptal LV access (26.4% vs. 12.5%, $P=0.04$). In a multivariate analysis, only retrograde LV access and advanced age were independent determinants of significant ABI.

Conclusion

Significant ABI after ablation of VT in patients with SHD can be detected in one-fifth of subjects. Retrograde access to LV is associated with a two-fold higher probability of significant ABI.

Keywords

Ventricular tachycardia • Catheter ablation • Complications

Introduction

Catheter ablation is an effective treatment option for recurrent ventricular tachycardia (VT) in patients with structural heart disease (SHD). One of the most devastating complications of this procedure is cerebral thromboembolism. Although the incidence of periprocedural stroke associated with VT ablation is low,^{1,2} a certain

proportion of events may be silent. Previous studies have evaluated the occurrence of asymptomatic brain injury (ABI) after catheter ablation of atrial fibrillation^{3,4} using diffusion-weighted magnetic resonance imaging (MRI) and/or transcranial measurement of cerebral microembolic signals.⁵ We have previously shown that assessment of biomarker S100B may be used as an alternative diagnostic method for the detection of periprocedural cerebral injury.⁶ In a recent study

* Corresponding author. Fax: +420 261 362 982. E-mail address: bore@ikem.cz

Published on behalf of the European Society of Cardiology. All rights reserved. © The Author(s) 2020. For permissions, please email: journals.permissions@oup.com.

What's new?

- Periprocedural brain injury can be detected in one-fifth of patients with structural heart disease undergoing ventricular tachycardia ablation at left ventricular endocardium under conscious sedation.
- Retrograde compared with transseptal left ventricular access showed a two-fold higher probability of significant brain damage.

by Whitman et al.,⁷ catheter ablation of VT was associated with detectable ABI in 58% of patients. The risk factors responsible for these events are speculative.

In the current study, we investigated whether the degree of periprocedural brain injury in patients with SHD undergoing catheter ablation of VT will differ with respect to the access route to the left ventricle (LV). Specifically, we hypothesized that ABI can be reduced using transseptal instead of retrograde LV access.

Methods

Study protocol

Patients referred for radiofrequency (RF) catheter ablation of VT were recruited in the period between September 2013 and March 2017. The presence of SHD with presumable LV endocardial arrhythmogenic substrate was the main inclusion criterion. Patients were excluded in case of a mechanical valve in either a mitral or aortic position that would preclude random assignment of LV access route. We did not enrol patients scheduled for pericardial access as well as those with suggestive LV outflow tract substrate, which would likely require a retrograde access. Patients with other (non-procedural) conditions that may result in the cerebral lesion (e.g. after cardiopulmonary resuscitation or recent ablation) or interfere with laboratory diagnostics (significant renal disease) were also excluded. Eligible patients were assigned to two treatment groups (retrograde or transseptal LV access) in 1:1 fashion by covariate-adaptive randomization algorithm considering age, gender, LV ejection fraction, and serum creatinine level.

Evaluation of brain injury

Peripheral venous blood sampling for assessment of protein S100B was performed immediately before the ablation procedure and in the morning on the next day. Serum samples were stored at -70°C for batch analysis by a commercially available electrochemiluminescence immunoassay (Elecys S100 R, Roche Diagnostics, Mannheim, Germany). The test can detect protein S100B concentrations ranging from 5 to 39,000 ng/L with inter- and intra-assay coefficient of variation of 5.6% and 2.3%. Significant ABI was defined as a post-ablation relative increase of S100B level $>30\%$.

Periprocedural anticoagulation management

In all patients with long-term anticoagulation therapy, the procedure was performed after temporary interruption of warfarin therapy, which was bridged by low-molecular-weight heparin. Direct oral anticoagulants were used only in a minority of patients in the study and if so, the treatment was interrupted 24–48 h prior to the procedure according to the renal function. In patients on antiplatelet therapy, no changes were made.

After achieving the vascular access, loading dose of unfractionated heparin (10,000 IU) was given (in case of transseptal LV access, 5000 IU prior and 5000 IU immediately after the puncture). Then, heparin was administered by intermittent boluses to maintain the activated clotting time (ACT) in the range of 300–350 s. The ACT was checked by Hemochron ACT+ (Accriva Diagnostics, San Diego, CA, USA) at 15-min intervals until therapeutic anticoagulation was achieved, and then every 15–30 min for the duration of the procedure. For purpose of the study, the mean and minimum ACT during the procedure was calculated. The mean time-weighted ACT (i.e. more representative index reflecting variable intervals between ACT sampling) was also computed.

After the ablation procedure and removal of sheaths, all patients received an infusion of unfractionated heparin with a target activated partial thromboplastin time ratio of 1.5–2.5. The next day after venous blood sampling for the assessment of S100B patients received either antiplatelet therapy for a minimum of 6 weeks or anticoagulation therapy for 3 months in case of an extensive ablation in the LV.

Catheter ablation procedure

The procedure was performed in conscious sedation using midazolam and alfentanil. Vascular access was achieved without ultrasound guidance. Mapping and ablation strategy was described elsewhere.² Briefly, if the VT did not occur spontaneously, the programmed stimulation protocol from the two right ventricular sites and up to three extrastimuli was applied to induce clinical VT. The mapping was performed under fluoroscopy guidance and with a three-dimensional electroanatomical mapping system (CARTO, Biosense Webster, Diamond Bar, CA, USA). The use of intracardiac echocardiography (ICE) was at the discretion of the operator. For ablation, a 3.5 mm, saline-irrigated tip ablation catheter (Navistar Thermocool, Biosense Webster) was used.

Left ventricle access (retrograde vs. transseptal) was obtained based on the randomization. Intracardiac echocardiography was used for the guidance of transseptal puncture in all cases. Substrate mapping was used in the majority of cases and was performed during the spontaneous rhythm and/or during right ventricular pacing. It predominantly consisted of sequential point-by-point bipolar voltage mapping with ablation catheter, tagging of late potentials or local abnormal ventricular activity regions, and pacing from different sites with a minimum output to assess slow ventricular conduction and morphology of the resulting QRS complex. No multipolar mapping catheter was used in the study. In patients with haemodynamically tolerated or incessant VT, three-dimensional activation mapping was initiated during tachycardia and entrainment manoeuvres were utilized. Subsequently, substrate mapping/ablation was finalized after abolition of clinical VT.

Ablation was performed in power control mode with an irrigation flow of 30 mL/min. Power was set up to 20–45 W, depending on location and catheter contact, and was down-regulated in case of catheter tip temperature rise above 43°C or rapid drop of impedance ($>10\text{--}15\ \Omega$) during ablation. Whenever ICE was used during the procedure, it was used to monitor RF delivery and prevent tissue overheating and steam pop. Radiofrequency current was applied in the majority of cases for a maximum of 60 s per target site. Pacing at 10 mA was used after RF delivery to verify non-capture at a given site. Catheter ablation was performed to abolish all inducible monomorphic VTs.

Study follow-up

The dedicated institutional tracking system was used to identify all complications during the procedure and within the minimum 3-month follow-up.

Table 1 The baseline and procedural characteristics

	Retrograde access	Transseptal access	P-value
Male (%)	88.9	91.7	0.57
Age (years)	65.9 ± 7.5	66.9 ± 9.7	0.52
BMI (kg/m ²)	29.7 ± 4.6	29.6 ± 5.5	0.96
Hypertension (%)	86.1	75.0	0.14
Diabetes (%)	37.5	38.9	1.00
Previous stroke/TIA (%)	4.2	18.1	0.02
Coronary artery disease (%)	87.5	91.7	0.59
LVEF (%)	30.4 ± 9.3	29.8 ± 7.4	0.67
CHA ₂ DS ₂ -VASc score	4.0 ± 1.2	4.3 ± 1.5	0.24
ICD (%)	86.1	94.4	0.16
Atrial fibrillation (%)	33.3	44.4	0.23
Warfarin (%)	37.5	50.0	0.18
NOAC (%)	8.3	4.2	0.49
Antiplatelet therapy (%)	55.6	52.8	0.87
Serum creatinine (μmol/L)	112.7 ± 31.7	112.0 ± 30.9	0.89
Radiofrequency time (min)	31.8 ± 15.7	30.1 ± 13.3	0.49
Procedure time (min)	187 ± 44	182 ± 48	0.47
Procedural DC shocks (n)	0.5 ± 0.8	0.5 ± 0.9	0.84
Activation mapping of VT (%)	25.0	20.8	0.55
Mean power (W)	28.8 ± 3.5	29.9 ± 2.4	0.06
Pre-procedural INR	1.22 ± 0.26	1.48 ± 0.57	0.12
Heparin dose (1000 IU)	23.0 ± 6.8	19.9 ± 6.3	0.006
Mean ACT (s)	308 ± 33	320 ± 25	0.05
Minimum ACT (s)	239 ± 49	255 ± 45	0.04
Mean time-weighted ACT (s)	314 ± 32	326 ± 23	0.05

ACT, activated clotting time; BMI, body mass index; DC, direct current; ICD, implantable cardioverter-defibrillator; INR, international normalized ratio; LVEF, left ventricular ejection fraction; NOAC, new oral anticoagulant; TIA, transient ischaemic attack; VT, ventricular tachycardia.

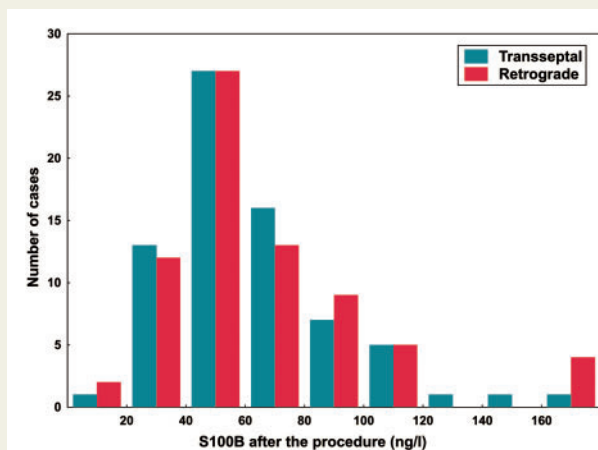


Figure 1 Histogram of absolute levels of S100B after the procedure.

Statistical analysis

Continuous variables were expressed as means with standard deviations and compared with *t*-test for independent samples or Mann–Whitney *U*

test or Wilcoxon paired test, as appropriate. Categorical variables were expressed as percentages and compared with χ^2 test or Fisher's exact test. Factors associated with outcome measure ($P < 0.20$) were entered into a multivariate linear regression model and investigated by a stepwise forward method. A P -value < 0.05 was considered significant. All analyses were performed using the STATISTICA version 10 software (Statsoft, Inc., Tulsa, USA).

Results

Altogether 144 patients were enrolled and randomly allocated into two study groups (72 in each group). Baseline characteristics and procedural data are shown in *Table 1*. Both groups were comparable in baseline characteristics except for the history of a previous cerebral ischaemic event that was more common in transseptal LV access group. In addition, patients in the retrograde LV access group required more intravenous heparin to achieve target ACT levels.

Level of S100B biomarker at baseline was comparable (67 ± 39 vs. 73 ± 50 ng/L, $P = 0.40$) in retrograde vs. transseptal LV access group. It non-significantly increased in patients with retrograde LV access (from 67 ± 39 to 75 ± 77 ng/L, $P = 0.20$) and decreased in patients with transseptal LV access (from 73 ± 50 to 63 ± 29 ng/L, $P = 0.16$). Post-procedure level of S100B for both study groups are displayed in

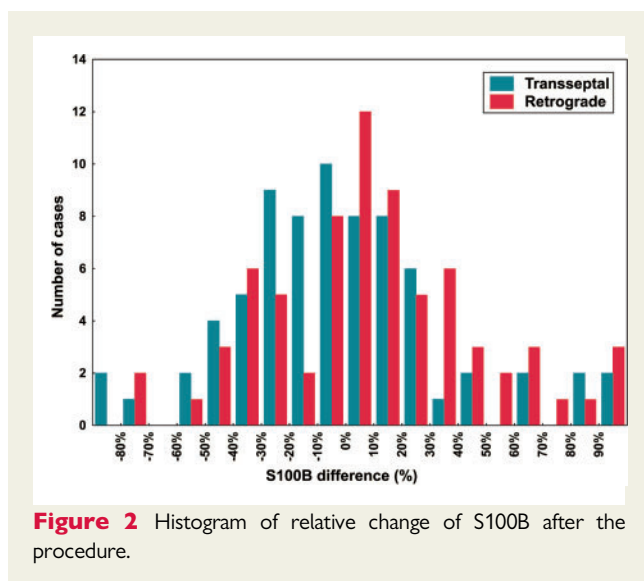


Figure 2 Histogram of relative change of S100B after the procedure.

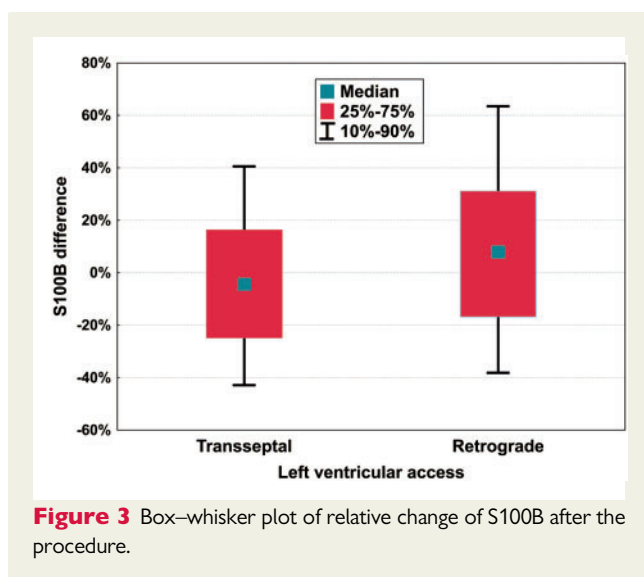


Figure 3 Box-whisker plot of relative change of S100B after the procedure.

Figure 1. Between-group differences in procedure-related change of S100B level were borderline non-significant: 8 ± 67 vs. -10 ± 48 ng/L ($P = 0.053$) in absolute units and $16 \pm 73\%$ vs. $0 \pm 44\%$ ($P = 0.052$) relatively for retrograde vs. transseptal LV access, respectively (Figures 2 and 3). The significant ABI defined as a post-ablation relative increase of S100B level $>30\%$ was found in 19.4% of patients. This was observed more often in patients from retrograde vs. transseptal LV access group: 19/72 (26.4%) vs. 9/72 (12.5%), $P = 0.04$. No symptomatic neurological events were noted during and after the procedure in any subject.

The results of linear regression analysis are shown in Table 2. Univariately, only retrograde LV access was associated with significant ABI. The association was borderline ($P < 0.20$) for four other factors: age, body mass index, LV ejection fraction, and procedure time. In multivariate analysis, only two factors were independently

Table 2 Predictors of significant ABI by linear regression analysis

	Univariate			Multivariate		
	Coeff	SE	P-Value	Coeff	SE	P-value
Age (years)	0.71	0.38	0.06	0.75	0.38	0.046
BMI (kg/m^2)	-1.2	0.7	0.08			
LVEF (%)	0.57	0.39	0.15			
Retrograde LV access (1/0)	13.9	6.5	0.04	14.6	6.5	0.03
Procedure time (min)	0.103	0.072	0.16			

Table shows only factors that were univariately associated ($P < 0.20$) with significant ABI.

ABI, asymptomatic brain injury; BMI, body mass index; Coeff = slope of regression line between individual factor (unit specified) and the rate of significant ABI (in percentages); LVEF, left ventricular ejection fraction; LV, left ventricle; SE, standard error of coefficient.

associated with significant ABI. Patients with retrograde LV access had the rate of significant ABI higher by absolute $15 \pm 6\%$ ($P = 0.03$) compared with patients with transseptal LV access. Each decade of age increased the rate of significant ABI by absolute $8 \pm 4\%$ ($P = 0.046$).

Acute efficacy of the procedure

In 24/144 (17%) procedures (12 in each study group), the final programmed ventricular stimulation was not performed due to initial VT non-inducibility. Programmed ventricular stimulation was applicable in 120 of the procedures, of which non-inducibility of any VT was achieved in 77 procedures (64%); 40/60 (67%) and 37/60 (62%) in the retrograde and transseptal group, respectively ($P = 0.57$). The acute outcome was not related to S100B change.

Periprocedural complications

The overall rate of complications was 6.3% without the difference between the retrograde vs. transseptal LV access (6.9% vs. 5.5%). One patient in each group presented with cardiac tamponade. One patient in the transseptal LV access group had acute haemodynamic decompensation with the need for inotropic support. There were two pseudoaneurysms in the retrograde group and none in the transseptal group. There were three local haematomas with a drop of haemoglobin >20 g/L; two in transseptal and one in retrograde LV access group.

Discussion

This randomized clinical trial compared two access routes with the LV during endocardial VT ablation in patients with SHD. Subclinical periprocedural brain damage as assessed by the S100B biomarker was the outcome measure. The main findings can be summarized as follows: (i) significant ABI after LV endocardial ablation can be detected in one-fifth of patients and (ii) retrograde access to LV is associated with a two-fold higher probability of significant ABI.

Because of the study design and the main objective, only a subset of VT patients was investigated excluding those with VT targeted in right ventricle only and those with restricted route to LV substrate either because of mechanical valves or preferential access like in case of LV outflow tract tachycardias. Patients scheduled for pericardial access were also excluded because: (i) epicardial ablation alone has low embolic potential but may be associated with local neural lesions resulting in S100B elevation⁸; (ii) concomitant endocardial ablation, if necessary, is usually performed in a retrograde fashion; and (iii) general anaesthesia is used for all patients with planned epicardial ablation unlike all other patients in our cohort. None of enrolled patients was converted to epicardial ablation during the study procedure.

Brain injury biomarker

The protein S100B is a relatively small protein that belongs to the family of calcium-binding proteins. It is found predominantly found in mature astrocytes, but it may be present in other nervous cells. Its escalated blood levels suggest a neurological dysfunction and cell death. It is released within 24 h after brain injury and its levels correlate with magnitude of neurological deficit and brain injury in stroke.⁹ Serial S100B testing has been used for monitoring during various cardiovascular interventions such as carotid endarterectomy,¹⁰ carotid stenting¹¹ or TAVI.¹² In our previous study, we evaluated correlation between serum S100B levels and cerebral lesions by MRI.⁶

Risk of periprocedural brain injury

Subclinical cerebral microembolism is reported frequently after cardiac interventional procedures. Coronary angiography has shown the incidence of 10–15% ischaemic events after procedure,¹³ and in diagnostic aortic valve procedures¹⁴ the number raised to 22%. Transcatheter aortic valve replacement could be associated with up to 84% occurrence of new brain embolic lesions.¹⁵

In patients undergoing catheter ablation of atrial fibrillation, the reported rate of ABI ranges between 1.7% and 67%, depending on diagnostic criteria, ablation strategy and diagnostic modality.^{3,5,16,17} Despite relatively high incidence of ABI, most of the lesions resolve.⁴ There is no evidence that neurological deficit could evolve during 6–12 months of follow up.¹⁸ On the other hand, some studies have demonstrated that even asymptomatic lesions may have adverse neurocognitive effects.^{19,20}

The rate of ABI and corresponding risk factors in a patient undergoing VT ablation has been much less studied. In a study by Whitman *et al.*,⁷ catheter ablation of VT (left-sided procedure) was associated with detectable ABI by MRI in 7/12 (58%) patients. This is substantially higher rate than that in our study (overall 19.4%) and the difference is more striking as our patients had mostly advanced heart disease with low LV ejection fraction and more ablation lesions were delivered. Obviously, methods for ABI detection in both studies are clearly not comparable. The major procedural differences between both studies were retrograde LV access in 92% of patients in a study by Whitman *et al.*, longer procedure time (351 ± 58 vs. 185 ± 46 min) and usage of general anaesthesia. Whether these additional factors could impact the ABI should be investigated in future studies.

The same applies to selecting the optimum ACT level. Anticoagulation was slightly more intensive in transseptal access group, but we did not observe a significant association between both mean and minimum ACT during the procedure and the rate of ABI.

However, ACT range as per protocol was rather narrow (300–350 s) which decreased the power to detect any relationship.

Procedural DC shocks may trigger thromboembolic events and contribute to the development of ABI. Direct current shock count did not differ between study groups and was not related to S100B rise. The mean number of shocks was relatively low as most of the induced VTs were terminated by overdrive pacing. In addition, no sustained VT was inducible in substantial proportion of patients (17%) at the beginning of the procedure.

Transseptal vs. retrograde left ventricle access

Multiple mechanisms might be responsible for documented higher rate of ABI associated with retrograde LV access. The cerebral lesions might be attributed to the disruption of either aortic atheroma or debris from the degenerative aortic valves due to multiple attempts to cross the valve. This is relevant to patients with SHD undergoing VT ablation, in whom vascular/valvular disease is common. Irrespective of study findings, preferential use of transseptal LV access facilitates the implementation of the strategy of uninterrupted anticoagulation, which has further potential to reduce the ABI even lower than that demonstrated in this study that enrolled earlier cohorts of patients who all discontinued their oral anticoagulation therapy.

Although retrograde LV access with arterial cannulation may be associated with a higher risk of vascular complications at the puncture site, no significant difference was observed in our study because the overall incidence of vascular complications was very low.

Limitations

The study has several limitations. First, it is a single-centre study that limits the transfer of results into clinical practice. Secondly, detailed neurological evaluation prior/after the ablation procedure was not a part of the study design and we did not verify the raise of S100B by MRI which is considered the gold standard for neural lesion detection. However, no patient showed neurological deficit after the procedure and the majority of patients had ICD, which constitutes relative contraindication to this imaging modality. Thirdly, rate of 'significant' S100B elevation was much lower than expected based on our previous study in population of patients after ablation for atrial fibrillation so that arbitrary cut-off value of >30% was selected for post hoc analysis. Fourthly, post-ablation sample of S100B was taken in the morning on the next day so that the latency was <24 h in small proportion of afternoon procedures. Finally, direct oral anticoagulants were used only sparsely during the study period. Whether their more frequent use would change the outcome of current study is unclear.

Conclusions

Periprocedural brain injury can be detected in one-fifth of patients with SHD undergoing VT ablation at LV endocardium under conscious sedation. Retrograde compared with transseptal LV access showed a two-fold higher probability of significant brain damage. Further studies are needed to elucidate clinical significance of asymptomatic elevation of the S100B marker.

Funding

This study was supported by the Research Grant of the Ministry of Health, Czech Republic—Conceptual development of research organization ('Institute for Clinical and Experimental Medicine—IKEM, IN 00023001').

Conflict of interest: P.P. has received speaker's honoraria from Abbott, BiosenseWebster, Pfizer, Biotronik, Medtronic, and MDS. R.Č. has received speaker's honoraria from Medtronic, Pfizer, and MSD. J.K. has received speaker's honoraria from Boehringer Ingelheim, Biosense Webster, Biotronik, Boston Scientific, Bristol Myers Squibb, Daiichi Sankyo, Medtronic, Merck Sharp & Dohme, Pfizer, and Abbott—St. Jude Medical and has served as a consultant for Bayer, Boehringer Ingelheim, Biosense Webster, Daiichi Sankyo, Medtronic, Merit Medical, and Abbott—St. Jude Medical. All other authors report no conflict of interest.

Data availability

The data underlying this article will be shared on reasonable request to the corresponding author.

References

1. Cronin EM, Bogun FM, Maury P, Peichl P, Chen M, Nambodiri N et al. HRS/EHRA/APHRS/LAHRS expert consensus statement on catheter ablation of ventricular arrhythmias. *Europace* 2019;**21**:1143–4.
2. Peichl P, Wichterle D, Pavlu L, Cihak R, Aldhoon B, Kautzner J. Complications of catheter ablation of ventricular tachycardia: a single-center experience. *Circ Arrhythm Electrophysiol* 2014;**7**:684–90.
3. Herrera Siklódy C, Deneke T, Hocini MM, Lehrmann H, Shin D-II, Miyazaki S et al. Incidence of asymptomatic intracranial embolic events after pulmonary vein isolation comparison of different atrial fibrillation ablation technologies in a multi-center study. *J Am Coll Cardiol* 2011;**58**:681–8.
4. Deneke T, Shin D-I, Balta O, Bünz K, Fassbender F, Mügge A et al. Postablation asymptomatic cerebral lesions: long-term follow-up using magnetic resonance imaging. *Heart Rhythm* 2011;**8**:1705–11.
5. Nagy-Baló E, Tint D, Clemens M, Beke I, Kovács KR, Csiba L et al. Transcranial measurement of cerebral microembolic signals during pulmonary vein isolation. *Circ Arrhythm Electrophysiol* 2013;**6**:473–80.
6. Sramko M, Peichl P, Wichterle D, Tintera J, Maxian R, Weichet J et al. A novel biomarker-based approach for the detection of asymptomatic brain injury during catheter ablation of atrial fibrillation. *J Cardiovasc Electrophysiol* 2014;**25**:349–54.
7. Whitman IR, Gladstone RA, Badhwar N, Hsia HH, Lee BK, Josephson SA et al. Brain emboli after left ventricular endocardial ablation. *Circulation* 2017;**135**:867–77.
8. Scherschel K, Hedenus K, Jungen C, Lemoine MD, Rübsamen N, Veldkamp MW et al. Cardiac glial cells release neurotrophic S100B upon catheter-based treatment of atrial fibrillation. *Sci Transl Med* 2019;**11**. DOI: 10.1126/scitranslmed.aav7770.
9. Elting JW, De Jager AEJ, Teelken AW, Schaaf MJ, Maurits NM, Van Der Naalt J et al. Comparison of serum S-100 protein levels following stroke and traumatic brain injury. *J Neural Sci* 2000;**181**:104–10.
10. Falkensammer J, Oldenburg WA, Hendrzak AJ, Neuhauser B, Pedraza O, Ferman T et al. Evaluation of subclinical cerebral injury and neuropsychologic function in patients undergoing carotid endarterectomy. *Ann Vasc Surg* 2008;**22**:497–504.
11. Mattusch C, Diederich KW, Schmidt A, Scheinert D, Thiele H, Schuler G et al. Effect of carotid artery stenting on the release of S-100B and neurone-specific enolase. *Angiology* 2011;**62**:376–80.
12. Reinsfelt B, Westerlind A, Ioanes D, Zetterberg H, Fredén-Lindqvist J, Ricksten SE. Transcranial Doppler microembolic signals and serum marker evidence of brain injury during transcatheter aortic valve implantation. *Acta Anaesthesiol Scand* 2012;**56**:240–7.
13. Büsing KA, Schulte-Sasse C, Flüchter S, Süsselbeck T, Haase KK, Neff W et al. Cerebral infarction: incidence and risk factors after diagnostic and interventional cardiac catheterization—prospective evaluation at diffusion-weighted MR imaging. *Radiology* 2005;**235**:177–83.
14. Omran H, Schmidt H, Hackenbroch M, Illien S, Bernhardt P, von der Recke G et al. Silent and apparent cerebral embolism after retrograde catheterisation of the aortic valve in valvular stenosis: a prospective, randomised study. *Lancet* 2003;**361**:1241–6.
15. Kahlert P, Knipp SC, Schlamann M, Thielmann M, Al-Rashid F, Weber M et al. Silent and apparent cerebral ischemia after percutaneous transfemoral aortic valve implantation: a diffusion-weighted magnetic resonance imaging study. *Circulation* 2010;**121**:870–8.
16. Gaita F, Leclercq JF, Schumacher B, Scaglione M, Toso E, Halimi F et al. Incidence of silent cerebral thromboembolic lesions after atrial fibrillation ablation may change according to technology used: comparison of irrigated radiofrequency, multipolar nonirrigated catheter and cryoballoon. *J Cardiovasc Electrophysiol* 2011;**22**:961–8.
17. Yu Y, Wang X, Li X, Zhou X, Liao S, Yang W et al. Higher incidence of asymptomatic cerebral emboli after atrial fibrillation ablation found with high-resolution diffusion-weighted magnetic resonance imaging. *Circ Arrhythm Electrophysiol* 2020;**13**:e007548.
18. Herm J, Fiebich JB, Koch L, Kopp UA, Kunze C, Wollboldt C et al. Neuropsychological effects of MRI-detected brain lesions after left atrial catheter ablation for atrial fibrillation: long-term results of the MACPAF study. *Circ Arrhythm Electrophysiol* 2013;**6**:843–50.
19. Medi C, Evered L, Silbert B, Teh A, Halloran K, Morton J et al. Subtle post-procedural cognitive dysfunction after atrial fibrillation ablation. *J Am Coll Cardiol* 2013;**62**:531–9.
20. Puskas JD, Stringer A, Hwang SN, Hatfield B, Smith AS, Kilgo PD et al. Neurocognitive and neuroanatomic changes after off-pump versus on-pump coronary artery bypass grafting: long-term follow-up of a randomized trial. *J Thorac Cardiovasc Surg* 2011;**141**:1116–27.

P. Kala a kol.

Deleterious Effects of Hyperactivity of the Renin-Angiotensin System and Hypertension on the Course of Chemotherapy-Induced Heart Failure after Doxorubicin Administration: A Study in Ren-2 Transgenic Rat

International Journal of Molecular Sciences
Impact Factor: 4,556



Article

Deleterious Effects of Hyperactivity of the Renin-Angiotensin System and Hypertension on the Course of Chemotherapy-Induced Heart Failure after Doxorubicin Administration: A Study in Ren-2 Transgenic Rat

Petr Kala ^{1,2,*}, Hana Bartušková ^{2,†}, Jan Piřha ², Zdenka Vaňourková ², Soňa Kikerlová ², Šárka Jířhová ², Vojtěch Melenovský ³, Lenka Hořková ³, Josef Veselka ¹, Elzbieta Kompanowska-Jeziarska ⁴, Janusz Sadowski ⁴, Olga Gawrys ^{2,4}, Hana Maxová ⁵ and Luděk Červenka ^{2,5}

¹ Department of Cardiology, University Hospital Motol and 2nd Faculty of Medicine, Charles University, 150 06 Prague, Czech Republic; josef.veselka@fnmotol.cz

² Center for Experimental Medicine, Institute for Clinical and Experimental Medicine, 140 21 Prague, Czech Republic; hana.bartuskova@ikem.cz (H.B.); jan.pitha@ikem.cz (J.P.); zdenka.vanourkova@ikem.cz (Z.V.); sona.kikerlova@ikem.cz (S.K.); sarka.jichova@ikem.cz (Š.J.); olga.gawrys@ikem.cz (O.G.); ludek.cervenka@ikem.cz (L.Č.)

³ Department of Cardiology, Institute for Clinical and Experimental Medicine, 140 21 Prague, Czech Republic; vojtech.melenovsky@ikem.cz (V.M.); lenka.hoskova@ikem.cz (L.H.)

⁴ Department of Renal and Body Fluid Physiology, Mossakowski Medical Research Centre, Polish Academy of Sciences, 01-224 Warsaw, Poland; ekompanowska@imdik.pan.pl (E.K.-J.); jsadowski@imdik.pan.pl (J.S.)

⁵ Department of Pathophysiology, 2nd Faculty of Medicine, Charles University, 110 00 Prague, Czech Republic; hana.maxova@lfmotol.cuni.cz

* Correspondence: petrkala@gmail.com

† These authors contributed equally to this work.

Received: 21 November 2020; Accepted: 4 December 2020; Published: 8 December 2020



Abstract: Doxorubicin's (DOX) cardiotoxicity contributes to the development of chemotherapy-induced heart failure (HF) and new treatment strategies are in high demand. The aim of the present study was to characterize a DOX-induced model of HF in Ren-2 transgenic rats (TGR), those characterized by hypertension and hyperactivity of the renin-angiotensin-aldosterone system, and to compare the results with normotensive transgene-negative, Hannover Sprague-Dawley (HanSD) rats. DOX was administered for two weeks in a cumulative dose of 15 mg/kg. In HanSD rats DOX administration resulted in the development of an early phase of HF with the dominant symptom of bilateral cardiac atrophy demonstrable two weeks after the last DOX injection. In TGR, DOX caused substantial impairment of systolic function already at the end of the treatment, with further progression observed throughout the experiment. Additionally, two weeks after the termination of DOX treatment, TGR exhibited signs of HF characteristic for the transition stage between the compensated and decompensated phases of HF. In conclusion, we suggest that DOX-induced HF in TGR is a suitable model to study the pathophysiological aspects of chemotherapy-induced HF and to evaluate novel therapeutic strategies to combat this form of HF, which are urgently needed.

Keywords: chemotherapy-induced heart failure; doxorubicin; hypertension; renin-angiotensin-aldosterone system

1. Introduction

The past two decades have brought a remarkable improvement in the treatment of diverse cancer forms. Worldwide, good outcomes of the disease are estimated at 4% of the population [1,2]. However, the success of cancer treatment was achieved at a considerable cost [3–5]. This was connected with the properties of anthracyclines, discovered 60 years ago but still listed among the World Health Organization (WHO) recommended drugs for the treatment of childhood and adult cancer [4,6–9]

Acute cardiotoxicity of anthracyclines, especially the most commonly used doxorubicin (DOX), is observed during the first year of treatment. In pediatric patients, its incidence is low, owing to a cautious dosing regime, which limits drug cumulation. Furthermore, in young patients, pre-existing cardiovascular diseases (hypertension, hyperlipidemia), the recognized risk factors, are uncommon [10–15].

Unfortunately, in the long run, because of the cardiotoxicity of DOX the susceptibility of the treated patients to cardiac damage and the development of heart failure (HF) is dramatically higher (15fold) than in the untreated population [8,16,17]. This is observed both in children and adults. While it is common knowledge that one in eight women will develop breast cancer, we are only rarely aware that one in ten breast cancer patients whose chemotherapy regime includes DOX will develop cardiac damage and not infrequently DOX-induced HF [3,9,15]. Its incidence increases progressively, and the current standard therapeutic measures applied in DOX-induced HF prove less effective than in HF patients of other etiology [8,13,18–20].

Important progress has been made in effort to develop mitochondria-specific delivery of DOX (or similar anthracyclines) to tumor mitochondria, which would increase its accumulation in the tumor tissue and reduce exposure of the heart. Hence, it should result in a simultaneous increase in the efficiency and safety of DOX in cancer chemotherapy. Such attempt has been made by amphiphilic modification of DOX, which seems to be a very promising tool in the future [21]. However, despite intensive research and progress, to the best of our current knowledge, no mitochondria-targeting formulations of DOX have been approved for the clinical use. In addition, it is important to recognize that even after potential introducing of new modification of DOX, with expected minimal off-target toxicity, for many decades a large cohort of patients, particularly childhood cancer survivors, will be still endangered by the development of HF induced by the classic doxorubicin [7].

Hence, it is recognized that new treatment strategies for chemotherapy-induced HF are needed, however, the prerequisite for any success is the profound understanding of the pathophysiology of this HF form.

Without disregarding some obvious limitations, the small animal models of HF have proven to be invaluable tools that have greatly advanced our understanding of the pathophysiology of HF, and have helped to define new targets in the development of novel treatment strategies [22,23]. A number of mouse, rat, and rabbit models of cardiotoxicity induced by cancer treatment regimes (particularly DOX and trastuzumab, a monoclonal antibody applied in breast and stomach cancer) were proposed [24]. They were mostly employed to investigate the mechanisms and/or protective measures against chemotherapy-induced cardiotoxicity [24–29]. The effects of DOX on cardiac function and the development of HF were only of marginal interest [30–33]. It is worth mentioning that the value of other models of HF, such as ischemic injury (coronary artery ligation [34]) and non-ischemic HF (chronic volume overload induced by aorto-caval fistula (ACF) [35]) have been characterized in detail [22,23].

Considering an urgent need to further elucidate the pathophysiology of chemotherapy-induced HF and the insufficient *in vivo* characterization of a DOX-induced model of HF, the major aim of the present study was to evaluate cardiac morphological structure and the function parameters in rats with DOX-induced HF. Echocardiography and invasive pressure-volume analysis of the left ventricle (LV) were employed at the very early phase of HF development. In addition, the systemic and intrarenal activity status of neurohormonal systems were simultaneously evaluated.

Since hypertension and inappropriate activation of the renin-angiotensin-aldosterone system (RAAS) are considered as risk factors for the development of chemotherapy-induced cardiotoxicity, cardiomyopathy and ultimately chemotherapy-induced HF [11,15], we decided to explore the characteristics of the DOX-induced model of HF in Ren-2 transgenic rats (TGR), in which the endogenous activation of the RAAS and hypertension are combined [33,36,37], and to compare them with those of normotensive transgene-negative, Hannover Sprague-Dawley (HanSD) rats.

2. Results

2.1. Series 1: Echocardiographic Assessment of the Longitudinal Changes in Cardiac Function throughout DOX Administration

Figures 1 and 2 summarize the results from evaluation of cardiac function and morphology by echocardiography. In HanSD rats the administration of DOX resulted in the decline in cardiac output, stroke volume, LV ejection fraction and in LV fractional shortening, without altering heart rates. All the above-mentioned changes were observed two weeks after the last injection (4 weeks values, Figure 1A–E). In the case of TGR, all the mentioned changes were also present, however, they were observed earlier and were also more pronounced, i.e., at the end of DOX administration (2 weeks values). Explicitly, two weeks after last injection (4 week values), DOX treatment caused in TGR significantly greater decreases than in HanSD rats in cardiac output (-34.6 ± 0.9 vs. $-24.1 \pm 0.7\%$), stroke volume (-25.9 ± 0.8 vs. $-20.6 \pm 0.4\%$), LV ejection fraction (-24.6 ± 0.6 vs. $-15.9 \pm 0.5\%$), and LV fractional shortening (-31.7 ± 2.4 vs. $13.1 \pm 0.6\%$)— $p < 0.05$ in all cases.

As shown in Figure 2A there was no significant difference in the LV diastolic diameter between TGR and HanSD rats under basal conditions, and administration of DOX did not change it in any of experimental groups or at any time point. The hypertensive TGR under basal conditions revealed, under basal conditions, markedly higher LV anterior and posterior wall thickness as compared with normotensive HanSD rats (both in diastole and systole) (Figure 2B–E). DOX treatment resulted in reduction of LV wall thickness in both TGR and HanSD rats as compared with the untreated counterparts (Figure 2B–E), as observed two weeks after termination of the treatment (4 week values). This effect was more distinct for LV posterior wall thickness (both in diastole and systole), than in the anterior wall (significant only in systole). In addition, as shown in Figure 2F, two weeks after the last injection (4 week values) DOX was seen to cause a significant decrease in the relative wall thickness in TGR. Moreover, DOX treatment two weeks after the last injection (4 week values) resulted in TGR a more pronounced reduction of wall thicknesses than in HanSD rats, explicitly in LV anterior wall thickness in systole (-20.6 ± 0.5 vs. $-14.1 \pm 0.4\%$), LV posterior wall thickness in diastole (-23.8 ± 0.5 vs. $-11.1 \pm 0.3\%$), and LV posterior wall thickness in systole (-28.1 ± 0.6 vs. $-11.3 \pm 0.3\%$)— $p < 0.05$ in all cases.

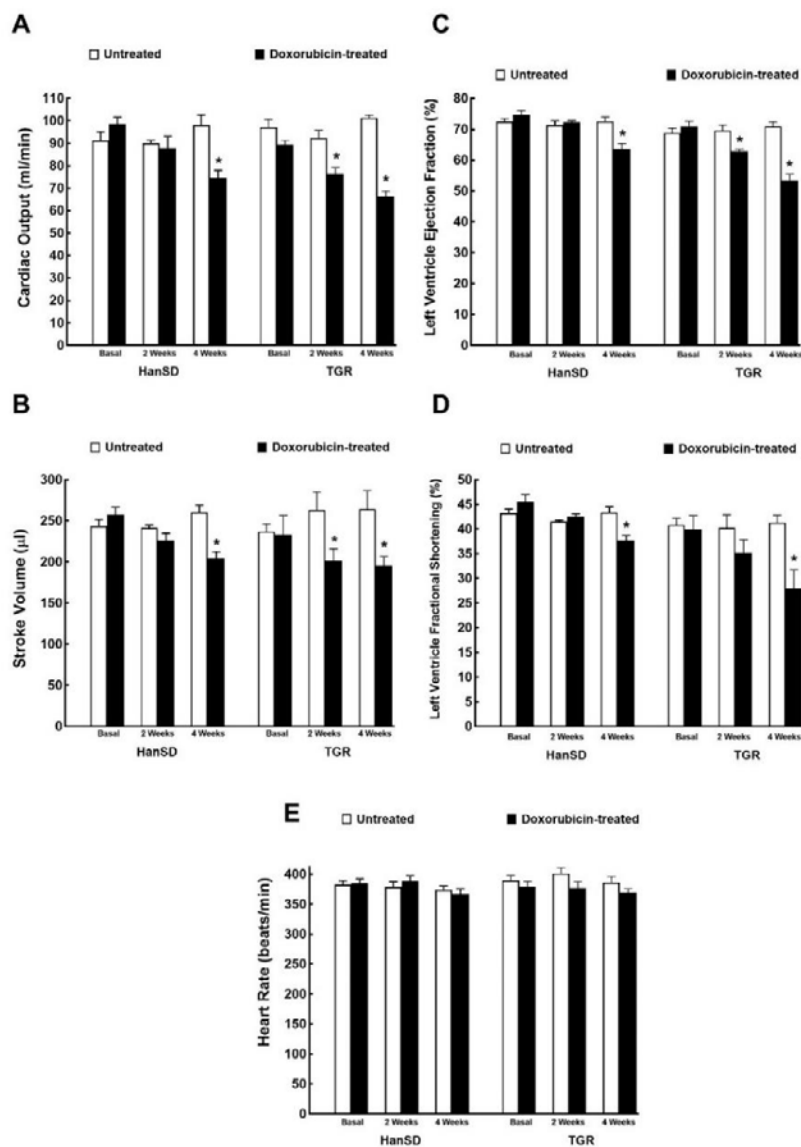


Figure 1. Assessment of the cardiac functional parameters by echocardiography before administration of doxorubicin (basal values), at the end of doxorubicin administration (2 weeks values) and two weeks after termination of doxorubicin treatment (4 weeks values) in normotensive, transgene-negative Hannover Sprague-Dawley (HanSD) and hypertensive, Ren-2 transgenic (TGR) rats. Cardiac output (A), stroke volume (B), left ventricle ejection fraction (C), left ventricle fractional shortening (D), heart rate (E). * $p < 0.05$ compared with untreated animals of the same strain at the same time point. The values are means \pm SEM.

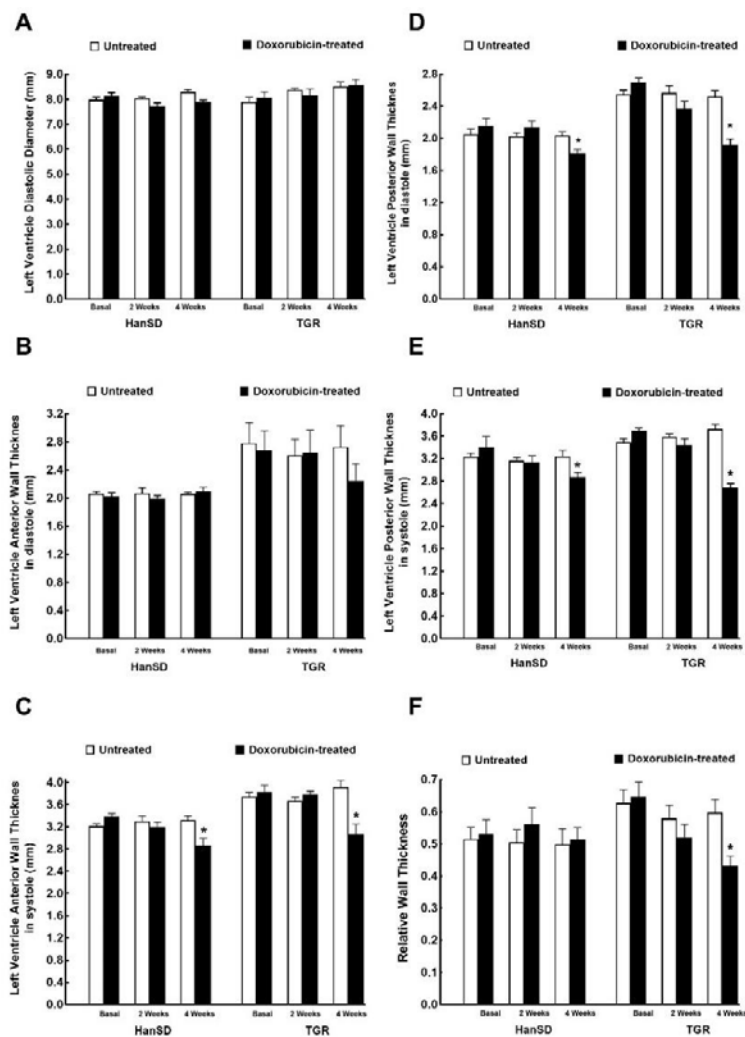


Figure 2. Assessment of the cardiac morphological parameters by echocardiography before administration of doxorubicin (basal values), at the end of doxorubicin administration (2 weeks values) and two weeks after termination of doxorubicin treatment (4 weeks values) in normotensive, transgene-negative Hannover Sprague-Dawley (HanSD) and hypertensive, Ren-2 transgenic (TGR) rats. Left ventricle diastolic diameter (A), left ventricle anterior wall thickness in diastole (B), left ventricle anterior wall thickness in systole (C), left ventricle posterior wall thickness in diastole (D), left ventricle anterior wall thickness in (E), relative wall thickness (F). * $p < 0.05$ compared with untreated animals of the same strain at the same time point. The values are means \pm SEM.

Figures 3 and 4 summarize the effect of DOX on body weight, organ weights and plasma albumin levels two weeks after the last DOX dose (i.e., 4 week values; at the end of the experimental protocol), both in HanSD rats and TGR. The data are pooled from all three series of experiments.

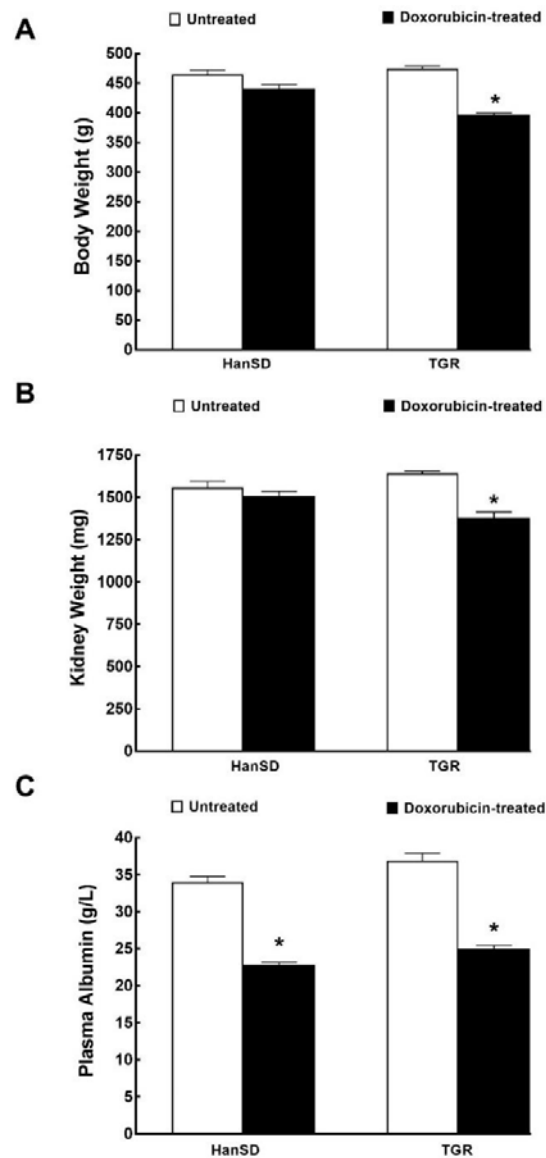


Figure 3. Weights and biochemical parameter. Body weight (A), kidney weight (B) and plasma albumin levels (C) two weeks after the last doxorubicin injection (at the end of the experimental protocol) in normotensive, transgene-negative Hannover Sprague-Dawley (HanSD) and hypertensive, Ren-2 transgenic (TGR) rats. * $p < 0.05$ compared with untreated animals of the same strain at the same time point. The values are means \pm SEM and are pooled from the three series of experiments.

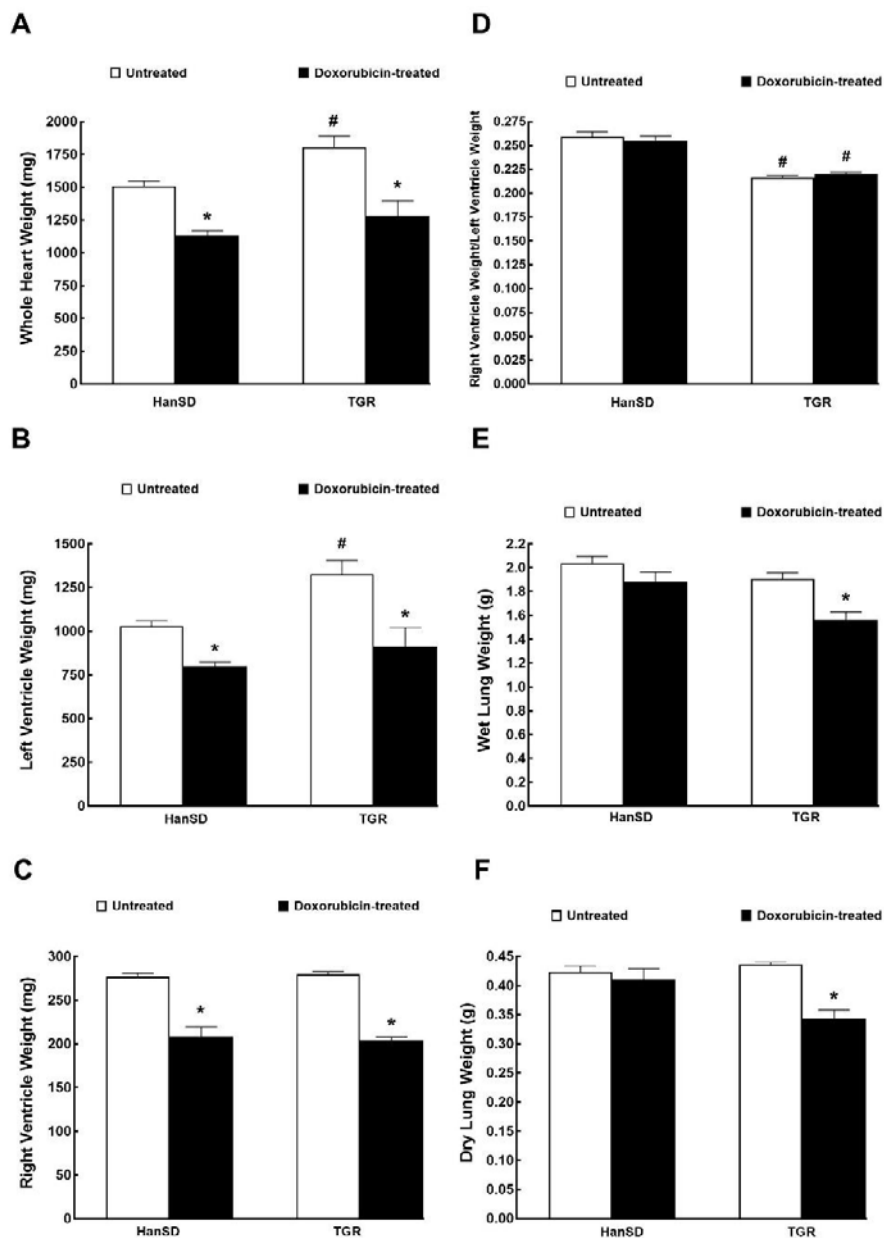


Figure 4. Whole heart weight (A), weights of individual components of the heart (B,C), their ratio (D) and wet and dry lung weights (E,F) two weeks after the last doxorubicin injection (i.e., at the end of the experimental protocol) in normotensive, transgene-negative Hannover Sprague-Dawley (HanSD) and hypertensive, Ren-2 transgenic (TGR) rats. * $p < 0.05$ compared with untreated animals of the same strain. # $p < 0.05$ versus HanSD rats within the same protocol. The values are means \pm SEM and are pooled from the three series of experiments.

As shown in Figure 3A,B, DOX did not cause significant decreases in body weight and kidney weight in HanSD rats, but did so in TGR. Moreover, DOX caused similar decreases in plasma albumin levels in HanSD rats and TGR (Figure 3C).

Figure 4A,B show that untreated TGR exhibited markedly higher whole heart and LV weights as compared with untreated HanSD rats, but there were no significant differences in the RV weights between them. DOX treatment elicited significant and proportional decreases in the whole heart, LV and RV weights as seen from equal ratios of the RV to LV weights with and without DOX administration (Figure 4A–D). As shown in Figure 4E,F, DOX did not alter lung weight (wet or dry) in HanSD rats but significantly decreased both parameters in TGR.

2.2. Series 2: Assessment of Cardiac Function with Invasive Hemodynamic Pressure-Volume Method

Figures 5 and 6 summarize the data from evaluation of cardiac function by the invasive hemodynamics method. The administration of DOX to HanSD rats caused only significant decrease in LV ejection fraction in comparison to untreated counterparts (Figure 6C). In contrast, administration of DOX to TGR resulted not only in reduced LV ejection fraction (Figure 6C), but also in the significant impairment in maximum rates of pressure rise $(+dP/dt)_{max}$ and maximum rates of pressure fall $(-dP/dt)_{max}$ (Figure 5D,E). In addition, the administration of DOX elicited significant decreases in end-systolic pressure volume relationship (ESPVR) and in preload recruitable stroke work (PRSW) in TGR as compared with untreated counterparts (Figure 6A,D), which was accompanied by significant increase in ventricular-arterial coupling (Figure 6F).

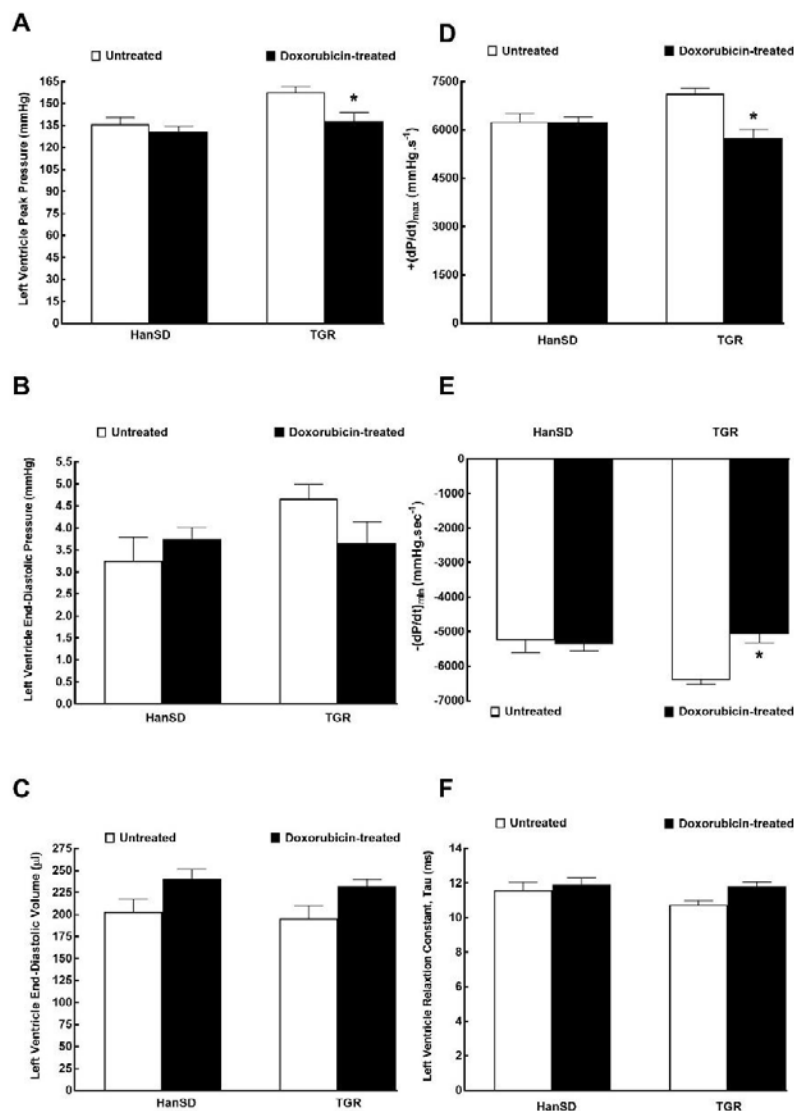


Figure 5. The first data part of the left ventricular cardiac function assessment by invasive hemodynamic analysis performed two weeks after the last doxorubicin injection (i.e., at the end of the experimental protocol) in normotensive, transgene-negative Hannover Sprague-Dawley (HanSD) and hypertensive, Ren-2 transgenic (TGR) rats. Left ventricle peak pressure (A), left ventricle end-diastolic pressure (B), left ventricle end-diastolic volume (C), maximum rates of pressure rise $(+dP/dt)_{max}$ (D), maximum rates of pressure fall $(-dP/dt)_{max}$ (E), relaxation constant tau (F). * $p < 0.05$ compared with untreated animals of the same strain. The values are means \pm SEM.

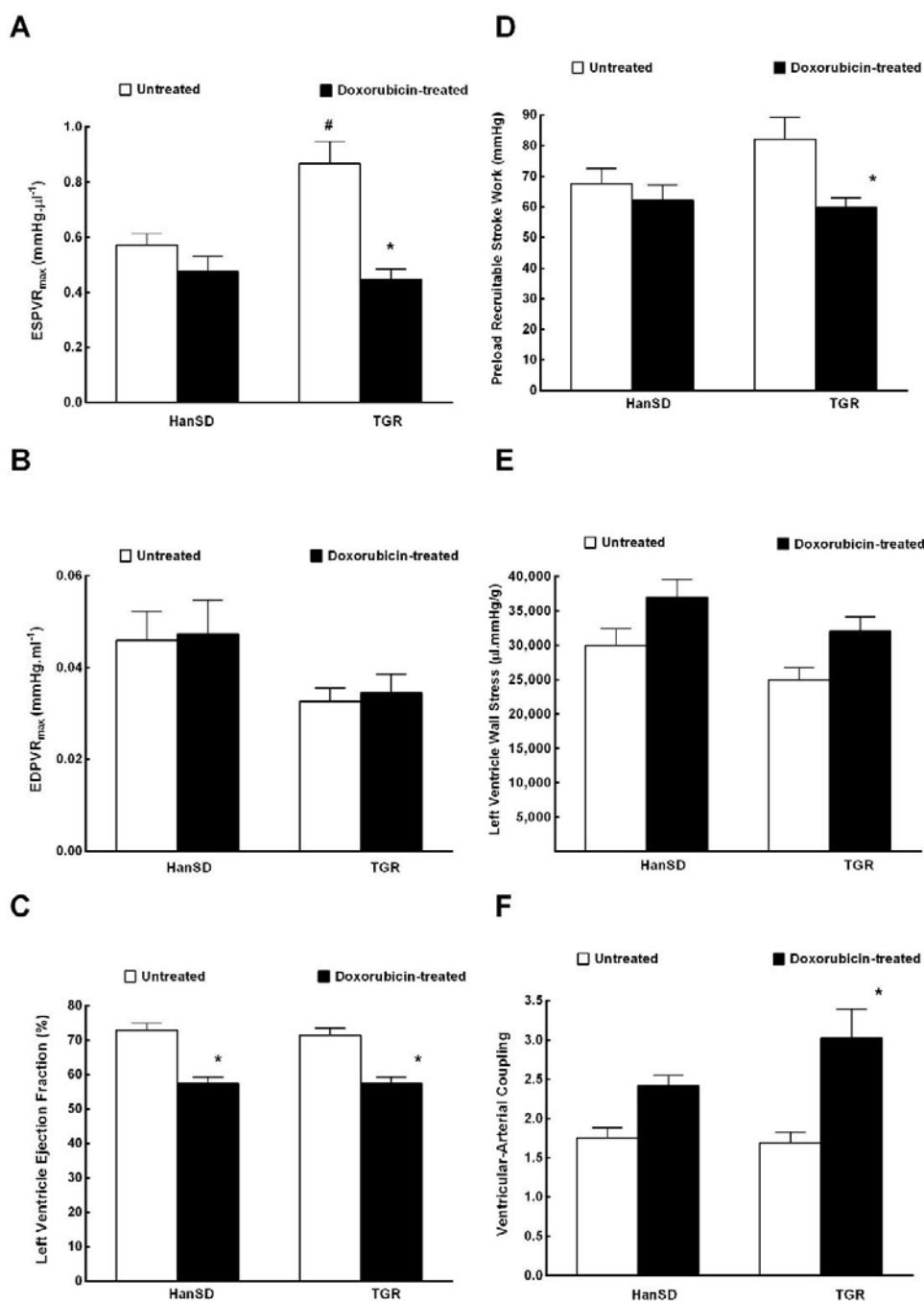


Figure 6. The second part of the data for the left ventricular cardiac function assessment by invasive hemodynamic analysis two weeks after the last doxorubicin injection (i.e., at the end of the experimental protocol) in normotensive, transgene-negative Hannover Sprague-Dawley (HanSD) and hypertensive, Ren-2 transgenic (TGR) rats. End-systolic pressure volume relationship (ESPVR) (A), end-diastolic pressure volume relationship (EDPVR) (B), left ventricle ejection fraction (C), preload recruitable stroke work (D), left ventricle wall stress (E), ventricular-arterial coupling (F). * $p < 0.05$ compared with untreated animals of the same strain. The values are means \pm SEM. # $p < 0.05$ compared with untreated HanSD rats.

Figure 7 shows representative steady-state loops from the pressure-volume analysis in untreated and DOX-treated HanSD rats and TGR. Inspection of the loops further supports the notion that TGR after DOX administration exhibit substantial impairment of systolic function when compared with the untreated counterparts.

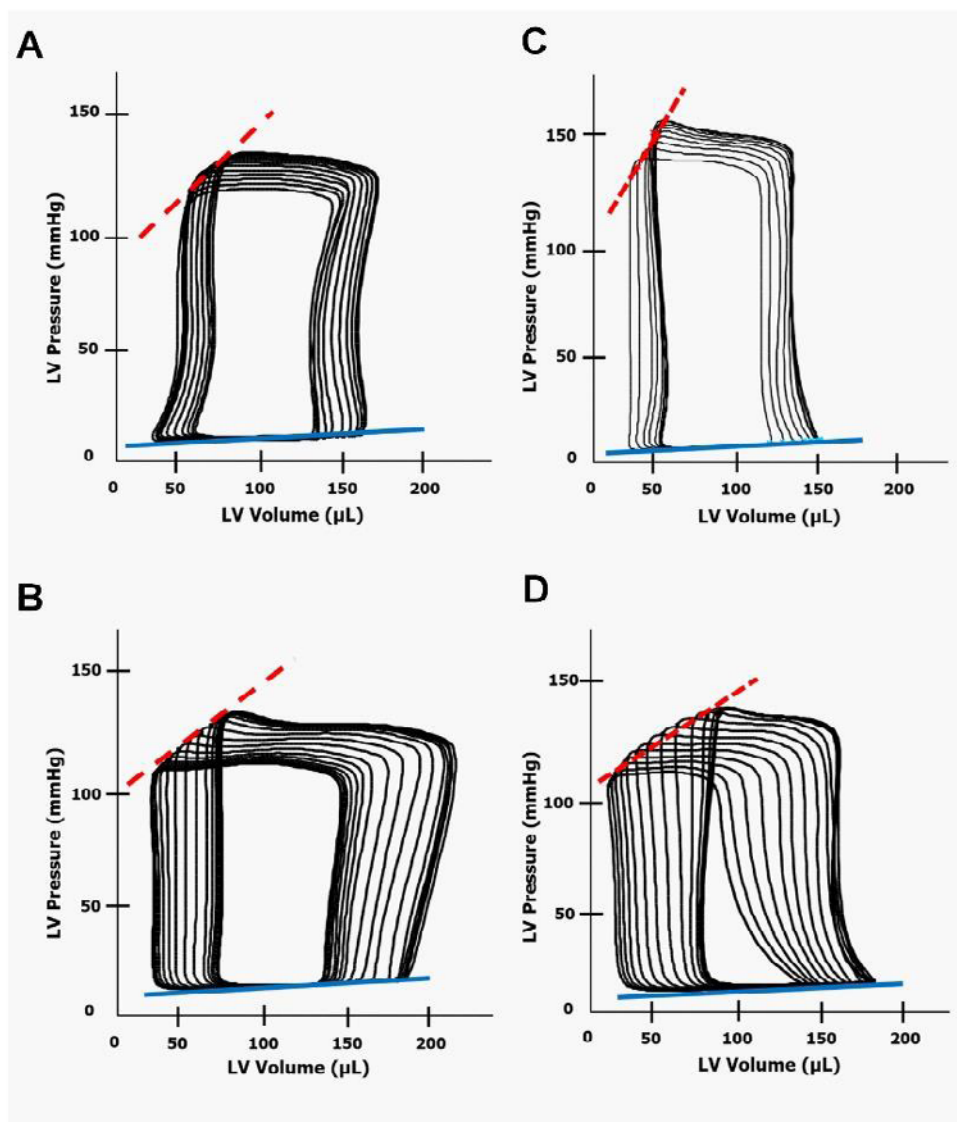


Figure 7. Representative steady-state loops from the pressure-volume analysis performed in (A) untreated normotensive, transgene-negative Hannover Sprague-Dawley (HanSD) rats, (B) HanSD rats two weeks after the last doxorubicin injection (i.e., at the end of the experimental protocol), (C) untreated hypertensive, Ren-2 transgenic (TGR) rats and (D) TGR after doxorubicin administration. ESPVR, end-systolic pressure volume relationship (dotted red line). EDPVR, end-diastolic pressure volume relationship (blue line).

Figure 8 summarizes the results from echocardiographic evaluation of the RV performed during the invasive hemodynamics analysis. As shown, there were no significant differences in the RV diastolic diameter and RV ejection fraction between untreated TGR and HanSD rats. The administration of DOX did not alter the RV diastolic diameter, either in TGR or HanSD rats. However, in both strains, it caused a significant and proportional decrease in RV ejection fraction (Figure 8B).

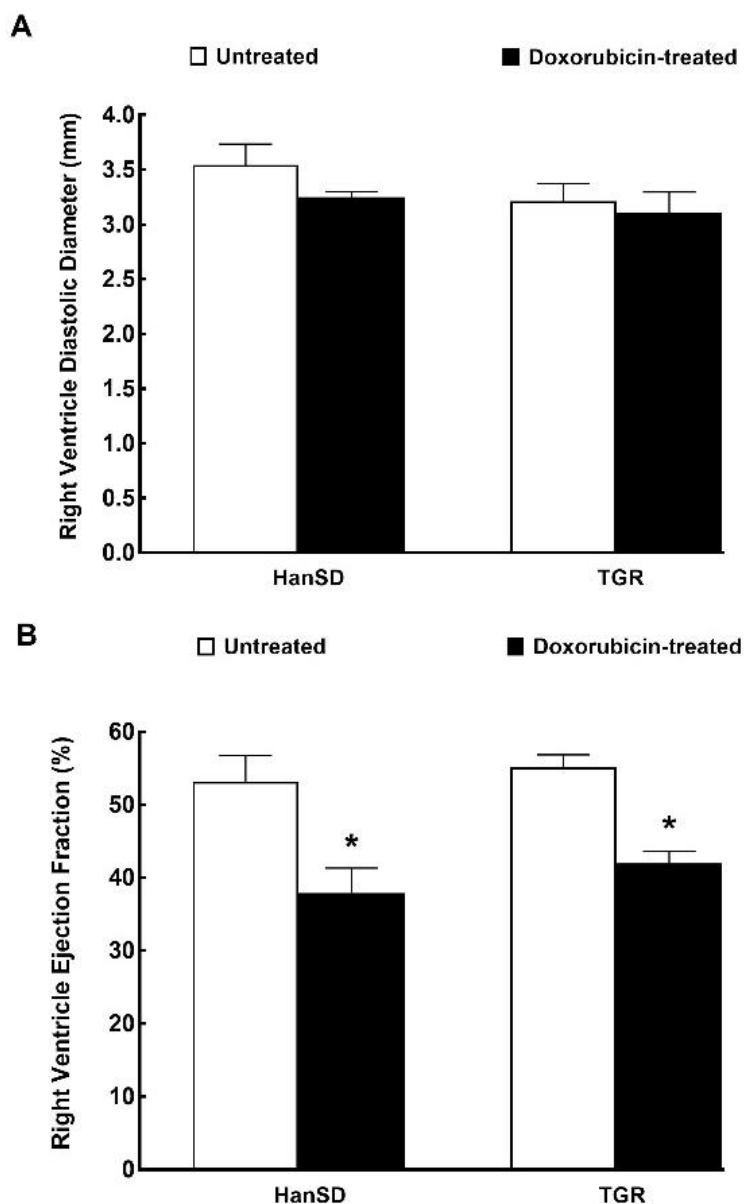


Figure 8. Right ventricle function. Assessment of the right ventricle diastolic diameter (A) and right ventricle ejection fraction (B) by echocardiography after the last doxorubicin injection (i.e., at the end of the experimental protocol) in normotensive, transgene-negative Hannover Sprague-Dawley (HanSD) and hypertensive, Ren-2 transgenic (TGR) rats. * $p < 0.05$ compared with untreated animals of the same strain. The values are means \pm SEM.

2.3. Series 3: Assessment of the Effects of DOX Administration on Plasma and Kidney Concentrations of Angiotensin II (ANG II), Angiotensin 1-7 (ANG 1-7) and Norepinephrine (NE)

Figure 9A shows that plasma NE levels in untreated HanSD rats and TGR were almost identical and that administration of DOX elicited significant increases in HanSD rats, but did not alter them in TGR. In contrast, renal NE concentrations were significantly higher in untreated HanSD rats when compared with untreated TGR, but the administration of DOX did not change renal NE concentrations, similarly in HanSD rats or in TGR (Figure 9E). Figure 9B,F show that plasma and the whole kidney ANG II levels were about twofold higher in untreated TGR than in untreated HanSD rats. Administration of DOX resulted in marked increases in plasma and kidney ANG II levels in both HanSD rats and TGR, but still the difference between the two strains were maintained (significantly higher concentrations in TGR as compared with HanSD rats after DOX treatment).

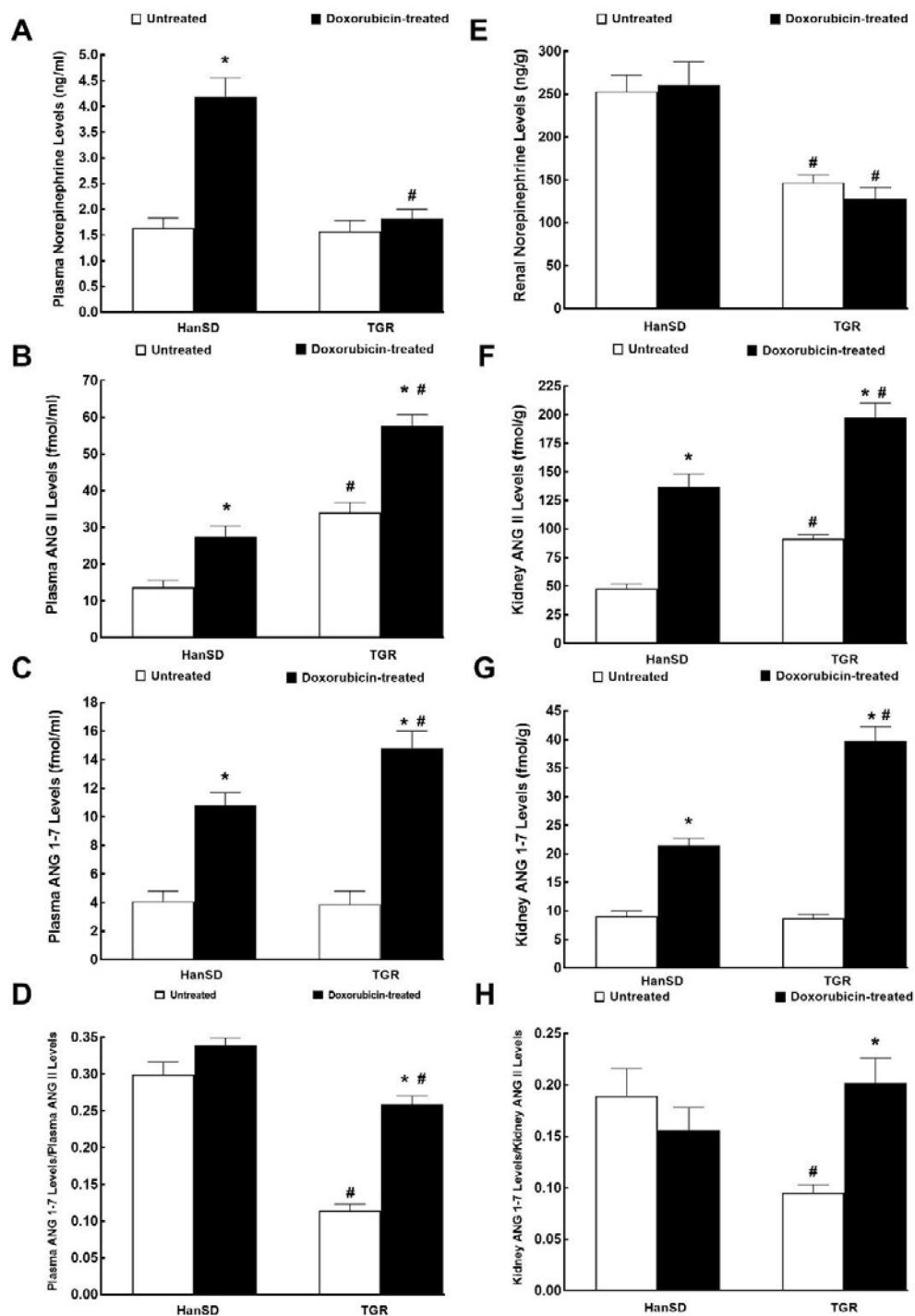


Figure 9. Plasma and kidney biochemical parameters. Plasma and kidney norepinephrine (A,E), angiotensin II (ANG II) (B,F), angiotensin 1-7 (ANG 1-7) (C,G) levels and the ratio of ANG 1-7 to ANG II (D,H) after the last doxorubicin injection (i.e., at the end of experimental protocol) in normotensive, transgene-negative Hannover Sprague-Dawley (HanSD) and hypertensive, Ren-2 transgenic (TGR) rats. * $p < 0.05$ compared with untreated animals of the same strain. # $p < 0.05$ versus HanSD rats exposed to the same protocol. The values are means \pm SEM.

Figure 9C,G show that there were no significant differences in plasma and kidney ANG 1-7 levels between untreated HanSD rats and TGR. DOX administration elicited significant increases in plasma and kidney ANG 1-7 concentrations in HanSD rats as well as in TGR, but they were more prominent in TGR.

Figure 9D,H help to assess the systemic and intrarenal balance between vasodilator and vasoconstrictor axes of the RAAS expressed as the ratio of ANG 1-7 to ANG II. In previous studies, including our own [38], this ratio has been validated as a reliable marker of the activity of the vasodilator axis of RAAS under conditions of vasoconstrictor axis hyperactivity.

Substantially lower values of this index were observed in plasma and kidneys of untreated TGR versus untreated HanSD rats (about twofold and threefold lower, respectively). In HanSD rats, the administration of DOX did not change the ratio of ANG 1-7 to ANG II, similarly in systemic and intrarenal compartments. In contrast, DOX administration resulted in significant increases in this index in TGR, and in the kidney its values reached the level observed in the untreated HanSD rats.

3. Discussion

The first important finding of the present study is that, two weeks after the end of DOX treatment, normotensive HanSD rats showed an impairment of cardiac function. Moreover, all the changes then observed closely resembled “chemotherapy-induced HF with reduced ejection fraction (HFrEF)” described in humans [4–8,12,13,17–19,39]. In HanSD rats, DOX caused bilateral cardiac atrophy and impairment of the liver synthetic function (see reduced plasma albumin levels) without affecting the whole body or other organs’ weight. Remarkably, the finding of marked cardiac atrophy agrees well with the recent report by Jordan et al. [40] who clearly demonstrated that the recipients of anthracycline-based chemotherapy showed a 5% decline in myocardial mass as early as six months post treatment, even under conditions of increased afterload. The study by Jordan et al. [40] was a milestone in the field because, up to this point, most of the surveillance strategies for the detection of early signs of chemotherapy-induced HF with HFrEF were focused on a serial assessment of LV ejection fraction to identify LV systolic dysfunction but did not include LV mass evaluation [41,42].

Of particular interest were also the data on systemic and intrarenal RAAS and SNS activities. In HanSD rats, DOX activated the systemic (but not intrarenal) SNS. Also enhanced were the systemic and intrarenal activity of the vasoconstrictor and vasodilator axes of the RAAS, however, the balance of the two axes was maintained. Given the recent finding that an elevated ANG 1-7/ANG II ratio predicts a beneficial outcome of HF [43], it is reassuring that at least the ratio was not lowered. Importantly, our biochemical findings indicate that the compensatory activation of neurohormonal systems was at the initial stage. It is now agreed that such activation is initially beneficial. However, if prominent and long-lasting, it might be extremely deleterious and substantially contribute to the progression of HF, which makes it a life-threatening disorder [44–47]. Taken together, our present functional and biochemical data indicate that, two weeks after the termination of DOX treatment, HanSD rats are at the very early phase of chemotherapy-induced HFrEF, with the dominant symptom of bilateral cardiac atrophy.

The second important set of findings is that, compared to HanSD rats, in the TGR model already at the end of the treatment DOX significantly decreased cardiac output with substantial impairment of systolic function, and these alterations progressed throughout the two weeks after cessation of the treatment. Moreover, in addition to bilateral cardiac atrophy and impairment of the liver synthetic function as observed in HanSD rats, DOX significantly decreased the whole BW and the weight of the kidney and lungs. Furthermore, besides LV atrophy DOX administration in TGR caused LV dilatation as indicated by a significant decrease in LV relative wall thickness. We noticed also that TGR subjected to DOX treatment did not show systemic and intrarenal activation of SNS, whereas there was a marked activation of both axes of the RAAS. Interestingly, based on the significant increase in plasma and kidney ANG 1-7/ANG II ratio, activation of the vasodilator axis of RAAS appeared more pronounced. As reported recently and already mentioned above [42], the increased ANG 1-7/ANG II ratio might be considered as the beneficial factor slowing down the progression of HF.

Our results indicate that, similarly to HanSD rats, TGR developed chemotherapy-induced HFrEF after DOX treatment. However, the substantial impairment of LV contractility, as apparent from decreased $(+dP/dt)_{\max}$, ESPVR, and PRSW, was more pronounced than in HanSD rats. Remarkably,

despite such an apparent impairment of LV contractility in TGR, when LV ejection fraction was assessed by the invasive hemodynamic pressure-volume method, the reduction was not more pronounced in TGR than in HanSD rats, as observed when cardiac function was evaluated by echocardiography. We cannot provide a fully satisfactory explanation for this discrepancy, but we assume that it is elicited by methodological factors, in particular by different anesthesia's employed for these two methods. Nevertheless, despite this discrepancy, overall, our findings are in agreement with our original hypothesis that hypertension and augmented activation of the RAAS might accelerate the onset of DOX-induced HF, and support the previously expressed notion that hypertension and over-activation of the RAAS constitute major risk factors for the development of chemotherapy-induced cardiomyopathy and HF [11–15,17,19,39].

In addition, our present findings extend those of Sharkey et al. [48] who found that the delayed toxic effects of DOX treatment were exacerbated in genetically hypertensive spontaneously hypertensive rats (SHR) and in rats genetically predisposed to develop hypertension combined with cardiomyopathy. In general, our present findings strongly support the widespread view that a crosstalk between the common risk factors can predispose to both cancer and cardiovascular diseases, particularly to heart failure [49–51].

Taking together the assessment of cardiac function, organ morphology and biochemical data from our current study and our previous results from the ACF-induced HFrEF model in TGR [52–54], we propose that after DOX treatment TGR exhibit signs of HFrEF in the phase of compensation resembling those in HanSD rats but with dominant bilateral cardiac atrophy combined with impairment of systolic functions.

On the whole, while admitting the limitations of small animal models of HF, they remain an irreplaceable tool for improving our understanding of various aspects of pathophysiology of HF and help us develop novel treatment strategies. Our current results indicate that the model of DOX-induced HFrEF strongly resembles clinical situation in patients with chemotherapy-induced HF. As defined more than 20 years ago, an optimal animal model of human cardiovascular disease should (i) mimic the human disease, (ii) allow studies in chronic, stable disease, (iii) produce symptoms which are predictable and controllable, (iv) satisfy economical, technical and animal welfare considerations, and (v) allow relevant measurement of cardiac, hemodynamic and biochemical parameters [55]. Based on our current results and recent reports we believe that all these prerequisites are fulfilled in HanSD rats, as well as in TGR two weeks after the cessation of DOX administration. Nevertheless, it should be emphasized that by this time TGR had displayed signs of compensated chemotherapy-induced HFrEF. However, a closer scrutiny of some data, especially of the analysis of the invasive hemodynamic pressure-volume studies, suggests that the rats were at the beginning of the transition stage from the compensated to the decompensated phase of HF. It is important to acknowledge that, in order to undoubtedly define the stage of transition from the compensated to the decompensated phase of DOX-induced HF in TGR (as well as in HanSD rats), long term studies evaluating HF-related morbidity and mortality are necessary. We performed similar studies that characterized the course of HF development in an ACF model in TGR and HanSD rats [51,56]. However, such studies are very challenging. We characterized the course of ACF-induced HF in normotensive rats and we found that first deaths occur around the 20th week and the median survival was around 43 weeks after ACF induction [56] and even if the onset of the phase of decompensation in TGR after ACF creation is markedly accelerated still the median survival is about five weeks [52,54,57,58]. It is plausible to assume that, in DOX-induced HFrEF, more long term studies will be also required and it is apparent that future studies are needed to precisely define the phases of compensated and decompensated chemotherapy-induced HFrEF in TGR as well as in HanSD rats. Nevertheless, despite this limitation, on the whole, the present results strongly support the view that DOX-induced HFrEF, particularly in TGR, is an optimal model to study the pathophysiological aspects of chemotherapy-induced HFrEF. Therefore, the model should be applied for evaluation of the urgently needed novel therapeutic strategies to combat this condition.

4. Methods

4.1. Experimental Animals and HF Induction

All animals used in the present study were bred at the animal house of the Center of Experimental Medicine, Institute for Clinical and Experimental Medicine (IKEM, Prague, Czech Republic), which is accredited by the Czech Association for Accreditation of Laboratory Animal Care. Heterozygous TGR were generated by breeding male homozygous TGR with female homozygous HanSD rats and age-matched HanSD rats served as controls. The animals were kept on a 12 h/12 h light/dark cycle. Throughout the experiments rats were fed a normal salt, normal protein diet (0.45% NaCl, 19–21% protein) manufactured by SEMED (Prague, Czech Republic) and had free access to tap water. Male TGR and HanSD rats, at the initial age of 8–9 weeks, derived from several litters, were randomly assigned to the experimental groups.

A simple and well-established procedure for DOX-induced cardiomyopathy followed by HF was employed, involving six intraperitoneal (i.p.) injections of DOX (Doxorubicin Ebewe 2mg/ml, Ebewe Pharma, Unterach, Austria), (2.5 mg/kg of body weight) over two weeks, resulting in cumulative dose of 15 mg/kg of body weight. This method has been frequently used for more than 30 years [59] and besides its simplicity, it reflects well the human clinical circumstances; the cumulated dose in our rats corresponds to 550–600 mg/m² body surface applied in patients. The incidence of DOX-induced cardiomyopathy with this dose is usually 18% and even higher in hypertensive patients [8,13–18,60]. Control animals received vehicle solution in the same volume (saline solution with lactose at the same concentration as used for dilution of DOX). It is evident that our experimental approach combines the advantage of a very simple experimental procedure with high clinical relevance.

4.2. Experimental Design

4.2.1. Series 1: Echocardiographic Assessment of the Longitudinal Changes in Cardiac Function throughout DOX Administration

The aim of this series was to assess the changes in cardiac morphology during DOX treatment. Echocardiographic examination was performed three days before the first DOX administration (basal values), at the end of 2 weeks' DOX treatment and then after additional two weeks (4 weeks values). It has been suggested that this time is sufficient to fully develop the signs of DOX-induced cardiomyopathy [23,24,30,31,59]. Echocardiographic assessment is described in detail in our recent study [61]. Briefly, the animals were anesthetized with 4% isoflurane combined with 3 L/min oxygen, the ventral thorax was shaved. During the image acquisition, the rats were maintained under isoflurane anesthesia (2–2.3%, at oxygen flow of 1 L/min, if necessary the dosage was slightly adjusted, depending on the animal's weight, its reaction and breathing), and fixed in the supine position. For standard measurements of cardiac parameters, B-MODE and M-Mode images were recorded in parasternal long axis and parasternal short axis view at the papillary muscle level. Morphological parameters of the LV, including dimension of LV inner diameter, anterior and posterior walls were measured in M-mode from long and short axis sections as previously described [61]. All ultrasound studies were done by Vevo[®] 2100 Imaging System with the MS250S transducer (13–24 MHz), (FUJIFILM VisualSonics, Inc., Toronto, ON, Canada). For each parameter, the mean of 3 optimally obtained measurements was used. The following experimental groups of animals were examined:

1. HanSD rats + vehicle ($n = 8$)
2. TGR + vehicle ($n = 7$)
3. HanSD rats + DOX ($n = 8$)
4. TGR + DOX ($n = 8$)

In addition, at the end of each experiment whole heart, LV (assessed as LV + septum), right ventricle (RV), liver, kidney and lung weights were measured.

4.2.2. Series 2: Assessment of Cardiac Function with Invasive Hemodynamic Pressure-Volume Method

The aim of this series was to evaluate the cardiac function by LV pressure-volume analysis two weeks after the last DOX administration. Based on recent reports [32,33] and the results from Series 1 of the present study, it is known that at this stage the animals show signs of cardiac dysfunction. The goal was to characterize its degree and to confirm that the rats exhibit signs of compensated HF. DOX- and vehicle-treated TGR and HanSD rats were prepared as ascribed above. Two weeks after the last injection, animals were anesthetized with ketamine/midazolam combination (50 and 5 mg/kg of body weight, respectively; i.p.) and echocardiography and subsequently invasive hemodynamic evaluation was performed as described in detail in our previous studies [52,62].

Rats were divided into the following experimental groups:

1. HanSD rats + vehicle ($n = 12$)
2. TGR + vehicle ($n = 12$)
3. HanSD rats + DOX ($n = 14$)
4. TGR + DOX ($n = 15$)

At the end organ weights were assessed as in Series 1.

4.2.3. Series 3: Assessment of the Effects of DOX Administration on Plasma and Kidney ANG II, ANG 1-7 and NE Concentrations

The aim of this series was to assess the degree of activation of two axes of RAAS: the vasoconstrictor axis, represented by ANG II concentration and the vasodilatory axis, represented by ANG 1-7 concentration, together with the determination of the sympathetic nervous system (SNS) activation, represented by NE concentration. It is well known that ANG II concentration under anaesthesia is higher than in conscious rats and there are also marked differences in the renin secretion in response to anaesthesia and surgery per se and in the activation of the RAAS between TGR and HanSD rats. Therefore ANG II, ANG 1-7, and catecholamine concentrations were measured in samples from decapitated animals by methods described in detail in our recent studies [38,53,54,63].

Animals were exposed to the same experimental protocol as in Series 1 and 2, and were decapitated two weeks after the last injection of DOX (the same time schedule as in Series 2). The same experimental groups were evaluated as in Series 1 and 2 ($n = 8$ in each group)

4.3. Statement of Ethics

The study followed the guidelines and practices established by the Animal Care and Use Committee of the IKEM, which accord with the national law and with American Physiological Society guiding principles for the care and use of vertebrate animals in research and training, and were approved by the Animal Care and Use Committee of the IKEM and, consequently, by the Ministry of Health of the Czech Republic (project decision 36388/2019-4/).

4.4. Statistical Analysis

Statistical analysis of the data was performed using Graph-Pad Prism software (Graph Pad Software, San Diego, CA, USA). Statistical comparison of other results was made by Student's *t*-test, Wilcoxon's signed-rank test for unpaired data or one-way ANOVA when appropriate. Values are expressed as mean \pm SEM. The values of *p* below 0.05 were considered statistically significant.

Author Contributions: P.K., V.M., J.V., E.K.-J., J.S. and L.Č. conceived and designed the experiments. P.K. and H.B. were involved in all series of experiments. J.P., Z.V. and L.H. were involved in echocardiographic analyses. J.V. performed invasive hemodynamics analyses. S.K., Š.J., O.G. and H.M. performed biochemical analyses. All authors have read and agreed to the published version of the manuscript.

Funding: This study was primarily supported by the Ministry of Health of the Czech Republic grant no. NV 18-02-00053 awarded to Luděk Červenka. All rights reserved. Peter Kala is Ph.D. student who is supported by the Grant Agency of Charles University, project number 32218.

Conflicts of Interest: Authors declare no conflict of interest.

Abbreviations

ACF	aorto-caval fistula
ANG II	angiotensin II
ANG 1-7	angiotensin 1-7
DOX	doxorubicin
(+dP/dt) _{max}	maximum rates of pressure rise
(−dP/dt) _{max}	maximum rates of pressure fall
ESPVR	end-systolic pressure volume relationship
HanSD	normotensive, transgene-negative, Hannover Sprague-Dawley rats
HF	heart failure
HFrEF	heart failure with reduced ejection fraction
LV	left ventricle
NE	norepinephrine
PRSW	preload recruitable stroke work
RAAS	renin-angiotensin-aldosterone system
RV	right ventricle
SNS	sympathetic nervous system
TGR	Ren-2 renin transgenic, hypertensive rats
WHO	World Health Organization

References

1. Bluethmann, S.M.; Mariotto, A.B.; Rowland, J.H. Anticipating the “Silver Tsunami”: Prevalence trajectories and co-morbidity burden among older cancer survivors in the United States. *Cancer Epidemiol. Biomark. Prev.* **2016**, *25*, 1029–1036. [[CrossRef](#)] [[PubMed](#)]
2. Siegel, R.L.; Miller, K.D.; Jemal, A. Cancer statistics, 2016. *CA Cancer J. Clin.* **2016**, *66*, 7–30. [[CrossRef](#)] [[PubMed](#)]
3. Trachtenberg, B.H. Future Directions in Cardio-Oncology. *Methodist Debaquey Cardiovasc. J.* **2019**, *15*, 300–302. [[PubMed](#)]
4. Lenneman, C.G.; Sawyer, D.B. Cardio-Oncology. An updated on cardiotoxicity of cancer-related treatment. *Circ. Res.* **2016**, *118*, 1008–1020. [[CrossRef](#)]
5. Bansal, N.; Blanco, J.G.; Sharma, U.C.; Pokharel, S.; Shisler, S.; Lipshult, S.E. Cardiovascular diseases in survivors of childhood cancer. *Cancer Metastasis Rev.* **2020**, *39*, 55–68. [[CrossRef](#)]
6. Corremans, R.; Adao, R.; De Keulenaer, G.W.; Leite-Moreira, A.F.; Brás-Silva, C. Update on pathophysiology of anthracycline-induced cardiotoxicity. *Clin. Exp. Pharmacol. Physiol.* **2019**, *46*, 204–215. [[CrossRef](#)]
7. Mancilla, T.R.; Iskra, B.; Aune, G.J. Doxorubicin-induced cardiomyopathy in children. *Compr. Physiol.* **2019**, *9*, 905–931.
8. Henriksen, P.A. Anthracycline cardiotoxicity: And update on mechanisms, monitoring and prevention. *Heart* **2018**, *104*, 971–977. [[CrossRef](#)]
9. Cai, F.; Luis, M.A.F.; Lin, X.; Wang, M.; Cai, L.; Cen, C.; Biskup, E. Anthracycline-induced cardiotoxicity in the chemotherapy treatment of breast cancer: Preventive strategies and treatment. *Mol. Clin. Oncol.* **2019**, *11*, 15–23. [[CrossRef](#)]
10. Cardinala, D.; Colombo, A.; Bacchiani, G.; Tedeschi, I.; Meroni, C.A.; Veglia, F.; Civelli, M.; Lamantia, G.; Colombo, N.; Curigliano, G.; et al. Early detection of anthracyclines cardiotoxicity and improvement with heart failure therapy. *Circulation* **2015**, *131*, 1981–1988. [[CrossRef](#)]
11. Szmit, S.; Jurczak, W.; Zaucha, J.M.; Drozd-Sokolowska, J.; Spychalowicz, W.; Joks, M.; Dlugosz-Danecka, M.; Torbicky, A. Pre-existing arterial hypertension as a risk factor for early left ventricular systolic dysfunction following (R)-CHOP chemotherapy in patients with lymphoma. *J. Am. Soc. Hypertens.* **2014**, *8*, 791–799. [[CrossRef](#)] [[PubMed](#)]
12. Von Hoff, D.D.; Layard, M.W.; Basa, P.; Davis, H.L., Jr.; Von Hoff, A.L.; Rozenzweig, M.; Muggia, F.M. Risk factors for doxorubicin-induced congestive heart failure. *Ann. Intern. Med.* **1979**, *91*, 710–717. [[CrossRef](#)] [[PubMed](#)]

13. Zamorano, J.L.; Lancellotti, P.; Munoz, R.D.; Aboyans, V.; Asteggiano, R.; Galderisi, M.; Habib, G.; Lenihan, D.J.; Lip, G.Y.H.; Lyon, A.R.; et al. 2016 ESC position paper on cancer treatments and cardiovascular toxicity developed under auspices of the ESC Committee for Practice Guidelines. *Eur. Heart J.* **2016**, *37*, 2768–2801. [[CrossRef](#)] [[PubMed](#)]
14. Hassen, L.J.; Lenihan, D.J.; Baliga, R.R. Hypertension in the cardio-oncology clinic. *Heart Fail. Clin.* **2019**, *15*, 487–495. [[CrossRef](#)]
15. Kalyanaraman, B. Teaching the basic of the mechanism of doxorubicin-induced cardiotoxicity: Have we been barking up the wrong tree? *Redox Biol.* **2020**, *29*, 101394. [[CrossRef](#)]
16. Feijen, E.A.; Leisenring, W.M.; Stratton, K.L.; Ness, K.K.; van der Pal, H.J.H.; van Dalen, E.C.; Armstrong, G.T.; Aune, G.J.; Green, D.M.; Hudson, M.M.; et al. Derivation of anthracyclines and anthraquinone equivalence ratios to doxorubicin for late-onset cardiotoxicity. *JAMA Oncol.* **2019**, *5*, 864–871. [[CrossRef](#)]
17. Agunbiade, T.; Zaghlol, R.Y.; Barac, A. Heat failure in relation to anthracyclines and other chemotherapies. *Methodist Debaquey Cardiovasc. J.* **2019**, *15*, 243–249.
18. Lefrak, E.A.; Pit'ha, J.; Rosenheim, S.; Gottlieb, J.A. A clinicopathologic analysis of adriamycin cardiotoxicity. *Cancer* **1973**, *32*, 302–314. [[CrossRef](#)]
19. Ponikowski, P.; Voors, A.A.; Anker, S.D.; Bueno, H.; Cleland, J.G.; Coats, A.J.; Falk, V.; González-Juanaatey, J.R.; Harjola, V.-P.; Jankowska, E.A.; et al. 2016 ESC Guidelines for the diagnosis and treatment of acute and chronic heart failure: The Task Force for the diagnosis and treatment of acute and chronic heart failure of the European Society of Cardiology (ESC). Developed with the special contribution of the Heart Failure Association (HFA) of the ESC. *Eur. Heart J.* **2016**, *37*, 2129–2200.
20. Seferovic, P.M.; Ponikowski, P.; Anker, S.D.; Bauersachs, J.; Chioncel, O.; Cleland, J.G.F.; de Boer, R.A.; Drexel, H.; Gal, T.B.; Hill, L.; et al. Clinical practice update on heart failure 2019, pharmacotherapy, procedures, devices and patients management. An expert consensus meeting report of the Heart Failure Association of the European Society of Cardiology. *Eur. J. Heart Fail.* **2019**, *21*, 1169–1186. [[CrossRef](#)]
21. Xi, J.; Li, M.; An, M.; Yu, C.; Pinnock, C.B.; Zhu, Y.; Lam, T.A.; Li, H. Long-circulating amphiphilic doxorubicin for tumor mitochondria-specific targeting. *ACS Appl. Mater. Interfaces* **2018**, *50*, 43482–43492. [[CrossRef](#)] [[PubMed](#)]
22. Houser, S.R.; Margulies, K.B.; Murphy, A.M.; Spinale, F.G.; Francis, G.S.; Prabhu, S.D. Animal models of heart failure: A scientific statement from the American Heart Association. *Circ. Res.* **2012**, *111*, 131–150. [[CrossRef](#)] [[PubMed](#)]
23. Riehle, C.; Bauersachs, J. Small animals models of heart failure. *Cardiovasc. Res.* **2019**, *115*, 1838–1849. [[CrossRef](#)] [[PubMed](#)]
24. Nakahara, T.; Tanimoto, T.; Petrov, A.D.; Ishikawa, K.; Strauss, H.W.; Narula, J. Rat model of cardiotoxic drug-induced cardiomyopathy. In *Experimental Models of Cardiovascular Diseases: Methods and Protocols*; Ishikawa, K., Ed.; Springer + Business Media, Part of Springer Nature: Berlin/Heidelberg, Germany, 2018; Volume 1816, pp. 221–232.
25. Singal, P.K.; Siveski-Iliskovic, N.; Hill, M.; Thomas, T.P.; Li, T. Combination therapy with probucol prevents adriamycin-induced cardiomyopathy. *J. Mol. Cell Cardiol.* **1995**, *27*, 1055–1063. [[CrossRef](#)]
26. Olson, H.M.; Capen, C.C. Subacute cardiotoxicity of Adriamycin in the rat. Biochemical and ultrastructural investigation. *Lab Invest.* **1977**, *37*, 386–394.
27. Baris, V.O.; Gedikli, E.; Yersal, N.; Muftuoglu, S.; Erdem, A. Protective effect of taurine against doxorubicin-induced cardiotoxicity in rats: Echocardiographical and histological findings. *Amino Acids.* **2019**, *51*, 1649–1655. [[CrossRef](#)]
28. Lódi, M.; Priksz, D.; Fulop, G.; Bodi, B.; Gyongyoi, A.; Nagy, L.; Kovács, A.; Kertész, A.B.; Kocsis, J.; Édes, I.; et al. Advantages of prophylactic versus conventionally scheduled heart failure therapy in and experimental model of doxorubicin-induced cardiomyopathy. *J. Transl. Med.* **2019**, *17*, 229–245. [[CrossRef](#)]
29. Zhu, W.; Reuter, S.; Field, J. Targeted expression of cyclin D2 ameliorates late stage anthracyclines cardiotoxicity. *Cardiovasc. Res.* **2019**, *115*, 960–965. [[CrossRef](#)]
30. Arnolda, L.; McGrath, B.; Cocks, M.; Sumithran, E.; Johnston, C. Adriamycin cardiomyopathy in the rabbit: An animal model of low output cardiac failure with activation of vasoconstrictor mechanisms. *Cardiovasc. Res.* **1985**, *19*, 378–382. [[CrossRef](#)]
31. Hayward, R.; Hydock, D.S. Doxorubicin cardiotoxicity in the rat: An in vivo characterization. *J. Am. Assoc. Lab. Anim. Sci.* **2007**, *46*, 20–32.

32. Medeiros-Lima, D.J.M.; Carvalho, J.J.; Tibirica, E.; Borges, J.P.; Matsuura, C. Time course of cardiomyopathy induced by doxorubicin in rats. *Pharmacol. Rep.* **2019**, *71*, 583–590. [[CrossRef](#)]
33. Razmari, B.H.; Assanassab, N.; Nayebi, M.G.; Azarmi, A.; Mohammadnejad, Y.; Azami, D. Ultrastructural and echocardiographic assessment of chronic doxorubicin-induced cardiotoxicity in rats. *Arch. Razi Inst.* **2020**, *75*, 55–62.
34. Pfeffer, M.A.; Pfeffer, J.M.; Fishbein, M.C.; Fletcher, P.J.; Spadaro, J.; Kloner, R.A.; Braunwald, E. Myocardial infarction size and ventricular function in rats. *Circ. Res.* **1979**, *44*, 503–512. [[CrossRef](#)] [[PubMed](#)]
35. Garcia, R.; Diebold, S. Simple, rapid, and effective method of producing aorto-caval shunts in the rat. *Cardiovasc. Res.* **1990**, *24*, 430–432. [[CrossRef](#)] [[PubMed](#)]
36. Husková, Z.; Kramer, H.J.; Vaňourková, Z.; Červenka, L. Effects of changes in sodium balance on plasma and kidney angiotensin II levels in anesthetized and conscious Ren-2 transgenic rats. *J. Hypertens.* **2006**, *24*, 517–527. [[CrossRef](#)]
37. Elased, K.M.; Cunha, T.S.; Marcondes, F.K.; Morris, M. Brain angiotensin-converting enzyme 2 in processing angiotensin II in mice. *Exp. Physiol.* **2008**, *93*, 665–675. [[CrossRef](#)]
38. Husková, Z.; Kopkan, L.; Červenková, L.; Doleželová, Š.; Vaňourková, Z.; Škaroupková, P.; Nishiyama, A.; Kompanowska-Jezierska, E.; Sadowski, J.; Kramer, H.J.; et al. Intrarenal alterations of the angiotensin-converting enzyme type 2/angiotensin 1-7 complex of the renin-angiotensin system do not alter the course of malignant hypertension in Cyp11a1-Ren-2 transgenic rats. *Clin. Exp. Pharmacol. Physiol.* **2016**, *43*, 438–449. [[CrossRef](#)]
39. Bertero, E.; Ameri, P.; Maack, C. Bidirectional relationship between cancer and heart failure: Old and new issues in cardio-oncology. *Card. Fail. Rev.* **2019**, *5*, 106–111. [[CrossRef](#)]
40. Jordan, J.H.; Castellino, S.M.; Meléndez, G.C.; Klepin, H.D.; Ellis, L.R.; Lamar, Z.; Vasu, S.; Kitzman, D.W.; Ntim, W.O.; Brubaker, P.H.; et al. Left ventricular mass change after anthracyclines chemotherapy. *Circ. Heart Fail.* **2018**, *11*, e004560. [[CrossRef](#)]
41. Plana, J.C.; Galderisi, M.; Barac, A.; Ewer, M.S.; Ky, B.; Scherrer-Crosbie, M.; Ganame, J.; Sebag, I.A.; Agler, D.A.; Badano, L.P.; et al. Expert consensus for multimodality imaging evaluation of adult patients during and after cancer therapy: A report from the American Society of Echocardiography and the European Association of Cardiovascular Imaging. *J. Am. Soc. Echocardiogr.* **2014**, *27*, 911–939. [[CrossRef](#)]
42. Russell, R.R.; Alexander, J.; Jain, D.; Poornima, I.G.; Srivastava, A.V.; Storozynsky, E.; Schwartz, R.G. The role and clinical effectiveness of multimodality imaging in the management of cardiac complications of cancer and cancer therapy. *J. Nucl. Cardiol.* **2016**, *23*, 856–884. [[CrossRef](#)]
43. Wang, K.; Basu, R.; Poglitsch, M.; Bakal, J.A.; Stat, P.; Oudit, G.Y. Elevated angiotensin 1-7/angiotensin II ratio predicts favorable outcomes in patients with heart failure. *Circ. Heart Fail.* **2020**, *13*, e006939. [[CrossRef](#)]
44. Dube, P.; Weber, K.T. Congestive heart failure: Pathophysiological consequences of neurohormonal activation and the potential for recovery: Part I. *Am. J. Med. Sci.* **2011**, *342*, 348–351. [[CrossRef](#)]
45. Hartupee, J.; Mann, D.L. Neurohormonal activation in heart failure with reduced ejection fraction. *Nat. Rev. Cardiol.* **2017**, *14*, 30–38. [[CrossRef](#)]
46. Packer, M.; McMurray, J.J. Importance of endogenous compensatory vasoactive peptides in broadening the effects of inhibitors of the renin-angiotensin system for the treatment of heart failure. *Lancet* **2017**, *389*, 1831–1840. [[CrossRef](#)]
47. Díaz, H.S.; Toledo, C.; Andrade, D.C.; Marcus, N.J.; Del Rio, R. Neuroinflammation in heart failure: New insights for an old disease. *J. Physiol.* **2020**, *598*, 33–59. [[CrossRef](#)]
48. Sharkey, L.C.; Radin, M.J.; Heller, L.; Rogers, L.K.; Tobias, A.; Matisse, I.; Wang, Q.; Apple, F.S.; McCune, S.A. Differential cardiotoxicity in response to chronic doxorubicin treatment in male spontaneous hypertension-heart failure (SHHF), spontaneously hypertensive (SHR), and Wistar Kyoto (WKY) rats. *Toxicol. Appl. Pharmacol.* **2013**, *273*, 47–57. [[CrossRef](#)]
49. Meijers, W.C.; de Boer, R.A. Common risk factors for heart failure and cancer. *Cardiovasc. Res.* **2019**, *115*, 844–853. [[CrossRef](#)]
50. Moslehi, J.; Zhang, Q.; Moore, K.J. Crosstalk between the heart and cancer. Beyond drug toxicity. *Circulation* **2020**, *142*, 684–687. [[CrossRef](#)]
51. Avraham, S.; Abu-Sharki, S.; Shofti, R.; Haas, T.; Korin, B.; Kalfon, R.; Friedman, T.; Shiran, A.; Saliba, W.; Shaked, Y.; et al. Early cardiac remodeling promotes tumor growth and metastasis. *Circulation* **2020**, *142*, 670–683. [[CrossRef](#)]

52. Červenka, L.; Melenovský, V.; Husková, Z.; Škaroupková, P.; Nishiyama, A.; Sadowski, J. Inhibition of soluble epoxide hydrolase counteracts the development of renal dysfunction and progression of congestive heart failure in Ren-2 transgenic hypertensive rats with aorto-caval fistula. *Clin. Exp. Pharmacol. Physiol.* **2015**, *42*, 795–807. [[CrossRef](#)] [[PubMed](#)]
53. Vacková, Š.; Kikerlová, S.; Melenovský, V.; Kolář, F.; Imig, J.D.; Kompanowska-Jeziarska, E.; Sadowski, J.; Červenka, L. Altered renal vascular responsiveness to vasoactive agents in rats with angiotensin II-dependent hypertension and congestive heart failure. *Kidney Blood Press Res.* **2019**, *44*, 792–809. [[CrossRef](#)] [[PubMed](#)]
54. Honetschlagerová, Z.; Gawrys, O.; Jíčovská, Š.; Škaroupková, P.; Kikerlová, S.; Vaňourková, Z.; Husková, Z.; Melenovský, V.; Kompanowska-Jeziarska, E.; Sadowski, J.; et al. Renal sympathetic denervation attenuates congestive heart failure in angiotensin II-dependent hypertension: Studies with Ren-2 transgenic hypertensive rats with aorto-caval fistula. *Kidney Blood Press Res.* **2020**, in press.
55. Doggrell, S.A.; Brown, L. Rat models of hypertension, cardiac hypertrophy and failure. *Cardiovasc. Res.* **1998**, *39*, 89–105. [[CrossRef](#)]
56. Melenovsky, V.; Skaroupkova, P.; Benes, J.; Torresova, V.; Kopkan, L.; Cervenka, L. The course of heart failure development and mortality in rats with volume overload due aorto-caval fistula. *Kidney Blood Press Res.* **2012**, *35*, 167–173. [[CrossRef](#)]
57. Červenka, L.; Škaroupková, P.; Kompanowska-Jeziarska, E.; Sadowski, J. Sex-linked differences in the course of chronic kidney disease and congestive heart failure: A study in 5/6 nephrectomized Ren-2 transgenic hypertensive rats with volume overload induced using aorto-caval fistula. *Clin. Exp. Pharmacol. Physiol.* **2016**, *43*, 883–895. [[CrossRef](#)]
58. Kala, P.; Sedláková, L.; Škaroupková, P.; Kopkan, L.; Vaňourková, Z.; Tábořský, M.; Nishiyama, A.; Hwang, S.H.; Hammock, B.D.; Sadowski, J.; et al. Effect of angiotensin-converting enzyme blockade, alone or combined with blockade with blockade of soluble epoxide hydrolase, on the course of congestive heart failure and occurrence of renal dysfunction in Ren-2 transgenic hypertensive rats with aorto-caval fistula. *Physiol. Res.* **2018**, *67*, 401–415.
59. Weinberg, L.E.; Singal, P.K. Refractory heart failure and age-related differences in adriamycin-induced myocardial changes in rats. *Can. J. Physiol. Pharmacol.* **1987**, *65*, 1957–1965. [[CrossRef](#)]
60. Volkova, M.; Russell, R. Anthracycline cardiotoxicity: Prevalence, pathogenesis and treatment. *Curr. Cardiol. Rev.* **2011**, *7*, 214–220. [[CrossRef](#)]
61. Pokorný, M.; Mrázová, I.; Kubátová, H.; Piřha, J.; Malý, J.; Pirk, J.; Maxová, H.; Melenovský, V.; Šochman, J.; Sadowski, J.; et al. Intraventricular placement of a spring expander does not attenuate cardiac atrophy of the healthy heart induced by unloading via heterotopic heart transplantation. *Physiol. Res.* **2019**, *68*, 567–580. [[CrossRef](#)]
62. Červenka, L.; Melenovský, V.; Husková, Z.; Sporková, A.; Burgelová, M.; Škaroupková, P.; Hwang, S.H.; Hammock, B.D.; Imig, J.D.; Sadowski, J. Inhibition of soluble epoxide hydrolase does not improve the course of congestive heart failure and the development of renal dysfunction in rats with volume overload induced by aorto-caval fistula. *Physiol. Res.* **2015**, *64*, 857–873. [[CrossRef](#)] [[PubMed](#)]
63. Čertíková Chábová, V.; Kujal, P.; Škaroupková, P.; Vaňourková, Z.; Vacková, Š.; Husková, Z.; Kikerlová, S.; Sadowski, J.; Kompanowska-Jeziarska, E.; Baranowska, I.; et al. Combined inhibition of soluble epoxide hydrolase and renin-angiotensin system exhibit superior renoprotection to renin-angiotensin system blockade in 5/6 nephrectomized Ren-2 transgenic hypertensive rats with established chronic kidney disease. *Kidney Blood Press Res.* **2018**, *43*, 329–349. [[CrossRef](#)] [[PubMed](#)]

Publisher's Note: MDPI stays neutral with regard to jurisdictional claims in published maps and institutional affiliations.



© 2020 by the authors. Licensee MDPI, Basel, Switzerland. This article is an open access article distributed under the terms and conditions of the Creative Commons Attribution (CC BY) license (<http://creativecommons.org/licenses/by/4.0/>).

M. Horváth a kol.

MicroRNA-331 and microRNA-151-3p as biomarkers in patients with ST-segment elevation myocardial infarction

Nature / Scientific Reports
Impact Factor: 4,120

OPEN

MicroRNA-331 and microRNA-151-3p as biomarkers in patients with ST-segment elevation myocardial infarction

Martin Horváth^{1*}, Veronika Horváthová^{2,3}, Petr Hájek¹, Cyril Štěchovský¹, Jakub Honěk¹, Ladislav Šenolt³ & Josef Veselka¹

We sought to analyse plasma levels of peripheral blood microRNAs (miRs) as biomarkers of ST-segment-elevation myocardial infarction (STEMI) due to type-1 myocardial infarction as a model situation of vulnerable plaque (VP) rupture. Samples of 20 patients with STEMI were compared both with a group of patients without angina pectoris in whom coronary angiogram did not reveal coronary atherosclerotic disease (no coronary atherosclerosis-NCA) and a group of patients with stable angina pectoris and at least one significant coronary artery stenosis (stable coronary artery disease-SCAD). This study design allowed us to identify miRs deregulated in the setting of acute coronary artery occlusion due to VP rupture. Based on an initial large scale miR assay screening, we selected a total of 12 miRs (three study miRs and nine controls) that were tested in the study. Two of the study miRs (miR-331 and miR-151-3p) significantly distinguished STEMI patients from the control groups, while ROC analysis confirmed their suitability as biomarkers. Importantly, this was observed in patients presenting early with STEMI, even before the markers of myocardial necrosis (cardiac troponin I, miR-208 and miR-499) were elevated, which suggests that the origin of miR-331 and miR-151-3p might be in the VP. In conclusion, the study provides two novel biomarkers observed in STEMI, which may be associated with plaque rupture.

Rupture of a vulnerable atherosclerotic plaque (VP), which leads to acute artery occlusion due to an overlying thrombosis, is a potentially devastating situation resulting in acute coronary syndromes (ACS), ischaemic stroke and other acute complications of atherosclerosis¹⁻⁵. Early detection of VP *in vivo* is essential for effective primary prevention of their rupture, which might aid in the reduction of cardiovascular morbidity and mortality⁶. A potent biomarker that would be sensitive enough for the presence of a VP with a reasonable specificity could be a very important piece of this puzzle.

MicroRNAs (miRs) are small, non-coding RNA molecules that act as modifiers of gene expression⁷⁻⁹. Once they bind to their target mRNA, they may cause its degradation or suppression of its translation⁷⁻⁹. Thus, miRs control many cellular processes and play a role in the pathogenesis of various diseases that include atherosclerosis⁷⁻⁹. The molecules are very stable, easy to detect with quantitative polymerase chain reaction (qPCR) and are relatively tissue specific⁹⁻¹². Due to these properties, miRs appear to be very suitable biomarkers.

The aim of this study was to identify plasma miRs from peripheral blood samples of patients with ST-segment-elevation myocardial infarction (STEMI) that might help quicken its diagnostics or may even be used directly as markers of VP. Such biomarkers might be used for the risk stratification of patients and both aid in tailoring the primary preventive measures and help as prognostic markers in patients with clinically manifested atherosclerosis.

¹Department of Cardiology, Charles University, 2nd Faculty of Medicine and Motol University Hospital, Prague, Czech Republic. ²Faculty of Science, Charles University, Prague, Czech Republic. ³Department of Rheumatology, Charles University, 1st Faculty of Medicine and Rheumatology Institute, Prague, Czech Republic. *email: martin@horvath.cz

	STEMI	SCAD	NCA	STEMI vs. SCAD (p-values)	STEMI vs. NCA (p-values)	SCAD vs. NCA (p-values)
Sex (male)-N(%)	17 (85)	13 (65)	8 (40)	0.273	0.008*	0.122
Age (mean \pm SD)	66.1 (\pm 9.5)	65.2 (\pm 5)	57.9 (\pm 12.9)	0.789	0.027*	0.077
BMI (mean \pm SD)	29.6 (\pm 6.8)	30.1 (\pm 4.7)	29.3 (\pm 4.6)	0.779	0.897	0.606
Arterial hypertension-N (%)	12 (60)	17 (85)	12 (60)	0.155	1.000	0.155
Dyslipidaemia-N (%)	6 (30)	15 (75)	11 (55)	0.010*	0.200	0.320
Diabetes mellitus-N (%)	8 (40)	9 (45)	3 (15)	1.000	0.155	0.082
Smoking-N (%)	13 (65)	11 (55)	4 (20)	0.748	0.010*	0.048*
Stroke-N (%)	1 (5)	2 (10)	1 (5)	1.000	1.000	1.000
Statin-N (%)	2 (10)	14 (70)	11 (55)	0.0002*	0.006*	0.515
ASA-N (%)	11 (55)	17 (85)	12 (60)	0.082	1.000	0.155
Clopidogrel-N (%)	0 (0)	10 (50)	1 (5)	0.0001*	1.000	0.003*

Table 1. Here we provide the baseline characteristics of all three study groups. The data that significantly differ between the groups are indicated with an asterisk. *Twenty patients were enrolled in each group. Normally distributed data are presented as means \pm standard deviation (\pm SD) and non-normally distributed data as medians with interquartile range (IQR). The distribution of the data was evaluated using the D'Agostino and Pearson omnibus normality test, the Shapiro-Wilk normality test and the Kolmogorov-Smirnov normality test. The differences in the background clinical data between the study groups were evaluated using the Student's t-test.

Results

Baseline characteristics. A total of 60 patients were evenly divided between patients with STEMI (20 patients, 66.1 \pm 9.5 years, 85% men), patients with SCAD (20 patients, 65.2 \pm 12.5 years, 65% men) and the NCA group (20 patients, 56.5 \pm 12.9 years, 55% men). Baseline characteristics of the study population are summarized in Table 1.

Safety and feasibility. No complications of the sample collection and evaluation were noted. All STEMI patients as well as all patients with SCAD were treated with a percutaneous coronary intervention (PCI). No complications of the diagnostic angiography or PCI were observed.

Markers of acute coronary syndrome. Amongst the miRNAs associated with ACS, which were selected as positive controls, four (miR-146a, miR-145, miR-24 and miR-323p) were significantly up-regulated in STEMI: miRNA-146a [STEMI: 2.970 (1.405–6.280) vs. SCAD: 0.760 (0.153–1.845), $p < 0.001$, STEMI: 2.970 (1.405–6.280) vs. NCA: 0.660 (0.175–1.370), $p < 0.001$]; miRNA-145 [STEMI: 1.955 (1.025–4.270) vs. SCAD: 0.750 (0.223–1.038), $p < 0.01$, STEMI: 1.955 (1.025–4.270) vs. NCA: 0.490 (0.193–1.178), $p < 0.01$]; miRNA-24 [STEMI: 1.675 (0.750–2.693) vs. SCAD: 0.765 (0.185–1.405), $p = \text{ns}$; STEMI: 1.675 (0.750–2.693) vs. NCA: 0.575 (0.105–0.883), $p < 0.01$] and miRNA-323p [STEMI: 2.805 (1.268–6.533) vs. SCAD: 0.405 (0.353–1.058), $p < 0.01$; STEMI: 2.805 (1.268–6.533) vs. NCA: 0.675 (0.300–1.670), $p < 0.001$] (Fig. 1A). MicroRNA-155 was not expressed in any of the study groups.

Markers of myocardial necrosis. Both of the miRs that were tested as markers of myocardial necrosis (miR-208 and miR-499) were not expressed in any of the study groups. The median level of high-sensitivity troponin I (hsTnI) did not exceed the cut-off value for myocardial infarction in the STEMI patients at the time of blood sample collection (median hsTnI in STEMI 107.6 ng/l). The median time from the onset of chest pain to blood sample collection in STEMI was 2.25 hours.

Markers of platelet activation. The relative expressions of miRs associated with platelet activation were significantly higher in patients with STEMI: miR-223 [STEMI: 4.810 (1.560–7.100) vs. SCAD: 0.475 (0.165–1.328); $p < 0.0001$; STEMI: 4.810 (1.560–7.100) vs. NCA: 0.550 (0.270–0.850); $p < 0.0001$] and miR-191 [STEMI: 3.000 (1.473–6.758) vs. SCAD: 0.630 (0.218–1.238); $p < 0.001$; STEMI: 3.000 (1.473–6.758) vs. NCA: 0.390 (0.163–0.808); $p < 0.0001$] (Fig. 1B).

Results of the study microRNAs. Amongst the study miRs, miR-331 and miR-151-3p, were significantly up-regulated in patients with STEMI. MicroRNA-518d was not deregulated in any of the study groups.

MicroRNA-331 distinguished patients with STEMI from both control groups [STEMI: 1.830 (0.775–4.313) vs. SCAD: 0.585 (0.243–1.050); $p < 0.05$; STEMI: 1.830 (0.775–4.313) vs. NCA: 0.525 (0.176–1.140); $p < 0.01$] (Fig. 2A). The ROC analysis confirmed the suitability of miR-331 as a biomarker (STEMI vs. NCA: AUC = 0.790 [95% CI; 0.649–0.931], $p = 0.002$; STEMI vs. SCAD: AUC = 0.773 [95% CI; 0.625–0.921], $p = 0.003$) (Fig. 2A). The results suggest a sensitivity of 65% and specificity of 85% for distinguishing STEMI patients from NCA with a cut-off value of 1.3x. Alternatively, the sensitivity was 65% and the specificity was 80% for separating STEMI from SCAD patients with a cut-off value of 1.2x (Fig. 2A).

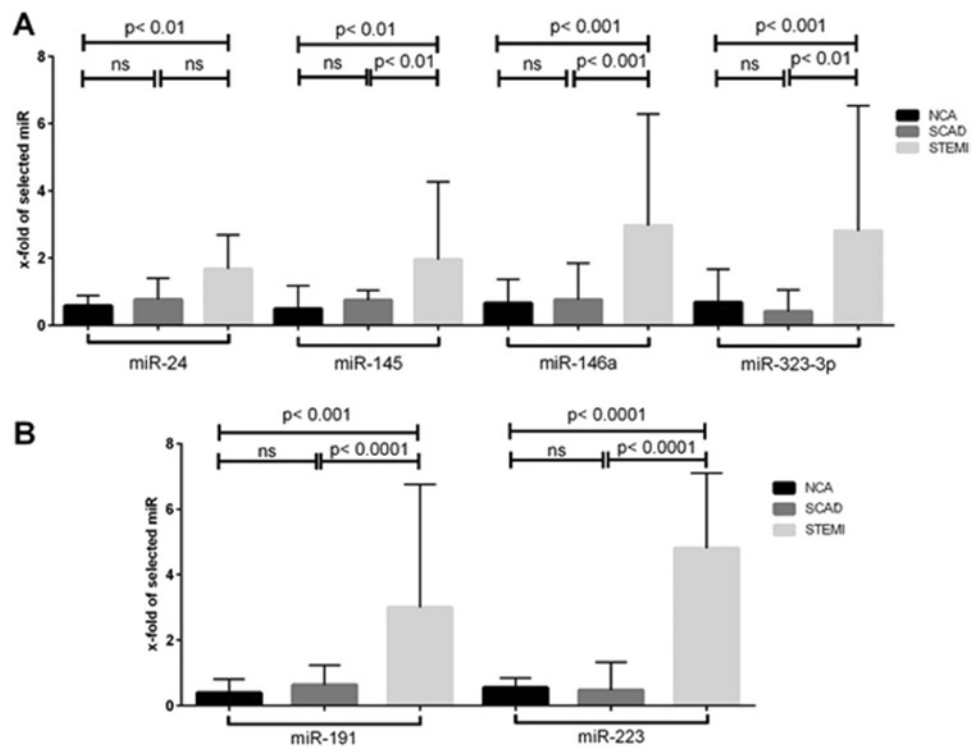


Figure 1. Amongst the miRNAs that were selected as positive controls, four (miR-146a, miR-145, miR-24 and miR-323p) were significantly up-regulated in STEMI. (A) The relative expressions of miRNAs associated with platelet activation (miR-223 and miR-191) were significantly higher in patients with STEMI. (B) There were twenty patients enrolled in each of the three study groups. For the purposes of the comparison between the relative expressions of miRNAs in the three study groups, the Kruskal-Wallis one-way analysis of variance was used.

The plasma levels of miR-151-3p were also significantly higher in patients with STEMI when compared to the control groups [STEMI: 1.430 (0.770–3.370) vs. SCAD: 0.625 (0.223–1.163); $p < 0.05$; STEMI: 1.430 (0.770–3.370) vs. NCA: 0.620 (0.243–1.083); $p < 0.05$] (Fig. 2B). The ROC analysis confirmed a good power to distinguish STEMI from the control groups (STEMI vs. NCA: AUC = 0.758 [95% CI; 0.602–0.931], $p = 0.005$; STEMI vs. SCAD: AUC = 0.754 [95% CI; 0.602–0.905], $p = 0.006$) (Fig. 2B). The sensitivity and specificity for the detection of STEMI patients when compared with NCA was 70% and 85% respectively with a cut-off value 1.1x. When using miR-151-3p to differentiate STEMI from SCAD the sensitivity was 70%, the specificity was 75% using the cut-off value was 1.1x (Fig. 2B).

An analysis of miR-151-3p and miR-331 was also performed. The combination of the two miRNAs did not provide a better power to predict STEMI from the control groups in a ROC analysis (STEMI vs. NCA: AUC = 0.790; STEMI vs. SCAD: AUC = 0.627).

Discussion

The principle findings of the study may be summarized as follows: (1) most important finding of this research is the newly described association between the plasma levels of miR-331 and miR-151-3p and STEMI, (2) the results of the positive control miRNAs demonstrate that the methodology in this pilot study was executed properly, (3) the results suggest that the source of miR-331 and miR-151-3p is outside of the myocardium since the markers of myocardial necrosis were still negative at the time of sampling and (4) the platelet-derived miRNAs were elevated in STEMI, which indicates that the STEMI patients suffered from a type-1 myocardial infarction (T1 MI) due to a rupture of a VP¹³.

Little is known about the molecular biology of miR-331. Its deregulation has been linked to the pathogenesis of several types of human cancer^{14–17}. Its down-regulation was observed in a very small study of human abdominal aortic aneurysm specimens¹⁸. Several observational studies have proposed its expression in macrophages^{19,20}. Interestingly, this miRNA is up-regulated in many types of leukaemia, including acute myeloid leukemia, indicating its possible association with the monocyte-macrophage system^{14,17}. A study conducted on patients with chronic lymphocytic leukaemia found an up-regulation of miR-331¹⁴. The authors described a possible association between this miRNA and the suppressor of cytokine signalling 1 (SOCS1) protein, an inhibitor of the Janus kinase/signal transducer and activator of transcription (JAK/STAT) pathway¹⁴. This may be one of the possible links between the observed over-expression of miR-331 and STEMI. Up-regulation of SOCS1 has been identified as an anti-inflammatory mechanism in atherosclerosis²¹. MicroRNAs have the ability to block SOCS1, leading to a pro-inflammatory response in atherosclerotic plaques²². This pathophysiological mechanism has been previously described with miR-155, which is however the only positive control that was not deregulated in the present

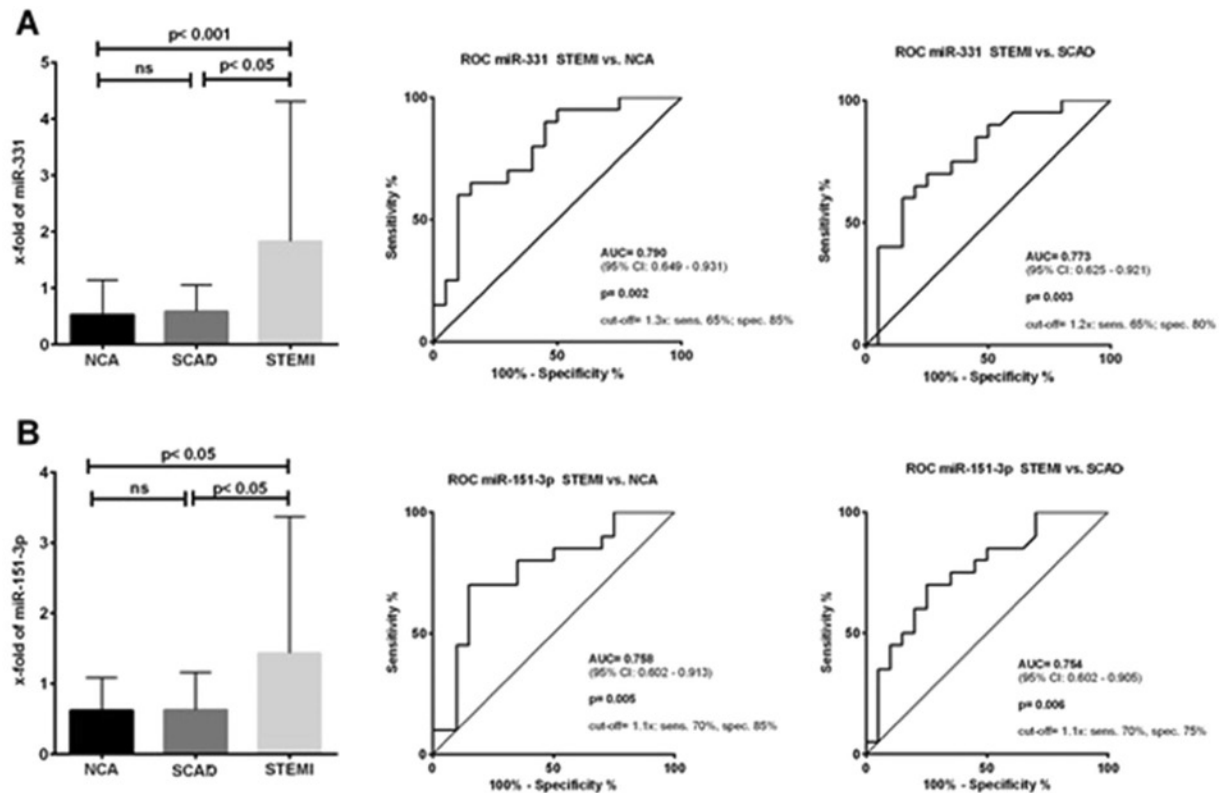


Figure 2. MicroRNA-331 distinguished patients with STEMI from both control groups. (A) The ROC analysis confirmed the suitability of miR-331 as a biomarker. (A) Plasma levels of miR-151-3p were also significantly higher in patients with STEMI when compared to the control groups. (B) The ROC analysis yielded a promising sensitivity and specificity for the differentiation of STEMI from both control groups (B).

study²². Another possible link between miR-331 and VP rupture might be its proposed impact on the phosphatidylinositol 3-kinase/protein kinase B (PI3K/AKT) signalling pathway, which has a role in the stabilization of Vp^{15,23,24}.

The evidence about miR-151-3p is even scarcer. Several studies have observed a relationship with cancer^{25,26}. Its association with atherosclerosis has not been reported to date. Liu *et al.* observed an interaction between miR-151-3p and STAT3, which regulates the inflammatory response in macrophages²⁷. This is a plausible explanation of its deregulation in STEMI. Moreover, the dependence of miR-151-3p expression on the amount of endothelial shear stress, a well-known modifier of atherosclerotic plaque progression and destabilization, has also been described^{28–31}. Another possible explanation of its deregulation might be an association with type 2 diabetes mellitus, although its prevalence was similarly high in the STEMI and SCAD groups³².

This study established the association between four previously described miRs (miR-146a, miR-145, miR-24 and miR-323p) and ACS confirming the well-executed methodology. The data are quite unique because they were obtained in a study with very well-defined groups. A more general definition of ACS was often used in the previously published research in order to simplify patient recruitment^{12,33}. Patients with non-ST segment elevations myocardial infarction or unstable angina pectoris were frequently included, which may be a source of inaccuracies when we focus directly on markers of VP rupture^{12,33}. Furthermore, all patients enrolled in this study, including the negative controls, had a well-defined coronary anatomy by coronary angiography and well-defined background clinical data. Another fact that differentiates our data from previous research is that the levels of miRs were determined from peripheral venous blood samples rather than samples obtained directly from the coronary arteries or the coronary sinus^{12,33}. This may certainly lead to an inability to detect small differences in miR levels. However, we believe that this approach may be much better convertible into common practice. The sole positive control that was not upregulated in the study was miR-155. A possible explanation for this inconsistency might be that the data about this miR are somewhat uncertain and contradictory^{7,34}. While some studies suggest that its upregulation may promote atherosclerosis, others suggested that it may have a protective role or no effect at all. The decision to use this miR as a positive control was thus to some extent unfortunate³⁴.

The levels of myocardial enriched miR-208 and miR-499 were not significantly elevated in STEMI patients at the time of blood sample collection³⁵. The median level of hsTnI in STEMI was below the cut-off value for myocardial infarction at the time of sample collection. These facts suggest that the patients enrolled in the STEMI group presented to the hospital before myocardial injury would compromise the results of a study designed to detect miRs associated with VP rupture. All STEMI patients had an acute arterial occlusion due to T1 MI confirmed on coronary angiography. Since rupture of a thin-cap fibroatheroma is the most common cause of VP

associated coronary artery thrombosis, we hypothesize that the study miRs may directly be associated with the presence of such atherosclerotic lesions^{36,37}. Clearly, this hypothesis remains to be tested in larger studies using invasive imaging techniques.

The plasma levels of the platelet derived miR-223 and miR-191 were elevated in STEMI. This suggests that the reason for the acute arterial occlusion was the formation of an intracoronary thrombus in the setting of a T1 MI. It also suggests an alternative explanation for the elevation of the study miR-331 and miR-151-3p, since their origin might be in activated platelets. However, no association between both of the study miRs and platelets has been noted to date^{38,39}. Importantly, the study miRs could serve as biomarkers of ACS even if their origin was in platelets. Platelet-derived miRs can directly affect gene expression in their neighbouring cells including the endothelium⁴⁰. Such miRs have indeed been proposed as potential prognostic markers in atherosclerosis⁴¹.

Present study has several limitations and should thus be appreciated as a pilot project aiming to generate hypotheses for further research. The most obvious limitations include its observational design and the relatively small study sample^{12,33}. This did not allow us to reliably verify whether the level of study miRs could be influenced by some possible confounding factors that were not evenly balanced between the patient groups. The differences in baseline clinical data are provided in Table 1. These are mainly due to the different distribution of characteristics in NCA, which is based on the very indication of coronary angiography in these patients. The relationship between the levels of peripheral blood miRs and age has been well-described before, and sex differences should not significantly influence the results⁴². There was no correlation between the level of miR-151-3p of miR-331 with age in any of the groups. We also did not find any statistically significant difference between the levels of both miR-151-3p and miR-331 between sexes in all of the groups. The combination of the two markers as a signature did not yield better results in our study. The reason for this might be the limited study sample and the close correlation between the markers. The prevalence of diabetes mellitus was lower among NCA, which could affect the levels of both study miRs, especially miR-151-3p where an association has previously been described³². If we assume that the origin of the study miRs might be in platelets, their levels could also be influenced by anti-platelet therapy, which was also unevenly distributed between the study groups^{38,39}. We believe that these limitations did not corrupt the results. The hypotheses provided in the study will be tested in larger studies which will account for the potential confounders and will also provide more insight with invasive imaging techniques.

In conclusion, the study provides two novel biomarkers observed in STEMI, which may be associated with plaque rupture.

Methods

Study design and population. A total of 60 patients who underwent coronary angiography (CAG) at the same institution were enrolled in this case-control observational study. The study population was divided evenly between a cohort of 20 patients with STEMI and two control groups. These were introduced in the study in order to determine whether the studied miRs are not only markers of atherosclerosis in general (STEMI vs. NCA), but rather potential markers of patients with VPs (STEMI vs. SCAD).

All patients included in the study were ≥ 18 years old and provided signed informed consent. Patients in the STEMI cohort met the definition according to the European Society of Cardiology guidelines (i.e. patients with persistent chest discomfort or other symptoms suggestive of ischaemia and significant ST-segment elevation in at least two contiguous leads) and had a proven coronary artery occlusion as a culprit on CAG⁴³. The NCA cohort consisted of patients without angina pectoris who underwent a clinically indicated coronary angiography that did not reveal any atherosclerotic affection of the coronary arteries. In most cases, these were patients with valvular heart disease. The SCAD consisted of patients with stable angina pectoris and at least one significant coronary artery stenosis (more than 50% stenosis) proven by CAG. The study was approved by the Ethics committee of the Motol University Hospital under the reference number EK-1158/18. All research was performed in accordance with the relevant guidelines and regulations.

Plasma collection and storage. Peripheral blood samples were collected into 9 ml EDTA tubes. In patients with STEMI, the blood was collected immediately after the admission of the patient to the hospital. Blood samples of SCAD patients were collected after a significant stenosis was revealed, but always before a PCI was performed. The blood samples of NCA patients were collected after the diagnostic CAG yielded a negative result.

Immediately after the collection, the whole blood samples were centrifuged at 1000 g for 10 minutes to separate plasma from red blood cells. Next, the plasma samples were transferred into DNase/RNase free tubes and centrifuged once again at 2000 g for 15 minutes in order to remove platelets from the sample. Finally, the resultant plasma was aliquoted per 500 μ l into DNase/RNase free Eppendorf tubes and stored at -80°C .

Total RNA isolation and its quantification. Total RNA was isolated from 100 μ l plasma samples using the miRNeasy Serum/Plasma kit (Qiagen, Hilden, Germany) according to the manufacturer's protocol and stored at -80°C .

Initial TaqMan screening. In order to identify previously unknown miRs that could be associated with VP, we performed an initial screening of a large number of miRs. From the isolated total RNA, we screened miRs which were differently expressed between a group of four patients with STEMI and a group of four NCA using TaqMan Array microRNA Cards (Thermo Fisher Scientific, Waltham, MA, USA). Screening of miRs in plasma samples started with reverse transcription (RT) using MegaplexTM RT Primers, Human Pool A + B v2.1 (Thermo Fisher Scientific, Waltham, MA, USA) with TaqMan MicroRNA Reverse Transcription Kit (Thermo Fisher Scientific, Waltham, MA, USA), followed by pre-amplification reaction using MegaplexPreAmp Primers (Thermo Fisher Scientific, Waltham, MA, USA) and TaqMan[®] PreAmp Master Mix (Thermo Fisher Scientific, Waltham, MA, USA), finished with quantitative polymerase chain reaction (qPCR) using TaqMan Array Human

MicroRNA A + B Cards (Thermo Fisher Scientific, Waltham, MA, USA) with TaqMan Universal PCR Master Mix, no AmpErase UNG (Thermo Fisher Scientific, Waltham, MA, USA) according to the company-provided protocol. The mean of all expressed miRs in TaqMan Array Human MicroRNA A + B Cards was used for the normalization of screened miRs.

Based on the results of the screening, we selected a total of 12 miRs for validation on the whole study population. Firstly, we selected three study miRs that were significantly deregulated in the initial screening (miR-331, miR-151-3p and miR-518d) and have not yet been associated with cardiovascular disease. We further selected miR-146a, miR-145, miR-155, miR-24 and miR-323p, which were previously linked to ACS, as positive controls^{44–49}. MicroRNA-208 and miR-499 associated with myocardial necrosis were selected as controls of timely sampling, since our aim was to detect miRs associated with plaque rupture rather than myocardial necrosis³⁵. Lastly, we selected miR-191 and miR-223 that are associated with platelet activation to prove the formation of coronary thrombus due to T1 MI in STEMI⁴¹.

Study miR analysis. The selected miRs were first reverse transcribed by particular TaqMan microRNA Assays (Thermo Fisher Scientific, Waltham, MA, USA) with TaqMan MicroRNA Reverse Transcription Kit (Thermo Fisher Scientific, Waltham, MA, USA) followed by qPCR reaction using specific TaqMan microRNA Assays (Thermo Fisher Scientific, Waltham, MA, USA) with TaqMan Universal PCR Master Mix, no AmpErase UNG (Thermo Fisher Scientific, Waltham, MA, USA). For all reverse transcription (RT) reactions, thermocycler Lab Cycler (Sensoquest, Göttingen, Germany) was used and all quantification reactions were performed using the QuantStudio 7 Flex Real-Time PCR System (Thermo Fisher Scientific, Waltham, MA, USA). Spike-in control cel-miR-39 (IDT, San Jose, CA, USA), originating from *Caenorhabditis elegans*, was used for the normalization of cell-free miRs. For calculation of miRNA levels was used $2^{-\Delta\Delta Ct}$ method determining fold change in miRNA expressions of the patient group relative to the control groups⁵⁰.

Heparinase I treatment. Patients with STEMI were treated with heparin prior to the admission to the hospital and the collection of blood samples. Since, heparin is a well-known inhibitor of RT and qPCR reactions, we incubated all STEMI samples with 0.3 U of heparinase I from *Flavobacterium heparinum* (Sigma-Aldrich, St. Louis, MO, USA) per 10 ng of total RNA at 26 °C for 1 h before the RT reaction, according to the protocol published by Li and colleagues^{51–54}.

Statistical analysis. Normally distributed data are presented as means \pm standard deviation (\pm SD) and non-normally distributed data as medians with interquartile range (IQR). The distribution of the data was evaluated using the D'Agostino and Pearson omnibus normality test, the Shapiro-Wilk normality test and the Kolmogorov-Smirnov normality test. The differences in the background clinical data between the study groups were evaluated using Student's t-test. For the purposes of the comparison between the relative expressions of miRs between the three study groups, the Kruskal-Wallis one-way analysis of variance was used. The power of the study miRs to predict STEMI was analysed by the receiver operating characteristic (ROC) curve analysis; the area under the curve (AUC) was calculated with 95% confidence intervals (CI). A p-value of ≤ 0.05 was considered to indicate a statistically significant difference. The statistical analyses were performed using GraphPad Prism version 6 (La Jolla, CA, USA). We used Binary logistic regression model to combine the levels of miR-151-3p and miR-331 as a signature. The combined probability model was then used to assess the power of this signature to predict patients with STEMI from the control groups in an ROC analysis. The IBM SPSS Statistics for Windows, Version 25.0 (IBM Corp., Armonk, NY) was used solely for this analysis.

Received: 2 January 2019; Accepted: 19 March 2020;

Published online: 03 April 2020

References

1. Townsend, N. *et al.* Cardiovascular disease in Europe: epidemiological update 2016. *Eur. Heart J.* **37**, 3232–3245 (2016).
2. Muller, J. E., Toffler, G. H. & Stone, P. H. Circadian variation and triggers of onset of acute cardiovascular disease. *Circulation* **79**, 733–743 (1989).
3. Friedman, M. & Van den Bovenkamp, G. J. The pathogenesis of a coronary thrombus. *Am. J. Pathol.* **48**, 19–44 (1966).
4. Go, A. S. *et al.* Heart Disease and Stroke Statistics—2014 Update. *Circulation* **129**, e28–e292 (2014).
5. Murray, C. J. L. & Lopez, A. D. Measuring the Global Burden of Disease. *N. Engl. J. Med.* **369**, 448–457 (2013).
6. Franco, M., Cooper, R. S., Bilal, U. & Fuster, V. Challenges and Opportunities for Cardiovascular Disease Prevention. *Am. J. Med.* **124**, 95–102 (2011).
7. Feinberg, M. W. & Moore, K. J. MicroRNA Regulation of Atherosclerosis. *Circ. Res.* **118**, 703–720 (2016).
8. Economou, E. K. *et al.* The role of microRNAs in coronary artery disease: From pathophysiology to diagnosis and treatment. *Atherosclerosis* **241**, 624–33 (2015).
9. Kaudewitz, D., Zampetaki, A. & Mayr, M. MicroRNA Biomarkers for Coronary Artery Disease? *Genetics*, <https://doi.org/10.1007/s11883-015-0548-z> (2015).
10. Kaudewitz, D., Zampetaki, A. & Mayr, M. MicroRNA Biomarkers for Coronary Artery Disease? *Curr. Atheroscler. Rep.* **17**, 70 (2015).
11. Fichtlscherer, S., Zeiher, A. M. & Dimmeler, S. Circulating MicroRNAs. *Arterioscler. Thromb. Vasc. Biol.* **31**, 2383–2390 (2011).
12. Leistner, D. M. *et al.* Transcoronary gradients of vascular miRNAs and coronary atherosclerotic plaque characteristics. *Eur. Heart J.* **37**, 1738–1749 (2016).
13. Thygesen, K. *et al.* Fourth universal definition of myocardial infarction (2018). *Eur. Heart J.*, <https://doi.org/10.1093/eurheartj/ehy462> (2018).
14. Zanette, D. L. *et al.* miRNA expression profiles in chronic lymphocytic and acute lymphocytic leukemia. *Brazilian J. Med. Biol. Res. = Rev. Bras. Pesqui. medicas e Biol.* **40**, 1435–40 (2007).
15. Zhao, D., Sui, Y. & Zheng, X. miR-331-3p inhibits proliferation and promotes apoptosis by targeting HER2 through the PI3K/Akt and ERK1/2 pathways in colorectal cancer. *Oncol. Rep.* **35**, 1075–1082 (2016).
16. Epis, M. R., Giles, K. M., Barker, A., Kendrick, T. S. & Leedman, P. J. miR-331-3p regulates ERBB-2 expression and androgen receptor signaling in prostate cancer. *J. Biol. Chem.* **284**, 24696–704 (2009).

17. Expression of microRNA-331 can be used as a predictor for response to therapy and survival in acute myeloid leukemia patients. - PubMed - NCBI. Available at, <https://www.ncbi.nlm.nih.gov/pubmed/25620533>. (Accessed: 14th October 2018).
18. Pahl, M. C. *et al.* MicroRNA expression signature in human abdominal aortic aneurysms. *BMC Med. Genomics* **5**, 25 (2012).
19. Luers, A. J., Loudig, O. D. & Berman, J. W. MicroRNAs are expressed and processed by human primary macrophages. *Cell. Immunol.* **263**, 1–8 (2010).
20. Naqvi, A. R. *et al.* Expression Profiling of LPS Responsive miRNA in Primary Human Macrophages. *J. Microb. Biochem. Technol.* **8**, 136–143 (2016).
21. Xiao, L., Ming, H., Tao, C. & Yuliang, W. The expression of SOCS is altered in atherosclerosis. *Heart* **97**, A51–A51 (2011).
22. Yang, Y., Yang, L., Liang, X. & Zhu, G. MicroRNA-155 Promotes Atherosclerosis Inflammation via Targeting SOCS1. *Cell. Physiol. Biochem.* **36**, 1371–81 (2015).
23. Zhai, C. *et al.* Selective Inhibition of PI3K/Akt/mTOR Signaling Pathway Regulates Autophagy of Macrophage and Vulnerability of Atherosclerotic Plaque. *Plos One* **9**, e90563 (2014).
24. Auge, N. *et al.* Oxidized LDL-Induced Smooth Muscle Cell Proliferation Involves the EGF Receptor/PI-3 Kinase/Akt and the Sphingolipid Signaling Pathways. *Arterioscler. Thromb. Vasc. Biol.* **22**, 1990–1995 (2002).
25. Concomitant dysregulation of microRNAs miR-151-3p and miR-126 correlates with improved survival in resected cholangiocarcinoma|Read by QxMD. Available at, <https://www.readbyqxmd.com/read/23458262/concomitant-dysregulation-of-micrornas-mir-151-3p-and-mir-126-correlates-with-improved-survival-in-resected-cholangiocarcinoma>, (Accessed: 14th October 2018).
26. Yeh, T.-C. *et al.* miR-151-3p Targets TWIST1 to Repress Migration of Human Breast Cancer Cells. *Plos One* **11**, e0168171 (2016).
27. Liu, X. *et al.* MicroRNA *in vivo* precipitation identifies miR-151-3p as a computational unpredictable miRNA to target Stat3 and inhibits innate IL-6 production. *Cell. Mol. Immunol.* **15**, 99–110 (2018).
28. Ni, C.-W., Qiu, H. & Jo, H. MicroRNA-663 upregulated by oscillatory shear stress plays a role in inflammatory response of endothelial cells. *Am. J. Physiol. Circ. Physiol.* **300**, H1762–H1769 (2011).
29. Groen, H. C. *et al.* High shear stress influences plaque vulnerability Part of the data presented in this paper were published in *Stroke* 2007;38:2379–81. *Neth. Heart J.* **16**, 280–3 (2008).
30. Cheng, C. *et al.* Atherosclerotic Lesion Size and Vulnerability Are Determined by Patterns of Fluid Shear Stress. *Circulation* **113**, 2744–2753 (2006).
31. Brown, A. J. *et al.* Role of biomechanical forces in the natural history of coronary atherosclerosis. *Nat. Rev. Cardiol.* **13**, 210–220 (2016).
32. Rome, S. Are extracellular microRNAs involved in type 2 diabetes and related pathologies? *Clin. Biochem.* **46**, 937–945 (2013).
33. Soeki, T. *et al.* Plasma MicroRNA-100 Is Associated With Coronary Plaque Vulnerability. *Circ. J.* **79**, 413–418 (2015).
34. Cao, R. Y. *et al.* The Emerging Role of MicroRNA-155 in Cardiovascular Diseases. *Biomed Res. Int.* **2016**, 1–5 (2016).
35. Li, C., Chen, X., Huang, J., Sun, Q. & Wang, L. Clinical impact of circulating miR-26a, miR-191, and miR-208b in plasma of patients with acute myocardial infarction. *Eur. J. Med. Res.* **20**, 58 (2015).
36. Virmani, R., Burke, A. P., Farb, A. & Kolodgie, F. D. Pathology of the Vulnerable Plaque. *J. Am. Coll. Cardiol.* **47**, C13–C18 (2006).
37. Bentzon, J. F., Otsuka, F., Virmani, R. & Falk, E. Mechanisms of Plaque Formation and Rupture. *Circ. Res.* **114**, 1852–1866 (2014).
38. Willeit, P. *et al.* Circulating MicroRNAs as Novel Biomarkers for Platelet Activation. *Circ. Res.* **112**, 595–600 (2013).
39. Sunderland, N. *et al.* MicroRNA Biomarkers and Platelet Reactivity. *Circ. Res.* **120**, 418–435 (2017).
40. Laffont, B. *et al.* Activated platelets can deliver mRNA regulatory Ago2bulletmicroRNA complexes to endothelial cells via microparticles. *Blood* **122**, 253–261 (2013).
41. Pordzik, J. *et al.* The Potential Role of Platelet-Related microRNAs in the Development of Cardiovascular Events in High-Risk Populations, Including Diabetic Patients: A Review. *Front. Endocrinol. (Lausanne)*. **9**, 74 (2018).
42. Meder, B. *et al.* Influence of the confounding factors age and sex on microRNA profiles from peripheral blood. *Clin. Chem.* **60**, 1200–8 (2014).
43. Ibanez, B. *et al.* 2017 ESC Guidelines for the management of acute myocardial infarction in patients presenting with ST-segment elevation. *Eur. Heart J.* **39**, 119–177 (2018).
44. Bao, M.-H. *et al.* Meta-Analysis of miR-146a Polymorphisms Association with Coronary Artery Diseases and Ischemic Stroke. *Int. J. Mol. Sci.* **16**, 14305–14317 (2015).
45. Wang, J., Yan, Y., Song, D. & Liu, B. Reduced Plasma miR-146a Is a Predictor of Poor Coronary Collateral Circulation in Patients with Coronary Artery Disease. *Biomed Res. Int.* **2016**, 4285942 (2016).
46. Raitoharju, E., Oksala, N. & Lehtimäki, T. MicroRNAs in the Atherosclerotic Plaque, <https://doi.org/10.1373/clinchem.2013.204917> (2013).
47. Zhu, X. *et al.* Investigating the Role of the Posttranscriptional Gene Regulator MiR-24- 3p in the Proliferation, Migration and Apoptosis of Human Arterial Smooth Muscle Cells in Arteriosclerosis Obliterans. *Cell. Physiol. Biochem.* **36**, 1359–70 (2015).
48. Di Gregoli, K. *et al.* MicroRNA-24 Regulates Macrophage Behavior and Retards Atherosclerosis. *Arterioscler. Thromb. Vasc. Biol.* **34**, 1990–2000 (2014).
49. Pilbrow, A. P. *et al.* Circulating miR-323-3p and miR-652: Candidate markers for the presence and progression of acute coronary syndromes. *Int. J. Cardiol.* **176**, 375–385 (2014).
50. Livak, K. J. & Schmittgen, T. D. Analysis of Relative Gene Expression Data Using Real-Time Quantitative PCR and the 2^{-ΔΔCT} Method. *Methods* **25**, 402–408 (2001).
51. Li, S., Chen, H., Song, J., Lee, C. & Geng, Q. Avoiding heparin inhibition in circulating MicroRNAs amplification. *Int. J. Cardiol.* **207**, 92–93 (2016).
52. Izraeli, S., Pfeleiderer, C. & Lion, T. Detection of gene expression by PCR amplification of RNA derived from frozen heparinized whole blood. *Nucleic Acids Res.* **19**, 6051 (1991).
53. Johnson, M. L., Navanukraw, C., Grazul-Bilska, A. T., Reynolds, L. P. & Redmer, D. A. Heparinase treatment of RNA before quantitative real-time RT-PCR. *Biotechniques* **35**, 1140–1144 (2003).
54. Kaudewitz, D. *et al.* Impact of intravenous heparin on quantification of circulating microRNAs in patients with coronary artery disease. *Thromb. Haemost.* **110**, 609–615 (2013).

Acknowledgements

Research supported by MH CZ – DRO, University Hospital Motol, Prague, Czech Republic; 00064203; SVV-2013-266509 from the Charles University in Prague and by MHCR 023728.

Author contributions

M.H., P.H., C.S. and J.H. participated on the peripheral blood sample collection. M.H., J.H. and C.S. participated on the collection of the background clinical data. J.V. and P.H. performed all the diagnostic coronary angiographies and the percutaneous coronary interventions. M.H., V.H. and L.S. participated on the laboratory analysis of the data. M.H., V.H. and P.H. worked on the interpretation and statistical analysis of the data. V.H.

prepared the figures and the table. M.H., V.H., J.V., J.H. and P.H. participated on the draft of the main manuscript text. All other authors contributed to its critical revision. All authors disclose any relationship with industry.

Competing interests

The authors declare no competing interests.

Additional information

Correspondence and requests for materials should be addressed to M.H.

Reprints and permissions information is available at www.nature.com/reprints.

Publisher's note Springer Nature remains neutral with regard to jurisdictional claims in published maps and institutional affiliations.



Open Access This article is licensed under a Creative Commons Attribution 4.0 International License, which permits use, sharing, adaptation, distribution and reproduction in any medium or format, as long as you give appropriate credit to the original author(s) and the source, provide a link to the Creative Commons license, and indicate if changes were made. The images or other third party material in this article are included in the article's Creative Commons license, unless indicated otherwise in a credit line to the material. If material is not included in the article's Creative Commons license and your intended use is not permitted by statutory regulation or exceeds the permitted use, you will need to obtain permission directly from the copyright holder. To view a copy of this license, visit <http://creativecommons.org/licenses/by/4.0/>.

© The Author(s) 2020

J. Beneš a kol.

*Exercise dynamics of cardiac biomarkers and hemoconcentration
in patients with chronic systolic heart failure*

Journal of Cardiac Failure
Impact Factor: 3,942

Brief Report

Exercise dynamics of cardiac biomarkers and hemoconcentration in patients with chronic systolic heart failure

JAN BENES, MD, PHD,^{1,2} MARTIN KOTRC, MD,¹ MICHAEL J. CONRAD, MLA,³ JOSEF KAUTZNER, MD, PHD,¹ VOJTECH MELENOVSKY, MD, PHD,¹ AND PETR JAROLIM, MD, PHD³

Prague, Czech Republic; and Boston, USA

Introduction

Cardiac troponin, natriuretic peptides, adrenomedullin, and copeptin capture different pathophysiological mechanisms and can be employed in the diagnosis and monitoring of patients with heart failure (HF).^{1,2}

The mid-regional fragment of proadrenomedullin, copeptin, the mid-regional fragment of the precursor of the atrial natriuretic peptide and N-terminal pro B-type natriuretic peptide are more stable than biologically active peptides and are, thus, used as surrogates.³⁻⁵ Cardiac troponin can be measured by highly sensitive cTnI assay based on single molecule counting (sm-cTnI), which allows measurement of plasma cTnI concentrations in all healthy individuals.⁶

Concentration of multiple biomarkers can significantly change upon exercise, which can be caused both by exercise-induced hemoconcentration^{7,8} and by various specific mechanisms such as increased myocardial stress.⁹ Whether the biomarker levels drawn after exercise provide additional prognostic information beyond resting levels remains unclear. The goal of this study was to analyze the dynamics of a set of biomarkers during exercise and to assess whether biomarker measurement immediately after exercise provides better prognostic information than the baseline values.

Methods

Patients with stable advanced HF of at least 6 months' duration with left ventricular ejection fraction < 40% were

From the ¹From the Department of Cardiology, Institute for Clinical and Experimental Medicine, Prague, Czech Republic; ²Department of Medicine, First Faculty of Medicine, Charles University and Military University Hospital Prague, Czech Republic; and ³Department of Pathology, Brigham and Women's Hospital, Harvard Medical School, Boston, MA, USA.

Reprint requests: Petr Jarolim, MD, PhD, Department of Pathology, Brigham and Women's Hospital, 75 Francis Street, Boston, MA 02115, USA. E-mail: pjarolim@partners.org

See page 1104 for disclosure information.

1071-9164/\$ - see front matter

© 2020 Elsevier Inc. All rights reserved.

<https://doi.org/10.1016/j.cardfail.2020.07.004>

enrolled together with controls matched for age, sex and body composition. Patients with recent (< 3 months) HF decompensation or potentially reversible left ventricular dysfunction were excluded. The protocol was approved by the Institutional Ethics Committee. All study subjects signed an informed consent. Patients were prospectively followed, and the adverse outcome was defined as the combined endpoint of death, urgent heart transplantation or ventricular assist device implantation. Subjects underwent symptom-limited upright cycle ergometry until exhaustion, and blood was drawn prior to exercise and immediately after exercise termination. First, we assessed an absolute change in biomarker concentration. Because the observed effect on biomarker dynamics could be influenced by hemoconcentration and achieved workload, we subsequently performed a correction for both these variables. Hemoconcentration was calculated as the difference between total protein (TP) concentrations before and after exercise.¹⁰ Data were analyzed using JMP 11 (SAS Institute, Cary, NC, USA). A full description of the methods is in the Online Supplement.

Results

The patients enrolled in our study had advanced HF, with left-ventricle ejection fractions of 24%, average New York Heart Association functional class of 2.7 and long histories of HF (mean 7.6 years), but they achieved high degrees of guideline-recommended HF therapy (97% were receiving beta-blockers, and 54.5% had implantable cardioverter defibrillators). During a follow-up of 1050 ± 664 days, 55.6% of patients experienced an adverse event. No adverse events occurred in the control group (Table 1).

Exercise-induced hemoconcentration

Exercise led to significant hemoconcentration as judged by the changes in TP concentration (Table 1). In patients with HF and control subjects, hemoconcentration was directly proportional to the maximum workload achieved. When adjusted for the maximum workload achieved, no

Table 1. Characteristics of study subjects

	Controls n = 25	HF n = 108	<i>P</i>
Anthropometry			
Age, years	50 ± 8	54 ± 8	0.07
Male gender, %	88	86	0.80
BMI, kg m ⁻²	28 ± 3	28 ± 4	0.40
Heart failure and comorbidities			
Ischemic etiology, %	-	47	-
HF duration, years	-	7.6	-
NYHA functional class (1-4)	1 ± 0	2.7 ± 0.6	<0.0001
MLHFQ score sum	1 ± 2	45 ± 23	<0.0001
Diabetes	0 (0 %)	33 (31 %)	0.0002
Obesity	6 (24 %)	34 (31 %)	0.466
Anemia	0 %	24 (22 %)	0.009
eGFR, mL·min ⁻¹ ·1.73m ⁻²	91.2 ± 15.0	72 ± 22.8	<0.001
Hemoglobin A1C, %	3.8 ± 0.4	5.2 ± 2	0.001
Hemoglobin, g·l ⁻¹	152 ± 12	143 ± 16	0.009
Cardiac function			
LV ejection fraction, %	60 ± 0	24 ± 6	<0.0001
LV end-diastolic diameter, mm	50 ± 5	70 ± 8	<0.0001
Left atrium (PLAX), mm	40 ± 1.3	50 ± 0.6	<0.0001
RV dysfunction grade	0	1.5 ± 1	<0.0001
IVC, mm	15 ± 12	20 ± 16	<0.0001
Medication			
Furosemide use, daily dose, mg	-	96%, 103 ± 80	-
Beta-blocker use, daily dose (0-3)	-	97%, 1.5 ± 0.7	-
ACEI or ARB use	-	90%	-
aldosterone antagonists use	-	85%	-
Cardiopulmonary exercise test			
Heart rate rest/peak, s ⁻¹	74 ± 9/161 ± 16	79 ± 12/123 ± 24	<0.01
Systolic BP rest/peak, mmHg	118 ± 15/194 ± 27	97 ± 16/123 ± 23	<0.01
Diastolic BP rest/peak, mmHg	85 ± 12/92 ± 14	68 ± 12/74 ± 13	<0.01
Rate-pressure product	31 317 ± 5756	15 241 ± 4615	< 0.0001
Work rate, peak, watt	172 ± 50	72 ± 27	< 0.0001
Peak VO ₂ , mL·kg ⁻¹ ·min ⁻¹	29.2 ± 7	15 ± 4	< 0.0001
Respiratory quotient, peak	1.1 ± 0.1	1.1 ± 0.1	0.238
VE/VCO ₂ slope	24.2 ± 3	35.7 ± 10	< 0.0001
Total protein baseline, g·dL ⁻¹	6.7 ± 0.3	7.1 ± 0.5	0.004
Total protein post-exercise, g·dL ⁻¹	7.8 ± 0.4	7.6 ± 0.5	0.06
Δ total protein/workload, g·dL ⁻¹ ·watt ⁻¹	0.006 ± 0.002	0.008 ± 0.005	0.11
Devices			
BiV-pacemaker	-	7 pts. (6.5%)	-
ICD	-	33 pts. (30.6%)	-

(continued)

Table 1 (Continued)

	Controls n = 25	HF n = 108	<i>P</i>
BiV-ICD	-	26 pts. (24.1%)	-
Follow-up			
Follow-up length, days	-	1050 ± 664	-
Alive at follow-up end	-	39	-
No. of deaths	-	23	-
No. of urgent heart transplants	-	26	-
No. of nonurgent heart transplants	-	9	-
No. of mechanical circulatory support implantations	-	11	-

Obesity was defined as BMI ≥ 30. Values are means ± SD. ACEI, angiotensin-converting enzyme inhibitor; ARB, angiotensin receptor blocker; BiV, biventricular; BMI, body mass index; BP, blood pressure; DM, diabetes mellitus; eGFR, estimated glomerular filtration rate; HF, heart failure; ICD, International Classification of Diseases; IVC, inferior vena cava; LV, left ventricle; MLHFQ, Minnesota Living with Heart Failure Questionnaire; NYHA, New York Heart Association; PLAX, parasternal long axis; RV, right ventricle; VCO₂, body carbon dioxide production; VE, minute ventilation; VO₂, body oxygen consumption.

difference in the extent of hemoconcentration between controls and patients with HF was found (Supplementary Fig. 1A,B) (Table 1).

Unadjusted exercise-induced changes in biomarker levels

Exercise induced modest but statistically significant increases in the levels of all analyzed biomarkers, including troponin in patients with HF (ΔMR-proANP + 34.2 ng/L, ΔNT-proBNP + 168.9 ng/L, Δcopeptin + 9.71 ng/L, ΔMR-proADM + 0.023 ng/L Δsm-TnI + 0.94 ng/L; values are given as medians; *P* < 0.05 for all). In controls, significant increases were observed only for NT-proBNP (+ 5.68 ng/L), MR-proANP (+ 14.71 ng/L) and copeptin (+ 8.06 ng/L); values are given as medians; *P* < 0.05 for all (Supplementary Fig. 2).

Adjusted exercise-induced changes in biomarker levels

When absolute changes in biomarker concentrations were corrected for changes in TP, the increase in NT-proBNP (+ 2.82 ng/L for controls, + 36.98 ng/L for patients with HF), MR-proANP (+7.85 ng/L for controls, +12.23 ng/L for patients with HF), and copeptin (+7.21 ng/L for controls, +7.42 ng/L for patients with HF) remained statistically significant (all values given as medians, *P* < 0.05), whereas there was no statistically significant change in sm-TnI. MR-proADM showed a statistically significant decrease (-0.04 ng/L for both controls and patients with

HF, $P < 0.05$) (Supplementary Fig. 3). When further adjusted for achieved workload, both MR-proANP and NT-proBNP increased more, and a decrease in MR-proADM was more prominent in patients with HF than in controls (Fig. 1).

Impact of exercise on prognostic value

Both TP-uncorrected and corrected values revealed that most biomarkers had statistically significant predictive powers for outcome both at rest and after exercise. Baseline and postexercise cTnI concentrations were statistically

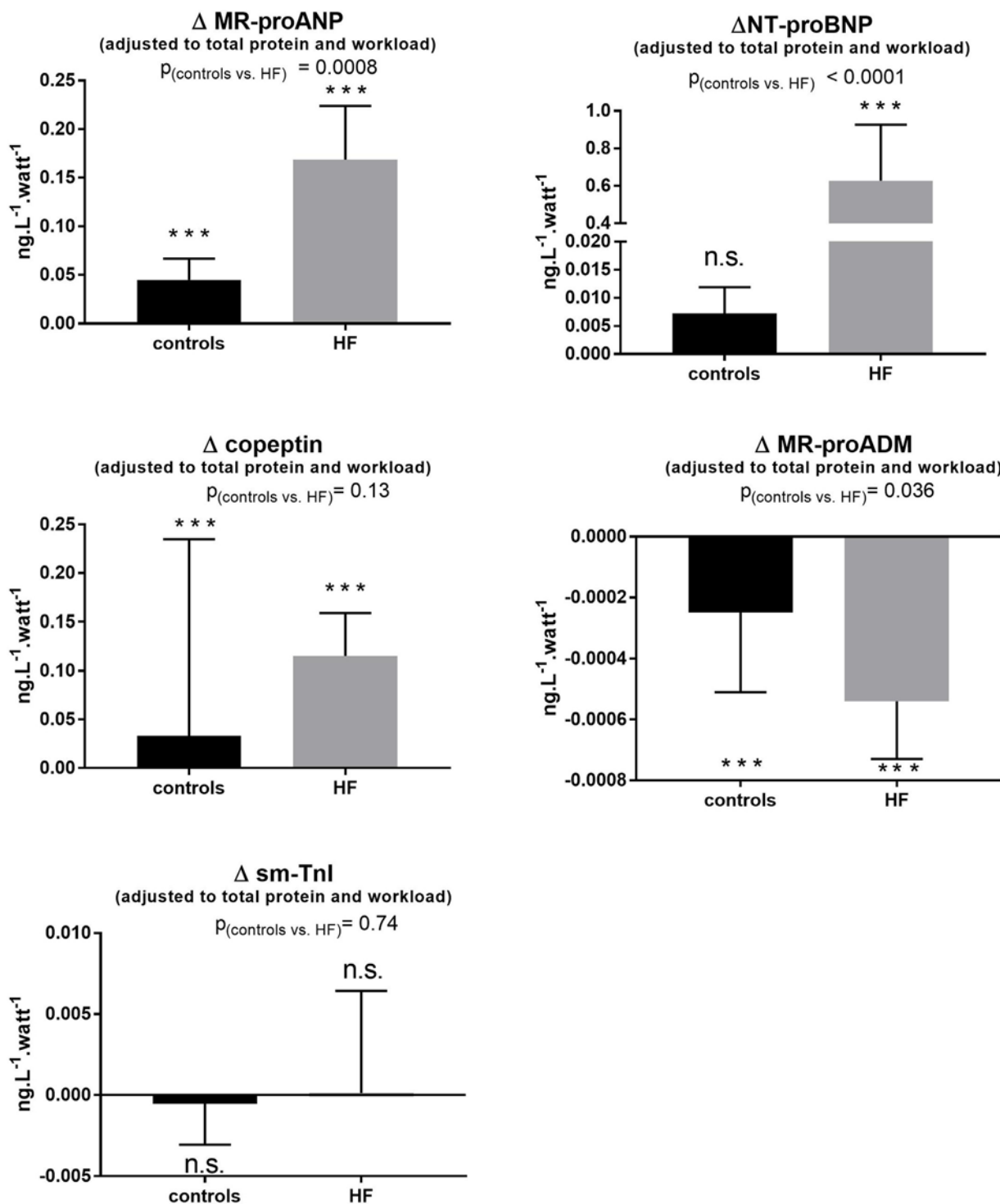


Fig. 1. Exercise-induced changes in biomarker concentration adjusted for total protein and normalized for maximal workload achieved. Data are presented as medians ± IQRs. Medians of both control subjects and patients with heart failure were tested for difference from zero. * $P < 0.05$. ** $P < 0.01$. *** $P < 0.001$. All P values are shown as uncorrected. All P values remained significant after Holm-Bonferroni correction.

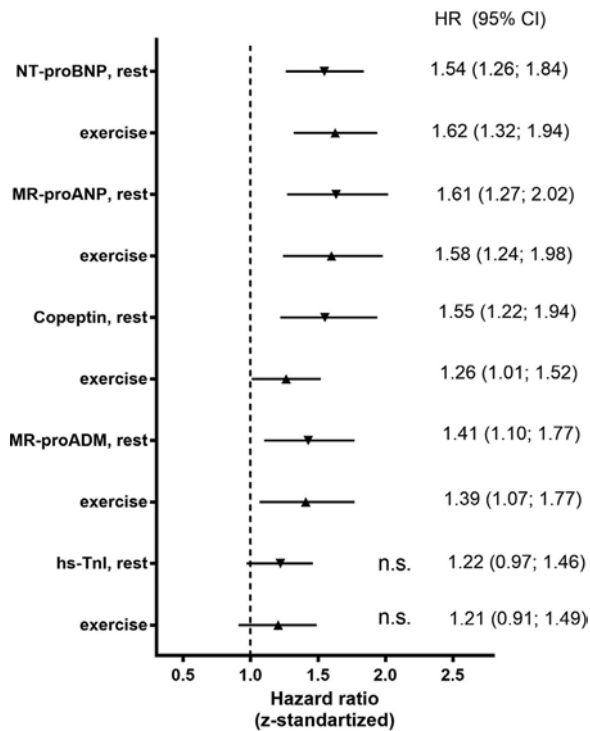


Fig. 2. Risk of adverse events for pre- and postexercise biomarker levels. Forest plot of hazard ratios after performing Z-standardization is shown. Postexercise biomarker levels are corrected for hemoconcentration.

insignificant. The prognostic values of both hemoconcentration-uncorrected and -corrected values were almost identical. Hemoconcentration alone was unrelated to outcome (P for TP change = 0.78). There was no statistically significant difference between the prognostic value of biomarker levels measured after exercise and at baseline (hemoconcentration corrected) (Fig. 2). Accordingly, receiver operating characteristic analysis showed nearly identical areas under receiver operating characteristic curves for resting and postexercise biomarker levels (Supplementary Table 1).

Discussion

Exercise-induced increase in troponin levels could be explained by hemoconcentration alone. In contrast, NT-proBNP, MR-proANP, copeptin, and MR-proADM showed an exercise-induced component that was independent of hemoconcentration. Both baseline and postexercise biomarker levels provided similar prognostic information.

Hemoconcentration-dependent biomarker changes

Exercise elevates lactate levels and increases extravascular osmotic pressure. Together with increased arterial pressure and sympathetic activation,⁷ this leads to fluid transfer from intravascular to extravascular space and ensuing hemoconcentration.^{8,11}

This is particularly important in patients with HF who have impaired increase in cardiac output during exercise, and hemoconcentration facilitates oxygen extraction.¹² The observed degree of hemoconcentration after adjustment for achieved workload did not differ between healthy subjects and patients with HF, as reported previously.^{7,8}

In order to dissect the impact of hemoconcentration from other potential causes of exercise-induced biomarker dynamics, we corrected the biomarker level for changes in total protein concentration. The observed increase in unadjusted sm-cTnI levels in patients with HF became insignificant after correction for total protein concentration. This suggests that hemoconcentration is the predominant mechanism leading to sm-cTnI increase in this cohort with HF with reduced ejection fraction. This is in accordance with the study by Sabatine and coworkers who observed an increase in hs-cTnI in patients with coronary artery disease after a 2-hour delay.⁶

Hemoconcentration-independent biomarker exercise dynamics

Adjustment for hemoconcentration revealed significant exercise-induced dynamics for natriuretic peptide surrogates MR-proANP and NT-proBNP as well as copeptin and MR-proADM. This effect must be due to mechanisms other than hemoconcentration.¹³⁻¹⁵ Additional adjustment for achieved workload revealed larger exercise-induced natriuretic peptide changes in patients with HF, suggesting larger degrees of exercise-induced myocardial stress compared to controls. The dynamics of natriuretic peptides on exercise have already been studied,¹⁶ but the novelty of our study is the ability to distinguish hemoconcentration-dependent and -independent changes. The rapid dynamics of natriuretic peptides correspond well with recently proposed mechanisms of BNP synthesis and release. BNP is likely produced constitutively also by unstressed ventricles as biologically inactive glycosylated proBNP. Cardiac stress limits the time for proBNP glycosylation and, thus, enables furin/corin processing, leading to the production of biologically active BNP.¹⁷

The adjustment for achieved workload revealed a larger decrease of MR-proADM in patients with HF compared to controls. ADM freely diffuses between blood and interstitium and helps to preserve endothelial integrity; disruption of the adrenomedullin (ADM) system results in vascular leakage and systemic and pulmonary edema.¹⁸ ADM binding to endothelial cells may be stimulated by exercise-induced volume transfer from intravascular to extravascular space, which may differ between healthy subjects and patients with HF. Whether the dynamics of the surrogate biomarker MR-proADM mirrors the action of the biologically active ADM needs to be further confirmed. The observed exercise-related decrease in adjusted plasma levels of MR-proADM contradicts previously reported exercise-induced increase^{13,19} or no change upon exercise.¹⁵ However, these studies did not adjust MR-proADM levels for hemoconcentration.

Prognosis assessment

Biomarker levels assessed immediately after the completion of exercise provided prognostic information similar to that of baseline values, which is in agreement with previous studies.^{20,21} Consequently, detection of exercise-induced changes in studied biomarker levels does not improve the prognostic assessment.

Limitations

The study is limited by its observational character and relatively small sample size. Patients were treated not only conservatively (i.e., by optimal pharmacotherapy and implantable cardioverter defibrillator device implantation and cardiac resynchronization therapy), but some of them underwent heart transplantation or implantation of mechanical circulatory support, which may bias outcome analysis. Patients were relatively young but had advanced HF, which is reflected by the high event rate. The blood was drawn immediately after exercise; specimens collected at later time points might have enabled better characterization of biomarker changes. Importantly, with the exception of TnI, the biomarkers used in this study are surrogates of the physiologically active molecules that have different half-lives in circulation and behave differently from their physiologically active counterparts.

Conclusion

MR-proANP, NT-proBNP, MR-proADM, and copeptin showed significant hemoconcentration-independent dynamics upon exercise. Biomarker assessment after exercise provided prognostic information similar to that of baseline biomarker levels.

Funding: This work was supported by Ministry of Health of the Czech Republic, grant #NV19-02-00130.

Disclosures: Disclosures of Petr Jarolim and Josef Kautzner are in the Online Supplement. Jan Benes, Martin Kotrc, Michael J. Conrad, and Vojtech Melenovsky have nothing to disclose.

Supplementary materials

Supplementary material associated with this article can be found, in the online version, at doi:10.1016/j.cardfail.2020.07.004.

References

1. Alehagen U, Dahlstrom U, Rehfeld JF, Goetze JP. Pro-A-type natriuretic peptide, proadrenomedullin, and N-terminal pro-B-type natriuretic peptide used in a multimarker strategy in primary health care in risk assessment of patients with symptoms of heart failure. *J Cardiac Failure* 2013;19:31–9.
2. Gegenhuber A, Struck J, Dieplinger B, Poelz W, Pacher R, Morgenthaler NG, et al. Comparative evaluation of B-type natriuretic peptide, mid-regional pro-A-type natriuretic peptide, mid-regional pro-adrenomedullin, and copeptin to predict 1-year mortality in patients with acute destabilized heart failure. *J Cardiac Failure* 2007;13:42–9.
3. Morgenthaler NG, Struck J, Alonso C, Bergmann A. Measurement of midregional proadrenomedullin in plasma with an immunoluminometric assay. *Clin Chem* 2005;51:1823–9.
4. Morgenthaler NG, Struck J, Alonso C, Bergmann A. Assay for the measurement of copeptin, a stable peptide derived from the precursor of vasopressin. *Clin Chem* 2006;52:112–9.
5. Morgenthaler NG, Struck J, Thomas B, Bergmann A. Immunoluminometric assay for the midregion of pro-atrial natriuretic peptide in human plasma. *Clin Chem* 2004;50:234–6.
6. Sabatine MS, Morrow DA, de Lemos JA, Jarolim P, Braunwald E. Detection of acute changes in circulating troponin in the setting of transient stress test-induced myocardial ischemia using an ultrasensitive assay: results from TIMI 35. *Eur Heart J* 2009;30:162–9.
7. Convertino VA, Keil LC, Bernauer EM, Greenleaf JE. Plasma volume, osmolality, vasopressin, and renin activity during graded exercise in man. *J Applied Physiol* 1981;50:123–8.
8. Agostoni P, Wasserman K, Guazzi M, Cattadori G, Palermo P, Marenzi G, et al. Exercise-induced hemoconcentration in heart failure due to dilated cardiomyopathy. *Am J Cardiol* 1999;83:278–80. A6.
9. Obokata M, Reddy YNV, Melenovsky V, Kane GC, Olson TP, Jarolim P, et al. Myocardial injury and cardiac reserve in patients with heart failure and preserved ejection fraction. *J Am Coll Cardiol* 2018;72:29–40.
10. Alis R, Sanchis-Gomar F, Primo-Carrau C, Lozano-Calve S, Dipalo M, Aloe R, et al. Hemoconcentration induced by exercise: revisiting the Dill and Costill equation. *Scand J Med Sci Sports* 2015;25:e630–7.
11. Sjogaard G, Saltin B. Extra- and intracellular water spaces in muscles of man at rest and with dynamic exercise. *Am J Physiol* 1982;243:R271–80.
12. Perego GB, Marenzi GC, Guazzi M, Sganzerla P, Assanelli E, Palermo P, et al. Contribution of PO₂, P₅₀, and Hb to changes in arteriovenous O₂ content during exercise in heart failure. *J Appl Physiol* (Bethesda, Md, 1985) 1996;80:623–31.
13. Tanaka M, Ishizaka Y, Ishiyama Y, Kato J, Kida O, Kitamura K, et al. Exercise-induced secretion of brain natriuretic peptide in essential hypertension and normal subjects. *Hyperten Res* 1995;18:159–66.
14. Huang WS, Lee MS, Perng HW, Yang SP, Kuo SW, Chang HD. Circulating brain natriuretic peptide values in healthy men before and after exercise. *Metabolism* 2002;51:1423–6.
15. Zurek M, Maeder MT, Brutsche MH, Luthi A, Twerenbold R, Freese M, et al. Midregional pro-adrenomedullin and copeptin: exercise kinetics and association with the cardiopulmonary exercise response in comparison to B-type natriuretic peptide. *Eur J Appl Physiol* 2014;114:815–24.
16. Steele IC, McDowell G, Moore A, Campbell NP, Shaw C, Buchanan KD, et al. Responses of atrial natriuretic peptide and brain natriuretic peptide to exercise in patients with chronic heart failure and normal control subjects. *Eur J Clin Invest* 1997;27:270–6.
17. Vodovar N, Seronde MF, Laribi S, Gayat E, Lassus J, Boukef R, et al. Post-translational modifications enhance NT-proBNP and BNP production in acute decompensated heart failure. *Eur Heart J* 2014;35:3434–41.
18. Tanaka M, Koyama T, Sakurai T, Kamiyoshi A, Ichikawa-Shindo Y, Kawate H, et al. The endothelial adrenomedullin-RAMP2 system regulates vascular integrity and suppresses tumour metastasis. *Cardiovasc Res* 2016;111:398–409.

19. Krzeminski K, Mikulski T, Nazar K. Effect of prolonged dynamic exercise on plasma adrenomedullin concentration in healthy young men. *J Physiol Pharmacol* 2006;57:571–81.
20. de Groote P, Soudan B, Lamblin N, Rouaix-Emery N, Mc Fadden E, Meurice T, et al. Is hormonal activation during exercise useful for risk stratification in patients with moderate congestive heart failure? *Am Heart* 2004;148:349–55.
21. Kallistratos MS, Pavlidis AN, Chamodraka ES, Varounis C, Dritsas A, Laoutaris ID, et al. Prognostic value of NT-proBNP at rest and peak exercise in patients with impaired left ventricular function. *Angiology* 2012;63:516–21.

I. Jurčová a kol.

Complete recovery of fulminant cytotoxic CD8 T-cell-mediated myocarditis after ECMELLA unloading and immunosuppression

ESC Heart Failure
Impact Factor: 3,902

Complete recovery of fulminant cytotoxic CD8 T-cell-mediated myocarditis after ECMELLA unloading and immunosuppression

Ivana Jurcova¹, Jan Rocek¹, William Bracamonte-Baran², Michael Zelizko¹, Ivan Netuka¹, Jana Maluskova¹, Josef Kautzner¹, Daniela Cihakova², Vojtech Melenovsky^{1*} and Jiri Maly¹

¹Department of Cardiology, Institute for Clinical and Experimental Medicine—IKEM, Videnska 1958/9, 140 21, Prague 4, Czech Republic; ²Department of Pathology, Johns Hopkins University, Baltimore, MD, USA

Abstract

A 19-year-old woman with no previous cardiac history was admitted to the hospital with third-degree atrioventricular block and left ventricular dysfunction. Her condition quickly deteriorated to severe biventricular failure and cardiogenic shock requiring mechanical circulatory support. An endomyocardial biopsy revealed lymphocytic myocarditis with no PCR-detectable viral genomes, with CD8 T-cell predominance and pro-inflammatory macrophage expansion shown by myocardial flow cytometry. The therapy consisted of immunosuppression (high-dose methylprednisolone) and temporary mechanical circulatory support with enhanced ability to achieve left ventricular unloading by combination of extracorporeal membrane oxygenation with Impella (ECMELLA). After 2 weeks of support, complete and sustained recovery from myocarditis was observed.

Keywords Fulminant myocarditis; Immunosuppression; Mechanical circulatory support; Extracorporeal membrane oxygenation (ECMO)

Received: 5 October 2019; Revised: 20 February 2020; Accepted: 13 March 2020

*Correspondence to: Vojtech Melenovsky, Department of Cardiology, Institute for Clinical and Experimental Medicine—IKEM, Videnska 1958/9, 140 21 Prague 4, Czech Republic. Email: vojtech.melenovsky@ikem.cz

Ivana Jurcova, Jan Rocek, Vojtech Melenovsky, and Jiri Maly contributed equally to this work.

Introduction

Fulminant myocarditis (FM) is a rare and severe form of myocarditis that presents with sudden onset of acute heart failure, cardiogenic shock, and/or life-threatening arrhythmias. FM may be viral, bacterial, toxic, or autoimmune in origin.^{1,2} The damage of the myocardium may result from direct cardiomyocyte insult or from indirect injury by immune-mediated cytotoxicity or tissue oedema. The diagnosis and treatment of FM are still a clinical challenge owing to variability of clinical presentation and limited use of myocardial biopsy. The management often requires intensive care, inotropic and mechanical circulatory support (MCS), and sometimes immunosuppressive therapy. Besides supporting circulation, unloading of the left ventricle by MCS may lead to additional disease-modifying effects over time that can be important for enhancing myocardial recovery.³

Case report

We report a case of a 19-year-old woman with past medical history of atopic eczema and asthma (chronically treated with desloratadine, montelukast, and salmeterol/fluticasone) who presented to a regional hospital after 2 days of gastrointestinal symptoms (diarrhoea and vomiting) with third-degree atrioventricular block, left ventricular (LV) systolic dysfunction (LV ejection fraction 40%), elevated cardiac biomarkers (high-sensitivity troponin T 13 850 ng/L and N terminal pro brain natriuretic peptide 19 686 ng/L). The condition progressed quickly to cardiogenic shock requiring inotropes, temporary transvenous pacing, and tracheal intubation. Coronary angiography showed patent arteries. Within the next day, her status further deteriorated with development of severe biventricular dysfunction, widening of QRS complex (*Figure 1A*), and multiple organ failure. She was transferred to our centre for further management. Urgent transfemoral

veno-arterial extracorporeal membrane oxygenation (VA ECMO) was introduced. Global LV ejection fraction dropped to <10% with further QRS widening (Figure 1B).

Right ventricular endomyocardial biopsy (EMB) revealed diffuse lymphocytic myocarditis, resembling severe cellular allograft rejection, with interstitial oedema and mild myocyte necrosis (Figure 2). PCR for detection of viral pathogens in the EMB specimen was negative (adenoviruses, enteroviruses, coxsackieviruses, parvoviruses, influenza A and B, herpes simplex virus 1 and 2, human herpes virus 6, varicella zoster virus, Epstein–Barr virus, and cytomegalovirus).

To comprehensively characterize infiltrating leucocyte subsets, multiparameter flow cytometry (FACS) analysis of EMB was performed in Dr. Čiháková's lab at Johns Hopkins University in Baltimore, MD, USA. Detailed description of the method is provided in the Supporting Information. Samples were shipped deep-frozen and were processed by cutting, digestion (collagenase II and DNase I), and mechanical dissociation using gentleMACS (Miltenyi Biotec). Cells were filtered, re-suspended, and counted. Surface immunostaining was performed using standard protocols using fluorochrome-labelled antibodies (eBiosciences, BD Biosciences, and BioLegend). Markers used for immunostaining

were as follows: CD45, TCR $\alpha\beta$, CD4, CD8, CXCR3, CCR6, CCR7, CCR2, IL23R, CD11b, CD66b, HLA-DR, CD16, CD14, CD68, and CD19. FACS data were acquired with an LSRFortessa and analysed with FlowJo v10.4 (Tree Star). Viability of cells based on competence of plasma membrane was ~12%. As a control, a similar analysis was performed in an autopsy specimen obtained from an individual without cardiac disease.

In the myocarditis EMB, we found a shift in the CD4⁺/CD8⁺ T-cell ratio of 1:3 as compared with 3:1 in the control, suggesting a predominant cytotoxic CD8 response (Figure 3A). In both CD4 and CD8 compartments, there was a change from the predominant naïve/central memory T-cell status (CCR7⁺CXCR3⁺) observed in the control toward a predominant effector/effector memory phenotype (CCR7^{neg}CXCR3⁺ CD4 T cells and CCR7^{neg}CXCR3^{neg} CD8 T cells) (Figure 3B, C), demonstrating activation of myocardium-infiltrating T-cell clones. We also observed expansion and functional changes in the myocardial myeloid compartment. In the autopsy control, the macrophages were almost exclusively CD14⁺CD16⁺ macrophages, whereas in myocarditis EMB sample, we found mainly pro-inflammatory CD14^{int/+}CD16^{neg} macrophages (Figure 3D). The latter suggests a pro-inflammatory role of

Figure 1 Twelve-lead electrocardiograms (ECG) (A) at presentation to the hospital, with temporary transvenous pacemaker spikes; (B) prior to ECMO implantation; (C) sustained monomorphic ventricular tachycardia during further deterioration; (D) prior discharge from the hospital.

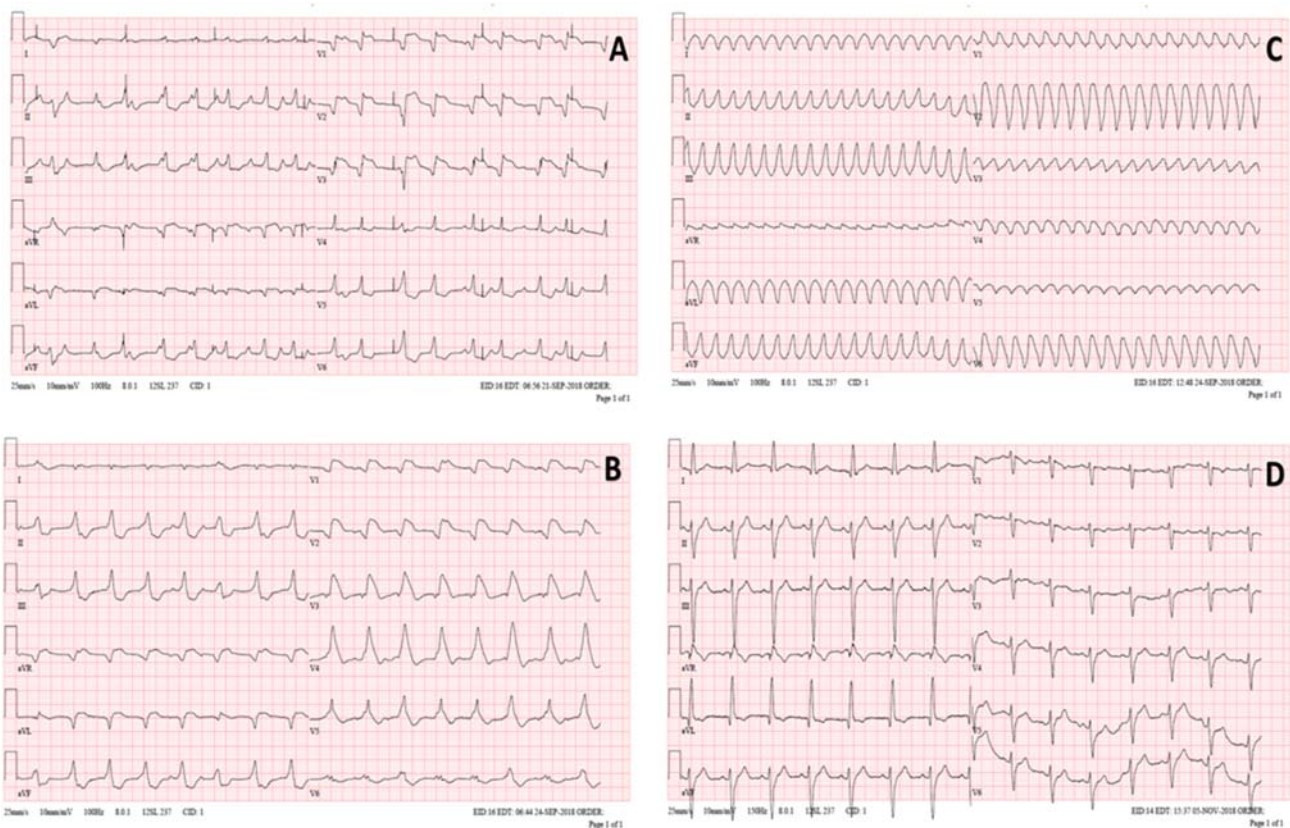
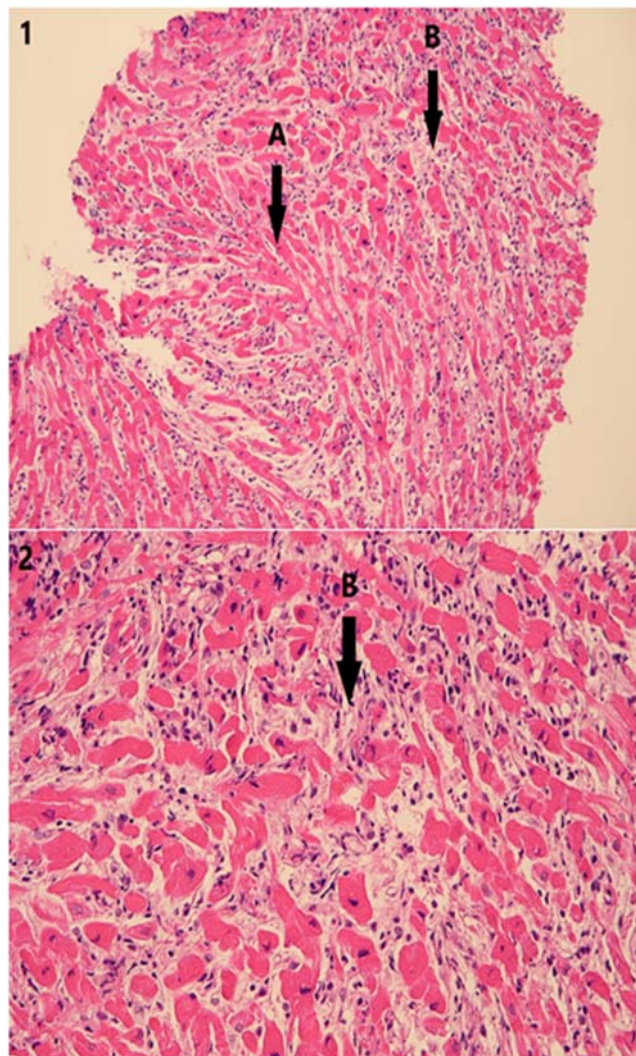


Figure 2 Lymphocytic myocarditis. Haematoxylin–eosin, original magnification (1) $\times 200$ and (2) $\times 400$. (A) Normal myocardial fibres. (B) Myocardial necrosis with interstitial inflammatory oedema and infiltrate, mostly lymphocytic.

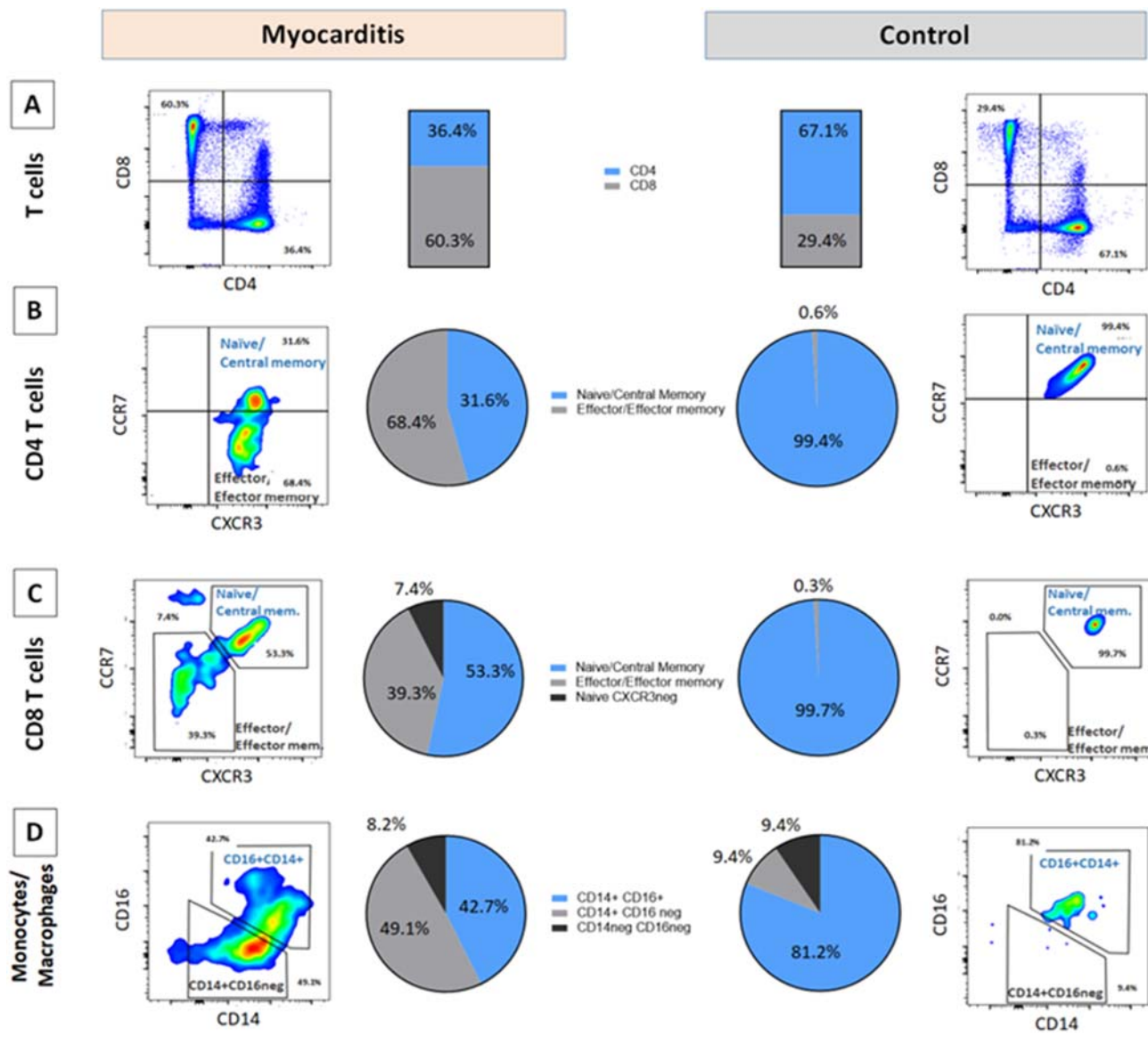


macrophages in supporting the T-cell response. Because of clear evidence of immune-mediated origin, immunosuppression with 1 g/day (in 3 days) of methylprednisolone (Solu-Medrol, Pfizer) and intravenous immunoglobulin G (0.5 g/kg of body weight; Privigen, Behring) was instituted.

Two days after ECMO implantation, the patient developed episodes of refractory sustained ventricular tachycardia (rate 224 b.p.m.) requiring cardioversion (*Figure 1C*), accompanied by complete LV akinesia and worsening pulmonary gas exchange. In order to achieve better venting of stagnating LV cavity, Impella 2.5 (Abiomed) pump was introduced transfemorally across the aortic valve. With such 'ECMELLA' (ECMO + Impella) configuration,³ prompt stabilization was achieved. Immediately after ECMELLA, ventricular tachycardia ceased and QRS complex narrowed (*Figure 1D*). Owing

to continued LV dysfunction after several days, Impella 2.5 was exchanged for Impella 5.0 device introduced via a graft sewn on right subclavian artery (*Figure 4*), a device that has longer durability and full-flow support capability. Immunosuppression was continued with oral prednisone 1 mg/kg/day. On Day 10, echocardiogram showed marked improvement of systolic function of ventricles (left ventricular ejection fraction > 60%). ECMO was discontinued on the Day 11, Impella was explanted on the Day 13, and the patient remained haemodynamically stable. Further recovery was uneventful, and the patient was discharged after 44 days. At the discharge, patient had normal cardiac function by echocardiography and cardiac magnetic resonance imaging, without evidence of late gadolinium enhancement, with normal BNP and troponin levels, and with incomplete right bundle branch

Figure 3 Composition and activation status of intramyocardial leucocyte compartments. Flow cytometry from endomyocardial biopsy (EMB) tissue shows (A) CD4/CD8 balance in myocarditis EMB vs. autopsy control (gated on CD3⁺CD11b^{neg}CD19^{neg} viable cells), showing a reversed CD4/CD8 ratio in myocarditis. (B, C) Activation status of CD4 T cells and CD8 T cells, respectively, based on CCR7/CXCR3 status, showing in both subsets a shift toward a predominant CCR7^{neg} effector status in myocarditis EMB. (D) Functional subsets of heart infiltrating macrophage/monocytes (gated on CD11b⁺CD19^{neg}CD3 should not be in normal case (not in superscript) ^{neg}CD66b^{neg} viable cells), showing a predominant pro-inflammatory phenotype CD14^{int/+}CD16^{neg} in myocarditis EMB.



block in electrocardiogram. Corticosteroids were gradually tapered off, and 360 days after discharge, the patient is in stable condition, back to school, with 2.5 mg/day of bisoprolol as the only cardiac medication.

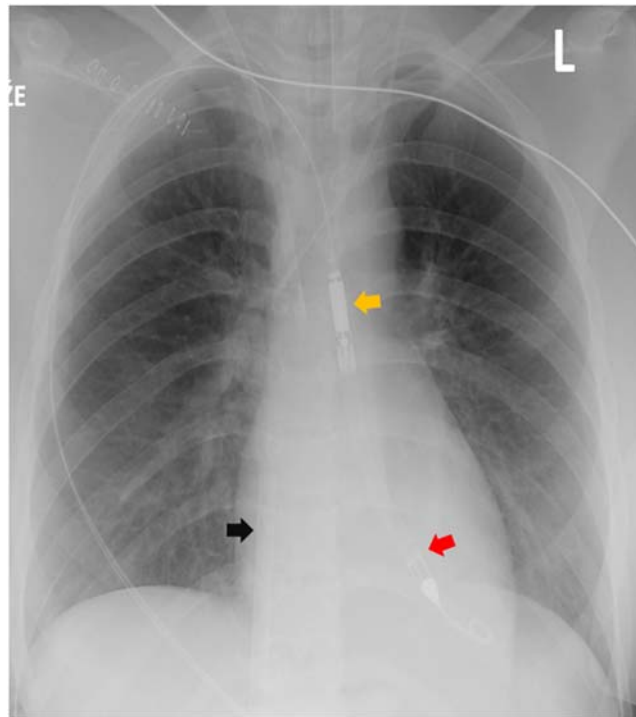
Discussion

Older studies suggested that patients with more severe presentation of myocarditis are more likely to improve cardiac

function over time,¹ but recent reports contradicted the finding.⁴ Even in patients with lymphocytic myocarditis, which is considered as more benign variant of FM, event rates are still high especially if associated with LV dysfunction or ventricular tachyarrhythmia.⁵ Early institution of MCS and early myocardial biopsy to ascertain prognosis and to guide immunosuppression is critical to successful management of FM.^{3,6}

While the role of immunosuppression in lymphocytic FM is not yet fully defined due to lack of randomized human studies, it may be considered if acute viral infection in the

Figure 4 Chest radiogram showing venous cannula of extracorporeal membrane oxygenation (ECMO) circuit (black arrow), Impella 5.0 inflow segment in the left ventricle (red arrow), and outflow segment in aorta (yellow arrow).



biopsy is ruled out and if there is high likelihood of autoimmune aetiology, for example in patients with pre-existing autoimmune disease.² In addition to conventional histology, we used multichannel flow cytometry of myocardial sample to better the nature of myocardial inflammation in our patient. We found striking evidence of CD8 T-cell predominance, accompanied by activation status of the entire T lymphoid compartment. The finding resembled acute cellular allograft rejection, a condition responsive to high-dosed course of methylprednisolone, which was also successfully used in our case. Interestingly, CD14^{int/+}CD16^{neg} macrophages were also involved in the inflammatory milieu that may contribute to the self-sustained inflammatory process *in situ*, supporting the important role of macrophages in the development of myocarditis.⁷ The presence of normal cardiovascular magnetic resonance (CMR) image in biopsy-proven myocarditis can be explained by an interval between the biopsy and CMR imaging that were performed already after administration of immunosuppressive therapy and after resolution of LV dysfunction. The absence of late gadolinium enhancement on CMR is consistent with lack of scar development in some patients with myocarditis.⁸

Temporary MCS using ECMO increases the chances of recovery/long-term survival for patients with the most dramatic presentations. However, ECMO is often not enough to achieve decompression of stagnating left ventricle,^{4,9}

which may lead to lung oedema, LV intracavitary thrombus, and impaired myocardial tissue drainage.³ From the methods for unloading of ECMO-supported left ventricle, the choice of intraaortic balloon pump, Impella, or direct surgical LV venting depends on the individual clinical settings, risk of the intervention, local experience, and the time expected for recovery.¹⁰ We chose Impella pump because of its feasibility, effective lowering of LV intracavitary pressures,³ and capability of almost complete support. The dislodgment and intravascular haemolysis are the potential risks of this device.

Our case suggests that adding Impella to ECMO (ECMELLA concept) might enhance LV cavity drainage, which can be important for enhancing myocardial recovery/remission.¹¹ Rapid resolution of QRS prolongation, followed by improvement of LV dysfunction after adding Impella to ECMO support, suggests a possible beneficial role of low end-diastolic LV pressure, with diminished wall tension, enhanced interstitial fluid clearance, and higher perfusion gradient for resolution of myocardial inflammation.^{3,6} High-flow Impella 5.0 is also very useful for weaning VA-ECMO circuit, and it allows patient rehabilitation in case of longer support.

In summary, our case illustrates that intense haemodynamic unloading with ECMO and Impella combined with immunosuppressive therapy may offer exciting new therapeutic ability to successfully manage even life-threatening myocardial inflammation.

Conflict of interest

None declared.

Funding

This work was supported by the Ministry of Health of the Czech Republic (grant AZV 17-28784A awarded to V.M.). All rights reserved.

Supporting information

Additional supporting information may be found online in the Supporting Information section at the end of the article.

Data S1. Supporting Information

References

- McCarthy RE 3rd, Boehmer JP, Hruban RH, Hutchins GM, Kasper EK, Hare JM, Baughman KL. Long-term outcome of fulminant myocarditis as compared with acute (nonfulminant) myocarditis. *New Engl J Med* 2000; **342**: 690–695.
- Caforio AL, Pankuweit S, Arbustini E, Basso C, Gimeno-Blanes J, Felix SB, Fu M, Helio T, Heymans S, Jahns R, Klingel K, Linhart A, Maisch B, McKenna W, Mogensen J, Pinto YM, Ristic A, Schultheiss HP, Seegewiss H, Tavazzi L, Thiene G, Yilmaz A, Charron P, Elliott PM. Current state of knowledge on aetiology, diagnosis, management, and therapy of myocarditis: a position statement of the European Society of Cardiology Working Group on Myocardial and Pericardial Diseases. *Eur Heart J* 2013; **34**: 2636–2648.
- Tschope C, Van Linthout S, Klein O, Mairinger T, Krackhardt F, Potapov EV, Schmidt G, Burkhoff D, Pieske B, Spillmann F. Mechanical unloading by fulminant myocarditis: LV-IMPELLA, ECMELLA, BI-PELLA, and PROPELLA concepts. *J Cardiovasc Transl Res* 2019; **12**: 116–123.
- Ammirati E, Cipriani M, Lilliu M, Sormani P, Varrenti M, Raineri C, Petrella D, Garascia A, Pedrotti P, Roghi A, Bonacina E, Moreo A, Bottiroli M, Gagliardone MP, Mondino M, Ghio S, Totaro R, Turazza FM, Russo CF, Oliva F, Camici PG, Frigerio M. Survival and left ventricular function changes in fulminant versus nonfulminant acute myocarditis. *Circulation* 2017; **136**: 529–545.
- Ammirati E, Veronese G, Brambatti M, Merlo M, Cipriani M, Potena L, Sormani P, Aoki T, Sugimura K, Sawamura A, Okumura T, Pinney S, Hong K, Shah P, Braun O, Van de Heyning CM, Montero S, Petrella D, Huang F, Schmidt M, Raineri C, Lala A, Varrenti M, Foa A, Leone O, Gentile P, Artico J, Agostini V, Patel R, Garascia A, Van Craenenbroeck EM, Hirose K, Isotani A, Murohara T, Arita Y, Sionis A, Fabris E, Hashem S, Garcia-Hernando V, Oliva F, Greenberg B, Shimokawa H, Sinagra G, Adler ED, Frigerio M, Camici PG. Fulminant versus acute nonfulminant myocarditis in patients with left ventricular systolic dysfunction. *J Am Coll Cardiol* 2019; **74**: 299–311.
- Tschope C, Cooper LT, Torre-Amione G, Van Linthout S. Management of myocarditis-related cardiomyopathy in adults. *Circ Res* 2019; **124**: 1568–1583.
- Hou X, Chen G, Bracamonte-Baran W, Choi HS, Diny NL, Sung J, Hughes D, Won T, Wood MK, Talor MV, Hackam DJ, Klingel K, Davogusto G, Taegtmeier H, Coppens I, Barin JG, Cihakova D. The cardiac microenvironment instructs divergent monocyte fates and functions in myocarditis. *Cell Rep* 2019; **28**: 172–189.
- Abdel-Aty H, Boye P, Zagrosek A, Wassmuth R, Kumar A, Messroghli D, Bock P, Dietz R, Friedrich MG, Schulz-Menger J. Diagnostic performance of cardiovascular magnetic resonance in patients with suspected acute myocarditis: comparison of different approaches. *J Am Coll Cardiol* 2005; **45**: 1815–1822.
- Ginsberg F, Parrillo JE. Fulminant myocarditis. *Crit Care Clin* 2013; **29**: 465–483.
- Donker DW, Brodie D, Henriques JPS, Broome M. Left ventricular unloading during veno-arterial ECMO: a simulation study. *ASAIO J* 2019; **65**: 11–20.
- Spillmann F, Van Linthout S, Schmidt G, Klein O, Hamdani N, Mairinger T, Krackhardt F, Maroski B, Schlabs T, Soltani S, Anker S, Potapov EV, Burkhoff D, Pieske B, Tschope C. Mode-of-action of the PROPELLA concept in fulminant myocarditis. *Eur Heart J* 2019; **40**: 2164–2169.

M. Kubánek a kol.

*Desminopathy: Novel Desmin Variants, a New Cardiac Phenotype,
and Further Evidence for Secondary Mitochondrial Dysfunction*

Journal of Clinical Medicine
Impact Factor: 3,303



Article

Desminopathy: Novel Desmin Variants, a New Cardiac Phenotype, and Further Evidence for Secondary Mitochondrial Dysfunction

Miloš Kubánek ^{1,*}, Tereza Schimerová ^{1,2}, Lenka Piherová ³ , Andreas Brodehl ⁴ , Alice Krebsová ¹, Sandra Ratnavadivel ⁴, Caroline Stanasiuk ⁴ , Hana Hansíková ⁵, Jiří Zeman ⁵ , Tomáš Paleček ⁶, Josef Houštek ⁷ , Zdeněk Drahota ⁷, Hana Nůšková ⁷, Jana Mikešová ⁷, Josef Zámečník ⁸, Milan Macek Jr. ⁹, Petr Ridzoň ¹⁰, Jana Malusková ¹¹, Viktor Stránecký ³, Vojtěch Melenovský ¹ , Hendrik Milting ⁴ and Stanislav Kmoch ³

¹ Department of Cardiology, Institute for Clinical and Experimental Medicine, 14021 Prague, Czech Republic; nedt@ikem.cz (T.S.); krea@ikem.cz (A.K.); vome@ikem.cz (V.M.)

² Institute of Physiology, First Faculty of Medicine, Charles University, 11636 Prague, Czech Republic

³ Research Unit for Rare Diseases, Department of Pediatrics and Adolescent Medicine, First Faculty of Medicine, Charles University, 11636 Prague, Czech Republic; Lenka.Piherova@lf1.cuni.cz (L.P.); Viktor.Stranecny@lf1.cuni.cz (V.S.); skmoch@lf1.cuni.cz (S.K.)

⁴ Erich and Hanna Klessmann Institute, Heart and Diabetes Center NRW, University Hospital of the Ruhr-University Bochum, 32545 Bad Oeynhausen, Germany; ABrodehl@hdz-nrw.de (A.B.); SRatnavadivel@hdz-nrw.de (S.R.); CStanasiuk@hdz-nrw.de (C.S.); HMilting@hdz-nrw.de (H.M.)

⁵ Department of Pediatrics and Adolescent Medicine, First Faculty of Medicine, Charles University and General University Hospital in Prague, 12108 Prague, Czech Republic; Hana.Hansikova@lf1.cuni.cz (H.H.); jzem@lf1.cuni.cz (J.Z.)

⁶ 2nd Department of Medicine—Department of Cardiovascular Medicine, First Faculty of Medicine, Charles University and General University Hospital in Prague, 12108 Prague, Czech Republic; Tomas.Palecek@lf1.cuni.cz

⁷ Institute of Physiology, Czech Academy of Sciences, 11720 Prague, Czech Republic; josef.houstek@fgu.cas.cz (J.H.); zdenek.drahota@fgu.cas.cz (Z.D.); h.nuskova@dkfz-heidelberg.de (H.N.); jana.mikesova@uochb.cas.cz (J.M.)

⁸ Department of Pathology and Molecular Medicine, Second Faculty of Medicine, Charles University, 11636 Prague, Czech Republic; josef.zamecnik@lfmotol.cuni.cz

⁹ Department of Biology and Medical Genetics, Second Faculty of Medicine, Charles University, 11636 Prague, Czech Republic; milan.macek.jr@lfmotol.cuni.cz

¹⁰ Department of Neurology, Thomayer's Hospital, 14059 Prague, Czech Republic; petr.ridzon@ftn.cz

¹¹ Department of Pathology, Institute for Clinical and Experimental Medicine, 14021 Prague, Czech Republic; Institute for Clinical and Experimental Medicine, 14021 Prague, Czech Republic; jana.maluszkova@ikem.cz

* Correspondence: milos.kubanek@ikem.cz; Tel.: +42-0236-055-047; Fax: +42-0236-052-989

Received: 13 February 2020; Accepted: 24 March 2020; Published: 29 March 2020



Abstract: Background: The pleomorphic clinical presentation makes the diagnosis of desminopathy difficult. We aimed to describe the prevalence, phenotypic expression, and mitochondrial function of individuals with putative disease-causing desmin (DES) variants identified in patients with an unexplained etiology of cardiomyopathy. **Methods:** A total of 327 Czech patients underwent whole exome sequencing and detailed phenotyping in probands harboring DES variants. **Results:** Rare, conserved, and possibly pathogenic DES variants were identified in six (1.8%) probands. Two DES variants previously classified as variants of uncertain significance (p.(K43E), p.(S57L)), one novel DES variant (p.(A210D)), and two known pathogenic DES variants (p.(R406W), p.(R454W)) were associated with characteristic desmin-immunoreactive aggregates in myocardial and/or skeletal biopsy samples. The individual with the novel DES variant p.(Q364H) had a decreased myocardial expression of desmin with absent desmin aggregates in myocardial/skeletal muscle biopsy and presented with familial left ventricular non-compaction cardiomyopathy (LVNC), a relatively novel

phenotype associated with desminopathy. An assessment of the mitochondrial function in four probands heterozygous for a disease-causing *DES* variant confirmed a decreased metabolic capacity of mitochondrial respiratory chain complexes in myocardial/skeletal muscle specimens, which was in case of myocardial succinate respiration more profound than in other cardiomyopathies. **Conclusions:** The presence of desminopathy should also be considered in individuals with LVNC, and in the differential diagnosis of mitochondrial diseases.

Keywords: desmin; dilated cardiomyopathy; mitochondrial dysfunction; myopathy; non-ischemic cardiomyopathy; whole exome sequencing

1. Introduction

Desminopathy (OMIM # 601409) represents a group of autosomal inherited disorders caused by pathogenic variants in the disease-causing desmin (*DES*) gene, encoding the major muscle specific intermediate filament protein desmin (OMIM: #125660) [1]. Desmin is the major component of intermediate filaments in cardiac, skeletal, and smooth muscle cells, with a particularly high content in Purkinje fibers and diaphragmatic muscle cells [1]. Consequently, cardiomyopathy, cardiac conduction disease, and progressive skeletal myopathy are the most common clinical presentations of desminopathy. It may occur as an isolated cardiac disease or in variable combinations and with different onsets. As summarized in a meta-analysis [1], 49%, 60%, and 74% of individuals harboring a pathogenic *DES* variant develop cardiomyopathy, cardiac conduction disease, and skeletal myopathy, respectively. The most common form of myocardial involvement is dilated cardiomyopathy (DCM) [1–3], followed by restrictive (RCM) [4–7], arrhythmogenic (ACM) and hypertrophic cardiomyopathy (HCM), and arrhythmogenic cardiomyopathy pattern [8–11]. On the other hand, there is low evidence regarding an association between desminopathy and left ventricular noncompaction cardiomyopathy (LVNC). Importantly, intermediate filaments are essential not only for cellular integrity, organization, and differentiation, but also for a signal transduction and adequate mitochondrial function [12]. Accordingly, several experimental [12–14] and clinical [15,16] studies have proven a secondary mitochondrial dysfunction in desminopathy, which in one case even mimicked mitochondrial disease [16].

The pleomorphic clinical presentation makes the diagnosis of desminopathy challenging. Fortunately, massively parallel sequencing (MPS) utilizing either cardiomyopathy panels and/or even whole exome sequencing (WES) aid in the diagnosis of desminopathy regardless of its clinical presentation. Hereby, we aimed to describe the prevalence of desminopathy and their phenotypes in a large representative cohort of patients with cardiomyopathy of unexplained etiology using WES.

2. Materials and Methods

A representative cohort of 327 Czech patients with an unexplained etiology of cardiomyopathy underwent WES between September 2015 and June 2017. The cohort consisted mainly of cases with familial and sporadic DCM (81%), LVNC (13%), and less frequently of RCM (6%) or ACM (6%). Rare and possibly pathogenic missense *DES* variants were identified in 6 (1.8%) index patients from 6 different families (Figure 1).

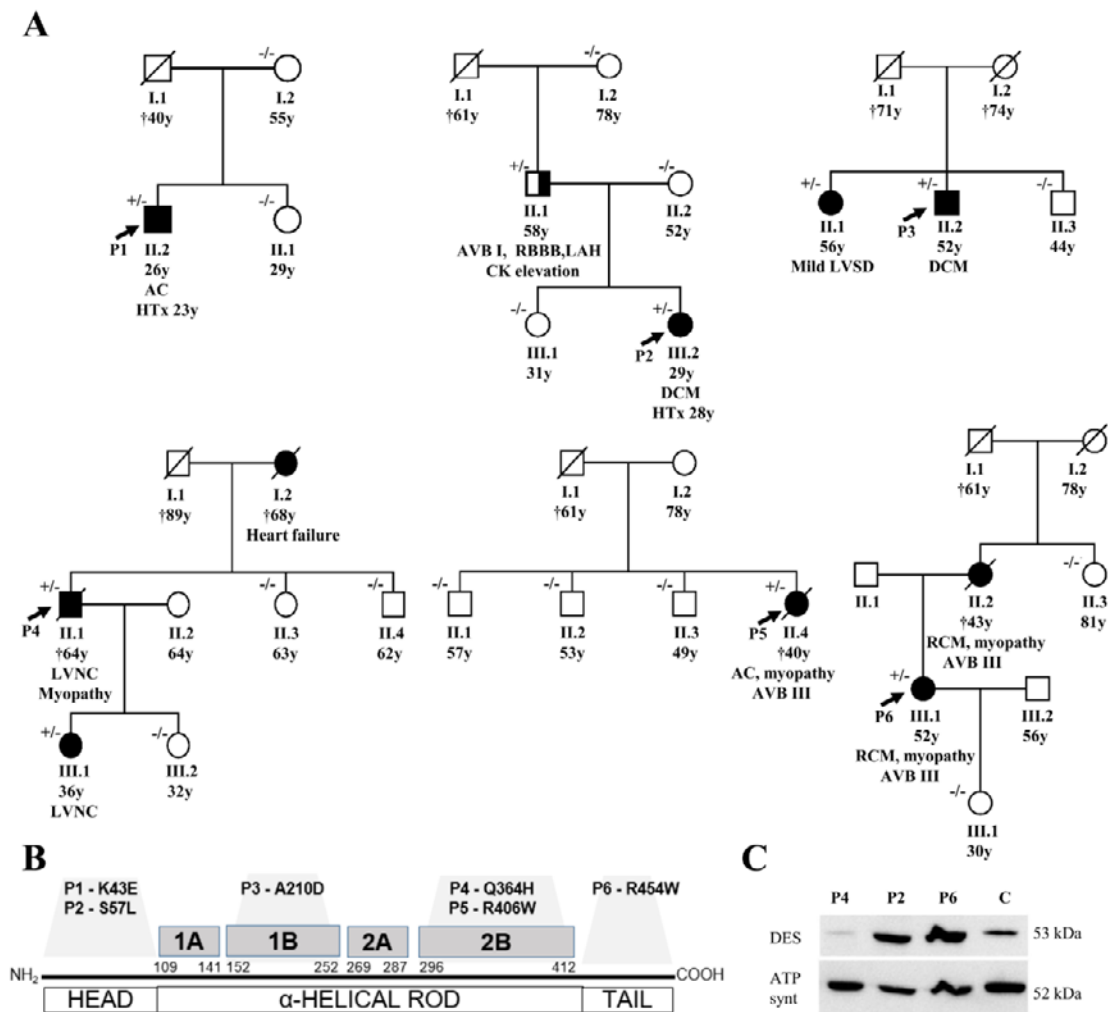


Figure 1. (A) shows pedigrees of the affected families and segregation of desmin variants (+/– heterozygous status, –/– wild type). In the fourth family (with P4) we also assessed a segregation of the rare variant of *MYH7* (NM_000257.3), c.4679G > C, p.(Arg1560Pro), which was present just in P4 (II/1) and absent in II/3, II/4, III/1, and III/2. (B) summarizes the structure of the desmin gene with localization of the detected variants. (C) illustrates the detection of desmin by western blot in myocardial samples (P2, P4, P6, control sample; 30ug protein aliquots) with an obvious reduction of signal in P4 with left ventricular non-compaction cardiomyopathy (*DES*-p.(Q364H)). Abbreviations: AC = arrhythmogenic cardiomyopathy, AVB = atrioventricular block, DCM = dilated cardiomyopathy, DES = desmin, HTx = heart transplantation, LAH = left anterior hemiblock, LVNC = left ventricular non-compaction cardiomyopathy, LVSD = left ventricular systolic dysfunction, RBBB = right bundle branch block, and RCM = restrictive cardiomyopathy.

2.1. Clinical Description of Studied Patients and of Their Families

Comprehensive clinical, laboratory, and electrophysiological data of all index cases were collected. Two probands of them (P2, P4) also underwent cardiovascular magnetic resonance imaging (Siemens Trio scanner, Siemens Medical Solutions, Erlangen, Germany) as described previously [17]. All available relatives undertook cardiologic screening, which included physical examination, electrocardiography, and echocardiography as well as a collection of blood samples for genetic analysis. Patients with suspected disease-causing *DES* variants were subjected to a detailed neurologic assessment, measurement of serum creatine phosphokinase, nerve conductance, and electromyography of two muscles (left vastus medialis and left deltoid muscle), as reported previously [17].

The study was approved by the Institutional Review Board's representing all clinical collaborators (Institute for Clinical and Experimental Medicine and Thomayer's Hospital; 1st Faculty of Medicine of the Charles University and General Faculty Hospital; both Prague) and was conducted in accordance with the principles of the Declaration of Helsinki. Written informed consent was obtained from all probands.

2.2. Genetic Analysis and Detection of Variants

To detect causal genetic variants, WES was performed according to internationally accepted guidelines [18]. Full technical details are provided in the Supplementary Materials. The criteria for classifying variants as putative disease-causing variants included their rare occurrence ($\leq 0.05\%$ among control samples), changes in predicted amino acid sequences, conservation across different species (<http://www.ncbi.nlm.nih.gov/BLAST/>), segregation within the family, and previously reported pathogenicity in databases.

Exons with identified variants of the *DES* gene were PCR amplified (Table S1) from genomic DNA of all available individuals from the analyzed families and sequenced using the version 3.1 Dye Terminator cycle sequencing kit with electrophoresis on an ABI 3500XL Avant Genetic Analyzer (both ThermoFisher Scientific; Waltham, MA, USA). Data were analyzed using Sequencing Analysis software version 6.0 (both ThermoFisher Scientific; USA) and the segregation of the candidate *DES* variants with the phenotype was evaluated.

2.3. In Vitro Analysis of DES Variants

As many but not all pathogenic *DES* variants cause an abnormal cytoplasmic desmin aggregation, we constructed for the identified *DES* variants expression plasmids by site-directed mutagenesis (Agilent Technologies, Santa Clara, CA, USA) according to the manufacturer's instructions. Desmin encoding parts of all plasmids were verified by Sanger sequencing (Macrogen, Amsterdam, Netherlands). The plasmid pmRuby-N1-DES and pmRuby-N1-DES-p.(Y122C) have been previously described [19,20]. Previously reported variant DES-p.(Y122C) was used as a positive control forming abnormal cytoplasmic aggregates [20]. HT1080 cells, which do not express endogenous desmin and cardiomyocytes derived from human induced pluripotent stem cells (iPSC) (NP00040-8) were transfected using Lipofectamin 3000 (ThermoFisher Scientific) or nucleofection using the 4D Nucleofector (Lonza, Cologne, Germany) in combination with the P3 Primary Cell 4D Nucleofector Kit according to the manufacturer's instructions. The differentiation of hiPSCs has been previously described [21]. Transfected HT1080 cells were fixed using 4% paraformaldehyde, permeabilized using 0.05% Triton X100, and stained with phalloidin conjugated with Alexa-488. Transfected hiPSC-derived cardiomyocytes were stained with primary antibodies against the Z-band protein α -actinin as a cardiomyocytes specific marker (Sigma-Aldrich, Missouri, MO, USA, #A7732) in combination with secondary antibodies conjugated to Alexa-488 (ThermoFisher). Confocal microscopy was performed as previously described [22].

2.4. Statistical Analysis of Aggregate Formation

A total of 3 to 4 independent transfection experiments were analyzed by counting the number of aggregate forming cells. Non-parametric Kruskal–Wallis for multiple comparison was performed using GraphPad Prism version 8.3.0 for Windows (GraphPad Software, San Diego, CA, USA). *p*-values < 0.05 were considered as significant.

2.5. Histopathology, Immunohistochemistry, Desmin Western Blot, and Electron Microscopy

In 5 probands (P1–P4, P6), formalin-fixed paraffin-embedded samples of myocardium were available either from endomyocardial biopsy (P2, P3) and/or from hearts explanted during transplantation (P1, P2, P6) or post-mortem (P4). The samples were snap frozen in liquid nitrogen and stored at $-70\text{ }^{\circ}\text{C}$. Resin-embedded myocardial samples for electron microscopy were analyzed in 4 patients (P1, P2, P4, and P6). A biopsy of skeletal muscle was performed in 3 individuals with

clinical signs of myopathy (P4 and P5: Soleus-, P6: Deltoid muscle). In P4, also we obtained samples of intercostal muscles post-mortem. The excisions from the skeletal muscle (approx. 10 × 5 × 5 mm in size) were snap frozen in isopentane (2-methylbutane; Merck, Kenilworth, NJ, USA) and cooled in liquid nitrogen. Cryosections were examined by routine hematoxylin–eosin staining and a conventional spectrum of histochemical reactions, including myofibrillary ATPase, nicotinamide adenine dinucleotide-tetrazolium reductase (NADH-TR), succinate dehydrogenase (SDH), and cytochrome c oxidase (COX), as described elsewhere [23].

Desmin immunohistochemistry and electron microscopy were performed on both skeletal muscle and myocardium samples according to standard protocols (Supplementary Materials).

2.6. Analysis of Mitochondrial Function in Biopsies

Skeletal muscle homogenate (5%, w/v) was prepared from fresh tissue by using a glass-Teflon homogenizer in a medium containing 150 mM KCl, 50 mM Tris-HCl, 2 mM EDTA, pH 7.4, and 0.2 ug/mL Aprotinin at 4 °C. Mitochondria were isolated from the homogenate by differential centrifugation as described elsewhere [24]. Heart tissue homogenates (7%, w/v) were prepared from –80 °C stored frozen samples of left and right heart ventricles in 0.32 M sucrose, 10 mM Tris-HCl, 1 mM EDTA, pH 7.4, and 1 µg/mL PIC (protease inhibitor mixture Sigma P8340) using glass-Teflon and glass-glass Dounce homogenizers. The subsequent methods are described in detail in Supplementary Materials. A western blot analysis of mitochondrial proteins, measurement of mitochondrial DNA content, measurement of activities of respiratory chain complexes and citrate synthase [25], high resolution oxygraphy, and measurement of the content of total coenzyme Q10 were described previously in details and in the Supplementary Materials.

3. Results

3.1. Description of DES Variants and Their Segregation in Families

Probably disease-causing *DES* variants in heterozygous constitution were identified in six index cases (1.8%). Two missense variants were identified within the non-helical head (amino-terminal) domain of desmin, i.e., in P1 with biventricular form of ACM (NM_001927.3: c.127A > G; NP_001918.3: p.(K43E)) and in P2 with DCM (NM_001927.3: c.170C > T; NP_001918.3: p.(S57L)) (Figure 1, Tables S2 and S3). Both of them were previously reported in Clinvar database as variants of uncertain significance. In addition, we analyzed the desmin filament formation in transfected HT1080 and in iPSC-derived cardiomyocytes, revealing an abnormal cytoplasmic aggregation in the DES-p.(K43E) variant and known pathogenic DES-p.(R406W) variant (Figure 2). Two novel variants were found in the highly conserved central α -helical rod domain, i.e., in P3 with familial DCM located in the 1B helical domain (NM_001927.3:c.629C > A; NP_001918.3: p.(A210D)) and in P4 with familial LVNC in combination with skeletal myopathy located in the 2B helical domain (NM_001927.3: c.1092G>T; NP_001918.3: p.(Q364H)) (Figure 1, Tables S2 and S3). The findings in the biopsies are described below. The remaining two probands had the following known *DES* pathogenic variants: P5 with ACM and skeletal myopathy in the 2B helical domain (NM_001927.3: c.1216C>T; NP_001918.3: p.(R406W); HGMD database (<http://www.hgmd.cf.ac.uk/ac/index.php>) CM000368) [6] and P6 with RCM and skeletal myopathy within the non-helical tail (carboxy-terminal) domain (NM_001927.3: c.1360C > T; NP_001918.3: p.(R454W); HGMD CM071700) [26] (Figure 1, Tables S2 and S3). Table S4 contains lists of rare genetic variants of further cardiomyopathy associated genes in all probands (frequency in Exac database less than 0.00001). Just the variant of *MYH7* (NM_000257.3) c.4679G > C, p.(Arg1560Pro) in proband 4 could be relevant in a patient with LVNC. However, it was not present in other members of the family tested (II 1, 3, 4; III 1, 2) (Figure 1) and did not co-segregate with the phenotype of LVNC. Importantly, any pathogenic variants in mitochondrial proteins coded by nuclear DNA or mitochondrial DNA were not found in these six probands.

Figure 1 illustrates the segregation of *DES* variants in families. Family history or clinical screening revealed a similar cardiac disease in a first-degree relative in P3, P4, and P6 segregating with occurrence of *DES* variants (Figure 1, Table S2). In the father of P2, heterozygous for *DES* p.(S57L) variant, we observed an incomplete penetrance of the disease with atrioventricular block grade I, right bundle branch block, left anterior hemiblock, normal echocardiography, and a mild elevation of creatinine phosphokinase of 6.1 μ kat/l (upper limit of normal 2.3 μ kat/L) without clinical signs of myopathy. Cases P1 and P5 seemed to be sporadic (segregation assessed in mother and sister of P1, and three siblings of P5).

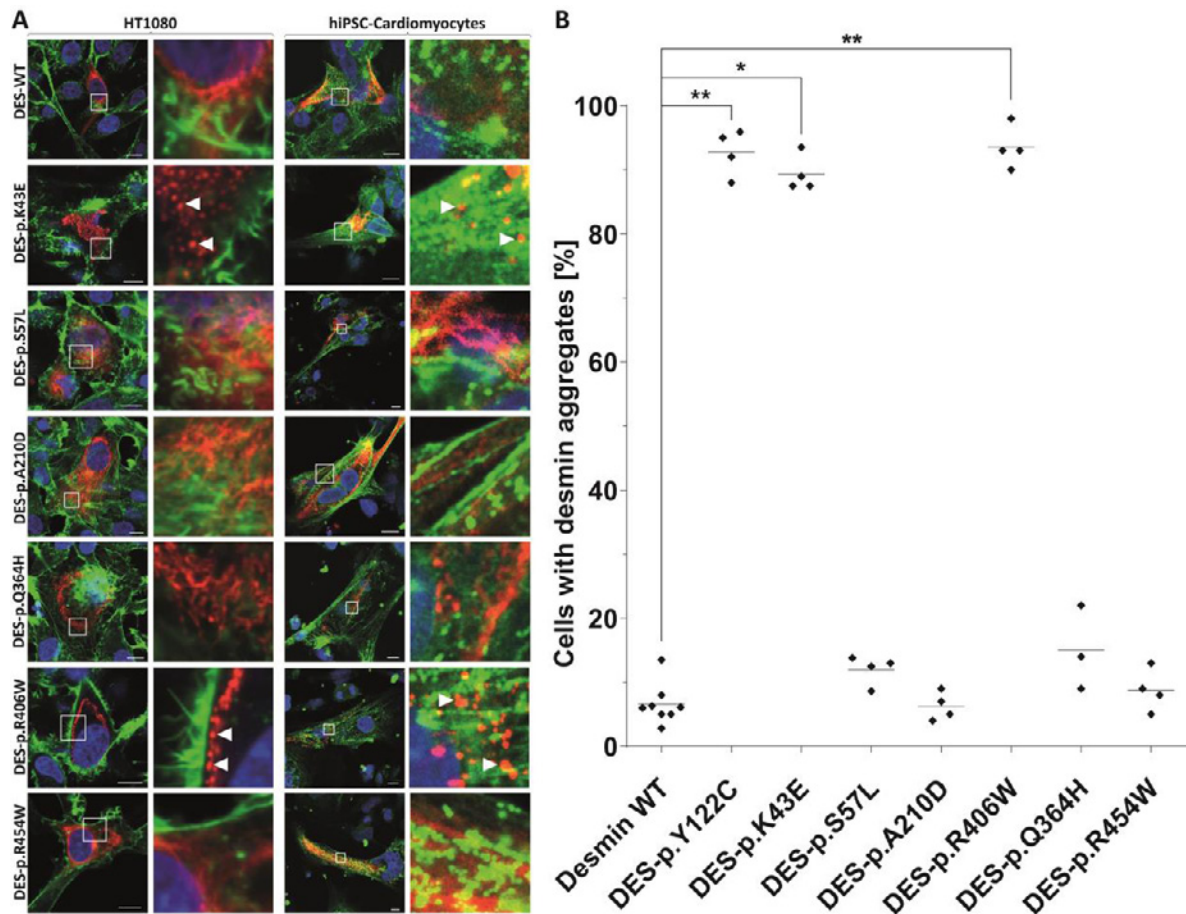


Figure 2. Cell transfection experiments of transfected HT1080 cells and iPSC-derived cardiomyocytes. Mutant and wild-type desmin was expressed with the red fluorescent protein-tag mRuby at the C-terminus (shown in red). Representative confocal images are shown (A). In case of HT1080 cells, F-actin was stained using phalloidin-Alexa488 (shown in green) and the nuclei were stained using 4',6-diamidin-2-phenylindole (shown in blue). In case of iPSC-cardiomyocytes, the cardiomyocyte marker α -actinin was stained using antibodies (shown in green) and the nuclei were stained with DAPI (shown in blue). Scale bars represent 10 μ m. (B) Quantification of aggregate formation was performed in three to four independent transfection experiments of HT1080 cells. * $p < 0.05$ and ** $p < 0.01$. The variant DES-p.(Y122C) was used as a positive control forming abnormal cytoplasmic aggregates [20].

3.2. Phenotypes of Desminopathy

The initial clinical presentation included cardiac arrest due to ventricular tachycardia in the 2nd decennium (P1), complete atrioventricular blockade in the 3rd decennium (P5, P6), and heart failure in the 3rd to 5th decennium (P2, P3, and P4). Skeletal myopathy and dysfunction of bulbar muscles became apparent during the 4th to 6th decennium in cases 4–6 (Table S2 and S3). An unusual clinical presentation had proband 2. A young female presented with acute heart failure, a severe

systolic dysfunction of mildly dilated left ventricle, persistent elevation of troponin T (> 10 times the upper limit of normal) (Table S3), and an extensive mid-wall late gadolinium enhancement of the septum and anterior wall of the left ventricle (Figure 3). These findings mimicked inflammatory cardiomyopathy however, there was no sign of inflammation as assessed by endomyocardial biopsy. Inflammation was absent also in her heart explanted during transplantation three years later. The arrhythmogenic left ventricular cardiomyopathy was considered as an alternative diagnosis in P2. However, her electrocardiogram was unremarkable and ventricular extrasystoles were infrequent. Proband 4 presented with a unique phenotype of LVNC. Magnetic resonance imaging (Figure 3) confirmed the diagnosis of LVNC with a percentage of non-compaction within the total left ventricular mass of 43%. Proband 6 was incorrectly diagnosed with mitochondrial disease based on skeletal muscle biopsy performed several years ago. This diagnosis was reclassified to desminopathy after the identification of known pathogenic desmin mutation (p.(R454W)) and morphological analysis of myocardial samples from the explanted heart. Table S3 illustrates additional clinical and laboratory data of the study group including echocardiography. During a median follow-up of 56 months (31–182), five probands (83%) developed end-stage heart failure.

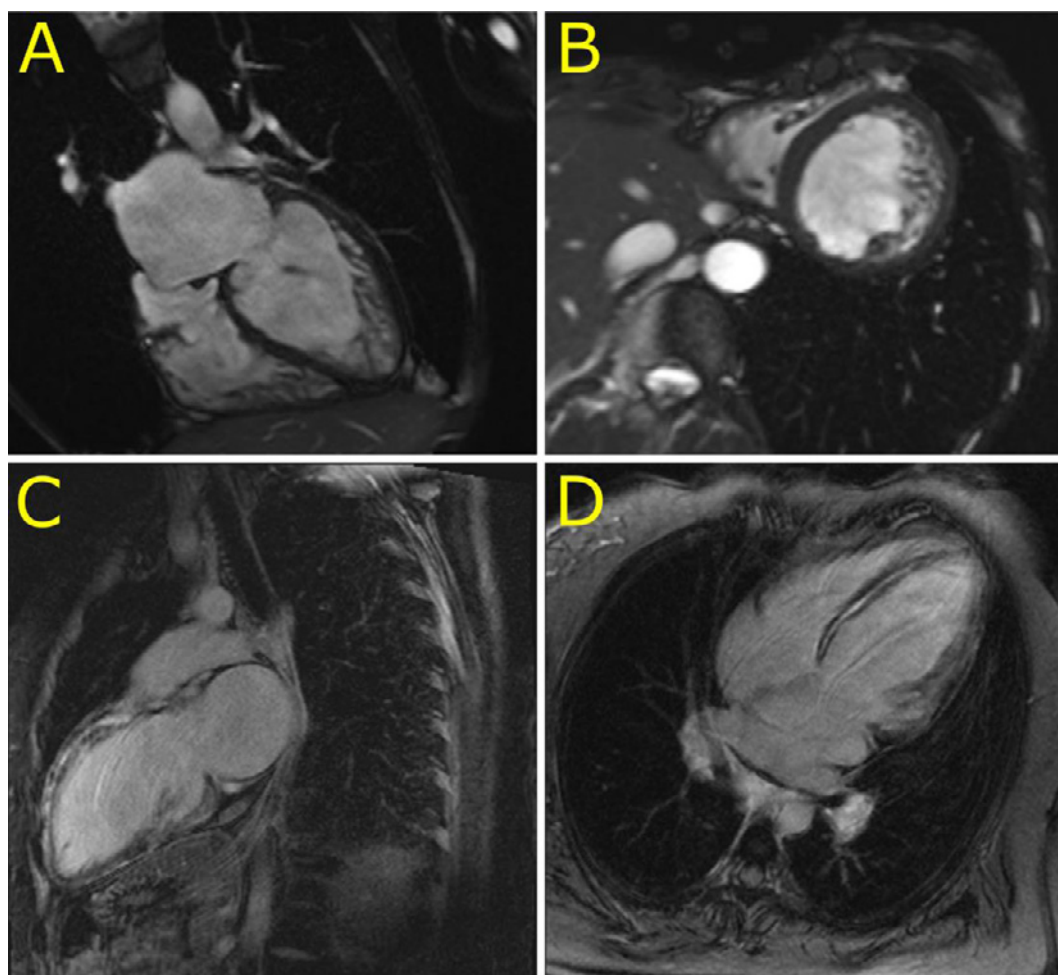


Figure 3. Cardiovascular magnetic resonance imaging in patients with left ventricular non-compaction cardiomyopathy (P4) and dilated cardiomyopathy with an extensive late gadolinium enhancement (P2). (A,B): Four chamber and short axis views of left ventricular non-compaction cardiomyopathy in P4. (C,D): Two chamber long axis and four chamber views of an extensive late gadolinium enhancement in the ventricular septum and left ventricular anterior wall mimicking inflammatory cardiomyopathy in P2.

3.3. Morphology of Desminopathy in Myocardial and Skeletal Muscle Samples

An immunohistochemical examination of myocardial samples in P1–P3 and P6 showed a diffuse alteration of desmin distribution in cardiomyocytes with a formation of desmin aggregates revealing strong immunoreactivity in the cytoplasm (shown in P1, P3; Figure 4A,E). Electron microscopy of cardiomyocytes in P1, P2, and P6 revealed myofibrillar disruption, streaming Z bands, and deposits of dense, amorphous granulofilamentous material of variable size and shape (shown in P1, P2; Figure 4B,C). In addition, we constructed a set of expression plasmids for the six *DES* missense variants and transfected HT1080 as a cell model without endogenous desmin expression and iPSC-derived cardiomyocytes. These experiments revealed a severe intermediate filament formation defect for *DES*-p.(K43E) and *DES*-p.(R406W) underlining their pathogenicity. Furthermore, electron microscopy of cardiac tissue demonstrated in P2, P4, and P6 focally increased the number of mitochondria, often in clusters, with loss of mitochondrial spatial organization (P2; Figure 4D). Importantly, desmin aggregates were absent in myocardial samples of P4 both at immunohistochemical and ultrastructural analysis. An expression of desmin in myocardium (P2, P4, and P6) was also assessed by Western blot analysis. There was an obvious reduction of the signal in P4 (Figure 1B).

Samples of the skeletal muscle (P4–P5 m. soleus, P4 intercostal muscle, P6 m. deltoideus) showed different findings in P4 and P6 as compared with P5. The morphological analysis in P4 and P6 detected only mild myopathic changes. The light microscopy with hematoxylin-eosin staining showed a marked variability in fiber size and increased number of internal nuclei (P4; Figure 4F). No inclusions were observed by light microscopy. Similarly, desmin immunohistochemistry did not reveal any protein aggregates in the sarcoplasm of P4 and P6 (P4; Figure 4G). In the NADH and SDH reactions, many fibers did not possess the characteristic checkerboard pattern, and in a proportion of fibers there was increased oxidative activity at the periphery of the muscle fibers, indicating the pathological accumulation of mitochondria (P4; Figure 4H). However, no typical ragged red fibers were observed. The distribution of COX reactivity was altered similarly to a NADH/SDH pattern with very few COX-negative fibers present (P4; Figure 4I). On the other hand, the muscle biopsy in P5 showed severe myopathic changes with a large amount of fibro-fatty tissue in the interstitium of the muscle. Desmin immunohistochemistry confirmed in P5 a diffuse alteration of desmin distribution with a formation of desmin aggregates in the cytoplasm of muscle fibers.

An ultrastructural analysis of skeletal muscle biopsies revealed a focally increased number of mitochondria, often in clusters, with an altered distribution in P4 and P6 (P4; Figure 4J) however, no ultrastructural abnormality in mitochondria morphology was observed. Typical deposits of dense granulofilamentous material were absent in P4 and were not observed in P6 at the first reading. Thus the first description of the skeletal muscle biopsy in P6 led to the diagnosis of mitochondrial myopathy. Nevertheless, the second reading of the skeletal muscle biopsy performed with the knowledge of the results of genetic tests and abnormal immunostaining of desmin in myocardium discovered a focus of dense amorphous material in a single fiber at electron microscopy (not shown).

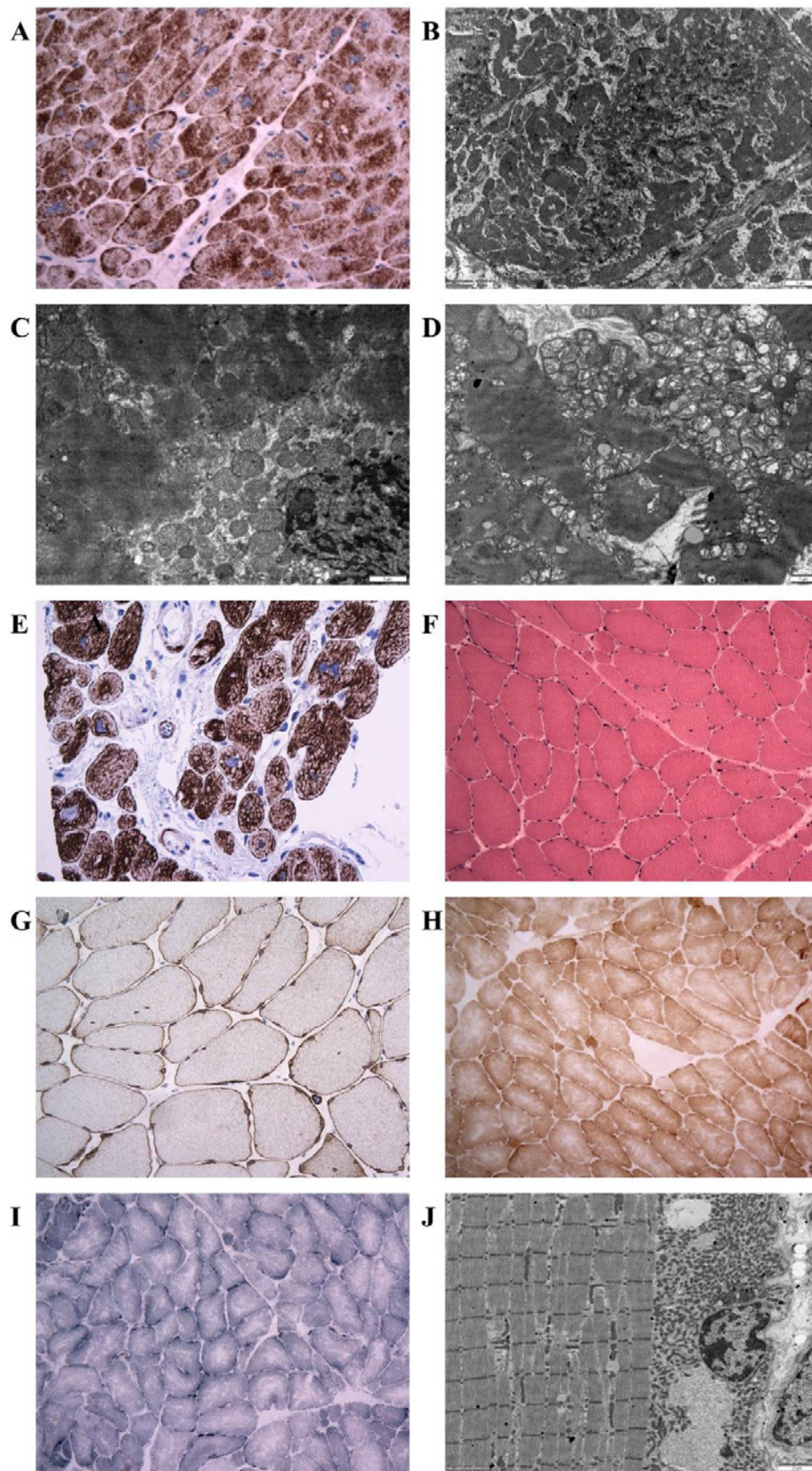


Figure 4. Illustration of histopathology, immunohistochemistry, and electron microscopy in individuals with the novel desmin variants. **(A):** Desmin immunohistochemistry (left ventricular myocardium, explanted heart, P1) documenting a diffuse alteration of desmin distribution with a formation of desmin aggregates revealing strong immunoreactivity in the cytoplasm. Original magnification $\times 400$. **(B):** Electron

microscopy (left ventricular myocardium, explanted heart, P1) detects amorphous granulofilamentous material in the cytoplasm of cardiomyocytes compatible with desmin aggregates. Original magnification $\times 10,000$. (C,D): Electron microscopy (left ventricular myocardium, explanted heart, P2). (C): Pathological dense granulofilamentous inclusions in the cytoplasm of cardiomyocyte. Original magnification $\times 12,000$. (D): Increased number of mitochondria in cardiomyocyte, often in clusters, with altered distribution. Original magnification $\times 8000$. (E): Desmin immunohistochemistry (right ventricular myocardium, endomyocardial biopsy, P3) revealed an abnormal staining of cardiomyocytes with a formation of desmin positive aggregates. Original magnification $\times 400$. (F–J) Diagnostic skeletal muscle biopsy specimens, Soleus muscle, P4, original magnification $\times 400$. (F): By light microscopy with hematoxylin-eosin, there was a marked variability in fiber size, absent inclusions, and increased number of internal nuclei. (G): Desmin immunohistochemistry did not reveal any protein aggregates in the sarcoplasm. (H): Nicotinamide adenine dinucleotide (NADH) and succinate dehydrogenase (SDH) immunohistochemistry identified few muscle fibers with increased oxidative activity at their periphery, indicating the pathological accumulation of mitochondria. However, no typical ragged red fibers were observed. (I): Very few COX-negative fibers were also present. (J): Electron-microscopic analysis revealed increased number of mitochondria, often in clusters, with altered distribution. No accumulation of intermediate filaments was observed. Original magnification $\times 6000$.

3.4. Indications for the Pathogenicity of the Novel Desmin Variants

A typical myocardial histopathology and ultrastructure with pathological desmin-immunoreactive aggregates strongly supported the pathogenicity of desmin variants p.(K43E), p.(S57L), and p.(A210D). In addition, the desmin filament formation experiments in transfected HT1080 and in iPSC-derived cardiomyocytes revealed an abnormal cytoplasmic aggregation of DES-p.(K43E). On the other hand, the pathogenicity of the novel desmin variant p.(Q364H) is supported mainly by decreased myocardial desmin expression and co-segregation of the above desmin variant in the family in the absence of other segregating cardiomyopathy-related genes as assessed by WES in the proband.

3.5. Mitochondrial Function and Content in Skeletal Muscle and Heart

An analysis of mitochondrial respiratory enzymes in skeletal muscle homogenates (Table 1) revealed a decreased activity of citrate synthase in P5, the activity of respiratory chain complex IV, and the quantity of mitochondrial respiratory chain proteins were decreased (Figure 5A). An oxygraphy analysis of P6 skeletal muscle fibers further showed a decrease in coupled (state 3-ADP) oxidation of NADH-dependent substrates (pyruvate + malate) to 35% of the mean of the controls (Table 1). More consistent data were provided by the analysis of isolated mitochondria from skeletal muscles of P4–P6. Specific activities of respiratory chain complexes I + III (NADH: Cytochrome c reductase), complex IV (cytochrome c oxidase), and citrate synthase were decreased to 30%–50% of the mean of the controls. Both P5 and P6 had a decreased content of coenzyme Q (Table 1). A low specific content of respiratory chain enzymes, citrate synthase, and porin was further apparent in isolated muscle mitochondria of P4–P6, with the most pronounced decrease observed in P5 (Figure 5A).

Table 1. Activities of respiratory chain enzymes in skeletal muscle homogenates (A), muscle fibers (B), and isolated mitochondria (C) of proband P4–P6. For analysis samples of m. tibialis (P4, P5) or m. deltoideus sin. (P6) were used. Enzyme activities and Coenzyme Q10 content are expressed per mg protein.

(A)				
Enzyme Activity of Muscle Homogenates (nmol/min/mg protein)	P4	P5	P6	Controls <i>n</i> = 30
Complex IV	130.1	38.1	81.8	68–213
Citrate synthase (CS)	109.5	41.4	97.8	48–128
Complex IV/CS	1.19	0.92	0.84	080–160
Coenzyme Q10 content (pmol/mg)	282.9	140.5	112.5	180–460
(B)				
Respiratory Activity of Permeabilized Muscle Fibers (pmol O ₂ /s/mg protein)				Controls <i>n</i> = 9
ADP-stimulated oxidation of NADH-dependent substrates	7.4			16–26
ADP-stimulated oxidation of succinate	10.7			9–18
Cytochrome <i>c</i> oxidase respiration	63			43–83
(C)				
Enzyme Activity of Isolated Mitochondria (nmol/min/mg protein)	P4	P5	P6	Controls <i>n</i> = 30
Complex I	328.5	230.8	131.2	110–290
Complex I+III	94.1	18.7	53.2	126–316
Complex II	69.7	50.5	49.5	21–93
Complex II+III	174.2	92.9	146.7	82–251
Complex III	303.0	342.7	535.0	200–600
Complex IV	578.4	311.6	236.6	658–1552
Citrate synthase	372.5	240.4	384.2	435–1234
Complex I/CS	0.88	0.96	0.34	0.17–0.41
Complex I+III/CS	0.25	0.07	0.13	0.07–0.27
Complex II/CS	0.19	0.21	0.13	0.04–0.12
Complex II+III/CS	0.47	0.39	0.38	0.35–0.36
Complex III/CS	0.81	1.43	1.39	0.56–1.46
Complex IV/CS	1.55	1.30	0.62	0.82–1.88

Abbreviations: ADP–adenosine diphosphate, ATP–adenosine triphosphate, and NADH–reduced form of nicotinamide adenine dinucleotide.

Myocardium of two patients with desminopathy (P2, P6) (Table 2) revealed a general decrease in respiratory chain enzyme activities. An oxidation of NADH and succinate and cytochrome *c* oxidase respiration decreased to 20%–55% of the controls and activities of respiratory complexes I+III, II+III, and IV decreased to 15%–81%, respectively, indicating more extensive impairment in P2 heart ventricles (Table 2). The impairment of succinate respiration was the most profound with a mean of 277 pmol O₂/s/mg. This was much lower than in our historical controls from donor hearts unsuitable for transplantation (653 ± 244 pmol O₂/s/mg, *n* = 38) and even myocardium explanted during heart transplantation or ventricular assist device implantation (508 ± 211 pmol O₂/s/mg, *n* = 91) [25]. Western blot quantification of mitochondrial proteins showed a decrease in specific content of respiratory chain complexes, also more pronounced in P2, where a very low content of complexes IV and I was associated with the upregulation of complex II (Figure 5B). Other mitochondrial proteins, as porin

(shown in Figure 5A) and adenine nucleotide translocator (not shown) were less affected. Analysis of native forms of respiratory chain complexes by BlueNative electrophoresis (Figure 5C) confirmed a marked reduction of complexes I and IV in P2 heart and further showed that it led to a pronounced decrease of high molecular weight respiratory supercomplexes consisting of complexes I, III, and IV. Similar, yet a smaller decrease of supercomplexes was observed in soleus of R349P desmin knock-in mouse [15] or heart of desmin knockout mouse [27]. The content of mitochondrial DNA (relative to nuclear DNA, D-loop/GAPDH, and 16S RNA/GAPDH) was slightly decreased in P6 heart ventricles (60%–90% of the average value of the controls) but was unchanged in P2 heart. These data indicate mild to pronounced attenuation of the energetic function of mitochondria due to a decreased content and activity of respiratory complexes and supercomplexes in failing hearts of patients with desminopathy.

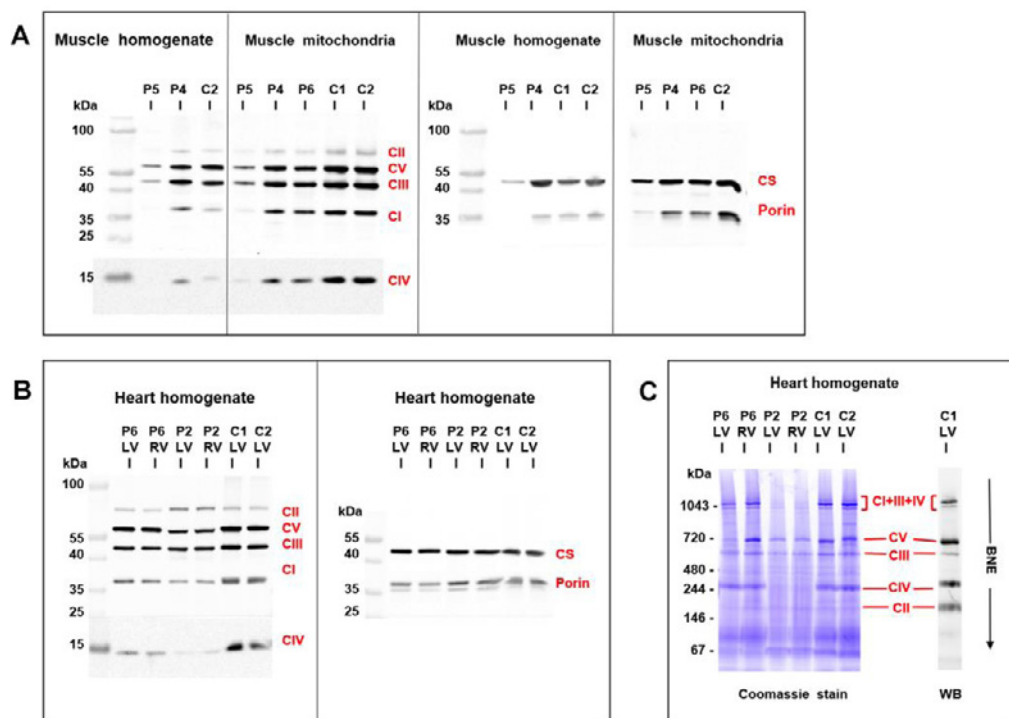


Figure 5. Western blot detection of mitochondrial proteins in skeletal muscle and heart. Analysis of SDS-PAGE resolved proteins from (A) muscle homogenates (6 µg protein aliquots) and isolated muscle mitochondria (2 µg protein aliquots) demonstrated a pronounced decrease of respiratory chain complexes (CI–CV), citrate synthase (CS), and porin in skeletal muscle of P5 compared to controls (C), P4 and P6 were less affected. Analysis of (B) heart homogenates (4 µg protein aliquots) from left and right heart ventricles (LV, RV) demonstrated a marked decrease of respiratory chain enzymes in P2 and a mild decrease in P6 compared to controls (C). CS and porin were less affected. BlueNative electrophoresis (C) further showed a marked decrease of native respiratory supercomplexes consisting of CI + CIII + CIV in P2 heart ventricles (12 µg protein aliquots).

Table 2. Activities of respiratory chain enzymes and mtDNA content in hearts of proband 2 and 6.

Respiratory/Enzyme Activity	P2 Left Ventricle	P2 Right Ventricle	P6 Left Ventricle	P6 Right Ventricle	Controls <i>n</i> = 38
(pmol O ₂ /s/mg)					
NADH respiration	245	203	448	229	235–2356
Succinate respiration	295	242	254	319	365–1529
Cytochrome <i>c</i> oxidase respiration	766	991	1003	1047	561–4120
(nmol/min/mg)					
Complex I+III	26.1	30.3	145.1	83.9	44–386
Complex II+III	88.0	71.3	59.5	56.7	27–195
Complex IV	262.6	432.4	430.5	276.8	389–1989
Citrate synthase (CS)	915.9	975.2	562.2	483.6	446–1207
(activity ratio)					
Complex I+III/CS	0.03	0.03	0.26	0.17	0.09–0.63
Complex II+III/CS	0.10	0.07	0.11	0.12	0.04–0.37
Complex IV/CS	0.29	0.44	0.77	0.57	0.54–2.60
mtDNA content (2 ^{-ΔCt})					
D-loop/GAPDH	4980	5499	2863	3592	2052–10519
16S RNA/GAPDH	11629	10914	8017	7299	3715–15843

Enzyme activities are expressed per mg protein, mtDNA content is expressed as 2^{-ΔCt} value indicating the number of mtDNA copies per a haploid genome. Abbreviation: GAPDH–glyceraldehyde 3-phosphate dehydrogenase.

As changes in mitochondria energetic function can affect a generation of reactive oxygen species, the content of antioxidative enzymes was analyzed by Western blot analysis in skeletal muscle and heart samples from patients with desminopathy (Figure 6). Both P4 and P5 muscle homogenates revealed highly increased glutathione reductase (GR) and superoxide dismutase 1 (SOD1) as well as a variable increase of catalase (CAT) and superoxide dismutase 2 (SOD2). Higher CAT was found in P5 isolated mitochondria, while the most increased SOD1 was of extra-mitochondrial origin (also apparent from the SOD1/SOD2 ratio). An increased content of GR and SOD1 was also found in heart ventricles of P6.

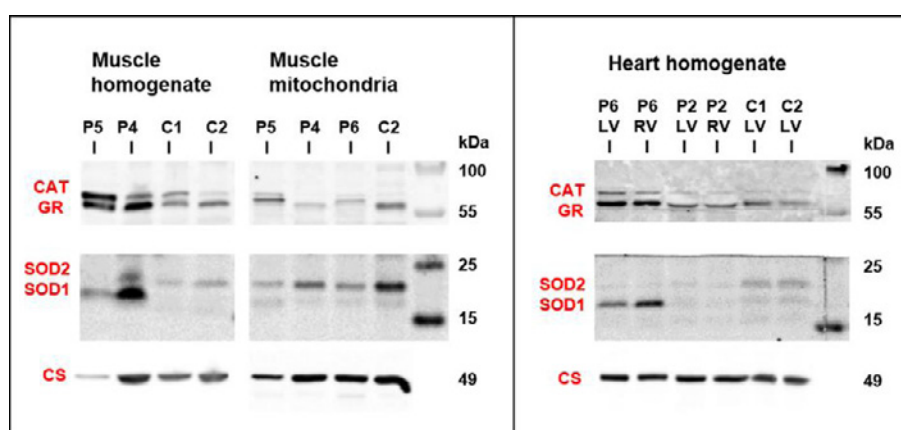


Figure 6. Western blot detection of antioxidative enzymes in skeletal muscle and heart. Both P4 and P5 muscle homogenates revealed variable increase in antioxidative enzymes glutathione reductase (GR), catalase (CAT), and superoxide dismutases 1 and 2 (SOD1, SOD2). Increased content of CAT, GR, and SOD1 was also found in heart ventricles of P6. Protein aliquots—muscle homogenate 30 μg, muscle mitochondria 15 μg, and heart homogenate 20 μg. For comparison, citrate synthase signal (CS) from Figure 5 is shown.

4. Discussion

Firstly, the prevalence of desminopathy in a large cohort of patients with an unexplained etiology of cardiomyopathy assessed with WES was 1.8%. Secondly, the presence of pathological desmin aggregates in myocardial/skeletal muscle samples of P1–P3 and decreased myocardial desmin expression in P4 suggested a pathogenicity of two novel *DES* variants and two *DES* variants previously classified as of uncertain significance. Thirdly, a pathogenicity of one variant of uncertain significance (*DES*-p.(K43E)) was supported also by abnormal desmin filament formation and its cytoplasmic aggregation in transfected HT1080 cells and in iPSC-derived cardiomyocytes. Fourthly, we provided further evidence for LVNC as a novel phenotype of desminopathy. Fifthly, we described secondary mitochondrial dysfunction in skeletal muscle and in myocardium, which was in case of myocardial succinate respiration more profound than in end-stage heart failure of other etiology. To the best of our knowledge, this seems to be the first comprehensive description of mitochondrial dysfunction in human myocardium affected by desminopathy. Finally, secondary mitochondrial dysfunction and/or an extensive left ventricular late gadolinium enhancement in desminopathy may imitate a primary mitochondrial disease or an inflammatory cardiomyopathy.

4.1. Clinical and Histopathological Correlates of Desminopathy

The majority of 68 pathogenic desmin variants that were reported so far are missense or small in-frame deletion variants localized in the helical rod domain [26,28]. A phenotype-genotype correlation meta-analyses revealed that pathogenic variants in the rod 2B domain of *DES* are common among patients with both skeletal and cardiac muscle phenotype, whereas head and tail domain pathogenic variants result mainly in clinically isolated cardiac phenotype [1,29,30]. In agreement with these findings, we found that two *DES* variants in head region (p.(K43E), p.(S57L)) and one novel *DES* variant (p.(A210D)) in the 1B helical domain had in probands isolated cardiac involvement. On the other hand, the novel *DES* mutation located in the 2B helical domain (p.(Q364H)) and two known *DES* variants (p.(R406W), p.(R454W)) affected both the cardiac and skeletal muscle.

Immunohistochemistry revealed pathological desmin aggregates in skeletal or cardiac myocytes in five probands from our study group. Importantly, desmin aggregates were absent in the deltoid muscle of proband 6 (*DES*-p.(R454W)), but present in her myocardial samples. Desmin aggregates were completely absent in proband 4 (*DES*-p.(Q364H)). Immunohistochemistry and electron microscopy of diagnostic muscle soleus biopsy and post-mortem myocardial and intercostal muscle samples failed to detect any pathological protein aggregates. Interestingly, Western blot analysis of the myocardial sample showed a decreased expression of desmin suggesting decreased protein synthesis. This is in agreement with the experience of pathologists that myopathological findings in genetically proven desminopathies may range from no overt pathology over subtle myopathic changes with sporadic protein aggregates to the picture of a vacuolar myopathy [31]. An absence of desmin aggregates has been recently documented both in autosomal dominant [32] and autosomal recessive [33] desminopathy.

4.2. Novel Cardiac Phenotypes of Desminopathy

In addition to known cardiac phenotypes of desminopathy like DCM, RCM HCM, and ACM [1,28,29], we observed LVNC as a relatively novel phenotype. So far, *DES* variants have been associated with LVNC just in a few individuals [34–37]. The first report from Arbustini et al. [34] described a family with a segregation of *DES* variant p.(G84S) with non-obstructive hypertrophic cardiomyopathy and one case of LVNC. Another group [35] reported one sporadic case of LVNC in a child with a *DES* variant p.(L398P). An occurrence of two cases of LVNC in one family has been recently associated with an in-frame mutation of desmin p.(Q113_L115del) affecting the α -helical rod domain [36] with a formation of typical desmin-immunoreactive aggregates. We expanded the available evidence by a description of another familial occurrence of two cases of LVNC associated

with the desmin variant p.(Q364H) with a decreased myocardial expression of desmin and absent desmin aggregates in myocardial/skeletal biopsy.

Recently, a novel phenotype of desminopathy describing left ventricular arrhythmogenic cardiomyopathy was reported to have a significant amount of subepicardial fibrosis [32]. A similar phenotype had our P2, which mimicked inflammatory cardiomyopathy by an extensive late gadolinium enhancement in the left ventricle and persistent elevation of cardiac troponins. However, ventricular ectopy and an inversion of T waves in inferior and precordial leads were absent. Taken together, the presence of desminopathy should be considered also in unexplained cases of LVNC and non-ischemic left ventricular systolic dysfunction with an extensive subepicardial or intramural fibrosis.

4.3. Mitochondrial Dysfunction in Desminopathy

Desminopathy may also imitate a mitochondrial disease, as was shown by Mc Cormic et al. [16]. The presence of SDH positive/COX negative muscle fibers, decreased activities of mitochondrial respiratory chain enzymes, and reduced mitochondrial DNA content in skeletal muscle biopsy lead to the suspicion of mitochondrial disease. We observed similar findings in our patient (P6) with an absence of desmin aggregates and signs of mitochondrial dysfunction in deltoid muscle biopsy. The correct diagnosis in our case provided genetic testing and immunostaining of myocardial samples.

Studies in desmin null mice and patients with recessive desmin-null muscular dystrophy revealed abnormalities in nuclear and mitochondrial localization and morphology, as well as impaired mitochondrial respiratory capacity [13,14]. Secondary mitochondrial dysfunction was also confirmed by Schröder et al. [38] and Vincent et al. [39] in skeletal muscle biopsies of heterozygous patients with desminopathy. Furthermore, Vincent et al. [39] reported a deficiency of respiratory chain complex I and IV compared to age matched controls and a low mitochondrial mass compared to controls. Our morphological and functional data from skeletal muscle samples are in agreement with the above mentioned studies and further evidence [40,41]. We observed a variable mitochondrial dysfunction characterized by a decreased expression of mitochondrial respiratory chain components and other mitochondrial proteins, as well as decreased enzyme activities, suggesting secondary changes in mitochondrial energetic function. The upregulation of several anti-oxidative enzymes, in particular that of superoxide dismutase 1 in homogenates, but not in isolated mitochondria, indicated increased antioxidative defense outside mitochondria.

Novel findings provided our analysis of myocardial energetic function in the explanted failing hearts of two probands with desminopathy. In one case harboring p.(R454W) desmin tail mutation we found a mild decrease in the content and activities of respiratory chain complexes while in the other case with p.(S57L) mutation in the desmin head region was present a very pronounced decrease in mitochondria proteins and an alteration of the bioenergetics function. Interestingly, changes in respiratory chain enzymes thus also caused a downregulation of respiratory supercomplexes that are expected to modulate the catalytic function as well as reactive oxygen species production by the respiratory chain [42]. This was associated with a decrease in several marker proteins of different mitochondrial compartments suggesting a complex mitochondrial dysfunction. The most pronounced was the impairment of myocardial succinate respiration, which was in our patients with desminopathy more profound than in end-stage heart failure of other etiologies.

4.4. Study Limitations

There are several limitations to our study. First, the small study group size reflects the rare occurrence of desminopathy and may limit the general applicability of the study results. Secondly, the small size of affected families limited the segregation studies. However, WES enabled us to exclude the presence of other pathogenic variants in cardiomyopathy- and skeletal myopathy-related genes, including genes coding mitochondrial proteins. Thirdly, an assessment of the mitochondrial function in tissues was possible only in a subgroup of patients with a clinical indication to biopsy or undergoing cardiac surgery. Finally, decreased desmin expression in P4 with a missense variant of *DES* might be

related to replacement fibrosis of the myocardium or epigenetic factors. Unfortunately, we cannot provide data supporting any of these hypotheses.

5. Conclusions

Desminopathy is a rare cause of cardiomyopathy and/or skeletal muscle myopathy with a pleomorphic clinical presentation and poor prognosis. This diagnosis should also be considered in individuals with LVNC. Differential diagnosis also includes mitochondrial and inflammatory myocardial diseases.

Supplementary Materials: The following are available online at <http://www.mdpi.com/2077-0383/9/4/937/s1>, Table S1 Primers for PCR Amplification of DES for segregation analysis in families, Table S2 Main clinical characteristics of probands, Table S3 Additional clinical, electrocardiographic, laboratory and echocardiographic data of probands, Table S4 Rare variants of non-desmin genes in probands, frequency in Exac database less than 0.00001.

Author Contributions: Conceptualization, M.K., T.S., L.P., A.K., V.M., and S.K.; Methodology, M.K., T.S., L.P., V.M., H.M., and S.K.; Validation, M.K. and S.K.; Formal Analysis, M.K., T.S., L.P., and S.K.; Investigation, clinical assessment M.K., A.K., T.P., and P.R.; Molecular-genetic analysis T.S., L.P., M.M., and V.S.; iPSC differentiation, cloning, transfection, confocal microscopy A.B.; Quantitative analysis of aggregate formation S.R.; site directed mutagenesis C.S.; analysis of mitochondrial function H.H., J.Z., J.H., Z.D., H.N., and J.M. (Jana Mikešová); histopathology and electron microscopy J.Z. and J.M. (Malusková); Resources, H.M., S.K.; Data Curation, M.K., T.S., and L.P.; Writing—Original Draft Preparation, M.K., T.S., L.P., and J.H.; Writing—Review & Editing, M.K., A.B., J.H., M.M., and S.K.; Visualization, T.S., L.P., and A.B.; Supervision, M.K., J.H., V.M., H.M., and S.K.; Project Administration, M.K. and T.S.; Funding Acquisition, H.M., M.K., and S.K. All authors have read and agreed to the published version of the manuscript.

Acknowledgments: M.K., T.S., and L.P. contributed equally to the manuscript. This study was supported by the research grant of the Ministry of Health, Czech Republic [MZ AZV 15-27682A], [NV19-08-00122], [MZ AZV 17-28784A], Ministry of Health, Czech Republic - conceptual development of research organization („Institute for Clinical and Experimental Medicine – IKEM, IN 00023001“) and by institutional support from the Ministry of Health (RVO-VFN64165) and Czech Academy of Sciences (RVO:67985823). We thank the National Center for Medical Genomics (LM2015091) for exome sequencing and providing ethnically matched population frequency data (project CZ.02.1.01/0.0/0.0/16_013/0001634). A.B. and H.M. are thankful for financial support by Deutsche Stiftung für Herzforschung (DSHF, F07/17) and by Deutsche Forschungsgesellschaft (DFG, MI-1146/2–2).

Conflicts of Interest: The authors have no conflicts of interest.

Abbreviations and Acronyms

ACM	arrhythmogenic cardiomyopathy
CAT	catalase
COX	cytochrome c oxidase
DCM	dilated cardiomyopathy
DES	desmin gene
GADPH	glyceraldehyde 3-phosphate dehydrogenase
GR	glutathione reductase
HCM	hypertrophic cardiomyopathy
LVNC	left ventricular non-compaction cardiomyopathy
NADH	reduced form of nicotinamide adenine dinucleotide
MPS	massively parallel sequencing
RCM	restrictive cardiomyopathy
SDH	succinate dehydrogenase
SOD	superoxide dismutase
WES	whole exome sequencing

References

1. van Spaendonck-Zwarts, K.Y.; van Hessem, L.; Jongbloed, J.D.; de Walle, H.E.; Capetanaki, Y.; van der Kooi, A.J.; van Langen, I.M.; van den Berg, M.P.; van Tintelen, J.P. Desmin-related myopathy. *Clin. Genet.* **2011**, *80*, 354–366. [[CrossRef](#)]

2. Li, D.; Tapscoft, T.; Gonzalez, O.; Burch, P.E.; Quiñones, M.A.; Zoghbi, W.A.; Hill, R.; Bachinski, L.L.; Mann, D.L.; Roberts, R. Desmin mutation responsible for idiopathic dilated cardiomyopathy. *Circulation* **1999**, *100*, 461–464. [[CrossRef](#)]
3. Taylor, M.R.; Slavov, D.; Ku, L.; Di Lenarda, A.; Sinagra, G.; Carniel, E.; Haubold, K.; Boucek, M.M.; Ferguson, D.; Graw, S.L.; et al. Prevalence of desmin mutations in dilated cardiomyopathy. *Circulation* **2007**, *115*, 1244–1251. [[CrossRef](#)]
4. Goldfarb, L.G.; Park, K.Y.; Cervenakova, L.; Gorokhova, S.; Lee, H.S.; Vasconcelos, O.; Nagle, J.W.; Semino-Mora, C.; Sivakumar, K.; Dalakas, M.C. Missence mutations in desmin associated with familial cardiac and skeletal myopathy. *Nat. Genet.* **1998**, *19*, 402–403. [[CrossRef](#)]
5. Arbustini, E.; Morbini, P.; Grasso, M.; Fasani, R.; Verga, L.; Bellini, O.; Dal Bello, B.; Campana, C.; Piccolo, G.; Febo, O.; et al. Restrictive cardiomyopathy, atrioventricular block and mild to subclinical myopathy in patients with desmin-immunoreactive material deposits. *J. Am. Coll. Cardiol.* **1998**, *31*, 645–653. [[CrossRef](#)]
6. Park, K.Y.; Dalakas, M.C.; Semino-Mora, C.; Lee, H.S.; Litvak, S.; Takeda, K.; Ferrans, V.J.; Goldfarb, L.G. Desmin myopathy, a skeletal myopathy with cardiomyopathy caused by mutations in the desmin gene. *N. Engl. J. Med.* **2000**, *342*, 770–780. [[CrossRef](#)]
7. Pruszczyk, P.; Kostera-Pruszczyk, A.; Shatunov, A.; Goudeau, B.; Dramińska, A.; Takeda, K.; Sambuughin, N.; Vicart, P.; Strelkov, S.V.; Goldfarb, L.G.; et al. Restrictive cardiomyopathy with atrioventricular conduction block resulting from a desmin mutation. *Int. J. Cardiol.* **2007**, *117*, 244–253. [[CrossRef](#)] [[PubMed](#)]
8. Olive, M.; Armstrong, J.; Miralles, F.; Pou, A.; Fardeau, M.; Gonzalez, L.; Martínez, F.; Fischer, D.; Martínez Matos, J.A.; Shatunov, A.; et al. Phenotypic patterns of desminopathy associated with three novel mutations in the desmin gene. *Neuromuscul. Disord.* **2007**, *17*, 443–450. [[CrossRef](#)] [[PubMed](#)]
9. Otten, E.; Asimaki, A.; Maass, A.; van Langen, I.M.; van der Wal, A.; de Jonge, N.; van den Berg, M.P.; Saffitz, J.E.; Wilde, A.A.; Jongbloed, J.D.; et al. Desmin mutations as a cause of right ventricular heart failure affect the intercalated disks. *Heart Rhythm* **2010**, *7*, 1058–1064. [[CrossRef](#)] [[PubMed](#)]
10. Klauke, B.; Kossmann, S.; Gaertner, A.; Brand, K.; Stork, I.; Brodehl, A.; Dieding, M.; Walhorn, V.; Anselmetti, D.; Gerdes, D.; et al. De novo desmin mutation N116S is associated with arrhythmogenic right ventricular cardiomyopathy. *Hum. Mol. Genet.* **2010**, *19*, 4595–4607. [[CrossRef](#)]
11. Lorenzon, A.; Beffagna, G.; Bauce, B.; De Bortoli, M.; Li Mura, I.E.A.; Calore, M.; Dazzo, E.; Basso, C.; Nava, A.; Thiene, G.; et al. Desmin mutations and arrhythmogenic right ventricular cardiomyopathy. *Am. J. Cardiol.* **2013**, *111*, 400–405. [[CrossRef](#)] [[PubMed](#)]
12. Capetanaki, Y.; Bloch, R.J.; Kouloumenta, A.; Mavroidis, M.; Psarras, S. Muscle intermediate filaments and their links to membranes and membranous organelles. *Exp. Cell. Res.* **2007**, *313*, 2063–2076. [[CrossRef](#)] [[PubMed](#)]
13. Milner, D.J.; Mavroidis, M.; Weisleder, N.; Capetanaki, Y. Desmin cytoskeleton linked to muscle mitochondrial distribution and respiratory function. *J. Cell. Biol.* **2000**, *150*, 1283–1298. [[CrossRef](#)] [[PubMed](#)]
14. Henderson, M.; Waele, L.D.; Hudson, J.; Eagle, M.; Sewry, C.; Marsh, J.; Charlton, R.; He, L.; Blakely, E.L.; Horrocks, I.; et al. Recessive desmin-null muscular dystrophy with central nuclei and mitochondrial abnormalities. *Acta Neuropathol. (Berl.)* **2013**, *125*, 917–919. [[CrossRef](#)] [[PubMed](#)]
15. Winter, L.; Wittig, I.; Peeva, V.; Eggers, B.; Heidler, J.; Chevessier, F.; Kley, R.A.; Barkovits, K.; Strecker, V.; Berwanger, C.; et al. Mutant desmin substantially perturbs mitochondrial morphology, function and maintenance in skeletal muscle tissue. *Acta Neuropathol.* **2016**, *132*, 453–473. [[CrossRef](#)]
16. McCormick, E.M.; Kenyon, L.; Falk, M.J. Desmin common mutation is associated with multi-systemic disease manifestations and depletion of mitochondria and mitochondrial DNA. *Front. Genet.* **2015**, *6*, 199. [[CrossRef](#)]
17. Hartmannova, H.; Kubanek, M.; Sramko, M.; Piherova, L.; Noskova, L.; Hodanova, K.; Stranecky, V.; Pristoupilova, A.; Sovova, J.; Marek, T.; et al. Isolated X-linked hypertrophic cardiomyopathy caused by a novel mutation of the Four-and-a-half LIM domain 1 gene. *Circ. Cardiovasc. Genet.* **2013**, *6*, 543–551. [[CrossRef](#)]
18. Kalia, S.S.; Adelman, K.; Bale, S.J.; Chung, W.K.; Eng, C.; Evans, J.P.; Herman, G.E.; Hufnagel, S.B.; Klein, T.E.; Korf, B.R.; et al. Recommendations for reporting of secondary findings in clinical exome and genome sequencing, 2016 update (ACMG SF v2.0): A policy statement of the American College of Medical Genetics and Genomics. *Genet. Med.* **2017**, *19*, 249–255. [[CrossRef](#)]

19. Brodehl, A.; Dieding, M.; Biere, N.; Unger, A.; Klauke, B.; Walhorn, V.; Gummert, J.; Schulz, U.; Linke, W.A.; Gerull, B.; et al. Functional characterization of the novel DES mutation p.L136P associated with dilated cardiomyopathy reveals a dominant filament assembly defect. *J. Mol. Cell. Cardiol.* **2016**, *91*, 207–214. [[CrossRef](#)]
20. Brodehl, A.; Pour Hakimi, S.A.; Stanasiuk, C.; Ratnavadivel, S.; Hendig, D.; Gaertner, A.; Gerull, B.; Gummert, J.; Paluszkiwicz, L.; Milting, H. Restrictive Cardiomyopathy is Caused by a Novel Homozygous Desmin (DES) Mutation p.Y122H Leading to a Severe Filament Assembly Defect. *Genes (Basel)* **2019**, *11*, 918. [[CrossRef](#)]
21. Debus, J.D.; Milting, H.; Brodehl, A.; Kassner, A.; Anselmetti, D.; Gummert, J.; Gaertner-Rommel, A. In vitro analysis of arrhythmogenic cardiomyopathy associated desmoglein-2 (DSG2) mutations reveals diverse glycosylation patterns. *J. Mol. Cell. Cardiol.* **2019**, *129*, 303–313. [[CrossRef](#)] [[PubMed](#)]
22. Brodehl, A.; Gaertner-Rommel, A.; Klauke, B.; Grewe, S.A.; Schirmer, I.; Peterschröder, A.; Faber, L.; Vorgerd, M.; Gummert, J.; Anselmetti, D.; et al. The novel α B-crystallin (CRYAB) mutation p.D109G causes restrictive cardiomyopathy. *Hum. Mutat.* **2017**, *38*, 947–952. [[CrossRef](#)] [[PubMed](#)]
23. Sheehan, D.C.; Hrapchak, B.B. *Theory and Practice of Histotechnology*, 2nd ed.; Mosby: Columbus, OH, USA, 1987.
24. Makinen, M.W.; Lee, C.P. Biochemical studies of skeletal muscle mitochondria. I. Microanalysis of cytochrome content, oxidative and phosphorylative activities of mammalian skeletal muscle mitochondria. *Arch. Biochem. Biophys.* **1968**, *126*, 75–82. [[CrossRef](#)]
25. Melenovsky, M.; Petrak, J.; Mracek, T.; Benes, J.; Borlaug, B.A.; Nuskova, H.; Pluhacek, T.; Spatenka, J.; Kovalcikova, J.; Drahota, Z.; et al. Myocardial Iron Content and Mitochondrial Function in Heart Failure: Direct Tissue Analysis. *Eur. J. Heart Fail.* **2017**, *19*, 522–530. [[CrossRef](#)]
26. Brodehl, A.; Gaertner-Rommel, A.; Milting, H. Molecular insights into cardiomyopathies associated with desmin (DES) mutations. *Biophys. Rev.* **2018**, *10*, 983–1006. [[CrossRef](#)]
27. Diokmetzidou, A.; Soumaka, E.; Kloukina, I.; Tsikitis, M.; Makridakis, M.; Varela, A.; Davos, C.H.; Georgopoulos, S.; Anesti, A.; Vlachou, A.; et al. Desmin and α B-Crystallin Interplay in Maintenance of Mitochondrial Homeostasis and Cardiomyocyte Survival. *J. Cell Sci.* **2016**, *129*, 3705–3720. [[CrossRef](#)]
28. Bär, H.; Goudeau, B.; Wälde, S.; Casteras-Simon, M.; Mücke, N.; Shatunov, A.; Goldberg, Y.P.; Clarke, C.; Holton, J.L.; Eymard, B.; et al. Conspicuous involvement of desmin tail mutations in diverse cardiac and skeletal myopathies. *Hum. Mutat.* **2007**, *28*, 374–386. [[CrossRef](#)]
29. Capetanaki, Y.; Paphanasiou, S.; Diokmetzidou, A.; Vatsellas, G.; Tsikitis, M. Desmin related disease: A matter of cell survival failure. *Curr. Opin. Cell Biol.* **2015**, *32*, 113–120. [[CrossRef](#)]
30. Kostera-Pruszczyk, A.; Pruszczyk, P.; Kamińska, A.; Lee, H.S.; Goldfarb, L.G. Diversity of cardiomyopathy phenotypes caused by mutations in desmin. *Int. J. Cardiol.* **2008**, *131*, 146–147. [[CrossRef](#)]
31. Clemen, C.S.; Herrmann, H.; Strelkov, S.V.; Schröder, R. Desminopathies: Pathology and mechanisms. *Acta Neuropathol.* **2013**, *125*, 47–75. [[CrossRef](#)]
32. Bermúdez-Jiménez, F.J.; Carriel, V.; Brodehl, A.; Alaminos, M.; Campos, A.; Schirmer, I.; Milting, H.; Abril, B.Á.; Álvarez, M.; López-Fernández, S.; et al. The Novel Desmin Mutation p.Glu401Asp Impairs Filament Formation, Disrupts Cell Membrane Integrity and Causes Severe Arrhythmogenic Left Ventricular Cardiomyopathy/Dysplasia. *Circulation* **2018**, *137*, 1595–1610. [[CrossRef](#)] [[PubMed](#)]
33. Cetin, N.; Balci-Hayta, B.; Gundesli, H.; Korkusuz, P.; Purali, N.; Talim, B.; Tan, E.; Selcen, D.; Erdem-Ozdamar, S.; Dincer, P. A novel desmin mutation leading to autosomal recessive limb-girdle muscular dystrophy: Distinct histopathological outcomes compared with desminopathies. *J. Med. Genet.* **2013**, *50*, 437–443. [[CrossRef](#)] [[PubMed](#)]
34. Arbustini, E.; Favalli, V.; Narula, N.; Serio, A.; Grasso, M. Left Ventricular Noncompaction: A Distinct Genetic Cardiomyopathy? *J. Am. Coll. Cardiol.* **2016**, *68*, 949–966. [[CrossRef](#)] [[PubMed](#)]
35. van Waning, J.I.; Caliskan, K.; Hoedemaekers, Y.M.; van Spaendonck-Zwarts, K.Y.; Baas, A.F.; Boekholdt, S.M.; van Melle, J.P.; Teske, A.J.; Asselbergs, F.W.; Backx, A.P.C.M.; et al. Genetics, Clinical Features, and Long-Term Outcome of Noncompaction Cardiomyopathy. *J. Am. Coll. Cardiol.* **2018**, *71*, 711–722. [[CrossRef](#)]
36. Marakhonov, A.V.; Brodehl, A.; Myasnikov, R.P.; Sparber, P.A.; Kiseleva, A.V.; Kulikova, O.V.; Meshkov, A.N.; Zharikova, A.A.; Koretsky, S.N.; Kharlap, M.S.; et al. Noncompaction cardiomyopathy is caused by a novel in-frame desmin (DES) deletion mutation within the 1A coiled-coil rod segment leading to a severe filament assembly defect. *Hum. Mutat.* **2019**, *40*, 734–741. [[CrossRef](#)]

37. Miszalski-Jamka, K.; Jefferies, J.L.; Mazur, W.; Głowacki, J.; Hu, J.; Lazar, M.; Gibbs, R.A.; Liczko, J.; Kłyś, J.; Venner, E.; et al. Novel Genetic Triggers and Genotype-Phenotype Correlations in Patients with Left Ventricular. *Noncompact. Circ. Cardiovasc. Genet.* **2017**, *10*, e001763. [[CrossRef](#)]
38. Schröder, R.; Goudeau, B.; Simon, M.C.; Fischer, D.; Eggermann, T.; Clemen, C.S.; Li, Z.; Reimann, J.; Xue, Z.; Rudnik-Schöneborn, S.; et al. On noxious desmin: Functional effects of a novel heterozygous desmin insertion mutation on the extrasarcomeric desmin cytoskeleton and mitochondria. *Hum. Mol. Genet.* **2003**, *12*, 657–669. [[CrossRef](#)]
39. Vincent, A.E.; Grady, J.P.; Rocha, M.C.; Alston, C.L.; Rygiel, K.A.; Barresi, R.; Taylor, R.W.; Turnbull, D.M. Mitochondrial dysfunction in myofibrillar myopathy. *Neuromuscul. Disord.* **2016**, *26*, 691–701. [[CrossRef](#)]
40. Galata, Z.; Kloukina, I.; Kostavasili, I.; Varela, A.; Davos, C.H.; Makridakis, M.; Bonne, G.; Capetanaki, Y. Amelioration of desmin network defects by α B-crystallin overexpression confers cardioprotection in a mouse model of dilated cardiomyopathy caused by LMNA gene mutation. *J. Mol. Cell. Cardiol.* **2018**, *125*, 73–86. [[CrossRef](#)]
41. Tsikitis, M.; Galata, Z.; Mavroidis, M.; Psarras, S.; Capetanaki, Y. Intermediate filaments in cardiomyopathy. *Bioph. Rev.* **2018**, *10*, 1007–1031. [[CrossRef](#)]
42. Milenkovic, D.; Blaza, J.N.; Larsson, N.G.; Hirst, J. The Enigma of the Respiratory Chain Supercomplex. *Cell Metab.* **2017**, *25*, 765–776. [[CrossRef](#)] [[PubMed](#)]



© 2020 by the authors. Licensee MDPI, Basel, Switzerland. This article is an open access article distributed under the terms and conditions of the Creative Commons Attribution (CC BY) license (<http://creativecommons.org/licenses/by/4.0/>).

P. Toušek a kol.

Modified Strategies for Invasive Management of Acute Coronary Syndrome during the COVID-19 Pandemic

Journal of Clinical Medicine
Impact Factor: 3,303



Article

Modified Strategies for Invasive Management of Acute Coronary Syndrome during the COVID-19 Pandemic

Petr Toušek^{1,*}, Viktor Kočka¹, Petr Mašek², Petr Tůma², Marek Neuberg², Markéta Nováčková¹, Josef Kroupa¹, David Bauer¹, Zuzana Mořovská¹ and Petr Widimský¹

¹ Department of Cardiology, Third Faculty of Medicine, Charles University, University Hospital Královské Vinohrady, 100 34 Prague, Czech Republic; viktor.kocka@fnkv.cz (V.K.); marketa.novackova@fnkv.cz (M.N.); josef.kroupa@fnkv.cz (J.K.); david.bauer@fnkv.cz (D.B.); zuzana.motovska@fnkv.cz (Z.M.); petr.widimsky@fnkv.cz (P.W.)

² Medtronic Czechia, Partner of INTERCARDIS Project, 190 00 Prague, Czech Republic; petr.masek@medtronic.com (P.M.); petr.tuma@fnkv.cz (P.T.); marek.neuberg@medtronic.com (M.N.)

* Correspondence: petr.tousek@fnkv.cz; Tel.: +420-267-162-621; Fax: +420-67-163-388

Abstract: The COVID-19 pandemic presents several challenges for managing patients with acute coronary syndrome (ACS). Modified treatment algorithms have been proposed for the pandemic. We assessed new algorithms proposed by The European Association of Percutaneous Cardiovascular Interventions (EAPCI) and the Acute Cardiovascular Care Association (ACCA) on patients with ACS admitted to the hospital during the COVID-19 pandemic. The COVID-19 period group (CPG) consisted of patients admitted into a high-volume centre in Prague between 1 February 2020 and 30 May 2020 ($n = 181$). The reference group (RG) included patients who had been admitted between 1 October 2018 and 31 January 2020 ($n = 834$). The proportions of patients with different types of ACS admitted before and during the pandemic did not differ significantly: in all ACS patients, KILLIP III-IV class was present in 13.9% in RG and in 9.4% of patients in CPG ($p = 0.082$). In NSTEMI-ACS patients, the ejection fraction was lower in the CPG than in the RG (44.7% vs. 50.7%, respectively; $p < 0.001$). The time from symptom onset to first medical contact did not differ between CPG and RG patients in the respective NSTEMI-ACS and STEMI groups. The time to early invasive treatment in NSTEMI-ACS patients and the time to reperfusion in STEMI patients were not significantly different between the RG and the CPG. In-hospital mortality did not differ between the groups in NSTEMI-ACS patients (odds ratio in the CPG 0.853, 95% confidence interval (CI) 0.247 to 2.951; $p = 0.960$) nor in STEMI patients (odds ratio in CPG 1.248, 95% CI 0.566 to 2.749; $p = 0.735$). Modified treatment strategies for ACS during the COVID-19 pandemic did not cause treatment delays. Hospital mortality did not differ.

Keywords: acute coronary syndrome; COVID-19; modified treatment; delays; outcome



Citation: Toušek, P.; Kočka, V.; Mašek, P.; Tůma, P.; Neuberg, M.; Nováčková, M.; Kroupa, J.; Bauer, D.; Mořovská, Z.; Widimský, P. Modified Strategies for Invasive Management of Acute Coronary Syndrome during the COVID-19 Pandemic. *J. Clin. Med.* **2021**, *10*, 24. <https://dx.doi.org/10.3390/jcm10010024>

Received: 2 November 2020

Accepted: 22 December 2020

Published: 24 December 2020

Publisher's Note: MDPI stays neutral with regard to jurisdictional claims in published maps and institutional affiliations.



Copyright: © 2020 by the authors. Licensee MDPI, Basel, Switzerland. This article is an open access article distributed under the terms and conditions of the Creative Commons Attribution (CC BY) license (<https://creativecommons.org/licenses/by/4.0/>).

1. Introduction

The global threat of COVID-19 and strict epidemiological containment measures have a significant impact on patients with acute coronary syndrome (ACS) in terms of contact with healthcare providers and treatment logistics after the first medical contact (FMC). The European Association of Percutaneous Cardiovascular Interventions (EAPCI) and the Acute Cardiovascular Care Association (ACCA) have proposed modified diagnostic and treatment algorithms for the COVID-19 outbreak [1].

The Czech Republic recorded some of the lowest numbers of confirmed COVID-19 cases and the lowest mortality rate in Europe during the first wave of the pandemic in spring 2020 [2]. Although the hospital system was partially re-organised, in general, there were no admission restrictions for patients with ACS.

We investigated the secondary impact of the COVID-19 pandemic on patients with ACS who were admitted to a high-volume centre in a country that was not severely affected

by the initial COVID-19 wave but that implemented the algorithms proposed by the EAPCI and ACCA.

2. Methods

We created a prospective registry of patients with ACS admitted to the University Hospital Královské Vinohrady Cardiocentre, Prague, Czech Republic, in September 2018 (supported by the EU project INTERCARDIS–INTERventional treatment of life-threatening CARDiovascular DISeases with the cooperation of project partner Medtronic). Consecutive patients admitted with confirmed ACS were entered in the registry from 1 October 2018. ACS types were defined according to the European guidelines for acute myocardial infarction with ST elevation (STEMI) and guidelines for ACS without ST elevation (NSTEMI-ACS) [3,4]. Data concerning 214 parameters including clinical characteristics, angiographic, laboratory and therapeutic findings, and financial costs and hospital outcomes were obtained for all patients. The registry was approved by the local ethics committee.

Patients admitted to hospital between 1 February and 30 May 2020 were included in the COVID-19 period group (CPG). The first social media reports of COVID-19 in other countries appeared in February, and the first case of COVID-19 disease in the Czech Republic was identified on 1 March 2020, followed by strict government restrictions and school closures on 10 March 2020. Major easing of restrictions was approved by the government on 25 May 2020. During the COVID-19 period, our centre used the diagnostic and treatment strategy algorithms recommended by the EAPCI and ACCA for patients with ACS [1].

Diagnostic and therapeutic procedures for patients with stable coronary syndromes were postponed or managed according to risk stratification, which was usually conducted by phone contact. All acutely admitted patients were tested for SARS-CoV-2 immediately after admission, and the test results were received within 4–6 h (laboratory testing was performed three times daily). All patients were managed as possible COVID-19-positive until negative test results were confirmed, with healthcare workers using appropriate personal protective equipment. However, the use of invasive management was guided by clinical presentation. Patients with ongoing ischemia, STEMI, and very high-risk NSTEMI-ACS patients underwent immediate invasive management, and SARS-CoV-2 testing was performed afterwards. A strategy for complete revascularisation within one hospital stay was established.

The reference group (RG) included all patients entered into the registry between 1 October 2018 and 31 January 2020. The RG was divided into four four-month periods to compare the number and type of ACS within the four-month COVID-19 period. Additionally, the clinical characteristics, times to FMC and treatment, length of stay in the intensive care unit (ICU) and total hospital stay (calculated only in patients who were not transferred back to regional hospitals after the initial treatment), hospital outcomes (in-hospital patient mortality and major adverse clinical events during hospitalisation including death, re-infarction, stroke and significant bleeding (Bleeding Academic Research Consortium class ≥ 2) and financial costs were compared between the CPG and RG. The calculation of financial costs was based on a model used nationally for diagnosis-related group costing and, for the needs of this project, was approved for the catheterisation laboratory. With the exception of expensive materials (e.g., coronary stents) and expensive drugs, which were directly registered for the patient, all expenses, including the costs of medical staff, were calculated using the cost drivers of the cost centres that provided health services, such as length of stay in bed, duration of surgery and points of procedure. The price unit calculation was based on the annual cost value of the cost centre. The costs were calculated in Czech crowns and then converted to euros according the exchange rate of the Czech National Bank on 2 July 2020.

Statistical Analyses

The Kolmogorov–Smirnov test or Shapiro–Wilk test was used to test for normality of the data set distribution. Continuous variables with non-normal (log-normal) distributions are expressed as box plots where the central line indicates the median. Continuous variables with normal distributions are expressed as means \pm standard deviations (SDs). Between-group differences were assessed using the Mann–Whitney *U*-test or Kruskal–Wallis test for non-normally distributed variables and Student's *t*-tests for normally distributed data. The chi-square test or Fisher's exact test was used to assess the difference between categorical variables. We also compared risk of mortality between groups expressed as odds ratio with a confidence interval (OR, CI). *p*-values < 0.05 were considered to indicate statistical significance. All statistical analyses were performed using SPSS version 26 (IBM Corp., Armonk, NY, USA). Graphical analysis was performed in Sigmaplot version 14 (Systat Software Inc., San Jose, CA, USA).

3. Results

3.1. ACS Types

The CPG consisted of 181 patients, and 834 patients were included in the RG. The proportion of acute myocardial infarction without ST-segment elevation (NSTEMI) and STEMI cases admitted in the months prior to the outbreak of COVID-19 and during the COVID-19 period were not significantly different (Figure 1). Although the number of patients with unstable angina admitted during the COVID-19 period ($n = 23$) was lower than that admitted in the previous 4-month blocks (39, 40, 37 and 46 patients, respectively), the difference was not statistically significant ($p = 0.138$).

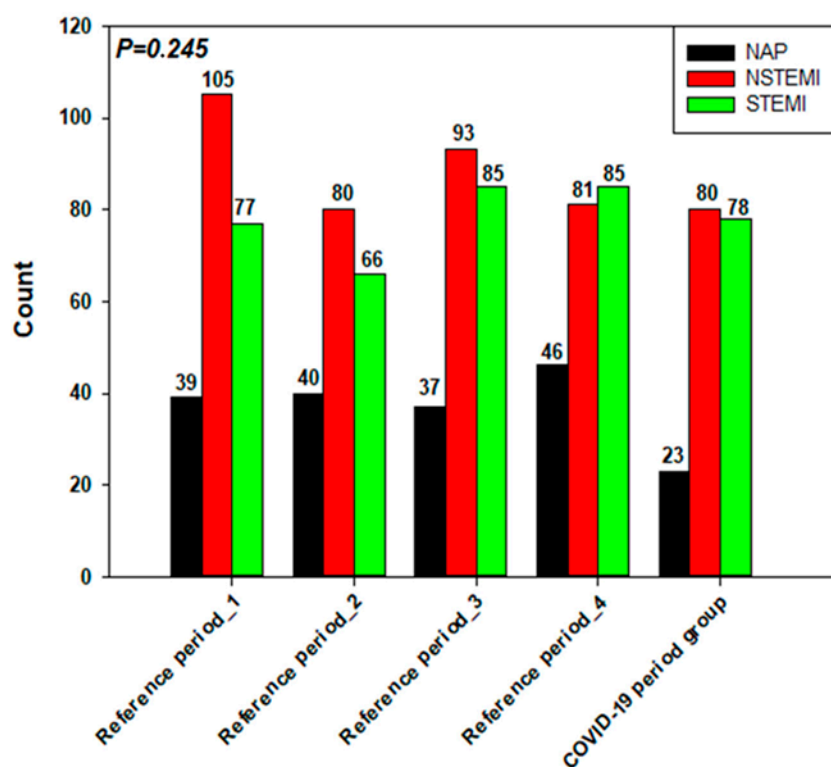


Figure 1. Number and types of acute coronary syndrome admitted during the four reference periods and the COVID-19 period (NAP—non-stable/unstable angina pectoris, NSTEMI—myocardial infarction with persistent ST elevation), STEMI—myocardial infarction with ST elevation).

3.2. Patient Characteristics

Table 1 shows the demographic and clinical characteristics of the CPG and RG patients according to ACS type (NSTE-ASC and STEMI). Age and medical history were not

significantly different between groups; however, some clinical aspects were worse in CPG patients than in those in the RG. Among patients with NSTEMI-ACS, the ejection fraction was lower in the CPG patients than in those in the RG (44.7% vs. 50.7%, respectively; $p < 0.001$). In all ACS patients, a non-significant, higher percentage of CPG patients presented with KILLIP III-IV class at admission (13.9% vs. 9.4%; $p = 0.082$).

3.3. Time Intervals and Treatment Strategies

3.3.1. NSTEMI-ACS Patients

The time from symptom onset to FMC and electrocardiogram (ECG) was less than 24 h in 49% of the CPG and in 46% of the RG ($p = 0.588$). Coronary angiography was performed in 99% of the patients in the CPG and in 99.8% of those in the RG. Of those, the procedure was performed within 24 h of admission in 49% of patients in the CPG and in 44.5% of those in the RG ($p = 0.462$).

3.3.2. STEMI Patients

The time from symptom onset to FMC did not differ between the CPG and RG patients admitted to the hospital within 24 h of symptom onset (Figure 2); however, 30% of the CPG patients and 33% of the RG patients presented with subacute STEMI (time from symptom onset to FMC longer than 24 h; $p = 0.728$). The time from FMC to vessel recanalization did not differ between the RG and CPG (Figure 2).

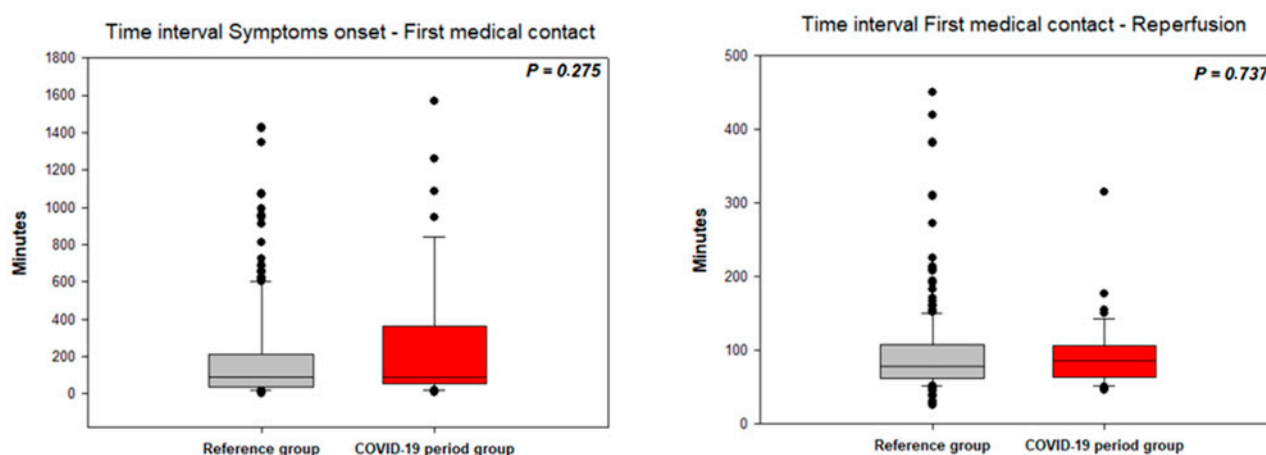


Figure 2. Time intervals in STEMI patients (symptoms onset—first medical contact and first medical contact to reperfusion).

The treatment strategies for NSTEMI-ACS and STEMI did not differ for the CPG and RG patients in the respective diagnostic groups (Figure 3).

Table 1. Patient’s demographic and clinical characteristics

	NSTE-ACS			STEMI		
	RG	CPG	p-Value	RG	CPG	p-Value
Age, mean (SD)	69.5 ± 11.6	70.4 ± 10.6	0.503	65.8 ± 13.1	65.2 ± 12.4	0.9
Male sex, N (%)	381 (73.1%)	81 (78.6%)	0.270	203 (64.9%)	55 (70.5%)	0.423
History of MI, n (%)	165 (31.9%)	24 (24.2%)	0.153	38 (12.3%)	16 (21.1%)	0.05
History of stroke, n (%)	69 (13.3%)	11 (10.8%)	0.628	17 (5.5%)	7 (9.2%)	0.286
Diabetes mellitus, n (%)	31 (6.0%)	4 (3.9%)	0.38	19 (6.1%)	4 (5.2%)	0.366
	Diet					
	PAD	115 (22.1%)	17 (16.5%)	55 (17.7%)	11 (14.3%)	
	Insulin therapy	50 (9.6%)	10 (9.7%)	28 (9.0%)	3 (3.9%)	
Hypertension, n (%)	408 (78.6%)	79 (77.5%)	0.793	182 (58.9%)	46 (60.5%)	0.896
Hyperlipidaemia, n (%)	244 (47.1%)	40 (39.2%)	0.304	92 (29.8%)	29 (38.2%)	0.158
Peripheral artery disease, n (%)	73 (14.1%)	13 (12.7%)	0.875	24 (7.8%)	7 (9.2%)	0.642
History of CABG	71 (13.7%)	11 (10.8%)	0.523	8 (2.6%)	4 (5.3%)	0.265
History of PCI	152 (29.4%)	28 (27.5%)	0.722	35 (11.4%)	15 (20.0%)	0.057
ECG rhythm						
	Sinus	434 (83.5%)	87 (84.5%)	268 (87.6%)	67 (87%)	0.876
	Atrial fibrillation/flutter	56 (10.8%)	10 (9.7%)	30 (9.8%)	7 (9.1%)	
	Pacemaker	24 (4.6%)	2 (1.9%)	4 (1.3%)	1 (1.3%)	
	Other	6 (1.2%)	4 (3.9%)	4 (1.3%)	2 (2.6%)	
KILLIP classification			0.652			0.324
	KILLIP I	437 (84.4%)	84 (82.4%)	244 (78.2%)	55 (71.4%)	
	KILLIP II	43 (8.3%)	7 (6.9%)	28 (9.0%)	8 (10.4%)	
	KILLIP III	19 (3.7%)	6 (5.9%)	8 (2.6%)	5 (6.5%)	
	KILLIP IV	19 (3.7%)	5 (4.9%)	32 (10.3%)	9 (11.7%)	
Mechanical ventilation at admission	23 (4.4%)	8 (7.7%)	0.271	21 (6.7%)	7 (9%)	0.69
Out-of-hospital cardiac arrest	18 (3.5%)	6 (5.8%)	0.416	25 (8%)	8 (10.3%)	0.72
Coronary angiography			0.481			0.665
	Single vessel disease	129 (25%)	24 (24%)	99 (32%)	23 (29.5%)	
	Multivessel disease	379 (73.6%)	76 (76%)	210 (68%)	55 (70.5%)	
	Left main disease	71 (13.9%)	16 (15.7%)	22 (7.1%)	9 (11.5%)	0.241
Ejection fraction	50.7 ± 11.1	44.7 ± 16.2	0.001	43.1 ± 10.8	42.5 ± 12.3	0.994

NSTE-ACS—acute coronary syndromes without ST elevation, STEMI—myocardial infarction with ST elevation, RG—reference group, CPG—COVID-19 reference group, MI—myocardial infarction, PAD—peroral antidiabetic treatment, CABG—coronary artery bypass graft, PCI—percutaneous coronary intervention.

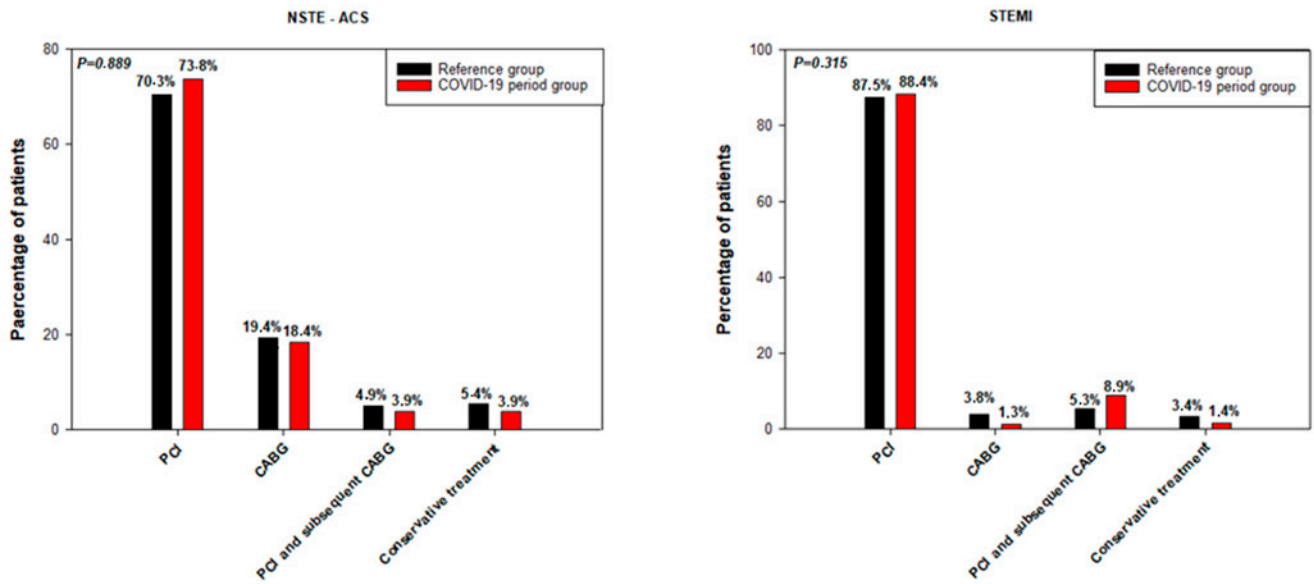


Figure 3. Treatment strategies for the NSTEMI-ACS and STEMI patients. PCI—percutaneous coronary intervention, CABG—coronary artery bypass graft.

3.4. Length of Hospital Stay

The length of stay in the ICU for patients not transferred to regional hospitals after initial treatment and the length of the total hospital stay were calculated for the patients with NSTEMI-ACS (Figure 4) and STEMI (Figure 5). In the NSTEMI-ACS patients, the ICU stay was 6.2 ± 6.6 days for the CPG and 4.7 ± 6.2 days for the RG ($p = 0.024$). The ICU stay for the STEMI patients was 4.6 ± 5.4 days for the CPG and 4.3 ± 4.3 days for the RG ($p = 0.751$). The total hospital stay for the NSTEMI-ACS patients was 11.1 ± 8.0 days for the CPG and 9.4 ± 9.2 days for the RG ($p = 0.016$). The total hospital stay for STEMI patients was 8.5 ± 7.0 days for the CPG and 8.0 ± 5.4 days for the RG ($p = 0.491$).

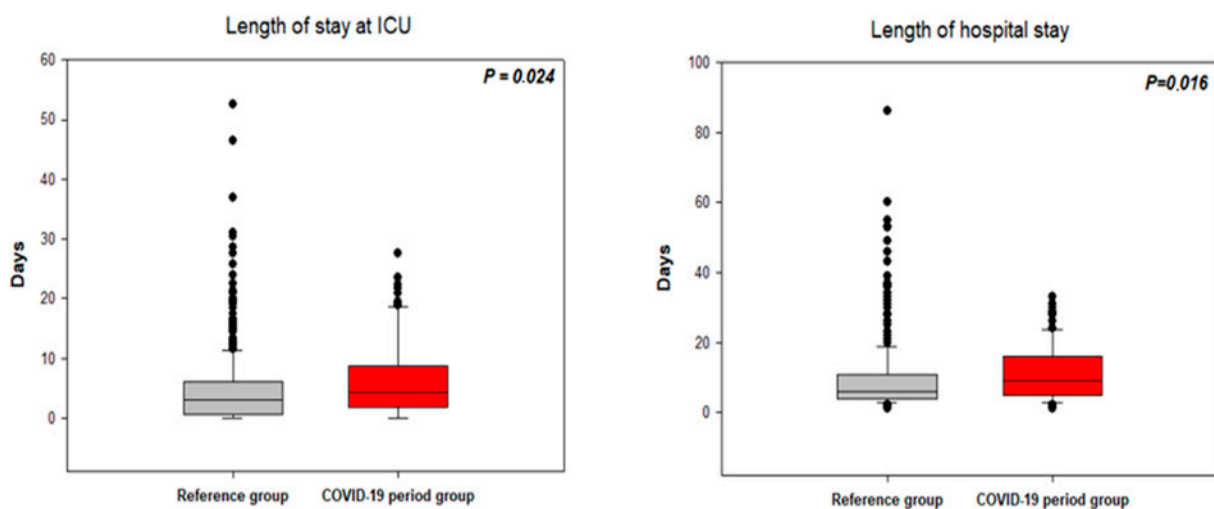


Figure 4. Length of stay in the intensive care unit (left figure) and total hospital stay (right figure) in patients with NSTEMI-ACS. ICU—Intensive care unit.

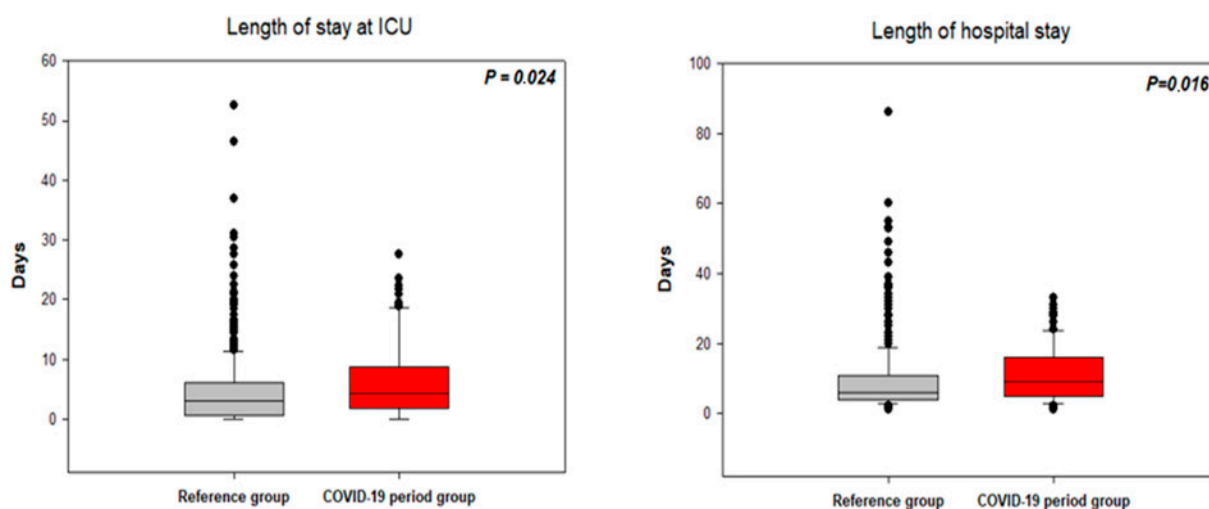


Figure 5. Length of stay in the intensive care unit (**left figure**) and total hospital stay (**right figure**) in patients with STEMI. ICU—Intensive care unit.

3.5. Hospital Outcomes

The in-hospital mortality rate for patients with NSTEMI-ACS was 3% in the CPG and 3.3% in the RG (odds ratio (OR) in the CPG 0.853, 95% confidence interval (CI) 0.247 to 2.951; $p = 0.960$). The in-hospital mortality rate for STEMI patients was 11.8% in the CPG and 9.6% in the RG (OR in CPG 1.248, 95% CI 0.566 to 2.749; $p = 0.735$). The major adverse event rates were not significantly different between the CPG and RG NSTEMI-ACS patients (8.7% vs. 6.3%, respectively; $p = 0.389$) or STEMI patients (17.9% vs. 15%, respectively; $p = 0.491$).

3.6. Financial Costs

The mean total hospital cost for NSTEMI-ACS patients was 8099 ± 6003 euros for the CPG ($p = 0.078$) and 7366 ± 6741 euros for the RG. In the STEMI patients, the total mean hospital cost was 6972 ± 5687 euros for the CPG and 6540 ± 5692 euros for the RG ($p = 0.262$).

4. Discussion

We reviewed an all-comers single-centre ACS registry of patient characteristics, treatment strategies, outcomes and financial costs before and during the COVID-19 pandemic when patients were managed using the EAPCI algorithms.

4.1. ACS Patient Characteristics

The COVID-19 outbreak was associated with a significant decline in the number of patients hospitalised for ACS in several countries, which may be explained by several patient- and system-related factors [5–9]. The fact that our centre did not experience a decrease in hospital admissions for patients with ACS (NSTEMI and STEMI) may be due to the relatively low involvement of the Czech Republic in the pandemic and good centre organisational protocols for ACS patients. The impact of low-intensity pandemic on hospital admissions is supported by the fact that we did not observe any patient with ACS and concomitant COVID-19 disease. Nevertheless, 8 out of the 34 patients (23.5%) admitted to the hospital with COVID-19 had slightly elevated high sensitive troponin I (less than five times higher of upper limit of range). These patients did not have other clinical symptoms of myocardial ischemia, and the troponin elevation was probably connected with myocardial injury during the inflammatory process.

4.2. Time Delays

In the STEMI group, the rates of primary percutaneous coronary intervention (PCI) did not differ between the CPG and RG patients and were similar to the findings of our previous large multicentre registries conducted in the Czech Republic over the last

two decades [10–12]. The COVID-19 pandemic did not cause system-related delays in time-to-treatment intervals. Surprisingly, no differences in patient-related time delays (from symptom onset to FMC) were found between the CPG and the RG. The higher number of patients in the KILLIP III-IV class can be partially explained by the hesitation in seeking medical attention in the very early phase of ACS after the onset of symptoms. An alternative explanation may be the inability of other hospitals to provide appropriate care for critically ill patients.

The majority of NSTEMI-ACS patients underwent invasive procedures, and coronary angiography was performed in approximately three-quarters of the patients within the first 24 h. This is relevant because, in most cases, SARS-CoV-2 testing was performed before coronary angiography. However, patients confirmed as COVID-19 negative immediately underwent coronary angiography, which was possible because a significant reduction in elective procedures increased catheterisation laboratory availability.

Our experience differs from those reported in an EAPCI survey, which assessed the impact of the COVID-19 pandemic on interventional cardiology practice [13]. In the EAPCI survey, approximately half of the 636 respondents reported delays in reperfusion in STEMI patients (48%) and delays in early invasive treatment for NSTEMI-ACS patients (57%). The authors concluded that, overall, it was not possible to test patients suspected of carrying COVID-19 systematically, and the availability of personal protective equipment in the catheterisation lab was suboptimal. We did not face these limitations at our centre. Thus, it is clear that testing availability and an adequate supply of protective equipment are essential for rapid treatment of patients with ACS during the pandemic. The crucial roles of testing and organising ACS patients during the COVID-19 pandemic was also established in Lombardy for effective treatment in spring 2020. A similar algorithm for ACS patients compared to the EAPCI algorithm was developed together with centralizing cardiovascular emergencies in a regional hub-and-spokes system [14–16].

4.3. Duration of Hospital Stay and Costs

We found that among NSTEMI-ACS patients, the ICU stay and total hospital stay were significantly longer in the CPG than in the RG, and the total financial cost was higher in the CPG than in the RG; however, the duration of ICU and total hospital stay and total financial cost were not significantly different between the CPG and RG in STEMI patients. The differences in the patients with NSTEMI-ACS cannot be explained by treatment delays or different treatment strategies (the PCI and coronary artery bypass graft rates were similar in both groups). Furthermore, this cannot be explained by the second PCI performed during hospital stay to achieve complete revascularisation, which was increased during the COVID-19 period in NSTEMI-ACS patients as well as in STEMI patients (4% in the RG vs. 8% in the CPG between NSTEMI-ACS and 10 vs. 15% in STEMI patients). The most likely explanation is that the clinical condition of the NSTEMI-ACS patients was worse (significantly lower ejection fraction, numerically higher rate of mechanical ventilation), and NSTEMI-ACS patients remained in the ICU longer to stabilise their condition. Furthermore, the longer mean total hospital stay in the NSTEMI-ACS CPG may have been skewed by deaths of three patients after a long hospital stay (mean time from admission to death was 19 days) compared with 12 deaths in the RG (mean time from admission to death was 8 days). As a consequence, the total hospital costs were higher in the NSTEMI-ACS CG. These observations were not seen in the patients with STEMI.

Regarding the in-hospital mortality rate of STEMI patients, we observed higher rates of mortality than expected with respect to randomised control trials or some registries [17]. However, our in-hospital mortality rate is very similar to those of large national registries collecting data from unselected STEMI population [18,19]. Secondly, it has to be put into context with the high number of patients who died after resuscitation (in CPG, 10.3% died following out-of-hospital cardiac arrest, and 12.8% died following resuscitation but before starting PCI). The mortality rate of resuscitated patients is ten times higher than that of STEMI patients who do not require resuscitation [20]. Our registry has the highest number

of resuscitated patients from all registries found in the literature. The prevalence of OHCA between STEMI patients is between 5 and 6% [21]. The in-hospital mortality rate of STEMI patients would decrease to 5.6% if OHCA STEMI patients were not included in the registry.

4.4. Limitations

Our study has several limitations. First, because it was a single-centre experience, our findings cannot be generalised to other European high-volume centres given that health-care organisational strategies and local epidemiological situations differ. Second, the CPG sample was relatively small; a larger sample drawn from multiple centres would have greater statistical power. However, our aim was to conduct a quick but detailed analysis of the relevance of the proposed EAPCI algorithms for ACS management because the epidemiological situation could worsen in the future, requiring the use of this management strategy again. Collecting a large amount of data from multiple centres with sufficient quality control would take significantly longer. Third, patients admitted for ACS in February were assigned to the CPG even though the first positive case in the Czech Republic was not confirmed until 1 March 2020. However, by that time the media focus on the pandemic may have altered patient attitudes towards seeking treatment; moreover, the first steps to reorganise hospital management were taken in February. Finally, the EAPCI position statement was published online on 14 May 2020, when the epidemiological situation had stabilised. Nevertheless, our centre's strategy, which had been established before the EAPCI publication, included all of the key EAPCI recommendations.

5. Conclusions

According to our centre's experience, the COVID-19 outbreak is not associated with a decrease in the number of patients admitted with ACS when the community spread of the virus is not severe. Nevertheless, more patients were admitted to our centre with serious clinical conditions. Modified treatment strategies for patients with ACS during the first four months of the COVID-19 pandemic were not associated with treatment delays when adequate SARS-CoV-2 testing and personal protective equipment were available. Moreover, the COVID-19 situation did not have an impact on treatment strategies and hospital outcomes at our centre. However, this conclusion must be put into the context of rates of viral spread. Further detailed analyses from multicentre registries are needed to reveal more accurately the secondary impact of COVID-19 on patients with ACS.

Author Contributions: P.T. (Petr Toušek), V.K. conceived and designed the study; D.B., M.N. (Marketa Novackova) and J.K. were responsible for data entering into the database, M.N. (Marek Neuberg) performed the statistical analysis; P.M. and P.T. (Petr Tuma) analyzed the data; P.W. and Z.M. performed final corrections of analysis and preparation of the article; P.T. (Petr Toušek) wrote the paper. All authors have read and agreed to the published version of the manuscript.

Funding: The registry and this manuscript was supported by the INTERCARDIS EU project Nr. CZ.02.1.01/0.0/0.0/16_026/0008388, Charles University Research Programmes UNCE/MED 02 and Progres Q38.

Acknowledgments: We acknowledge administrative support of Antonin Chlum and Petr Macek.

Conflicts of Interest: The authors do not have any conflicts of interest regarding this manuscript.

References

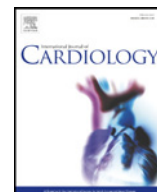
1. Chieffo, A.; Stefanini, G.G.; Price, S.; Barbato, E.; Tarantini, G.; Karam, N.; Moreno, R.; Buchanan, G.L.; Gilard, M.; Halvorsen, S.; et al. EAPCI Position Statement on Invasive Management of Acute Coronary Syndromes during the COVID-19 pandemic. *Eur. Heart J.* **2020**, *41*, 1839–1851. [[CrossRef](#)] [[PubMed](#)]
2. Widimsky, P.; Beneš, J.; Celko, A.M. Czech Republic and low COVID-19 mortality in the heart of Europe: Possible explanations. *Eur. Heart J.* **2020**, *41*, 3876–3879. [[CrossRef](#)] [[PubMed](#)]

3. Ibanez, B.; James, S.; Agewall, S.; Antunes, M.J.; Bucciarelli-Ducci, C.; Bueno, H.; Caforio, A.L.P.; Crea, F.; Goudevenos, J.A.; Halvorsen, S.; et al. 2017 ESC Guidelines for the management of acute myocardial infarction in patients presenting with ST-segment elevation: The Task Force for the management of acute myocardial infarction in patients presenting with ST-segment elevation of the European Society of Cardiology (ESC). *Eur. Heart J.* **2018**, *39*, 119–177. [[PubMed](#)]
4. Roffi, M.; Patrono, C.; Collet, J.P.; Mueller, C.; Valgimigli, M.; Andreotti, F.; Bax, J.J.; Borger, M.A.; Brotons, C.; Chew, D.P.; et al. 2015 ESC Guidelines for the management of acute coronary syndromes in patients presenting without persistent ST-segment elevation: Task Force for the Management of Acute Coronary Syndromes in Patients Presenting without Persistent ST-Segment Elevation of the European Society of Cardiology (ESC). *Eur. Heart J.* **2016**, *37*, 267–315.
5. Metzler, B.; Siostrzonek, P.; Binder, R.K.; Bauer, A.; Reinstadler, S.J. Decline of acute coronary syndrome admissions in Austria since the outbreak of COVID-19: The pandemic response causes cardiac collateral damage. *Eur. Heart J.* **2020**, *41*, 1852–1853. [[CrossRef](#)]
6. De Filippo, O.; D’Ascenzo, F.; Angelini, F.; Bocchino, P.P.; Conrotto, F.; Saglietto, A.; Secco, G.G.; Campo, G.; Gallone, G.; Verardi, R.; et al. Reduced Rate of Hospital Admissions for ACS during Covid-19 Outbreak in Northern Italy. *N. Engl. J. Med.* **2020**, *383*, 88–89. [[CrossRef](#)]
7. De Rosa, S.; Spaccarotella, C.; Basso, C.; Calabrò, M.P.; Curcio, A.; Filardi, P.P.; Mancone, M.; Mercurio, G.; Muscoli, S.; Nodari, S.; et al. Reduction of hospitalizations for myocardial infarction in Italy in the COVID-19 era. *Eur. Heart J.* **2020**, *41*, 2083–2088.
8. Garcia, S.; Albaghdadi, M.S.; Meraj, P.M.; Schmidt, C.; Garberich, R.; Jaffer, F.A.; Dixon, S.; Rade, J.J.; Tannenbaum, M.; Chambers, J.; et al. Reduction in ST-Segment Elevation Cardiac Catheterization Laboratory Activations in the United States During COVID-19 Pandemic. *J. Am. Coll. Cardiol.* **2020**, *75*, 2871–2872. [[CrossRef](#)]
9. Piccolo, R.; Bruzzese, D.; Mauro, C.; Aloia, A.; Baldi, C.; Boccalatte, M.; Bottiglieri, G.; Briguori, C.; Caiazzo, G.; Calabrò, P.; et al. Population Trends in Rates of Percutaneous Coronary Revascularization for Acute Coronary Syndromes Associated With the COVID-19 Outbreak. *Circulation* **2020**, *141*, 2035–2037. [[CrossRef](#)]
10. Tousek, P.; Staskova, K.; Mala, A.; Sluka, M.; Vodzinska, A.; Jancar, R.; Maluskova, D.; Jarkovsky, J.; Widimsky, P. Incidence, treatment strategies and outcomes of acute coronary syndrome with and without ongoing myocardial ischaemia: Results from the CZECH-3 registry. *Eur. Heart J. Acute Cardiovasc. Care* **2019**, *8*, 687–694. [[CrossRef](#)]
11. Tousek, P.; Toušek, F.; Horak, D.; Červinka, P.; Rokyta, J.R.; Pešl, L.; Jarkovsky, J.; Widimsky, P. The incidence and outcomes of acute coronary syndromes in a central European country: Results of the CZECH-2 registry. *Int. J. Cardiol.* **2014**, *173*, 204–208. [[CrossRef](#)] [[PubMed](#)]
12. Widimsky, P.; Želízko, M.; Janský, P.; Toušek, F.; Holm, F.; Aschermann, M. The incidence, treatment strategies and outcomes of acute coronary syndromes in the “reperfusion network” of different hospital types in the Czech Republic: Results of the Czech evaluation of acute coronary syndromes in hospitalized patients (CZECH) registry. *Int. J. Cardiol.* **2007**, *119*, 212–219.
13. Roffi, M.; Capodanno, D.; Windecker, S.; Baumbach, A.; Dudek, D. Impact of the COVID-19 pandemic on interventional cardiology practice: Results of the EAPCI survey. *EuroIntervention* **2020**, *16*, 247–250. [[CrossRef](#)] [[PubMed](#)]
14. Stefanini, G.; Azzolini, E.; Condorelli, G. Critical Organizational Issues for Cardiologists in the COVID-19 Outbreak A Frontline Experience from Milan, Italy. *Circulation* **2020**, *141*, 1597–1599. [[CrossRef](#)] [[PubMed](#)]
15. Cosentino, N.; Assanelli, E.; Merlino, L.; Mazza, M.; Bartorelli, A.L.; Marenzi, G. An In-hospital Pathway for Acute Coronary Syndrome Patients During the COVID-19 Outbreak: Initial Experience Under Real-World Suboptimal Conditions. *Can. J. Cardiol.* **2020**, *36*, 961–964. [[CrossRef](#)]
16. Cosentino, N.; Bartorelli, A.L.; Marenzi, G. Time to treatment still matters in ST-elevation myocardial infarction: A call to maintain treatment effectiveness during the COVID-19 pandemic. *Eur. Heart J. Cardiovasc. Pharmacother.* **2020**, *6*, 408–409. [[CrossRef](#)]
17. Danchin, N.; Lettino, M.; Zeymer, U.; Widimsky, P.; Bardaji, A.; Barrabes, J.A.; Cequier, A.; Claeys, M.J.; De Luca, L.; Dörler, J.; et al. Use, patient selection and outcomes of P2Y12 receptor inhibitor treatment in patients with STEMI based on contemporary European registries. *Eur. Heart J. Cardiovasc. Pharmacother.* **2016**, *2*, 152–167. [[CrossRef](#)]
18. Freisinger, E.; Fuerstenberg, T.; Malyar, N.M.; Wellmann, J.; Keil, U.; Breithardt, G.; Reinecke, H. German nationwide data on current trends and management of acute myocardial infarction: Discrepancies between trials and real-life. *Eur. Heart J.* **2014**, *35*, 979–988. [[CrossRef](#)]
19. Chung, S.-C.; Gedeberg, R.; Nicholas, O.; James, S.K.; Jeppsson, A.; Wolfe, C.; Heuschmann, P.; Wallentin, L.; Deanfield, J.; Timmis, A.; et al. Acute myocardial infarction: A comparison of short-term survival in national outcome registries in Sweden and the UK. *Lancet* **2014**, *383*, 1305–1312. [[CrossRef](#)]
20. Karam, N.; Bataille, S.; Marijon, E.; Tafflet, M.; Benamer, H.; Caussin, C.; Garot, P.; Juliard, J.-M.; Pirès, V.; Boche, T.; et al. Incidence, Mortality, and Outcome-Predictors of Sudden Cardiac Arrest Complicating Myocardial Infarction Prior to Hospital Admission. *Circ. Cardiovasc. Interv.* **2019**, *12*, e007081. [[CrossRef](#)]
21. Hauguel-Moreau, M.; Pillière, R.; Prati, G.; Beaune, S.; Loeb, T.; Lannou, S.; Mallet, S.; Mustafic, H.; Bégué, C.; Dubourg, O.; et al. Impact of Coronavirus Disease 2019 outbreak on acute coronary syndrome admission: Four weeks to reverse the trend. *J. Thromb. Thrombolysis* **2020**, *29*, 1–2. [[CrossRef](#)] [[PubMed](#)]

E. Polaková a kol.

Effectiveness of alcohol septal ablation for hypertrophic obstructive cardiomyopathy in patients with late gadolinium enhancement on cardiac magnetic resonance

International Journal of Cardiology
Impact Factor: 3,229



Effectiveness of alcohol septal ablation for hypertrophic obstructive cardiomyopathy in patients with late gadolinium enhancement on cardiac magnetic resonance

Eva Polaková^{a,*,1}, Max Liebrechts^b, Natália Marková^c, Theodor Adla^c, Basak Kara^b, Jurriën ten Berg^b, Jiří Bonaventura^a, Josef Veselka^{a,1}

^a Department of Cardiology, Second Medical School, Charles University, Motol University Hospital, Prague, Czech Republic

^b Department of Cardiology, St. Antonius Hospital, Nieuwegein, the Netherlands

^c Department of Radiology, Second Medical School, Charles University, Motol University Hospital, Prague, Czech Republic

ARTICLE INFO

Article history:

Received 20 April 2020

Received in revised form 21 May 2020

Accepted 24 June 2020

Available online 17 July 2020

Keywords:

Alcohol septal ablation

Hypertrophic cardiomyopathy

Cardiac magnetic resonance

Late gadolinium enhancement

Septal scarring

Septal fibrosis

ABSTRACT

Background: According to European guidelines, alcohol septal ablation (ASA) for hypertrophic obstructive cardiomyopathy (HOCM) may be less effective in patients with extensive septal scarring on cardiac magnetic resonance (CMR). This study aimed to analyze the impact of late gadolinium enhancement (LGE) on CMR on the effectiveness of ASA.

Method: We conducted an observational retrospective study involving adult patients with symptomatic drug-refractory HOCM who underwent CMR before ASA at two European centres from May 2010 through June 2019. Patients were compared in binary format based on LGE presence. Moreover, a subanalysis focused on patients with septal fibrosis was performed. The effectiveness of ASA was evaluated by echocardiographic, ECG and clinical findings.

Results: Of the 113 study patients, 54 (48%) had LGE on CMR. The LGE quantification performed in 29 patients revealed septal fibrosis in 17. The mean follow-up was 4.4 ± 2.6 years. Baseline parameters were similar between groups except for basal septal thickness that was greater in LGE+ group (21.1 ± 3.9 mm for LGE+ vs. 19.2 ± 3.2 mm for LGE-; $p = .005$). ASA improved symptoms in all groups and reduced left ventricular outflow tract obstruction (LVOTO) (delta gradient reduction: LGE+: $62 \pm 37.3\%$; septal LGE+: $75.6 \pm 20.8\%$; LGE-: $72.5 \pm 21.0\%$). However, 13% of the LGE+ and 2% of the LGE- group had residual LVOTO above 30 mmHg ($p = .027$).

Conclusion: ASA was effective in all patients with HOCM, whether they had LGE on CMR or not and whether they had septal fibrosis or not.

© 2020 Elsevier B.V. All rights reserved.

1. Introduction

Hypertrophic cardiomyopathy (HCM) is a common inherited cardiovascular disease characterized by thickened left ventricular (LV) wall in the absence of abnormal loading conditions [1]. The expression of disease varies widely among HCM patients, ranging from asymptomatic

patients expected to live a normal lifespan to severely symptomatic patients with poor prognosis. The treatment focuses on management of symptoms, prevention of complications and sudden cardiac death [1–4]. In symptomatic drug-refractory patients with significant left ventricular outflow tract obstruction (LVOTO) the therapy of choice is invasive septal reduction aiming to provide haemodynamic and clinical improvement. Although both surgical myectomy and alcohol septal ablation (ASA) have gained acceptance over the past decades, uncertainty over efficacy in subgroups of patients persists. According to the European Society of Cardiology (ESC) guidelines, ASA may be less effective in patients with extensive septal scarring on cardiac magnetic resonance (CMR) [1]. This statement is based on the assumption that fibrotic tissue stays unchanged after ASA, but sufficient evidence is lacking. [5–7] CMR provides accurate, non-invasive assessment of regional myocardial fibrosis using LGE [8,9]. [10] We therefore analyzed the impact of fibrosis assessed by LGE on CMR on the effectiveness of ASA. Moreover, we performed a subanalysis focused on patients with septal fibrosis.

Abbreviations: ASA, alcohol septal ablation; CMR, cardiac magnetic resonance; ESC, European Society of Cardiology; HCM, hypertrophic cardiomyopathy; HOCM, hypertrophic obstructive cardiomyopathy; LGE, late gadolinium enhancement; LV, left ventricle; LVOT, left ventricular outflow tract; LVOTO, LVOT obstruction; IVS, interventricular septum; PG, peak gradient.

* Corresponding author at: Department of Cardiology, Motol University Hospital, V Úvalu 84, Prague 15006, Czech Republic.

E-mail address: eva.polakova@fnmotol.cz (E. Polaková).

¹This author takes responsibility of all aspects of the reliability and freedom from bias of the data presented and their discussed interpretation.

<https://doi.org/10.1016/j.ijcard.2020.06.049>

0167-5273/© 2020 Elsevier B.V. All rights reserved.

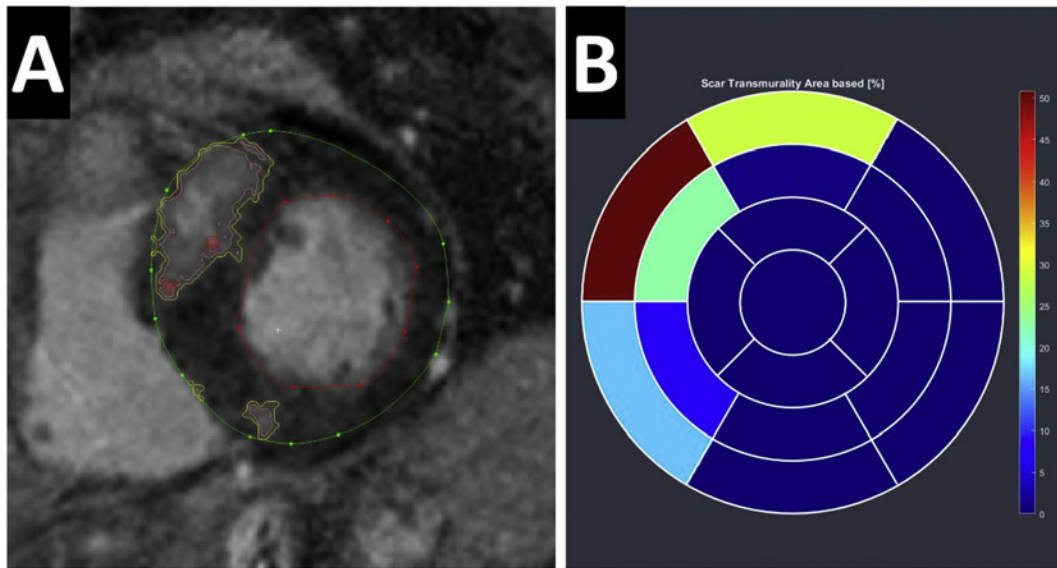


Fig. 1. 65-years old female with HOCM. ASA with 3,5 ml alcohol resulted in decrease of LVOT gradient from 107 mmHg to 10 mmHg. A) Example of MRI T1 PSIR image in basal short axis with LGE mainly at the anteroseptal region. The EWA method has been used for myocardial scar quantification after manual delineation of the endocardium (red) and epicardium (green). The yellow line denotes the complete affected area, and the pink line a graphical representation of the corresponding weighted area. B) Bullseye 17 AHA model shows area based scar transmurality. The most affected basal anteroseptal region with about 50% scar. Segments without LGE are blue.

2. Material and methods

2.1. Study design

We conducted an observational retrospective study involving adult patients with hypertrophic obstructive cardiomyopathy (HOCM) who underwent CMR imaging before ASA. CMR studies and ASA procedures were performed at two European tertiary HCM care centres (the Netherlands-Nieuwegein; Czech Republic-Prague). Patients were divided into two groups based on LGE presence. The effectiveness of ASA was evaluated by echocardiographic, electrocardiographic (ECG) and clinical findings. Data were collected at each outpatient visit. A dedicated ASA database was kept at the 2 centres. Subsequently, we performed a subanalysis to compare patients with septal fibrosis based on LGE quantification to LGE negative patients. The study was conducted in accordance with the principles of the Declaration of Helsinki.

2.2. Study population

We conducted a search in our ASA registries and identified patients who had undergone CMR before ASA. All patients had been previously enrolled in institutional registries and provided informed written consent before participation. Some of the patients were included in previous reports. [11–13] The diagnosis of HOCM was made by experienced cardiologists based on established criteria [1]. ASA was offered to patients with left ventricular outflow tract (LVOT) gradient ≥ 30 mmHg at rest or ≥ 50 mmHg after provocation who were symptomatic in spite of maximally tolerated drug therapy, or had experienced syncope. The need for ASA was established after consensus between HCM experts at individual sites. All procedures were performed by experienced interventional cardiologists. Details of the ASA technique have been published previously [14–17].

2.3. Cardiac magnetic resonance

2.3.1. CMR examination

CMR examinations were performed as previously described [18]. In both centres imaging was performed on a 1.5 T magnetic resonance scanners (Magnetom Avanto Siemens Medical System, Erlangen,

Germany) with dedicated cardiac coil. Details of image acquisition are discussed in the Appendix. The image evaluation was made independently at each site, however, the same protocol was followed. In the subanalysis using LGE quantification, LGE volume and LV myocardial volume were measured by the software Segment (Medviso, Lund, Sweden) using viability automatic EWA method (Expectation Maximization, weighted intensity, a priori information) after manual delineation of the endocardial and epicardial contours (Fig. 1) [19]. Areas identified as LGE by software but visually assessed as artefact were manually excluded.

2.4. Statistical analysis

Data are presented as mean \pm standard deviations for continuous variables and counts and proportions for categorical variables. The Shapiro-Wilk normality test was used to check for skewness and based on its outcome either the Student's *t*-test or Mann-Whitney test was used to assess equality of means between continuous variables. The difference between the categorical variables was evaluated using the Fisher's exact test.

To establish the impact of LGE presence on the effectiveness of ASA, we evaluated the variables in a univariate model (Table 1). *P*-value $< .05$ was considered statistically significant. All reported *p*-values are two-sided. The software Prism (release 6.05, GraphPad Software Inc., La Jolla, CA, USA) was used for statistical analysis.

3. Results

3.1. Baseline characteristics

From May 2010 through June 2019, a total of 113 patients with HOCM underwent ASA with prior CMR evaluation: 34 patients at the Czech centre, 79 at the Dutch centre. In this cohort, 54 patients (48%) had LGE on visual assessment (LGE+ group) and were compared to 59 patients without any LGE (LGE- group). Clinical, echocardiographic and ECG characteristics at baseline and at the last medical contact are summarized in Table 1.

Table 1
Clinical, ECG and echocardiographic characteristics at baseline and at the last check-up.

	A	B	C	A vs C	B vs C
	LGE +Group N = 54	Septal LGE +Group N = 17	LGE-Group N = 59	P value	P value
Age of ASA, years	58.6 ± 11.4	59.0 ± 10.8	59.7 ± 12.5	0.482	0.672
Age of MR, years	58.3 ± 11.5	58.3 ± 11.1	59.4 ± 12.6	0.482	0.594
Females, n (%)	21 (39)	8 (47)	32 (54)	0.132	0.784
Alcohol, ml	2.1 ± 0.5	2.1 ± 0.5	2.1 ± 0.6	0.576	0.746
Dyspnea, NYHA class					
Baseline	2.8 ± 0.5	2.7 ± 0.6	2.8 ± 0.5	0.345	0.308
Last clinical check-up	1.3 ± 0.5	1.3 ± 0.5	1.5 ± 0.6	0.261	0.345
NYHA class III/IV					
Baseline, n (%)	38 (70)	11 (65)	49 (83)	0.123	0.173
Last clinical check-up, n (%)	1 (2)	0	4 (7)	0.366	0.569
Angina, CCS class					
Baseline	0.7 ± 1.0	1.1 ± 1.2	0.5 ± 1.0	0.218	0.061
Last clinical check-up	0.1 ± 0.4	0.1 ± 0.3	0.1 ± 0.4	0.980	0.611
Maximal LV outflow gradient at rest, mmHg					
Baseline	62.7 ± 40.9	67.4 ± 34.8	57.6 ± 37.3	0.411	0.146
Last clinical check-up	18.2 ± 15.4	12.8 ± 9.1	12.3 ± 7.8	0.065	0.928
> 30 mmHg, n (%)	7 (13)	1 (6)	1 (2)	0.027	0.400
Delta gradient, %	62.4 ± 37.3	75.6 ± 20.8	72.5 ± 21.0	0.395	0.349
LV diameter, mm					
Baseline	40.9 ± 5.8	42.4 ± 5.0	39.4 ± 5.6	0.190	0.065
Last clinical check-up	43.7 ± 5.3	45.4 ± 4.5	41.9 ± 6.1	0.084	0.025
LV ejection fraction, %					
Baseline	70 ± 7	70 ± 8	71 ± 8	0.360	0.607
Last clinical check-up	68 ± 7	69 ± 7	68 ± 8	0.931	0.559
Basal septum thickness, mm					
Baseline	21.1 ± 3.9	22.7 ± 4.7	19.2 ± 3.2	0.005	0.003
Last clinical check-up	14.0 ± 4.4	13.6 ± 3.7	12.3 ± 3.6	0.021	0.148
Delta septum thickness, mm	7.2 ± 4.1	9.1 ± 3.9	7.4 ± 4.7	0.921	0.169
BBB					
Baseline, n (%)	4 (7)	2 (12)	3 (5)	0.708	0.310
Last clinical check-up, n (%)	31 (57)	11 (65)	35 (59)	0.851	0.783
Complete heart block					
Last clinical check-up, n (%)	11 (20)	5 (29)	19 (32)	0.202	1.000

Table 2
Cardiovascular adverse events in the first 30 days after ASA.

Event	A	B	C	A vs C	B vs C
	LGE + Group N = 54	Septal LGE + Group N = 17	LGE - Group N = 59	P-value	P-value
Transient complete heart block (%)	8 (14.8)	3 (17.6)	13 (22.0)	0.346	1.000
Pacemaker implantation, n (%)	4 (7.4)	3 (17.4)	6 (10.2)	0.745	0.410
Cardiovascular death, n (%)	0	0	0	1.000	1.000
Electrical cardioversion for VT/VF or ICD discharge, n (%)	1 (1.9)	0	2 (3.4)	1.000	1.000
Cardiac tamponade, n (%)	0	0	0	1.000	1.000

3.2. Alcohol septal ablation procedure

The volumes of injected alcohol during ASA were almost identical in both groups, the mean volume was 2.1 ml in the LGE+ group and in the LGE- group and it ranged from 1 ml to 3.5 ml and from 1 ml to 3 ml, respectively. The amount of alcohol injected was dependent at discretion of each operator. The correlation between the amount of injected alcohol, LGE presence and LVOT gradient is described in the Supplementary Fig. 1 and Supplementary Fig. 2.

None of the patients died during the procedure or in the first 30 days thereafter. The complication rate was very low with no significant differences between the groups (Table 2). The complete heart block requiring pacemaker implantation was present in 7.4% of the LGE+ group, 17.4% in the septal LGE+ group and 10.2% in the LGE- group (NS).

3.3. Outcome data

The mean follow-up after ASA was 4.4 ± 2.6 years in all patients, 3.9 ± 2.9 years in LGE+ group and 4.9 ± 2.3 years in LGE- group. At the last check-up, after ASA was performed, the symptoms improved in both groups almost equally (Table 1). ASA reduced basal septum thickness by 7.2 mm in LGE+ group and by 7.4 mm in LGE- group. Overall left ventricular outflow tract obstruction (LVOTO) decreased considerably in all patients (see Supplementary Fig. 3). However, 13% of the LGE+ group had residual LVOTO higher than 30 mmHg compared to only 2% of the LGE- group ($p = .027$).

A total of 5 deaths occurred during follow-up: 1 sudden cardiac death in the LGE+ group, 3 non-cardiovascular deaths in the LGE+ group, and 1 unknown death in the LGE- group. Further, 6 patients required electrical cardioversion for VT/VF or experienced appropriate implantable cardioverter-defibrillator (ICD) discharge (2 in the LGE+ group and 4 in the LGE- group). A total of 10 patients underwent 12 repeated septal reduction procedures with no significant difference between the groups.

3.4. Subanalysis

We intended to perform LGE quantification in all Czech patients ($n = 34$). Five of them were excluded from the analysis due to insufficient image quality that did not allow LGE quantification. Out of the 29 patients, 23 (79%) were classified as LGE+. The amount of LGE ranged between 1% to 14% of LV mass. In two cases the LGE was of ischemic origin due to previous myocardial infarction. We selected patients ($n = 17$) with any LGE in basal and midventricular septal segments (basal anteroseptal, basal inferoseptal, midventricular anteroseptal, midventricular inferoseptal) and compared them with the LGE- group ($n = 59$). The results are shown in Table 1. The percentage of LGE in basal and midventricular septal segments against reduction of LVOT gradient is shown in Fig. 2.

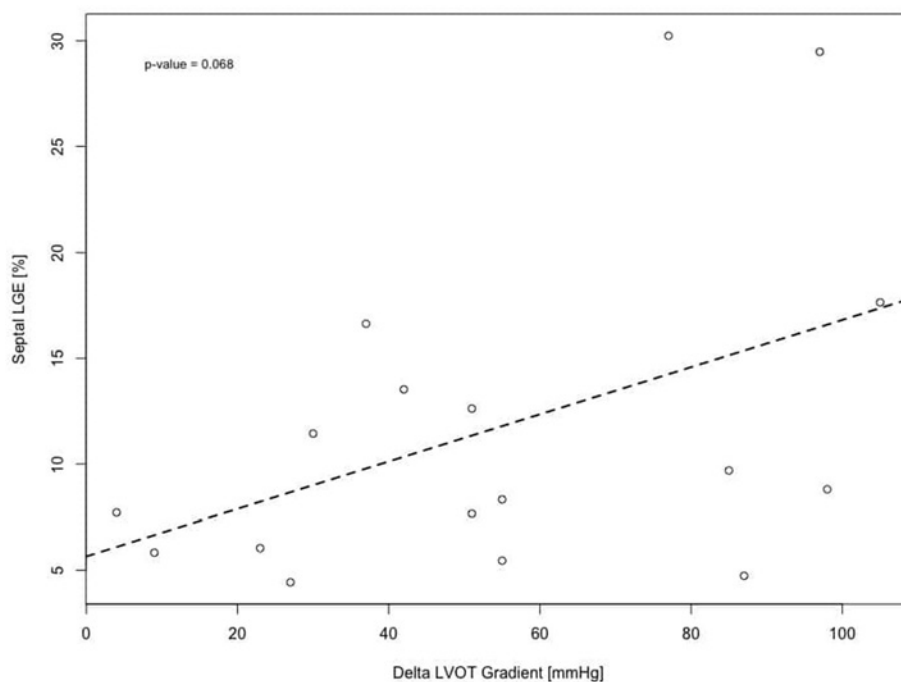


Fig. 2. The percentage of LGE in basal and midventricular septal segments against reduction of LVOT gradient. The ordinary least squares (OLS) regression estimated that increase in reduction of LVOT gradient by 1 mmHg increases septal LGE by 0.11% (p -value = .068).

4. Discussion

We assessed the impact of fibrosis, defined as LGE presence on CMR, on ASA outcomes in adult symptomatic patients with HOCM. Our results suggest that from haemodynamic and clinical point of view ASA was highly effective among all study groups whether they had LGE or not (LGE+, septal LGE+, LGE-).

In our cohort, the LGE+ group is associated with a more severe HCM phenotype and hence it is logical that the effectiveness of ASA in such a population might be slightly lower. We should emphasize that the LGE+ group had greater IVS thickness not only at baseline but also at follow-up. In fact, in the LGE+ group the LVOTO after ASA persisted more likely above 30 mmHg (13% LGE+ vs 2% LGE-), which might imply a worse prognosis as described in previous studies [11], [20]. However, based on the results of Euro-ASA registry [12] the rate of residual LVOT gradient above 30 mmHg was 12% in the group with severe hypertrophy (IVS > 16 mm) and 7% in the group with mild hypertrophy (IVS < 16 mm). In this study, we demonstrated that ASA was effective in LGE+ group, decreasing the LVOTO below 30 mmHg in 87% of LGE+ patients and improving NYHA class by ≥ 1 . Moreover, even in the LGE+ and septal LGE+ groups ASA significantly reduced the basal septum thickness, while the differences in reduction did not vary among all study groups.

Occurrence of complications did not differ significantly among the study groups. The rate of pacemaker implantations corresponds to the known rate in Euro-ASA registry [11] which revealed the rate of 12%, and Nationwide Inpatient Sample [21] which demonstrated complete heart block requiring pacemaker insertion in 8.7% patients.

Our results suggest that ASA can be performed independently of LGE presence and the choice of septal reduction therapy (ASA or surgical septal reduction) should not be directed by it. Based on the above findings we could challenge the ESC HCM guidelines – while ASA is not recommended in patients with septal fibrosis, our data show excellent outcome even in this population.

4.1. Limitations

As for the limitations of our study, the main drawback of our design is its retrospective character. Therefore, the selection and referral of patients who underwent CMR is not randomized and could possibly be determined by severity of illness. On the other hand, patients with CMR non-conditional implantable cardioverter defibrillator or pacemaker were excluded from the analysis by its design. In addition, our cohort was rather small and could potentially give biased results, especially in the septal LGE+ group. Our results may not be generalizable on non-tertiary care centres with less experience with ASA.

Another limitation is that only a small number of our patients underwent LGE quantification. We suggest that for the further studies LGE should not be assessed in binary format due to a wide spectrum of disease severity associated with LGE extent.

Moreover, as a novel technique LGE quantification method is not standardized and has a burden of huge variability. A CMR core lab was not established – the CMR evaluation was performed at each centre independently, and therefore inter-observer variability in our study is not excluded.

5. Conclusion

Our data suggest that ASA is effective in all patients with HOCM, whether they had LGE on CMR or not and whether they had septal fibrosis or not.

Supplementary data to this article can be found online at <https://doi.org/10.1016/j.ijcard.2020.06.049>.

Acknowledgments

The authors are grateful to statisticians Eva Hansvenclova and Filip Gleta for their assistance with statistical analysis. The authors also thank colleagues responsible for the HCM clinics in all participated centres.

Funding

Supported by Ministry of Health, Czech Republic - conceptual development of research organization, Motol University Hospital, Prague, Czech Republic 00064203.

Appendix A. Appendix

A.1. CMR

A.1.1. CMR examination:

The examination was performed using 1.5 Tesla systems (Magnetom Avanto Siemens Medical System, Erlangen, Germany) with dedicated cardiac coil. Study protocol included cine steady-state free precession pulse sequence images, 3 cine images in LV long axis (LVLA, LV 3Ch, 4ch) and short axis stack of consecutive cine images through whole ventricles. SA cine images parameters were: 25 phases, slice thickness 8 with 2 mm gap, FOV 35–40 cm, acquisition matrix 192 × 156, flip angle 74°, TR 70.8, TE 1.4.

LGE images acquisition was started 10 min after the administration of Gd-DTPA with a dosage of 0.15–0.2 mmol/kg in short-axis views with T1-weighted phase-sensitive inversion recovery (PSIR) sequence with appropriate setting of inversion time to null normal myocardium signal using a TI-scout, slice thickness 8 with 2 mm gap, FOV 35–40 cm, acquisition matrix 256 × 156, flip angle 25°, TR 650, TE 3.3.

A.1.2. CMR assessment:

LGE volume and LV myocardial mass were measured in the software Segment (Medviso, Lund, Sweden) using viability automatic EWA method (Expectation maximization, weighted intensity, a priori information) after manual delineation of endocardial and epicardial contour. Papillary muscles and trabeculae were excluded from LV myocardial mass. [19]

Declarations of Competing Interest. The authors report no relationships that could be construed as a conflict of interest.

Credit Author Statement. Eva Polaková: Data curation, Formal analysis, Investigation, Methodology, Project administration, Visualization, Writing original draft. Max Liebrechts: Investigation, Writing – review & editing. Natália Marková: Investigation, Writing – review & editing. Theodor Adla: Investigation, Writing – review & editing. Kara Basak: Investigation, Writing – review & editing. Jurrien ten Berg: Investigation, Writing – review & editing. Jiří Bonaventura: Investigation, Writing – review & editing. Josef Veselka: Conceptualization, Funding acquisition, Investigation, Methodology, Supervision, Writing – review & editing.

References

- [1] P.M. Elliott, J.L. Zamorano, A. Anastasakis, et al., 2014 ESC guidelines on diagnosis and management of hypertrophic cardiomyopathy: the task force for the diagnosis and management of hypertrophic cardiomyopathy of the European Society of Cardiology (ESC), *Eur. Heart J.* 35 (2014) 2733–2779, <https://doi.org/10.1093/eurheartj/ehu284>.
- [2] B.J. Gersh, B.J. Maron, R.O. Bonow, et al., 2011 ACCF/AHA guideline for the diagnosis and treatment of hypertrophic cardiomyopathy: a report of the American college of cardiology foundation/American heart association task force on practice guidelines, *Circulation.* 124 (2011) 783–831, <https://doi.org/10.1161/CIR.0b013e318223e2bd>.
- [3] C. Fumagalli, M.G. De Gregorio, M. Zampieri, et al., Targeted medical therapies for hypertrophic cardiomyopathy, *Curr. Cardiol. Rep.* 10 (2020) <https://doi.org/10.1007/s11886-020-1258-x>.
- [4] R.M. Cooper, C.E. Raphael, M. Liebrechts, N.S. Anavekar, J. Veselka, New developments in hypertrophic cardiomyopathy, *Can. J. Cardiol.* 33 (2017) 1254–1265, <https://doi.org/10.1016/j.cjca.2017.07.007>.
- [5] M. Lu, H. Du, Z. Gao, et al., Predictors of outcome after alcohol septal ablation for hypertrophic obstructive cardiomyopathy an echocardiography and cardiovascular magnetic resonance imaging study, *Circ. Cardiovasc. Interv.* 9 (2016) <https://doi.org/10.1161/CIRCINTERVENTIONS.115.002675>.
- [6] A.G. Rigopoulos, F. Panou, D.T. Kremastinos, H. Seggewiss, Alcohol Septal ablation in hypertrophic obstructive cardiomyopathy, *Hell. J. Cardiol.* 50 (2009) 511–522.
- [7] M.A. Fifer, Through thick and thin: what are the septal thickness limits for alcohol septal ablation? *Circ. Cardiovasc. Interv.* 9 (2016) <https://doi.org/10.1161/CIRCINTERVENTIONS.116.003588>.
- [8] L.M. Iles, A.H. Ellims, H. Llewellyn, et al., Histological validation of cardiac magnetic resonance analysis of regional and diffuse interstitial myocardial fibrosis, *Eur. Heart J. Cardiovasc. Imaging* 16 (2015) 14–22, <https://doi.org/10.1093/ehjci/jeu182>.
- [9] J.C.C. Moon, E. Reed, M.N. Sheppard, et al., The histologic basis of late gadolinium enhancement cardiovascular magnetic resonance in hypertrophic cardiomyopathy, *J. Am. Coll. Cardiol.* 43 (2004) 2260–2264, <https://doi.org/10.1016/j.jacc.2004.03.035>.
- [10] A. Rudolph, H. Abdel-Aty, S. Bohl, et al., Noninvasive detection of fibrosis applying contrast-enhanced cardiac magnetic resonance in different forms of left ventricular hypertrophy. relation to remodeling, *J. Am. Coll. Cardiol.* 53 (2009) 284–291, <https://doi.org/10.1016/j.jacc.2008.08.064>.
- [11] J. Veselka, M.K. Jensen, M. Liebrechts, et al., Long-term clinical outcome after alcohol septal ablation for obstructive hypertrophic cardiomyopathy: results from the euro-ASA registry, *Eur. Heart J.* 37 (2016) 1517–1523, <https://doi.org/10.1093/eurheartj/ehv693>.
- [12] J. Veselka, L. Faber, M. Liebrechts, et al., Short- and long-term outcomes of alcohol septal ablation for hypertrophic obstructive cardiomyopathy in patients with mild left ventricular hypertrophy: a propensity score matching analysis, *Eur. Heart J.* 40 (2019) 1681–1687, <https://doi.org/10.1093/eurheartj/ehz110>.
- [13] J. Veselka, M. Jensen, M. Liebrechts, et al., Alcohol Septal Ablation in Patients with Severe Septal Hypertrophy, *Heart*, 2019 <https://doi.org/10.1136/heartjnl-2019-315422>.
- [14] U. Sigwart, Non-surgical myocardial reduction for hypertrophic obstructive cardiomyopathy, *Lancet.* 346 (1995) 211–214, [https://doi.org/10.1016/s0140-6736\(95\)91267-3](https://doi.org/10.1016/s0140-6736(95)91267-3).
- [15] J. Veselka, D. Zemánek, J. Fiedler, P. Šváb, Real-time myocardial contrast echocardiography for echo-guided alcohol septal ablation, *Arch. Med. Sci.* (2009) 271–272.
- [16] M.A. Fifer, U. Sigwart, Hypertrophic obstructive cardiomyopathy: Alcohol septal ablation, *Eur. Heart J.* 32 (2011) <https://doi.org/10.1093/eurheartj/ehr013>.
- [17] J. Veselka, E. Polaková, J. Bonaventura, Update on alcohol septal ablation for hypertrophic obstructive cardiomyopathy, *Kardiol. Pol.* 77 (2019) 160–161, <https://doi.org/10.5603/KP.2019.0019>.
- [18] J.C.C. Moon, W.J. McKenna, J.A. McCrohon, P.M. Elliott, G.C. Smith, D.J. Pennell, Toward clinical risk assessment in hypertrophic cardiomyopathy with gadolinium cardiovascular magnetic resonance, *J. Am. Coll. Cardiol.* 41 (2003) 1561–1567, [https://doi.org/10.1016/S0735-1097\(03\)00189-X](https://doi.org/10.1016/S0735-1097(03)00189-X).
- [19] H. Engblom, J. Tufvesson, R. Jablonowski, et al., A new automatic algorithm for quantification of myocardial infarction imaged by late gadolinium enhancement cardiovascular magnetic resonance: Experimental validation and comparison to expert delineations in multi-center, multi-vendor patient data, *J. Cardiovasc. Magn. Reson.* 18 (2016) <https://doi.org/10.1186/s12968-016-0242-5>.
- [20] S.F. Nagueh, B.M. Groves, L. Schwartz, et al., Alcohol septal ablation for the treatment of hypertrophic obstructive cardiomyopathy: a multicenter north american registry, *J. Am. Coll. Cardiol.* 58 (2011) 2322–2328, <https://doi.org/10.1016/j.jacc.2011.06.073>.
- [21] S.S. Panaich, A.O. Badheka, A. Chothani, et al., Results of ventricular septal myectomy and hypertrophic cardiomyopathy (from Nationwide inpatient sample [1998–2010]), *Am. J. Cardiol.* 114 (2014) 1390–1395, <https://doi.org/10.1016/j.amjcard.2014.07.075>.

J. Veselka a kol.

Long-term outcome of repeated septal reduction therapy after alcohol septal ablation for HOCM

Archives of Medical Science
Impact Factor: 2,807

Long-term outcome of repeated septal reduction therapy after alcohol septal ablation for hypertrophic obstructive cardiomyopathy: insight from the Euro-ASA registry

Josef Veselka¹, Lothar Faber², Max Liebrechts³, Robert Cooper⁴, Jaroslav Januska⁵, Jan Krejci⁶, Maciej Dabrowski⁷, Peter Riis Hansen⁸, Hubert Seggewiss^{2,9}, Dieter Horstkotte², Eva Hansvenclova¹, Henning Bundgaard¹⁰, Jurriën ten Berg³, Morten Kvistholm Jensen¹⁰

¹Department of Cardiology, Second Medical School, Charles University, University Hospital Motol, Prague, Czech Republic

²Department of Cardiology, Heart and Diabetes Centre NRW, Ruhr-University Bochum, Bad Oeyenhausen, Germany

³Department of Cardiology, St. Antonius Hospital Nieuwegein, Nieuwegein, the Netherlands

⁴Institute of Cardiovascular Medicine and Science, Liverpool Heart and Chest Hospital, Liverpool, England

⁵Cardiocentre Podlesí, Trinec, Czech Republic

⁶First Department of Internal Medicine/Cardioangiology, International Clinical Research Centre, St. Anne's University Hospital and Masaryk University, Brno, Czech Republic

⁷Department of Interventional Cardiology and Angiology, Institute of Cardiology, Warsaw, Poland

⁸Department of Cardiology, Gentofte Hospital, Copenhagen University Hospital, Hellerup, Denmark

⁹Department of Internal Medicine, Juliusspital Wuerzburg, Germany

¹⁰Unit for Inherited Cardiac Diseases, Department of Cardiology, Copenhagen University Hospital, Rigshospitalet, Copenhagen, Denmark

Corresponding author:

Josef Veselka MD, PhD
Department of Cardiology
Second Medical School
Charles University
University Hospital Motol
V úvalu 84
Prague 5, 15000
Czech Republic
Phone: +420 224434900
Fax: +420 2 24434920
E-mail: Veselka.josef@seznam.cz

Submitted: 27 March 2018

Accepted: 25 May 2018

Arch Med Sci 2020; 16 (5): 1239–1242

DOI: <https://doi.org/10.5114/aoms.2020.97969>

Copyright © 2020 Termedia & Banach

Two-thirds of patients with hypertrophic cardiomyopathy (HCM) have a significant left ventricular outflow tract (LVOT) obstruction that may be treated with alcohol septal ablation (ASA) dependent on symptoms [1]. However, some degree of obstruction may remain after ASA and if the patient remains symptomatic repeated septal reduction therapy (RSRT) may be indicated [1–5]. The outcome of RSRT remains unknown. In this study, we sought to determine the long-term outcomes of patients treated with ASA or myectomy after previous ASA.

A total of 1385 consecutive patients (48% women, mean age: 58 ± 14 years) from nine European centres (Euro-ASA registry) who had been treated once with ASA as first time septal reduction therapy were enrolled in the study. We identified 145 (10%) patients who subsequently underwent RSRT, including 99 (68%) who underwent re-ASA, 31 (21%) who underwent myectomy, 12 (8%) who underwent re-ASA and myectomy, and 3 (2%) who underwent two further ASA procedures.

Patients were divided into those who had undergone only the initial ASA (group A, 1240 patients) and those who had undergone RSRT (group B, 145 patients). The primary end-point was major adverse cardiovascular events (MACE), defined as death related to any cardiovascular dis-

Table I. Clinical and echocardiographic characteristics at baseline and at the last check-up

Parameter	Group A (n = 1240)	Group B (n = 145)	P-value
Age at baseline [years]	58.7 ±13.4	55.1 ±14.0	0.005
Females, n (%)	597 (48)	70 (48)	1.000
Dyspnoea, NYHA class:			
Baseline	2.9 ±0.5	2.9 ±0.4	0.760
Last clinical follow-up	1.7 ±0.7	2.0 ±0.8	< 0.001
NYHA class III/IV, n (%):			
Baseline	1041 (84)	124 (86)	0.628
Last clinical follow-up	142 (11)	38 (26)	< 0.001
Angina, CCS class:			
Baseline	1.2 ±1.2	1.1 ±1.1	0.339
Last clinical follow-up	0.7 ±0.8	0.5 ±0.8	< 0.001
LV outflow gradient at rest [mm Hg]:			
Baseline	69 ±38.9	78.3 ±37.1	< 0.001
Last clinical follow-up	15.4 ±20.8	21.5 ±26.6	< 0.001
> 30 mm Hg, n (%)	170 (14)	30 (21)	0.033
Delta gradient, % reduction	74.6 ±30.3	71.2 ±28.8	0.143
LV systolic diameter [mm]:			
Baseline	43.0 ±6.3	42.3 ±6.0	0.271
Last clinical check-up	45.4 ±6.2	45.7 ±6.2	0.639
LV ejection fraction (%):			
Baseline	70 ±9	69 ±9	0.061
Last clinical follow-up	66 ±10	65 ±8	0.054
Basal interventricular septum thickness [mm]:			
Baseline	20.5 ±4.2	21.4 ±4.2	0.004
Last clinical check-up	15.3 ±4.5	16 ±4.1	0.022
Left atrium diameter [mm]:			
Baseline	47.4 ±6.8	47.6 ±5.7	0.702
Last clinical check-up	45.8 ±7.2	46.1 ±6.5	0.499
Alcohol [ml]	2.1 ±0.9	3 ±1.5	< 0.001
Pacemaker, n (%):			
Baseline	51 (4.1)	6 (4.1)	1.000
Last clinical check-up	198 (16.0)	37 (25.5)	0.007
Implantable cardioverter-defibrillator, n (%):			
Baseline	63 (5.1)	6 (4.1)	0.840
Last clinical check-up	110 (8.9)	19 (13.1)	0.098
Mean follow-up duration [years]	5.4 ±4.2	6.5 ±4.1	

LV – left ventricular, NYHA – New York Heart Association, CCS – Canadian Cardiovascular Society.

ease, sudden death, an appropriate implantable cardioverter-defibrillator discharge, resuscitation for ventricular fibrillation or death due to an unknown cause. Secondary endpoints were clinical symptoms and echocardiographic variables and number of implanted pacemakers at the last clinical check-up.

The septal reduction procedure was performed as described previously [1–6]. The indication for RSRT was at the discretion of each participating centre. Most patients underwent a routine clinical examination 3–6 months after ASA and then once per year including echocardiography [7–9]. All adverse events were confirmed by reviewing the medical records and/or national death registries.

Student's *t*-test, χ^2 test and Kaplan-Meier analysis were used as appropriate. The long-term occurrence of MACE was estimated using the Kaplan-Meier method, with the curves of groups A and B adjusted for age at ASA (60 years), baseline LVOT gradient (70 mm Hg), baseline septum thickness (20 mm) and baseline NYHA class (2.5). A *p*-value of < 0.05 was considered statistically significant.

A total of 1385 consecutive patients underwent ASA. A total of 12 (0.9%) patients died within 30 days after the first ASA and none died early after RSRT. In group B, the first RSRT was performed 1.9 ± 1.9 years (range: 0.04–10.77 years) after the first ASA. The mean follow-up period was 6.5 ± 4.1 years and none of the patients were lost to follow-up. The baseline (before first ASA) and long-term results are summarised in Table I. At the most recent clinical follow-up, group B patients were more symptomatic, had a higher residual LVOT gradient, and a larger proportion of the patients had a pacemaker implanted compared to group A patients (Table I). A total of 24 (24%) patients treated with ASA and re-ASA and 6 (19%) patients treated with ASA and myectomy underwent pacemaker implantation ($p = 0.81$). The percentage reduction of LVOT gradient was similar in patients who underwent ASA and re-ASA versus ASA and myectomy ($71 \pm 29\%$ vs. $70 \pm 29\%$; $p = 0.84$).

Survival free from MACE is presented in Figure 1.

The major findings in this study were as follows: 1) the incidence of MACE was similar among both groups of patients; 2) patients who required RSRT were younger, had a higher LVOT gradient and had a thicker interventricular septum at baseline; 3) RSRT is safe; 4) despite RSRT the patients had a higher residual LVOT gradient and worse dyspnoea and chest pain at the most recent follow-up; 5) repeated procedures were associated with an increased cumulative need for pacemaker implantation.

Currently, patients with only mild basal hypertrophy and redundant mitral apparatus, marked papillary muscle abnormalities, and mid-cavity

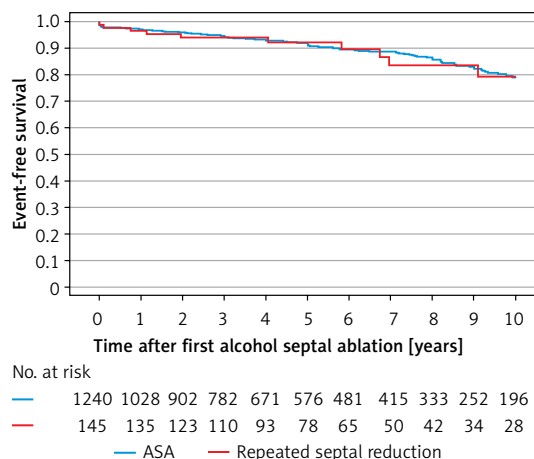


Figure 1. Kaplan-Meier curves showing MACE in patients after the first ASA (group A) and RSRT (group B) ($p = 0.165$)

obstruction are considered good candidates for myectomy. On the other hand, patients with less complex pathology might be treated with ASA. A growing body of evidence suggests that patients with HCM and a high LVOT gradient should be treated aggressively in order to eliminate or reduce the gradient to < 30 mm Hg [2, 3, 7]. However, it has not yet been established whether these patients should be submitted to the risk of undergoing RSRT or whether a conservative treatment approach would be more beneficial. Although this was an observational study only, our results suggest that the risk of MACE after repeated procedures is not increased compared to patients with a clinically satisfactory result after the first ASA.

In conclusion, repeated septal reduction therapy after ASA is not associated with a higher risk of major cardiovascular events over a long-term follow-up period but patients more often require pacemaker implantation.

Acknowledgments

This work was supported by the Project for conceptual development of research organization (no. 00064203) and by the AZV Grant awarded by the Ministry of Health, Czech Republic (15-34904A).

Conflict of interest

The authors declare no conflict of interest.

References

- Elliott PM, Anastasakis A, Borger MA, et al. 2014 ESC Guidelines on diagnosis and management of hypertrophic cardiomyopathy. *Eur Heart J* 2014; 35: 2733-79.
- Veselka J, Tomašov P, Krejčí J, Januška J, Adlová R. Obstruction after alcohol septal ablation is associated with cardiovascular mortality events. *Heart* 2016; 102: 1793-6.

3. Maron MS, Olivotto I, Betocchi S, et al. Effect of left ventricular outflow tract obstruction on clinical outcome in hypertrophic cardiomyopathy. *N Engl J Med* 2005; 384: 295-303.
4. Veselka J, Krejčí J, Tomašov P, et al. Outcome of patients after alcohol septal ablation with permanent pacemaker implanted for periprocedural complete heart block. *Int J Cardiol* 2014; 171: e37-8.
5. Veselka J, Duchonova R, Palenickova J, et al. Age-related hemodynamic and morphologic differences in patients undergoing alcohol septal ablation for hypertrophic obstructive cardiomyopathy. *Circ J* 2006; 70: 880-4.
6. Veselka J, Zemánek D, Fiedler J, Šváb P. Real-time myocardial contrast echocardiography for echo-guided alcohol septal ablation. *Arch Med Sci* 2009; 5: 271-2.
7. Ziolkowska L, Petryka J, Boruc A, Kawalec W. Comparison of echocardiography with tissue Doppler imaging and magnetic resonance imaging with delayed enhancement in the assessment of children with hypertrophic cardiomyopathy. *Arch Med Sci* 2017; 13: 328-36.
8. Veselka J. Alcohol septal ablation for hypertrophic obstructive cardiomyopathy: a review of literature. *Med Sci Monitor* 2007; 13: RA62-8.
9. Scisło P, Kochanowski J, Kołtowski Ł, Opolski G. Utility and safety of three-dimensional contrast low-dose dobutamine echocardiography in the evaluation of myocardial viability early after an acute myocardial infarction. *Arch Med Sci* 2018; 14: 488-93.

J. Bonaventura a kol.

Patients with hypertrophic obstructive cardiomyopathy after alcohol septal ablation have favorable long-term outcome irrespective of their genetic background

Cardiovascular Diagnosis and Therapy
Impact Factor: 2,615

Patients with hypertrophic obstructive cardiomyopathy after alcohol septal ablation have favorable long-term outcome irrespective of their genetic background

Jiří Bonaventura¹, Patricia Norambuena², Pavel Votýpka², Hana Hnáťová¹, Radka Adlová¹, Milan Macek Jr², Josef Veselka¹

¹Department of Cardiology, ²Department of Biology and Medical Genetics, 2nd Faculty of Medicine, Charles University and Motol University Hospital, Prague, Czech Republic

Contributions: (I) Conception and design: J Bonaventura, P Norambuena, M Macek Jr, J Veselka; (II) Administrative support: none; (III) Provision of study materials or patients: All authors; (IV) Collection and assembly of data: J Bonaventura, P Norambuena, P Votýpka, J Veselka; (V) Data analysis and interpretation: J Bonaventura, P Norambuena, J Veselka; (VI) Manuscript writing: All authors; (VII) Final approval of manuscript: All authors.

Correspondence to: Jiri Bonaventura, MD. Department of Cardiology, Motol University Hospital, 2nd Medical School, Charles University, V Uvalu 84, Prague, 15006, Czech Republic. Email: jiri.bonaventura@fnmotol.cz.

Background: The genetic background of patients with hypertrophic cardiomyopathy (HCM) treated with alcohol septal ablation (ASA) and its relationship to the outcomes are not known. We aimed to investigate whether the outcome of genotype positive (G+) patients differs from genotype negative (G-) patients treated with ASA.

Methods: We included 129 HCM patients (mean age 54±13 years) treated with ASA in a tertiary cardiovascular center and performed next generation sequencing (NGS) based genomic testing. All patients were followed-up three months after the procedure and yearly thereafter.

Results: A total of 30 (23%) HCM patients were G+ patients. At the 3-months follow-up, both groups of patients had similar left ventricular outflow tract PG (16.9±15.7 mmHg in G+ vs. 16.3±18.8 mmHg in G-, P=0.73) and symptoms (follow-up NYHA class 1.40±0.62 vs. 1.37±0.53, P=0.99, follow-up CCS class 0.23±0.52 vs. 0.36±0.65, P=0.36). The independent predictors of all-cause mortality were baseline interventricular septum (IVS) thickness (HR 1.12, 95% CI: 1.00–1.26, P=0.049) and age at the time of ASA (HR 1.11, 95% CI: 1.06–1.17, P<0.01). The adjusted all-cause mortality rate did not differ significantly between G+ and G- patients (P=0.52). The adjusted combined mortality event rate did not differ between both groups (P=0.78).

Conclusions: Despite more severe phenotype in G+ HCM patients, ASA is an equally effective treatment for LVOTO in G+ patients as it is for treating LVOTO in G- patients. The long-term outcome after ASA is similar in G+ and G- patients.

Keywords: Cardiomyopathy; hypertrophic cardiomyopathy (HCM); hypertrophic obstructive cardiomyopathy; alcohol septal ablation (ASA); genetics

Submitted Nov 29, 2019. Accepted for publication Jan 15, 2020.

doi: 10.21037/cdt.2020.01.12

View this article at: <http://dx.doi.org/10.21037/cdt.2020.01.12>

Introduction

Hypertrophic cardiomyopathy (HCM) is a heterogeneous condition in both its genetic origin and phenotypic features (1). Two-thirds of HCM patients have left ventricular (LV) outflow tract obstruction (LVOTO) (2,3). Alcohol septal ablation (ASA) is a safe and effective method of treating LVOTO (4,5). The genetic background of patients treated by ASA and its possible relationship with the outcomes of the procedure are not known. The aim of this study was to investigate whether the outcome of genotype positive (G+) patients differs from genotype negative (G-) patients in a highly symptomatic group of HCM patients treated with ASA.

Methods

Study population

We included 129 consecutive unrelated patients with a clinical diagnosis of HCM in a single tertiary cardiovascular center. The patients were treated with ASA between 1998 and 2017. An HCM diagnosis was established by experienced cardiologists based on a clinical examination, electrocardiography (ECG), and findings of LV hypertrophy ≥ 15 mm on echocardiography and/or magnetic resonance imaging (2,3). Secondary hypertrophy attributable to aortic valve stenosis or amyloidosis was excluded. When patients presented with mild concomitant systemic hypertension, the HCM echocardiography specialists had to claim the hypertension to be either controlled or the severity insufficient to cause the degree of LV hypertrophy. Symptomatic patients [New York Heart Association (NYHA) class III–IV or syncope on exertion] with significant LVOTO (maximal gradient at rest or during physiological provocation ≥ 50 mmHg), despite maximal tolerated pharmacotherapy, were offered septal reduction therapy. ASA was indicated after a careful assessment by a multidisciplinary heart team, in addition to local experience with ASA, and the patient's preference. All ASA procedures were performed by a single operator as previously described (6–8), and all procedures were guided by myocardial contrast echocardiography. A temporary pacemaker lead was placed in the right ventricle in all patients without previous permanent pacemaker implantation. Patients were observed in the coronary care unit for at least 48 hours, and the temporary pacemaker lead was then removed if no episode of high-degree atrioventricular block occurred. All the patients remained on continuous ECG monitoring for up

to seven days until discharge. Basic demographic, clinical, and echocardiographic data were collected at baseline, and the patients were followed up three months after the ASA procedure and yearly thereafter. The study protocol conforms to the ethical guidelines of the Declaration of Helsinki (2000, Fifth revision) and was approved by the institutional ethical committee. Written informed consent was obtained from all patients.

Genetic testing

The DNA samples for next generation sequencing (NGS) testing were obtained between 2005 and 2017. Genetic testing was performed in all patients treated with ASA who provided written informed consent. Genomic DNA was isolated from whole blood of all included patients. Our targeted NGS enrichment panel and methods of variant identification, prioritization, and classification were described in detail in our previous paper (9). All identified variants were classified according to the American College of Medical Genetics and Genomics (ACMG) and the Association for Molecular Pathology (AMP) guidelines (10). Patients, whose variants were classified as pathogenic or likely pathogenic (P/LP), were marked as genotype positive (G+ patients). The rest of the cohort, including patients with variants of unknown significance, was considered genotype negative (G- patients).

Statistical analysis

Data are presented as mean \pm standard deviation (SD) for continuous variables and proportions for categorical variables. The Student's *t*-test, Mann-Whitney test, and Fisher's exact test were used where appropriate. Cox proportional hazards regression was used to identify predictors of mortality events. The following clinical and echocardiographic variables with potential impact on mortality events were first evaluated in a univariate model: age at the time of ASA, sex, LVOTO, interventricular septum (IVS) thickness, and left atrial diameter. Variables with P values < 0.15 were then entered into a multivariable analysis, which was performed using backward stepwise Cox regression. The long-term occurrence of mortality was estimated using the Kaplan-Meier method, and differences between groups were assessed by the log-rank test. Kaplan-Meier curves of G+ and G- patients were adjusted for age at the time of ASA and baseline IVS. The level of statistical significance was set to 0.05. The Prism v.8.1.1 (GraphPad

Table 1 Clinical and echocardiographic data at baseline and during follow-up in G+ compared to G- patients

	Genotype+ (n=30)	Genotype- (n=99)	P value
Male sex [%]	19 [63]	46 [46]	0.10
Age at ASA, years	47.3±12.3	58.8±11.3	<0.01
LVEF baseline, %	78.7±5.6	79.4±5.7	0.48
LVEF follow-up, %	70.3±9.3	72.5±7.3	0.34
LVEDD baseline, mm	40.1±4.9	43.6±4.6	<0.01
LVEDD follow-up, mm	45.6±4.8	47.2±4.7	0.11
Angina, CCS class baseline	1.9±1.2	1.3±1.0	0.46
Angina, CCS class follow-up	0.2±0.5	0.4±0.7	0.36
Dyspnoea, NYHA class baseline	2.8±0.6	2.8±0.5	0.81
Dyspnoea, NYHA class follow-up	1.4±0.6	1.4±0.5	0.99
Episodes of syncope baseline [%]	4 [13]	14 [14]	0.99
Episodes of syncope follow-up [%]	1 [3]	13 [13]	0.19
IVS thickness baseline, mm	23.9±5.0	20.3±3.6	<0.01
IVS thickness follow-up, mm	15.5±4.0	13.0±4.0	<0.01
LVOTO baseline, mmHg	63.6±31.4	63.5±40.2	0.50
LVOTO follow-up, mmHg	16.9±15.7	16.3±18.8	0.73
Pacemaker implanted before ASA	2 [7]	4 [4]	0.62
ICD implanted before ASA	2 [7]	3 [3]	0.33

LVEF, left ventricular ejection fraction; LVEDD, left ventricular enddiastolic diameter; NYHA, New York Heart Association; CCS, Canadian Cardiovascular Society; IVS, interventricular septum; LVOTO, left ventricular outflow tract obstruction.

Software Inc., USA) statistical software was used for statistical analysis.

Results

The baseline characteristics of all 129 patients are shown

in *Table 1*. In 53 (41%) HCM patients, we identified 68 genetic variants in 25 different genes. The complete list of genes is shown in *Table S1*. Thirty of these variants (localized in 8 genes) identified in 30 (23%) HCM patients were classified as P/LP. The distribution of genetic variants is shown in *Figure 1*, and patients sorted by classified variants are shown in *Table 2*. Variants were identified in two major genes, *MYBPC3* and *MYH7*, wherein the dominant role of *MYBPC3* was even more apparent in the group of P/LP genetic variants (62% of identified variants).

Compared to G- patients, G+ patients were treated with ASA at a younger age (47.3±12.3 vs. 58.8±11.3 years, $P<0.01$), had greater hypertrophy of the IVS (23.9±5.0 vs. 20.3±3.6 mm, $P<0.01$), and a smaller LV end-diastolic diameter (40.1±4.9 vs. 43.6±4.6 mm, $P<0.01$).

At baseline, both groups had similar maximal LVOT pressure gradients (PG) (63.6±31.4 vs. 63.5±40.2 mmHg, $P=0.50$) and symptoms (NYHA class 2.77±0.57 vs. 2.81±0.49, $P=0.81$; Canadian Cardiovascular Society (CCS) class 1.93±1.17 vs. 1.83±1.04, $P=0.45$).

At the three-month follow-up, both groups of patients had similar maximal LVOT PG (16.9±15.7 mmHg in the G+ group vs. 16.3±18.8 mmHg in the G- group, $P=0.73$) and symptoms (follow-up NYHA class 1.40±0.62 vs. 1.37±0.53, $P=0.99$, follow-up CCS class 0.23±0.52 vs. 0.36±0.65, $P=0.36$).

Early adverse events

None of the patients died or suffered a stroke within 30 days after the procedure. Sustained ventricular tachycardia/ventricular fibrillation requiring urgent electrical cardioversion during the hospital stay occurred in 5 patients (4%). Either transient or persistent complete heart block was documented in 22 patients (17%), and a new permanent pacemaker was implanted in 9 patients (7%) during the hospital stay. Access site complication occurred in 2 patients (2%). There were no significant differences in complication rate within 30 days between G+ and G- patients (*Table 3*).

Long-term survival

The median (interquartile range) follow-up in the survival analysis was 9.1 (6.3–12.9) years. The mean follow-up in the survival analysis was 9.9±4.8 years. A total of 21 patients (16.3%) died during 1,211 patient-years of follow-up, which resulted in an all-cause mortality rate of 1.7 deaths per 100 patient-years. In the G+ group, 2 (6.7%) of 30

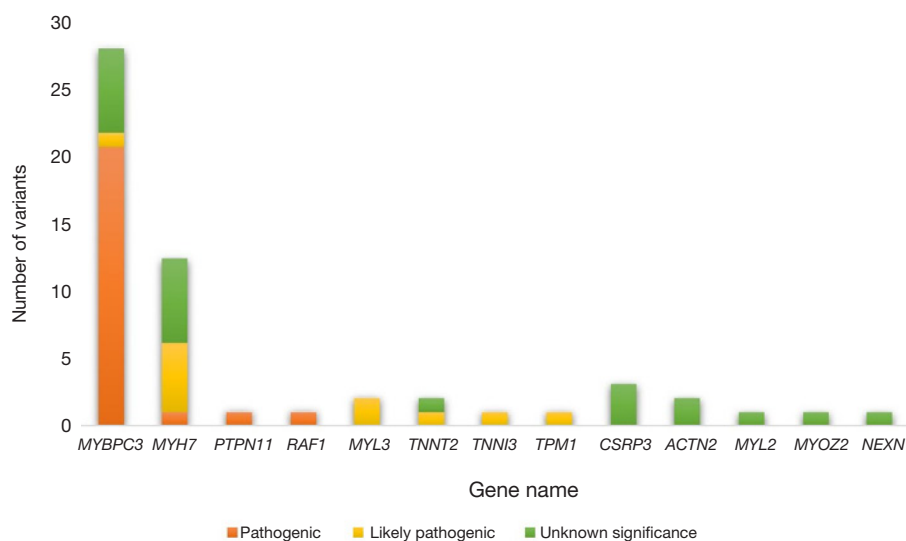


Figure 1 The distribution of genetic variants in HCM patients treated with ASA. HCM, hypertrophic cardiomyopathy; ASA, alcohol septal ablation.

Table 2 Patients sorted by identified variant class (N=129)

Variant classification	Number of patients [%]
Pathogenic or likely pathogenic	30 [23]
Unknown significance	23 [18]
No significant findings*	76 [59]

*, includes benign and likely benign variants.

Table 3 Incidence of complications within 30 days after ASA in G+ and G- patients

Adverse event	Genotype+ (n=30)	Genotype- (n=99)	P value
Death (%)	0 (0)	0 (0)	NA
Stroke (%)	0 (0)	0 (0)	NA
Ventricular tachycardia/fibrillation (%)	1 [3]	4 [4]	0.99
Complete heart block (%)	2 [7]	20 [20]	0.10
Permanent pacemaker implantation (%)	1 [3]	8 [8]	0.68
Cardiopulmonary resuscitation (%)	1 [3]	4 [4]	0.99
Vascular access complication (%)	0	2 [2]	0.99

patients died during follow-up. In the G- group during follow-up, 19 (19.2%) of 99 patients died. The unadjusted all-cause mortality rate did not differ significantly between G+ and G- patients ($P=0.087$), as shown in *Figure 2*. The independent predictors of all-cause mortality were baseline IVS thickness (HR 1.12, 95% CI: 1.00–1.26, $P=0.049$) and age at the time of ASA (HR 1.11, 95% CI: 1.06–1.17, $P<0.001$). The all-cause mortality rate adjusted for age at the time of ASA and baseline IVS thickness did not differ significantly between the G+ and G- patients ($P=0.288$), as shown in *Figure 3*. Combined mortality event endpoint [all-cause mortality and appropriate implantable cardioverter-defibrillator (ICD) discharge] occurred in 24 patients (18.6%) during 1,211 patient-years of follow-up, resulting in an event rate of 2.0 per 100 patient-years. The unadjusted combined mortality event rate did not differ significantly between the G+ and the G- groups ($P=0.518$), as shown in *Figure 4*. The independent predictors of combined mortality event rate were IVS thickness (HR 1.14, 95% CI:

1.03–1.26, $P=0.011$) and age at the time of ASA (HR 1.07, 95% CI: 1.03–1.12, $P<0.001$). The combined mortality event rate adjusted for age at the time of ASA and baseline IVS thickness did not differ significantly between G+ and G- patients ($P=0.777$), as shown in *Figure 5*.

Discussion

Our study suggests that ASA is an equally effective treatment of LVOTO in G+ HCM patients as in G-

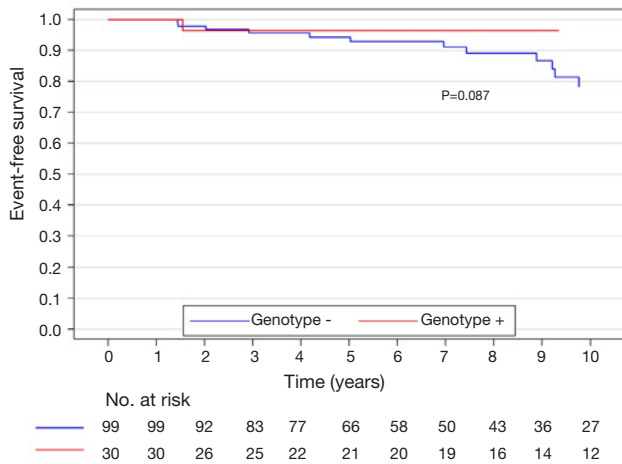


Figure 2 All-cause mortality rate (unadjusted) of genotype positive and genotype negative patients.

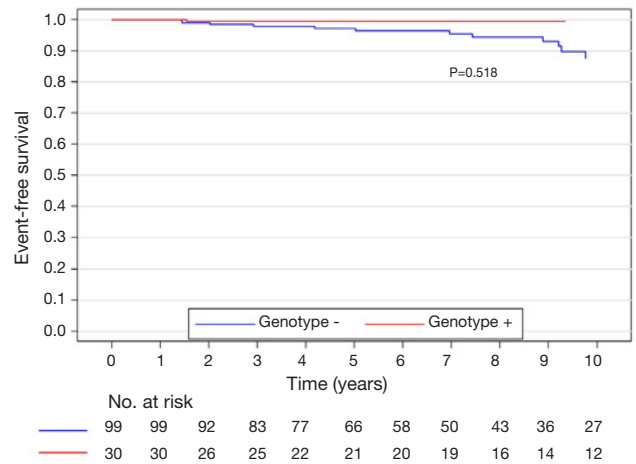


Figure 4 Combined mortality event rate (unadjusted) of genotype positive and genotype negative patients.

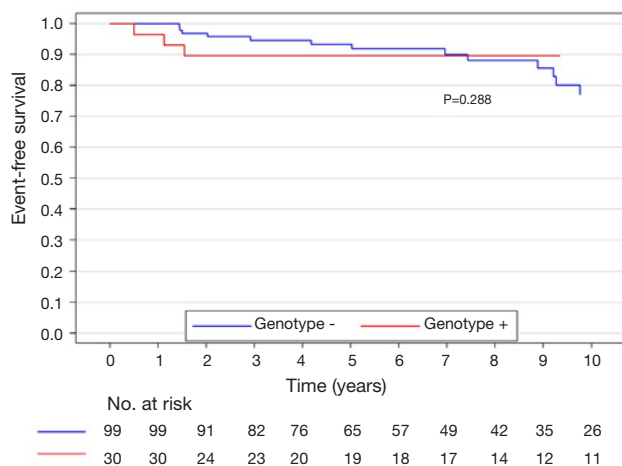


Figure 3 All-cause mortality rate adjusted for age at the time of ASA and baseline IVS thickness of genotype positive and genotype negative patients. ASA, alcohol septal ablation; IVS, interventricular septum.

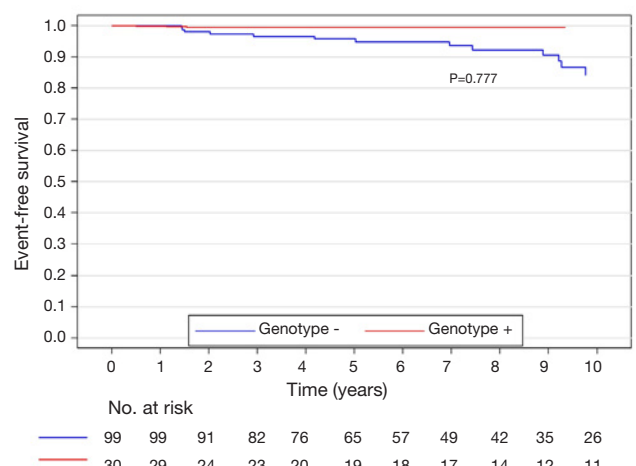


Figure 5 Combined mortality event rate adjusted for age at the time of ASA and baseline IVS thickness of genotype positive and genotype negative patients. ASA, alcohol septal ablation; IVS, interventricular septum.

patients. This finding is important, regarding the fact, that G+ patients are considered to have more severe phenotype and worse outcome than G- patients (11,12). To date, the reported data about G+ patients included a presentation at an earlier age, greater hypertrophy of IVS and smaller LV enddiastolic diameter (13-15). Increased risk for the combined endpoints of cardiovascular death, nonfatal stroke, or progression to NYHA functional class III or IV compared to G- HCM patients was also reported (16). Recent data from a large Portuguese registry of HCM

patients suggest a higher risk of sudden cardiac death in G+ patients (12). Our patients' baseline characteristics are in line with the previously reported data; G + patients are younger at the time of diagnosis, have greater hypertrophy of IVS and smaller LV enddiastolic diameter. Surprisingly, the severity of the LVOTO was similar between both groups in our study. Furthermore, the symptoms (angina CCS class, dyspnea NYHA class, syncope) were not significantly different at baseline. In both groups, the symptoms improved after ASA procedures. This finding

further supports the previously reported data from the Euro-ASA registry showing comparable outcomes among various subgroups of HCM patients treated with ASA (4). Since the residual LVOTO after ASA is known to be associated with worse prognosis (17), the favorable results in G+ patients are of great importance.

We included highly symptomatic HCM patients with significant LVOTO. After ASA, their symptoms greatly improved, as it has been already demonstrated by several studies (4,5,16,17). It is also known, that more pronounced reduction of LVOTO is associated with a lower NYHA class during the follow-up (4). This was confirmed by the current study, where both groups of patients had very low LVOT PG and only mild symptoms during the follow up. Severe LVOTO is known to be an independent predictor of adverse clinical outcome (18,19). Taking this into account, the clinical consequence of ASA is largely important. Resulting lower LVOT gradient is associated not only with better functional class, but also with better survival (18,20,21). The important finding of our current study is that HCM patients after ASA gained all these benefits irrespective of their genetic background. The possible explanation of relatively higher number of syncope after ASA in G- patients could be the fact, that the G- patients were on average 11.5 years older than G+ patients and had higher incidence of complete heart block after ASA, as shown in *Table 3*. Nevertheless, most of the complete heart blocks were transient and did not require permanent pacemaker implantation.

The long-term survival was not statistically different between G+ and G- patients. Neither differed the occurrence of combined mortality endpoint (all-cause mortality and appropriate ICD discharge). Despite the long follow-up, the number of endpoints is relatively low, emphasizing the favorable prognosis of post-ASA patients. Prediction of post-ASA clinical outcome is challenging because of the marked heterogeneity of the treated HCM cohort. In our study, the independent predictors of all-cause mortality were baseline IVS thickness and age at the time of ASA. Patients in the G+ group were on average 11.5 years younger than G- patients. Despite their greater IVS thickness at baseline, their mortality rate was lower than in G- patients, that is probably attributed to lower age. The genotype positivity was not found to be independent of these two main predictors. Nevertheless, the low number of endpoints in the G + group compromised the multivariate analysis.

Another important finding is that the genetic

background of HCM patients did not influence the safety of the procedure. None of our study patients died or suffered a stroke within 30 days after ASA. Despite the greater hypertrophy of IVS, the occurrence of malignant arrhythmias and cardiopulmonary resuscitation in G+ patients were similar to G- patients. The G- patients inclined towards higher rates of a complete heart block after ASA, but the difference was not statistically significant. Neither the rates of permanent pacemaker implantation differed between our two groups.

Marked genetic heterogeneity of HCM, including incomplete penetrance, variable expressivity and existence of HCM phenocopies, makes the genotype results interpretation complicated. It is likely, that factors other than the sarcomere mutation itself influence clinical course and outcomes. These genetic, epigenetic, and environmental modifiers play an important role but are not yet fully characterized or understood. All of these aspects of heterogeneity in HCM have prevented identifying clear correlations between genotype and phenotype to date.

In our study, we present the largest ASA cohort evaluated with NGS. We identified genetic variants in 41% of patients. Only 23% of identified variants were classified as pathogenic or likely pathogenic (P/LP). This relatively low yield of genetic testing is in line with our recent findings (9). Advances in contemporary DNA-sequencing methodology make gene-based diagnosis faster and cheaper in clinical practice. Screening large numbers of genes results in the identification of many genetic variants of unknown significance (VUS) (18,19) which are not clinically actionable. In our study, we used a strict classification ACMG guidelines criteria (10), that explains the lower number of patients with P/LP variants than described in the past (13,14) but in line with the most recent works (12,20). Even with analysis of up to 229 genes, 59% of our patients do not carry any genetic variant susceptible of causing HCM. Together with a known low yield of genetic testing in patients with sigmoid septal morphology (13), these findings suggest, that some of the patients, despite having significant LVOTO treated with ASA, may not suffer from a true monogenic disorder.

While historically viewed as an autosomal dominant inherited heart condition, in patients with negative genetic tests, the inheritance pattern and utility of family screening are unclear. Recent studies have shown that expanded panel for genetic testing offers limited additional sensitivity for most patients with HCM (21-23). Also, in our study of ASA patients, almost all P/LP variants were found in

sarcomeric genes, with only two exceptions. It is clear, that a large proportion of individuals with a clinical diagnosis of HCM but without sarcomere gene mutations may exhibit a distinct disease process that has a more complex, non-Mendelian inheritance pattern (24). Their phenotype fulfils the clinical criteria for the diagnosis of HCM (2,3) and they commonly suffer from typical features of the disease, including LVOTO. The results of our study revealed that both these groups of patients can be treated effectively with ASA resulting in similar clinical outcomes. Therefore, the decision about ASA procedure should not be influenced by genetic background in clinical practice.

Our study has several limitations. It is a retrospective analysis of prospectively collected data. The study is underpowered in terms of mortality, since our study groups are relatively small. We cannot be confident that these data are generalizable for non-tertiary referral centers with less experience with HCM patients and ASA. Institutional experience is a key determinant of successful outcomes and lower complication rates of ASA (25). This fact results in another selection bias—patients were carefully selected for ASA, considering the presence of septal and mitral apparatus anatomy appropriate for the procedure. Moreover, the results are only applicable to the adult HCM population, since no pediatric patients were included in our study.

Conclusions

Despite a more severe phenotype in G+ HCM patients, ASA is an equally effective treatment for LVOTO in G+ patients as it is for treating LVOTO in G- patients. The long-term outcome after ASA is similar in G+ and G- patients.

Acknowledgments

The authors would like to thank Dr. Marek Maly and Eva Hansvenclova for their assistance with statistical analysis.

Funding: Supported by the Ministry of Health of the Czech Republic (grant No. 15-34904A) and Conceptual Development of Research Organization, Motol University Hospital, Prague (grant No. 00064203).

Footnote

Conflicts of Interest: The authors have no conflicts of interest

to declare.

Ethical Statement: The authors are accountable for all aspects of the work in ensuring that questions related to the accuracy or integrity of any part of the work are appropriately investigated and resolved. The study protocol conforms to the ethical guidelines of the Declaration of Helsinki (2000, Fifth revision) and was approved by the institutional ethical committee. Written informed consent was obtained from all patients.

References

1. Maron BJ, Maron MS, Semsarian C. Genetics of hypertrophic cardiomyopathy after 20 years: clinical perspectives. *J Am Coll Cardiol* 2012;60:705-15.
2. Elliott PM, Anastakis A, Borger M, et al. 2014 ESC Guidelines on diagnosis and management of hypertrophic cardiomyopathy. *Eur Heart J* 2014;35:2733-79.
3. Gersh BJ, Maron BJ, Bonow RO, et al. 2011 ACCF/AHA guideline for the diagnosis and treatment of hypertrophic cardiomyopathy: A report of the American College of cardiology foundation/American heart association task force on practice guidelines. *Circulation* 2011;124:e783-831.
4. Veselka J, Jensen MK, Liebrechts M, et al. Long-term clinical outcome after alcohol septal ablation for obstructive hypertrophic cardiomyopathy: Results from the Euro-ASA registry. *Eur Heart J* 2016;37:1517-23.
5. Veselka J, Polaková E, Bonaventura J. Update on alcohol septal ablation for hypertrophic obstructive cardiomyopathy. *Kardiol Pol* 2019;77:160-1.
6. Veselka J. Alcohol septal ablation for hypertrophic obstructive cardiomyopathy: a review of the literature. *Med Sci Monit* 2007;13:RA62-8.
7. Veselka J, Zemánek D, Fiedler J, et al. Real-time myocardial contrast echocardiography for echo-guided alcohol septal ablation. *Arch Med Sci* 2009;5:271-2.
8. Veselka J, Lawrenz T, Stellbrink C, et al. Early outcomes of alcohol septal ablation for hypertrophic obstructive cardiomyopathy: A European multicenter and multinational study. *Catheter Cardiovasc Interv* 2014;84:101-7.
9. Bonaventura J, Norambuena P, Tomašov P, et al. The utility of the Mayo Score for predicting the yield of genetic testing in patients with hypertrophic cardiomyopathy. *Arch Med Sci* 2019;15:641-9.

10. Richards S, Aziz N, Bale S, et al. Standards and guidelines for the interpretation of sequence variants: A joint consensus recommendation of the American College of Medical Genetics and Genomics and the Association for Molecular Pathology. *Genet Med* 2015;17:405-24.
11. Ho CY, Day SM, Ashley EA, et al. Genotype and Lifetime Burden of Disease in Hypertrophic Cardiomyopathy. *Circulation* 2018;138:1387-98.
12. Lopes LR, Brito D, Belo A, et al. Genetic characterization and genotype-phenotype associations in a large cohort of patients with hypertrophic cardiomyopathy - An ancillary study of the Portuguese registry of hypertrophic cardiomyopathy. *Int J Cardiol* 2019;278:173-9.
13. Bos JM, Will ML, Gersh BJ, et al. Characterization of a phenotype-based genetic test prediction score for unrelated patients with hypertrophic cardiomyopathy. *Mayo Clin Proc* 2014;89:727-37.
14. Lopes LR, Syrris P, Guttmann OP, et al. Novel genotype-phenotype associations demonstrated by high-throughput sequencing in patients with hypertrophic cardiomyopathy. *Heart* 2015;101:294-301.
15. Binder J, Ommen SR, Gersh BJ, et al. Echocardiography-guided genetic testing in hypertrophic cardiomyopathy: Septal morphological features predict the presence of myofilament mutations. *Mayo Clin Proc* 2006;81:459-67.
16. Olivotto I, Girolami F, Ackerman MJ, et al. Myofilament protein gene mutation screening and outcome of patients with hypertrophic cardiomyopathy. *Mayo Clin Proc* 2008;83:630-8.
17. Veselka J, Tomašov P, Januška J, et al. Obstruction after alcohol septal ablation is associated with cardiovascular mortality events. *Heart* 2016;102:1793-6.
18. Fokstuen S, Munoz A, Melacini P, et al. Rapid detection of genetic variants in hypertrophic cardiomyopathy by custom DNA resequencing array in clinical practice. *J Med Genet* 2011;48:572-6.
19. Meder B, Haas J, Keller A, et al. Targeted Next-Generation Sequencing for the Molecular Genetic Diagnostics of Cardiomyopathies. *Circ Cardiovasc Genet* 2011;4:110-22.
20. Murphy SL, Anderson JH, Kapplinger JD, et al. Evaluation of the Mayo Clinic Phenotype-Based Genotype Predictor Score in Patients with Clinically Diagnosed Hypertrophic Cardiomyopathy. *J Cardiovasc Transl Res* 2016;9:153-61.
21. Walsh R, Thomson KL, Ware JS, et al. Reassessment of Mendelian gene pathogenicity using 7,855 cardiomyopathy cases and 60,706 reference samples. *Genet Med* 2017;19:192-203.
22. Ingles J, Goldstein J, Thaxton C, et al. Evaluating the Clinical Validity of Hypertrophic Cardiomyopathy Genes. *Circ Genomic Precis Med* 2019;12:e002460.
23. Alfares AA, Kelly MA, McDermott G, et al. Results of clinical genetic testing of 2,912 probands with hypertrophic cardiomyopathy: Expanded panels offer limited additional sensitivity. *Genet Med* 2015;17:880-8.
24. Ko C, Arscott P, Concannon M, et al. Genetic testing impacts the utility of prospective familial screening in hypertrophic cardiomyopathy through identification of a nonfamilial subgroup. *Genet Med* 2018;20:69-75.
25. Veselka J, Faber L, Jensen MK, et al. Effect of Institutional Experience on Outcomes of Alcohol Septal Ablation for Hypertrophic Obstructive Cardiomyopathy. *Can J Cardiol* 2018;34:16-22.

Cite this article as: Bonaventura J, Norambuena P, Vošpka P, Hnáťová H, Adlová R, Macek M Jr, Veselka J. Patients with hypertrophic obstructive cardiomyopathy after alcohol septal ablation have favorable long-term outcome irrespective of their genetic background. *Cardiovasc Diagn Ther* 2020. doi: 10.21037/cdt.2020.01.12

Supplementary

Table S1 The complete list of genes and identified variants

Gene	Pathogenic	Likely pathogenic	VUS
<i>MYBPC3</i>	20	1	6
<i>MYH7</i>	1	5	6
<i>PTPN11</i>	1	0	0
<i>RAF1</i>	1	0	0
<i>MYL3</i>	0	2	0
<i>TNNT2</i>	0	1	1
<i>TNNI3</i>	0	1	0
<i>TPM1</i>	0	1	0
<i>CSRP3</i>	0	0	3
<i>ACTN2</i>	0	0	2
<i>DSP</i>	0	0	2
<i>CACNA1C</i>	0	0	1
<i>DES</i>	0	0	1
<i>DMD</i>	0	0	1
<i>DSG2</i>	0	0	1
<i>FHL2</i>	0	0	1
<i>LDB3</i>	0	0	1
<i>MYH6</i>	0	0	1
<i>MYL2</i>	0	0	1
<i>MYOZ2</i>	0	0	1
<i>NEXN</i>	0	0	1
<i>PKP2</i>	0	0	1
<i>SCN10A</i>	0	0	1
<i>SOS1</i>	0	0	1
<i>SCN2B</i>	0	0	1

VUS, variants of unknown significance.